



This is to certify that the

dissertation entitled


The characterization of thermal degradation of peptides
utilizing K+IDS - K+ ionization of desorbed species
and an investigation of collision-induced dissociation (CID)
of deprotonated peptides

presented by

Huaiqin Wu

has been accepted towards fulfillment
of the requirements for

Ph.D. _____ degree in Chemistry



John Allison
Major professor

Date 10-25-94

**THE CHARACTERIZATION OF THERMAL DEGRADATION OF PEPTIDES
UTILIZING K⁺IDS - K⁺ IONIZATION OF DESORBED SPECIES
AND
AN INVESTIGATION OF COLLISION-INDUCED DISSOCIATION (CID)
OF DEPROTONATED PEPTIDES**

By

Huaiqin Wu

A DISSERTATION

**Submitted to
Michigan State University
in partial fulfillment of the requirements
for the degree of .**

DOCTOR OF PHILOSOPHY

Department of Chemistry

1994

ABSTRACT

THE CHARACTERIZATION OF THERMAL DEGRADATION OF PEPTIDES UTILIZING K^+ IDS - K^+ IONIZATION OF DESORBED SPECIES AND AN INVESTIGATION OF COLLISION-INDUCED DISSOCIATION (CID) OF DEPROTONATED PEPTIDES

By

Huaiqin Wu

The desorption/ionization technique, K^+ IDS, was developed in 1984 at MSU. In this work, the K^+ IDS technique was further developed and characterized. A new probe was designed and constructed; a new material was used for the thermionic emitter; local pressure in the ion source chamber was estimated; the stabilization theory for K^+ -adducts was re-evaluated.

Thermal degradation of peptides was characterized utilizing the K^+ IDS technique. Charge is not involved in this process; thus it can be treated as the ultimate model for charge-remote fragmentation, one of the processes proposed for CID of protonated and deprotonated peptides. Our understanding of thermal degradation of peptides may provide insights into the CID process of charged peptides.

The study is based on the use of deuterated, derivatized and specifically-designed peptides, to trace the source of the shifting hydrogen atom in thermal degradation. It is concluded that thermal degradation of peptides, at a temperature about 600K, proceeds via the lowest energy process - cyclization involving their termini.

A new phenomenon - the discrimination in the formation of K^+ adducts of thermal degradation products - was uncovered in this study. It is found that there is a discrimination against small and cyclic molecules, which are weakly bonded to K^+ ions.

In studying fragmentation of charged species, CID of deprotonated peptides was investigated. Derivatization/charge-localization and deuteration are the major tools in discovering the sites of deprotonation as well as the fragmentation pathways. The amides are found to be very important sites - for the first time - in the formation of fragment ions. Mechanisms are proposed for the formation of the major fragment ions from both regular and charge-localized peptides. The results obtained are found to be different from those reported in the literature for dipeptides. The applicability of CID-MS/MS of deprotonated peptides for peptide sequencing is discussed, as is the low sensitivity of both MS and MS/MS in negative ion mode.

**Dedicated to my mother
and
in memory of my father
Baoshi and Dekui Wu**

ACKNOWLEDGMENTS

I would like to express my sincere gratitude to my mentor, Dr. John Allison, for his guidance and constant support during my graduate study at MSU, especially for the time and effort in correcting this manuscript and in coaching the seminars. My gratitude also goes to Dr. Watson for correcting this dissertation, and for his encouragement and support; to Dr. Leroi and Dr. Reusch for serving on my committee; and to Dr. Hiller for his many advice about job hunting and for reading this dissertation.

To all the Allison group members, Karen, Jason, Kurt, Kate, Guy, Paochi, Gabi, Tom, and Garys, thank you all for your help and your friendship during my stay at MSU.

I also owe many thanks to all members of the Mass Spectrometry Facility: Dr. Gage, Dr. Huang, Mike, Mel, Melinda and Bev. Without their technical support and friendship, my study here would have been extremely difficult.

And last, but not the least, I would like to thank my wife, Shudong, my mother, brother and sisters, and to all my relatives and friends for their loving, caring and supporting during my graduate study at Michigan State University.

TABLE OF CONTENTS

List of Tables	ix
List of Figures	xiii
 Chapter 1 Introduction and Research Objectives	 1
I. Introduction - A Historical Review of Peptide Sequencing	1
II. Research Objectives	6
A. Thermal Degradation of Peptides	7
B. Fragmentation of Deprotonated Peptides.....	9
References.....	10
 Chapter 2 K ⁺ IDS: The Technique and Its Further Characterization.....	 12
I. Introduction	12
II. Experimental Section.....	13
A. Experiment Setup and K ⁺ IDS Probe.....	13
B. The Making of a Thermionic Emitter	17
III. K ⁺ IDS: Operational Principles	20
A. Thermionic Emission.....	20
B. Desorption Vs. Degradation	21
C. K ⁺ -Adduct Formation and Stabilization	24
IV. (M+K) ⁺ Stability Studied by Using a Directly Heated K ⁺ IDS Probe.....	26
A. Characterization of a Novel Direct-Heating K ⁺ IDS Probe.....	26

B. (M+K) ⁺ Stability Studied by Direct Heating	27
References.....	31
 Chapter 3 Peptide Analysis by K ⁺ IDS Mass Spectrometry.....	32
I. Introduction.....	32
II. Experimental Section	34
III. K ⁺ IDS Mass Spectra of Typical Peptides	35
A. Nomenclature of K ⁺ IDS Fragments.....	35
B. Typical K ⁺ IDS Spectra of Peptides	37
C. K ⁺ IDS Spectra of Polar Peptides and Dehydration Reactions	40
D. K ⁺ IDS Spectra of Peptide Derivatives	48
1. Peptide Amides.....	48
2. N-Terminally Derivatized Peptides.....	51
3. C-Terminal Esterification.....	55
4. Peptide Variants	55
E. Internal Ions from Peptides.....	61
IV. Peptide Sequencing by K ⁺ IDS Mass Spectrometry	61
References.....	65
 Chapter 4 The Characterization of the Primary Thermal Degradation Processes of Peptides	
I. Introduction.....	66
II. Experimental Section	67
III. The Primary Thermal Degradation Processes of Peptides	68
A. Deuterium-Labeling Experiments	70
B. Peptide Derivatization - Evidence for Cyclization.....	77
C. Termini, Sidechains and Steric Effects.....	83
D. Thermodynamic Aspects of the Thermal Degradation of Small Peptides	86

IV. Conclusion.....	90
References.....	91
 Chapter 5 Response Discrimination in K ⁺ -Adduct Formation	92
I. Introduction.....	92
II. Experimental Section	93
III. Binding Energies and Stabilities of K ⁺ -adducts	94
IV. Discrimination in the Formation of K ⁺ -adducts.....	96
A. Size Discrimination	97
B. Structure Discrimination	105
C. Discrimination Studied by Thermal Degradation of Tri- and Tetra-peptides: .	107
D. Discrimination Against Weak Binding:	
Experiments with Mixed Ionic Emitters.....	108
E. Summary (Discrimination in Interpretation of K ⁺ IDS Spectra).....	112
References.....	113
 Chapter 6 Collision-Induced Dissociation of Deprotonated Peptides	114
I. Introduction.....	114
II. Tandem Mass Spectrometry	116
A. Introduction.....	116
B. CID-B/E Linked Scans.....	117
III. Experimental Section	119
IV. Deprotonation of Peptides	124
A. Deprotonation in the Gas-phase or the Liquid-phase?.....	124
1. In Zwitterionic Form or in Neutral Form?	127
2. Thermodynamic Support for Gas-phase Deprotonation	128

B.	The Site of Deprotonation of Peptides.....	131
1.	Deprotonation at α -carbon Position?.....	133
2.	Deprotonation at Amides or at α -carbon?	134
3.	Why Is Deprotonation of Amides Favored over That of α -carbon?....	135
4.	Charge-localization: Evidence for Amide Deprotonation	137
5.	Final Comments on Site of Deprotonation	139
V.	Fragment Ions from CID-MS/MS Spectra of Deprotonated Peptides	139
A.	Nomenclature.....	139
B.	Common Fragment ions	141
C.	Ion Structure and Stability	142
VI.	Mechanisms for the Fragmentation of Deprotonated Peptides.....	146
A.	H-Shift: Mechanistic Study by Using Deuterated Peptides	147
B.	CID Fragments from Derivatized and Underivatized Peptides	148
VII.	Mechanisms: The Formation of Major Fragment Ions	151
A.	Ions from Amide-Deprotonated Peptides	151
B.	Ions from C-terminally Deprotonated Peptides.....	156
VIII.	Fragmentation of Charge-localized Peptides	160
A.	Charge-localization on Peptides.....	160
B.	Fragmentation of Deprotonated Peptides with Charge-localization	163
1.	Fragment Ions of C-terminally Charge-localized Peptides	164
2.	Fragment Ions of N-terminally Charge-localized Peptides.....	167
IX.	Sequencing with Negative Ion FAB-B/E Linked Scan.....	170
A.	Peptide Sequencing with CID-MS/MS of negative ions	170
B.	Why is Negative Mode not Favorable?.....	177
X.	Conclusions	184
	References.....	186

Appendices	188
-------------------------	------------

Appendix I. Local Pressure at the Sample Holder in the Ion Source	
and Collision frequency in K+IDS experiments.....	188

Appendix II. Enthalpies of Thermal Degradation of Peptides	
from Model Compounds.....	198

LIST OF FIGURES

Figure 2.1	a) Schematic of a dual-filament K^+ IDS probe;.....	14
	b) Schematic diagram of the K^+ IDS instrument.....	15
	c) Schematic of a K^+ IDS experiment in operation.....	16
Figure 2.2	K^+ IDS mass spectrum of a mixture of PEG200 and PPG725.....	18
	PEG = poly(ethylene glycol) $[H-(OCH_2CH_2)-OH]$;	
	PPG = Poly(propylene glycol) $\{H-[OCH(CH_3)CH_2]-OH\}$.	
Figure 2.3	Temperature dependence of thermal degradation vs. desorption.....	22
Figure 2.4	K^+ IDS spectra of H-YGGFM-NH ₂ :	
	a) with the original probe, $I = 2.70$ A;	
	b) with the new probe. $I(\text{sample}) = 2.0$ A,	
	direct heating delay = 3 seconds.....	28
Figure 3.1	1,2 - Elimination mechanism for the CO-NH bond cleavage of peptides..	33
Figure 3.2	Nomenclature for peptide fragments and ions.....	36
Figure 3.3	K^+ IDS mass spectra of H-FGGF-OH.	
	a) Time dependence. b) Average spectrum.....	39
Figure 3.4	K^+ IDS mass spectra of H-VGVAPG-OH.....	41
Figure 3.5	K^+ IDS mass spectra of H-FLEEI-OH.....	44
Figure 3.6	K^+ IDS mass spectra of H-PFGK-OH.....	45
Figure 3.7	K^+ IDS mass spectra of H-RKEVY-OH.....	47
Figure 3.8	K^+ IDS mass spectra of: a) H-YGGFL-OH; b) H-YGGFLNH ₂	49

Figure 3.9	K ⁺ IDS mass spectra of: a) H-GGFL-OH; b) H-GGFLNH ₂	50
Figure 3.10	K ⁺ IDS mass spectrum of Ac-VGVAPG-OH.....	52
Figure 3.11	K ⁺ IDS spectra of: a) CBZ-GPGGPA-OH; b) CBZ-GPFPL-OH;.....	53
	a) CBZ-GPGGPA-OH; c) t-BOC-PPPP-OH.....	54
Figure 3.12	K ⁺ IDS mass spectra of:	
	a) H-YGGFL-OCH ₃ ; b) H-VGVAPG-OCH ₃	56
Figure 3.13	K ⁺ IDS mass spectra of: a) H-VGGFL-OH; b) H-GGVFL-OH.....	57
Figure 3.14	K ⁺ IDS mass spectra of:	
	a) H-AGGFL-OH; b) H-(β-A)GGFL-OH.....	58
	a) H-AGGFL-OH; c) H-AG(Sar)FL-OH.....	59
Figure 3.15	K ⁺ IDS spectrum of a 22-mer peptide melittin (MW 2846.7). The sequence of the peptide is H-GIGAVLKVLTTTGLPALISWIKRKRQQ-NH ₂	64
Figure 4.1	Schematic diagram of 1,2 - elimination mechanism.....	69
Figure 4.2	K ⁺ IDS spectrum of:	
	a) H-GP-OH that had been exposed to D ₂ O;	
	b) H-FM-OH that had been exposed to D ₂ O.....	71
Figure 4.3	K ⁺ IDS spectra of variants of H-VGVAPG-OH.	
	a) unlabeled; b) peptide after exposure to D ₂ O.....	75
Figure 4.4	K ⁺ IDS spectra of α-incorporated peptides.	
	a) H-VGVA ^α dPG-OH; b) H-V ^β dGV ^β dAPG-OH.....	76
Figure 4.5	K ⁺ IDS spectrum of CH ₃ CO-VGVAPG-OH.....	79
Figure 4.6	Thermal degradation of peptides.....	80
Figure 4.7	K ⁺ IDS spectra of a) H-AGGFL-OH and b) H-(β-A)GGFL-OH.....	82
Figure 4.8	K ⁺ IDS spectra of a) H-YGGFL-OH and b) H-VGGFL-OH.....	84
Figure 4.9	K ⁺ IDS spectrum of H-GGVFL-OH.....	85
Figure 4.10	Thermal degradation pathways of peptides.....	87

Figure 5.1	Relative responses of five amino acids (a mixture of alanine, valine, leucine, threonine and phenylalanine) in K^+ IDS.	98
Figure 5.2	Relative responses of alanine and phenylalanine in K^+ IDS.	99
Figure 5.3	Relative responses of alanine and glycine in K^+ IDS.	100
Figure 5.4	Relative responses of alanine, H-AA-OH and H-AAA-OH at m/z 128, 199 and 270.	102
Figure 5.5	Relative responses of H-GGGG-OH and -H-AAA-OH in K^+ IDS.	104
Figure 5.6	Mass chronograms showing the relative responses for molecules H-GP-OH and cyclo-GP in the K^+ IDS experiments.	106
Figure 5.7	Relative responses of K^+ and Na^+ to a peptide <i>H-VGGFL-OH</i> and its degradation products.	110
Figure 5.8	Relative responses of K^+ and Cs^+ to a peptide <i>H-VGGFL-OH</i> and its degradation products.	111
Figure 6.1	The CID linked scan spectra for H-VGGFL-OH with precursors set at: a) m/z 490.2, (M-H) $^-$; b) m/z 489.2. a) m/z 490.2, (M-H) $^-$; c) m/z 491.2.	120 121
Figure 6.2	Deprotonation of peptides in glycerol matrix with FAB.	125
Figure 6.3	CID-B/E linked scan spectrum of deprotonated peptides (derivatives): a) H-VGGFL-AMSA; b) H-VGGFL-ABSA.	129
Figure 6.4	Kinetic reasoning for favored deprotonation at amides over that of α -carbon positions.	136
Figure 6.5	CID-B/E linked scan spectrum of deprotonated peptide SBA-VGGFL-OH.	138
Figure 6.6	a) Roepstorff nomenclature for peptide fragments; b) Common fragment ions from deprotonated peptides.	140

Figure 6.7	CID-B/E linked scan spectra of deprotonated peptides:	
	a) H-VGVAPG-OH; b) H-VGVA ^{αd} PG-OH;	143
	a) H-VGVAPG-OH; c) H-V ^{αd} GV ^{αd} APG-OH.....	144
Figure 6.8	CID-B/E linked scan spectra of deprotonated peptides:	
	a) H-VGGFL-OCH ₃ ; b) Ac-VGGFL-OCH ₃	150
Figure 6.9	The formation of Y _{n-1} and C _{n-1} ions via 1,3-elimination mechanisms:	
	a) charge-induced fragmentation; b) charge-remote fragmentation.....	152
Figure 6.10	The formation of Y _n and C _n ions via 1,3-elimination mechanisms (charge-induced fragmentation).....	153
Figure 6.11	C _n and Y _n ions from displacement reactions.....	154
Figure 6.12	CID-B/E linked scan spectrum of deprotonated peptides:	
	a) H-YGGFL-OH; b)H-YGGFL-NH ₂	157
Figure 6.13	The formation of C ions from C-terminally deprotonated peptide amides. (H-YGGFL-NH ₂ as an example).	158
Figure 6.14	The formation of C _n ions via a 1,4-elimination mechanism.....	159
Figure 6.15	The formation of Y ions from charge-remote processes such as E _{1,6} reactions shown here.....	161
Figure 6.16	CID-B/E linked scan spectrum of a deprotonated peptide H-VHLTEVEK-OH.....	173
Figure 6.17	CID-B/E linked scan spectrum of a deprotonated peptide H-RPPGFSPF-OH.....	174
Figure 6.18	CID-B/E linked scan spectra of deprotonated peptides:	
	a) H-FLEEI-OH; b) H-RKDVY-OH.....	176
Figure 6.19	CID-B/E linked scan spectrum of a deprotonated peptide H-WAGGDASGE-OH.	178
Figure 6.20	CID-B/E linked scan spectrum of a deprotonated peptide H-RVYIHPF-OH.....	179

LIST OF TABLES

Table 5.1	Binding energies and dipole moments of various molecules.	94
Table 5.2	Relative responses factors, R_{rel}, for amino acids and small peptides.....	101
Table 6.1	Negative ion FAB responses of a peptide and its derivatives.	126
Table 6.2	Gas-phase acidities of various functionalities in peptides.....	132
Table 6.3	Relative intensities of (M-1)⁻ and (M-2)⁻ ions for (deuterated) peptides..	133
Table 6.4	Relative intensities of (M-1)⁻ and (M-2)⁻ ions for (deuterated) peptide esters.....	135
Table 6.5	Fragment ions from peptides and their deuterated analogs.	147

Chapter 1

Introduction and Research Objectives

I. Introduction - Peptide Sequencing: Historical Review

The utility of mass spectrometry for peptide sequencing, the elucidation of the primary structure of peptides (amino acid sequence), was established in the late 1950s [1]. For many years in the following two decades, this sophisticated technique was demonstrated only in a few highly skilled laboratories, and limited to the analysis of very small peptides. When fast atom bombardment, FAB [2], was introduced in 1981, explosive growth in new methods and applications began, because the requirements for sample volatility were eliminated. Advances in high mass-range instrument development, especially those made the late 1980s, as well as the evolution of electrospray [3] and matrix-assisted laser desorption/ionization (MALDI) [4], made mass spectrometry applicable to an ever-increasing number of peptides.

With traditional techniques for peptide sequencing, analysis involves sequential degradation of the molecule from one end or the other, removing and identifying the amino acids one at a time. Compared with techniques such as the Edman degradation method [5], sequencing with mass spectrometry has many potential advantages such as high sensitivity and high speed. In addition, mass spectrometry can solve many problems that defy Edman degradation. For example, N-terminally blocked peptides can be sequenced with mass spectrometry; post-translational modification of protein/peptides can be identified with mass spectrometry; and peptide mixtures can be analyzed by mass spectrometry.

Furthermore, mass spectrometry can provide precise, accurate confirmation on the molecular mass of proteins derived from recombinant techniques in molecular biology.

Sequencing a peptide by the recording of a single mass spectrum is a very attractive proposition which has stimulated considerable research [6]. In fact, as an aid to microsequencing (automated Edman Degradation), mass spectrometry can improve both the efficiency and the accuracy of the operation. One of the greatest contributions of mass spectrometry to protein structure determination has been the ability to obtain precise, accurate molecular weights of peptides.

Over the last two decades mass spectrometry has advanced to the point where it has become one of the most broadly applicable tools in analytical chemistry. The rapid pace of this evolution has been spurred by periodic advances in mass spectrometer hardware, computer interfacing, new extended mass spectrometric methods (e.g., tandem mass spectrometry), interfacing with separation science methods, mass range extension into the millions of Daltons, and an increasing performance/cost ratio.

In mass spectrometry, the ion formation/ionization process is the starting point for mass spectrometric analysis. The ionization method used dictates the scope and utility of the methods in peptide sequencing analysis. The development of various ionization techniques over the years virtually reflected the advance of mass spectrometry techniques.

The most common ionization technique in mass spectrometry is electron impact (EI), which is well characterized and understood [7]. This technique has been traditionally used for the analysis of volatile species or those that can be easily derivatized to some volatile species. For this reason, the earliest and, for many years, the only way to obtain the mass spectra of peptides was by making volatile derivatives of small peptides. Two principal derivatives are often made: polyamino alcohols [8] and N-acetyl-N,O,S-permethylated peptides [9].

In recent years, desorption/ionization (DI) techniques have become increasingly popular for analyzing nonvolatile, thermally labile molecules such as peptides. Making

volatile derivatives is undesirable because the process is time consuming, leads to unwanted products, and usually requires large amounts of sample. Furthermore, there is a mass limit above which not even derivatized peptides are sufficiently volatile. The variety of available DI techniques, each of which has its particular advantages for certain applications, generally eliminates the need for derivatization reactions and opens the door to direct analysis of even higher mass compounds.

The DI techniques developed in the 1960s and 1970s include field desorption (FD) [10] plasma desorption (PD) [11], direct chemical ionization (DCI) [12], laser desorption (LD) [13] and secondary ion mass spectrometry (SIMS) [14]. The development of these techniques gradually demonstrated that mass spectrometry can be used for the determination of large, thermally labile biopolymers such as proteins. However, each of these techniques at that time presented at least one of the following problems such as signal stability, durability, reproducibility, and difficulty in operation.

Fast atom bombardment (FAB), developed in 1981 by Barber et al. [2] provides for the first time a technique for ionizing nonvolatile samples that is both simple to use and gives reproducible results. It has become the dominant ionization technique used for peptide sequence determination. FAB mass spectra of peptides show MH^+ , the protonated molecules, as the predominant ions at the high-mass end of the spectrum, which could be used as the precursor ion in MS/MS analysis. Although the FAB-MS spectrum usually displays some sequence ions, they are usually very weak and difficult to be isolated from matrix peaks. In addition, the mass range of FAB ionization is limited to 3000 Da (frequently lower than this) for peptides. Techniques with greater mass range need to be developed.

In the late 1980s, the evolution of ionization techniques such as electrospray (ES) [3] and MALDI [4] greatly extended the mass range. Compounds with mass up to millions of Daltons have been determined [15]. Most importantly, the electrospray technique also

provides a simple and successful way in coupling separation techniques such as electrophoresis and liquid-chromatography to mass spectrometry.

It should be pointed out that single stage mass spectrometry usually provides only molecular weight information, frequently from the mass of the most abundant pseudo-molecular ions such as protonated peptides (MH^+). These ions, formed by commonly used ionization techniques such as FAB or electrospray, have very little tendency to fragment.

The lack of fragmentation is very useful for the accurate determination of molecular weights of peptides, even in quite complex mixtures, but the resulting absence of structural information is a definite drawback. This problem can be overcome by transferring additional energy sufficient to force fragmentation of the stable MH^+ ions formed in the initial ionization process. Collision with a neutral gas is the most frequently used method leading to collision-induced dissociation (CID) [16]. The resulting fragment ions are then mass analyzed in a second stage of mass spectrometry, hence the term tandem mass spectrometry (MS/MS). Frequently, the necessary energy can be acquired by multiple collisions at low energy (eV) or single collisions at high energy (keV).

Tandem mass spectrometry has many advantages over conventional mass spectrometry. First, it increases the fragmentation of protonated peptides by CID. Therefore, more structural information can be obtained from a CID spectrum of a peptide. Secondly, it eliminates peaks that originate from matrix and impurities. Therefore it is capable of mixture analysis without pre-separation. Thirdly, all ions thus produced are structurally-related to the precursor ions MH^+ . In addition, tandem mass spectrometry is capable of differentiating isomeric and isobaric amino acids in peptides in high energy CID experiments [17-18].

When CID is performed for MS/MS experiments, collisions can be carried out at different energies. For low-energy collisions, such as those occurring in a triple quadrupole instrument, the collision energy is usually below 100 eV. With peptides,

cleavage of amide bonds is most frequently observed. With high-energy collisions, such as those occurring in sector instruments, the collision energy is usually in the range of 1 to 10 keV. This high-energy collision generates more fragments than it does in low-energy collisions. Side-chain specific fragments - different for different amino acids, are observed. For peptide sequencing, these fragment ions are extremely important [17-18] in distinguishing isomeric leucine and isoleucine. However, these ions are usually not observed in the low-energy CID spectra.

When precursor ions of a peptide are subjected to collision-induced dissociation, fragment ions indicative of the peptide structure are formed subsequently. Frequently, the dominant ions and ion series observed are dependent on the amino-acid composition (such as number of basic amino acids and their positions along the peptide chain) of the peptides and amino-acid sequence of the peptide. To date, the formation of many ion series have been proposed - some of them have been experimentally supported. However, questions like the following are still to be answered: Why does one specific ion series dominate over another in a CID spectrum of a peptide? For a regular peptide CID-MS/MS spectrum, what ions are produced by charge-induced processes? What ions are from charge-remote processes? Which ion series will dominate a spectrum? Why? A better understanding about the formation of various fragment ions can certainly speed up interpretation of mass spectra thus peptide sequencing.

In the study of CID fragmentation mechanisms of protonated peptides, various methods have been utilized. When a hydrogen shift is involved in the formation of a specific ion series, deuterated peptides were used frequently to trace the source of the shifting hydrogen atom. Frequently, the CID spectra of partially deuterated peptides (such as those via H/D exchange in a deuterated solvent), α -carbon deuterated peptides are used. In tracing the formation of secondary ions derived from specific side-chain cleavages of regular sequence ions, precursor scans (B^2/E linked scan) are frequently used to trace

possible precursors of a fragment ion. Product scans (B/E linked scan) are then performed to confirm the products from that possible precursor ion.

To date, mass spectrometry has become one of the most important tools in protein chemistry. Examples are the determination of molecular weight, molecular weight confirmation, identification of post-translational modification, sequencing of N-blocked peptides. In this dissertation, the research will be focused on fragmentation of peptides in both neutral and charged (negatively charged form). An example of application of mass spectrometry for peptide analysis will also be discussed.

II. Research Objectives

In this dissertation, two processes pertinent to peptides will be characterized. The first one is the primary thermal degradation chemistry of peptides, studied by using K^+IDS . This study will provide a detailed description of thermal degradation of peptides, based on experiments with peptides and their chemically modified variants such as derivatized peptides, deuterated peptides and specifically designed peptides. Since thermal degradation is a charge-free process, the results from this study may provide insight into charge-remote processes in CID of protonated peptides, as will be explained in more detail in Chapter 4. The second process is metastable and CID fragmentation of deprotonated peptides. This process is too complicated to draw much attention until recently, but still only di- and tri- peptides have been studied so far. Preliminary study with larger peptides in this research will add much more to our understanding on metastable fragmentation and CID of deprotonated peptides. At the end of this dissertation, one sample application of mass spectrometry to peptide analysis will be presented.

A. Thermal degradation of Peptides:

In this research, the primary thermal degradation chemistry of peptides will be characterized by using a mass spectrometric ionization technique, K^+ - Ionization of Desorbed Species (K^+IDS). This technique, based on thermionic emission of K^+ ions and subsequent K^+ attachment to thermally desorbed neutral analyte molecules and their thermal degradation products, was introduced in 1984 from this laboratory [19]. The strength of the K^+IDS technique is in the simplicity of both the experiment and the resulting mass spectra. Since each thermal degradation product gives one peak in the mass spectrum, K^+IDS mass spectra reflect a "molecular weight distribution" of the thermal degradation products of the analyte molecules, which, in combination with analogous studies of derivatized and isotope-labeled compounds, can be used for the study of unimolecular, condensed phase thermal degradation chemistry. However, the simplicity of the mass spectra is also a complication since *only* the molecular weight of each degradation product is directly determined. The approaches presented here are designed to provide insights into the structures of the thermal degradation products, and to demonstrate a unique and simple tool for characterizing thermal degradation processes for biomolecules, as well as other thermally-labile compounds.

There is a number of reasons why the thermal degradation chemistry of peptides is of current interest. First, thermal degradation of peptides is a process of rich chemistry itself. Traditional techniques such as Pyrolysis-Gas Chromatography (Py-GC) are very difficult to apply to the study of such processes because the degradation products (pyrolytes) are either too small to provide much useful structure information, too large to survive GC conditions (undergo further reaction, for example), or too polar to be analyzed by GC (not volatile enough, for instance). In fact, detailed study on pyrolysis has been extended only to dipeptides to date. Not much information has been obtained for larger peptides [20-21]. K^+IDS provides a unique way to circumvent this problem and make it possible to study the thermal degradation of peptides.

A second reason for the interest in thermal degradation is a process in mass spectrometry (MS) called charge-remote chemistry. When MS is used for structural analysis of peptides, the analyte molecules undergo desorption and ionization via techniques such as fast atom bombardment (FAB). When a peptide, M, is converted into a gas phase cation in the FAB ion source, it appears as a protonated molecule, MH^+ , which subsequently fragments (or is induced to fragment), giving structural information. There are two types of processes through which protonated peptides can fragment. The first is that most commonly considered in mass spectrometry for even-electron ions - the chemistry occurs at the site of protonation, and is charge-initiated. A second possibility is a charge-remote [22-24] mechanism. In the latter, bonds are broken far from the charge site, and are unaffected by the charge. They are driven by excess energy in the protonated molecule (as are charge-initiated processes). It is very difficult to distinguish between these two mechanisms, because, while the precursor to all fragment ions is the protonated peptide molecule in positive ion FAB, the initial site of protonation is not known and cannot be controlled. The advantage of the K^+IDS technique is that the molecules undergo fragmentation (thermal degradation) before a charge is placed on the molecule. Thus, for mass spectrometrists it may represent a model for charge-remote chemistry. Molecular fragmentation occurs due to energy deposition in the unionized molecule. It is hoped that the chemistry of bond cleavage in peptides will be sufficiently different for these two cases, charge-initiated and charge-free, such that the contributions from each in the fragmentation of protonated peptides can be deduced.

Thirdly, there have been a number of experimentally simple, "direct probe" approaches for the MS analysis of compounds such as small peptides. In such experiments, solid samples are introduced into an electron impact (EI) or chemical ionization (CI) source, and heated. Mass spectra are generated, which are either simple mass spectra of desorbed molecules, or complex spectra, resulting from the simultaneous ionization of desorbed molecules and desorbed thermal degradation products [25-26]. The

results of K^+ IDS experiments may provide direct information on such processes, to assist in the evaluation of the results of such experiments.

Finally, the average energy obtained by analyte molecules from K^+ IDS is about the same as that from FAB experiment. For a peptide of 500 Da (approximately 70 atoms, $3N-6 = 400$ degrees of freedom), assuming 50% of the atoms reach the temperature of 600K (experimental condition) with starting temperature at 300K ($\Delta T = 600-300 = 300K$), the energy gain of the peptide will be roughly about $50\% \times 400 \times R\Delta T/2 = .5 \times 400 \times 8.3 \times 300/2$ J = 240 kJ/mole = 60 kcal/mole = 3eV, very close to the average energy deposited in a high-energy collision process [27]. Therefore, K^+ IDS spectra may be compared with FAB spectra under certain circumstances.

B. Fragmentation of Deprotonated Peptides

The second topic in this dissertation is an investigation of fragmentation of deprotonated peptides induced by collision-induced dissociation. A mechanistic study was carried out on peptides larger than three amino-acid residues. In this study, extensive derivatization was performed to vary the site of deprotonation, and the effect of charge site on fragmentation was evaluated for deprotonated peptides. Deuterated peptides were used to trace the hydrogen shifts. Based on these experiments, mechanisms for the formation of the most commonly occurring ions from deprotonated peptides are proposed. Results from this study may provide valuable insight into CID of protonated peptides.

In mass spectrometry, the effect of charge site for even-electron ions such as protonated molecules and deprotonated molecules on fragmentation may be very similar. Therefore, fragmentation of charge-localized peptides in negative mode may produce the same fragments as those from charge-localized positive ions. Comparison of spectra obtained from different charge states (positive, neutral and negative mode) may provide important insights into ion fragmentation processes.

In Chapter 2, the K⁺IDS technique will be introduced in detail and further characterization and refinement of the technique will be described. In Chapter 3, application of K⁺IDS for the analysis of peptides will be studied. The applicability of this technique for peptide sequencing will be discussed. In Chapter 4, the primary thermal degradation of peptides will be studied by using K⁺IDS. Mechanisms for thermal degradation of peptides will be proposed and experimentally supported. In Chapter 5, a previously un-revealed phenomenon - response discrimination, will be described and the results will be used to interpret K⁺IDS spectra. In Chapter 6, fragmentation of deprotonated peptides will be discussed.

References

1. Biemann, K.; Gapp, F.; Seibl, J. *J. Am. Chem. Soc.* **1959**, 81, 2274.
2. Barber, M.; Bordoli, R. S.; Sedwick R. D.; Tyler, A. N. *J. Chem. Soc. Commun.* **1981**, 325.
3. Fenn, J. B.; Mann, M.; Meng, C. K.; Wong, S. F.; Whitehouse, C. M. *Science* **1989**, 246, 64.
4. Karas, M.; Hillenkamp, F. *Anal. Chem.* **1988**, 60, 2299.
5. Edman, P. *Acta Chem. Scand.* **1950**, 4, 238.
6. Biemann, K.; Martin, S. A. *Mass Spectrom. Rev.* **1987**, 6, 1-76.
7. McLafferty, F. W. *Interpretation of Mass Spectra*, 3rd Ed., University Science Books: Mill Valley, CA, **1980**.
8. Biemann K.; Vetter, W. *Biochem. Biophys. Res. Commun.* **1960**, 3, 578-584.
9. Vilkas, E. Lederer, E. *Tetrahedron Lett.* **1968**, 3089.
10. Beckey, H. D. , *Int. J. Mass Spectrom. Ion Phys.*, **1969**, 2, 500.

11. Torgenson, D. F.; Showronski R. P.; Macfarlane, R. D. *Biochem. Biophys. Res. Commun.*, **1974**, 60, 616.
12. Baldwin, M. A.; McLafferty, F. W. *Org. Mass Spectrom.* **1973**, 7, 1353.
13. Posthumas, P. G.; Kinstemaker, P. G.; Meuzelaar, H. L. C.; Ten Noever de Brauw, *Anal. Chem.* **1978**, 50, 985.
14. Benninghoven, A. *Int. J. Mass Spectrom. Ion Phys.* **1983**, 46, 459.
15. Chen, R.; Mitchell, D. W.; Chen X.; Wu, Q.; Hofstadlere, S. A.; Bruce, J. E.; Smith, R. D. *The 42nd ASMS Conference on Mass Spectrometry and Allied Topics*, Chicago, (1994), MP203.
16. McLafferty, F. W., Ed., *Tandem Mass Spectrometry*; Wiley: New York, **1983**.
17. Johnson, R. S.; Martin, S. A.; Biemann K.; Stults, J. T.; Watson, J. T. *Anal. Chem.* **1987**, 59, 2621
18. Johnson, R. S.; Martin, S. A.; Biemann K. *Int. J. Mass Spectrom. Ion Processes* **1988**, 86, 137.
19. Bombick D.; Pinkston, J. D.; Allison J. *Anal. Chem.* **1984**, 56, 396-402.
20. Irwin, W. J. *Analytical Pyrolysis: A Comprehensive Guide*; M. Dekker: New York, **1982**; pp 3-44.
21. Irwin, W. J.; Slack, J. A. *Analyst* **1978**, 103, 673-704.
22. Gierlich, H. H.; Rollgen, F. W.; Borchers, F.; Levsen, K. *Org. Mass Spectrom.* **1977**, 12, 541-543.
23. Jensen, N. J.; Tomer, K. B.; Gross, M. L. *J. Am. Chem. Soc.* **1985**, 107, 1863-1868.
24. Adams, J. *Mass Spectrom. Rev.* **1990**, 9, 141-186.
25. Svec, H. J.; Junk, G. A. *J. Am. Chem. Soc.* **1964**, 86, 2278-2282.
26. Biemann, K.; Seibl, J.; Gapp, F. *J. Am. Chem. Soc.* **1961**, 83, 3795-3804.
27. Wysocki, V. H.; Kentlamaa, H. I.; Cooks, R. G. *Int. J. Mass Spectrom. Ion Processes*, **1987**, 75, 189.

Chapter 2

K⁺IDS: The Technique and Its Further Characterization

I. Introduction

Mass spectrometry has been traditionally used for the analysis of volatile species and those that can be easily derivatized to volatile compounds. Before the evolution of fast atom bombardment (FAB), peptide analysis by mass spectrometry was hampered by the low volatility and thermal instability of peptides. That is, the volatility of a peptide can not be increased simply by heating, which leads to thermal degradation of the peptide. In the 1960s and 1970s, much effort in mass spectrometry research has been put into developing new ionization techniques to circumvent the problem. Various so-called desorption/ionization (D/I) techniques were developed, all based on a simple concept: Energy deposited on a sample surface in a very short time will induce desorption more effectively than thermal degradation.

In the search for better techniques at Michigan State University, K⁺-Ionization of Desorbed Species, K⁺IDS, a desorption/ionization technique, was introduced in 1984 by Bombick and Allison [1] from this laboratory. This technique is based on thermionic emission of K⁺ ions and subsequent K⁺ attachment to thermally desorbed neutral analyte molecules and their thermal degradation products. Since the introduction of the technique, K⁺IDS has been successfully used for the analysis of various compounds such as saccharides, polymers, peptides and steroids [2-6]. A detailed description on how this technique works will be presented below.

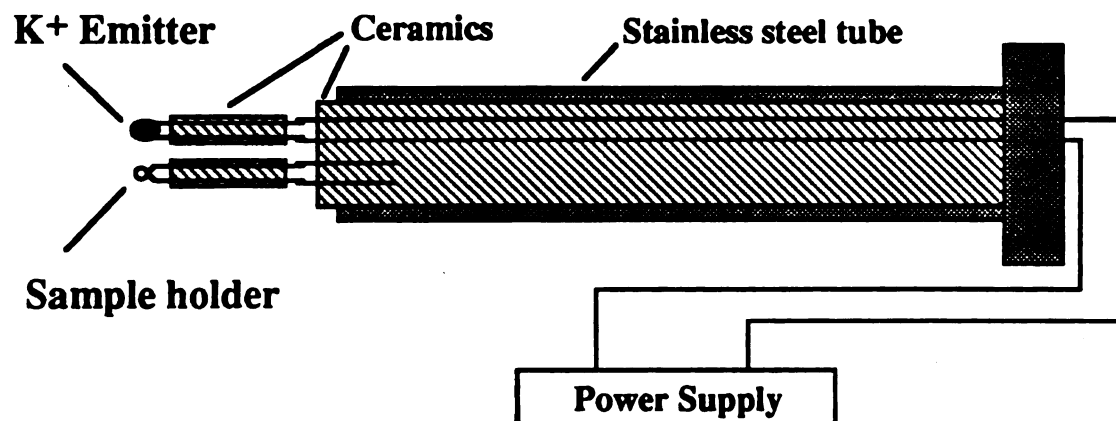
II. Experimental

A. Experiment setup and K⁺IDS probe

The K⁺IDS experiment is performed on an HP 5985 GC/MS/DS quadrupole mass spectrometer with a mass range of 10-1000 Da. A schematic of the ion source and K⁺IDS apparatus is shown in Figure 2.1. The key device for this K⁺IDS technique is the K⁺IDS probe (Figure 2.1a-c), a modified direct insertion probe. This probe is used to insert the K⁺ aluminosilicate bead, the K⁺ emitter, into the center of the ion source. The K⁺ bead filament is made by threading rhenium wire through a two-holed ceramic leaving a 1-2 mm loop at the top. The ends of the tip are spot-welded to nickel-wire leads that are fed through the K⁺IDS probe. The K⁺ bead is made by methods described in part B of this section [7]. Before use, the bead has to be conditioned inside the ion source of the mass spectrometer by slowly ramping the current applied to the bead (0-3.0 A, 0.5 A/min.). A low voltage power supply is used to provide to the K⁺ bead a bias voltage of 0-10 volts with respect to the repeller. K⁺IDS experiments are generally performed with a current of 2.2-3.0 A and a bias voltage of 0 V.

Because the K⁺IDS signals are usually too short-lived to allow for good calibration of the instrument with K⁺IDS adduct ions, the calibration of the instrument with perfluorotributylamine (PFTBA), especially the mass axis, is performed in the positive EI mode in the traditional way for GC/MS and/or DIP analyses. The voltages applied on all the lenses are adjusted for optimum EI results. After the source is cooled down, the EI filament is turned off for K⁺IDS. The K⁺ emission is monitored in the override tuning program and the bead position and direction are adjusted for optimum K⁺ transmission. Following this K⁺ bead position adjustment, the calibration was checked with K⁺IDS using palmitic acid [CH3(CH2)14COOH] as a benchmark compound to test the mass accuracy in Karen Light's experiments.

K⁺IDS Probe



K⁺ emitter: A solid (potassium aluminosilicate) emits K⁺ when heated.

made from a mixture of KNO₃: SiO₂: Al₂O₃ = 2: 2: 1 (molar ratio).

Figure 2.1a Schematic of a dual-filament K⁺IDS probe.

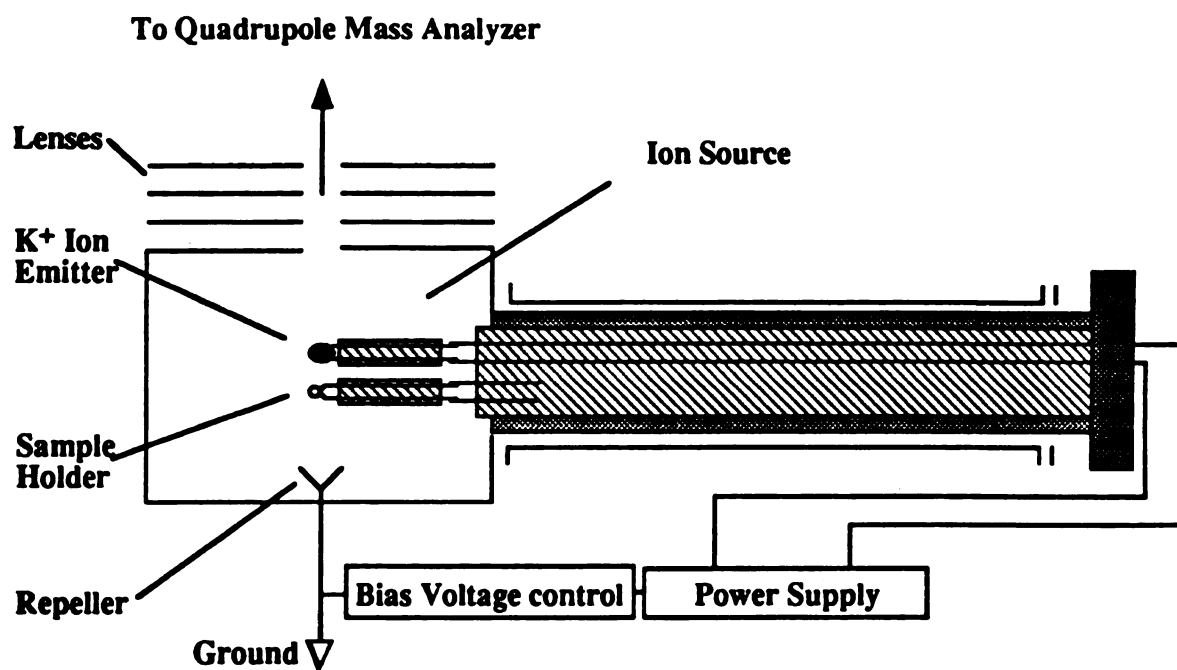
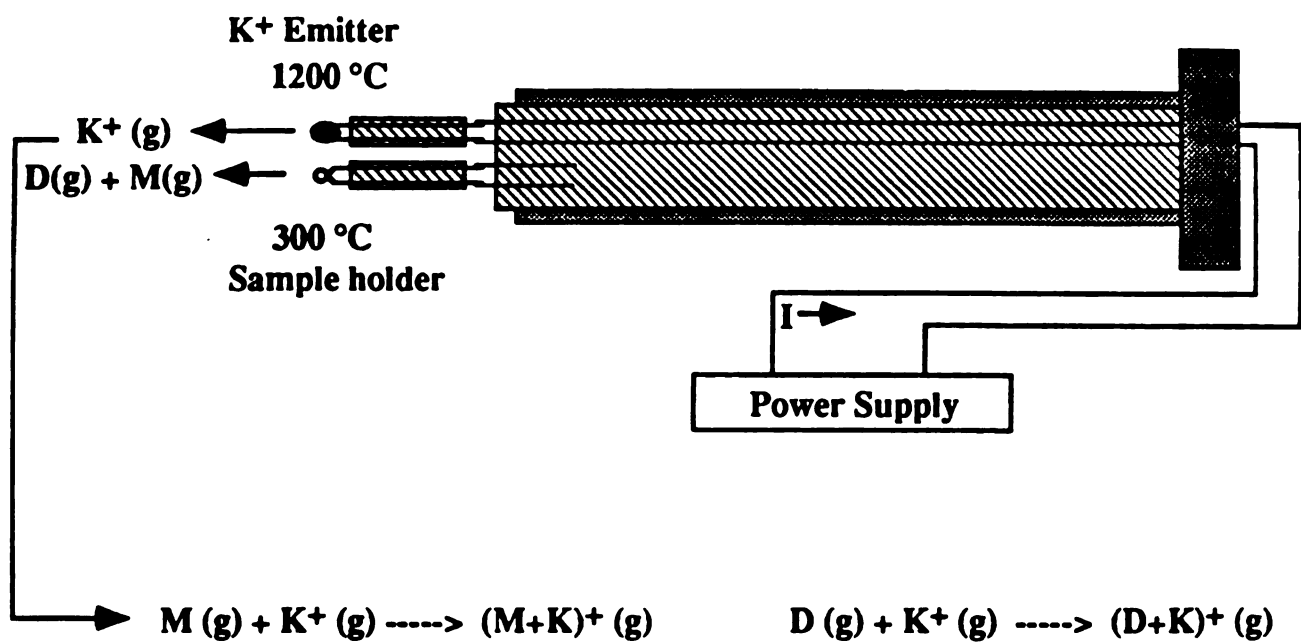


Figure 2.1b Schematic diagram of K⁺IDS instrumentation.



M: Intact analyte molecule.

D: Thermal degradation products of M.

Figure 2.1c Schematic of a K⁺IDS experiment in operation.

It has been noticed, in my experience with K^+IDS , that testing calibration with a single compound such as palmitic acid does not always give reliable results because calibration in other mass regions could be off even if the mass for the $(M+K)^+$ of palmitic acid is correct. To ensure better results, a mixture of polymers such as PEG 200 (polyethylene glycol, average molecular mass 200 Da) and PPG 725 (polypropylene glycol, average molecular mass 725) were used. Both the low-mass region and higher mass region were considered. The quality of the spectra of the mixture (Figure 2.2), both in mass accuracy and isotope distribution, was used to judge the quality of a mass calibration. In the spectrum, peaks at m/z 189, 233, 277, 321, 365 and 409 are $(M+K)^+$ ions of PEG200 with $n = 3, 4, 5, 6, 7$ and 8 , respectively; peaks at m/z 463, 521, 579, 637, 695, 753, 811, 869 and 927 are $(M+K)^+$ ions of PPG 725 with $n = 9, 10, 11, 12, 13, 14, 15, 16, 17$ and 18 respectively. Because these polymers are even-mass compounds and K^+ has an odd mass (39 Da), $(M+K)^+$ ions of these polymers should have odd m/z values. All peaks labeled with odd m/z values indicate a good calibration. Any peak labeled with even m/z value indicates a bad calibration.

All of the samples used in K^+IDS experiments were dissolved or suspended in methanol to allow transfer of 1-2 μl of sample (approximately 10 μg) onto the sample holder. The solvent was evaporated before the probe was inserted into the mass spectrometer.

B. The making of a thermionic emitter

The most difficult part in making a thermionic emitter is making a good glass mixture and attaching the glass on the rhenium wire. Traditionally, a mixture of KNO_3 , SiO_2 and Al_2O_3 , in a molar ratio of 2:2:1 is ground and a slurry in acetone is made. A small drop (Pasteur dropper) of slurry is applied onto the rhenium wire loop, to cover it evenly. The bead is heated on a Benson burner flame and the solvent is evaporated. The dried bead is heated in the flame carefully. Gases (NO_2 and O_2) are released and some

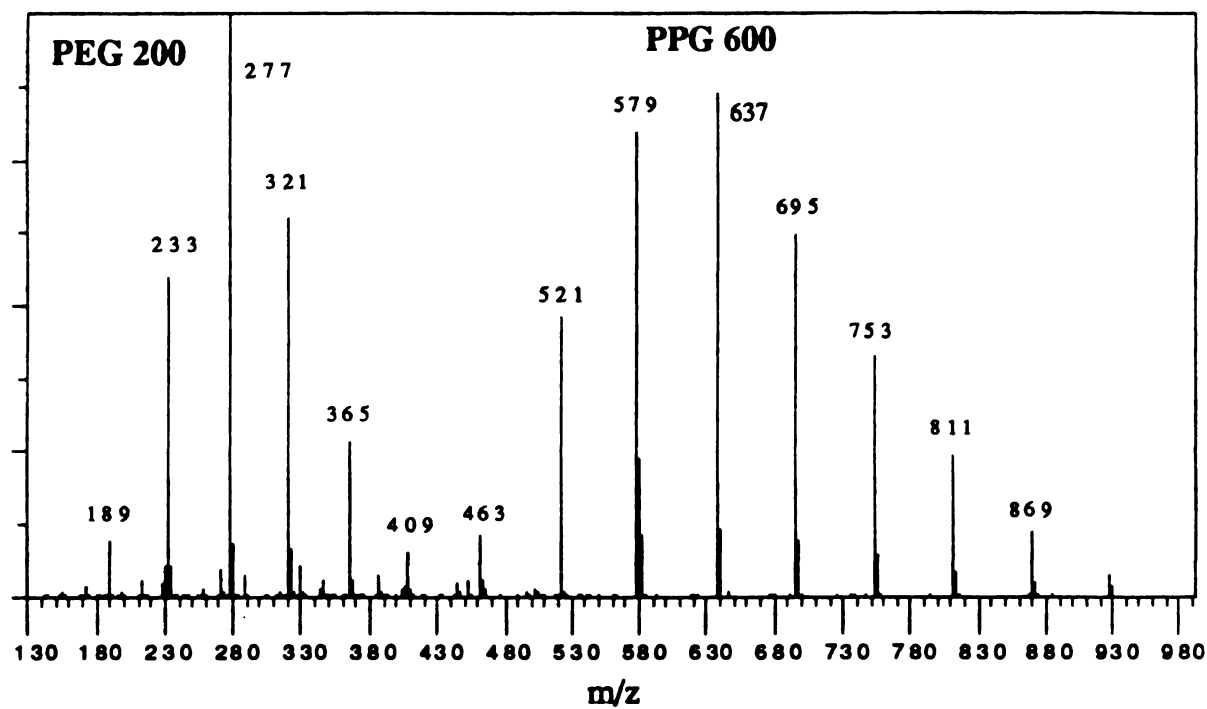


Figure 2.2 K^+ IDS mass spectrum of a mixture of PEG 200 & PPG 600.
 PEG = Poly(ethylene glycol) [$H-(OCH_2CH_2)_n-OH$].
 PPG = poly(propylene glycol) { $H-[OCH(CH_3)CH_2]_n-OH$ }.

binding between different particles develops. This bead is conditioned in the ion source by ramping the current from 0 to 3.0 A at 0.5 A/min. The probe is then cooled for use.

Although the recipe for making a glass mixture has not changed during the evolution of K^+ IDS technique, no one in this group has made a better glass mixture than that prepared by Daniel Bombick many years ago. The quality of the mixture determines the easiness for bead making and conditioning. With a bad glass mixture, it is very difficult to attach the mixture to the wire loop without pop-off after preliminary heating, or the bead does not survive the conditioning process. Because it is so difficult to make a good mixture this way, I tried a different way of making the glass mixture.

Since the glass was made from a mixture of KNO_3 , SiO_2 and Al_2O_3 , the result of heating is the formation of potassium aluminosilicate with the release of NO_2 and O_2 gases at the same time, especially during the conditioning processes. The preliminary heating removes the glass-carrying solvent such as acetone/methanol, and partly decomposes the KNO_3 to K_2O which reacts with the other two components to form an aluminosilicate which binds the mixture together. During the conditioning process, more aluminosilicates are formed and the beads become more homogeneous with the increase of temperature. Because of the zeolite structure of the aluminosilicate, in which large channels are formed, the bead is good for continuous K^+ emission when heated.

With this in consideration, ground molecular sieves with K^+ as the cation (K^+ aluminosilicate) were examined as the glass mixture because it contains potassium aluminosilicate. With the same process, a K^+ bead was made (adding a small amount of SiO_2 may prevent the bead from becoming too glassy which is bad for heat dissipation). It was found that ground molecular sieves with K^+ as the counter ions is a very good structural material for the K^+ IDS bead. There are several advantages for this new bead material: much shorter grinding time for molecular sieves than that for the traditional glass mixture, shorter conditioning time because no gas is released during conditioning,

higher success probability (less pop-off) because no gas is released during heating, and much shorter time is needed to make a quality bead.

III. K⁺IDS: Operational Principles

There are two basic processes that are important to the K⁺IDS technique. One is the use of a thermionic emitter to form gas-phase K⁺ ions that are used as reagent ions in a way similar to those used in chemical ionization. The other concept is the use of rapid heating of a thermally labile compound to promote vaporization of the sample with little thermal degradation. When these two processes are combined and occur simultaneously in the ion source of a mass spectrometer, a K⁺IDS spectrum can be obtained. The K⁺ ions attach to neutral gas-phase species and are observed as K⁺ adducts. This K⁺ attachment induces little or no fragmentation and it samples only the neutrals present in the gas phase produced by heating the sample.

A. Thermionic emission

The most important aspect of the K⁺IDS technique is the production of a large flux of K⁺ ions in the gas phase. This is accomplished by the use of thermionic emission materials that are patterned after the aluminosilicate mixtures described by Blewett and Jones [8] in 1936. They determined that the mixture of Al₂O₃, Li₂O and SiO₂ in a 1:1:2 ratio, was the best mixture for producing a large flux of Li⁺ ions. The same mixture doped with K₂O instead of Li₂O has proven to be a good source of K⁺ ions when the mixture is heated to temperatures between 800 °C and 1200 °C. The emission of K⁺ ions is dependent primarily on the work function of the surface and the ionization energy of

the potassium atom. Extensive discussion of how these materials are capable of emitting metal ions can be found in D. B. Bombick's dissertation [9].

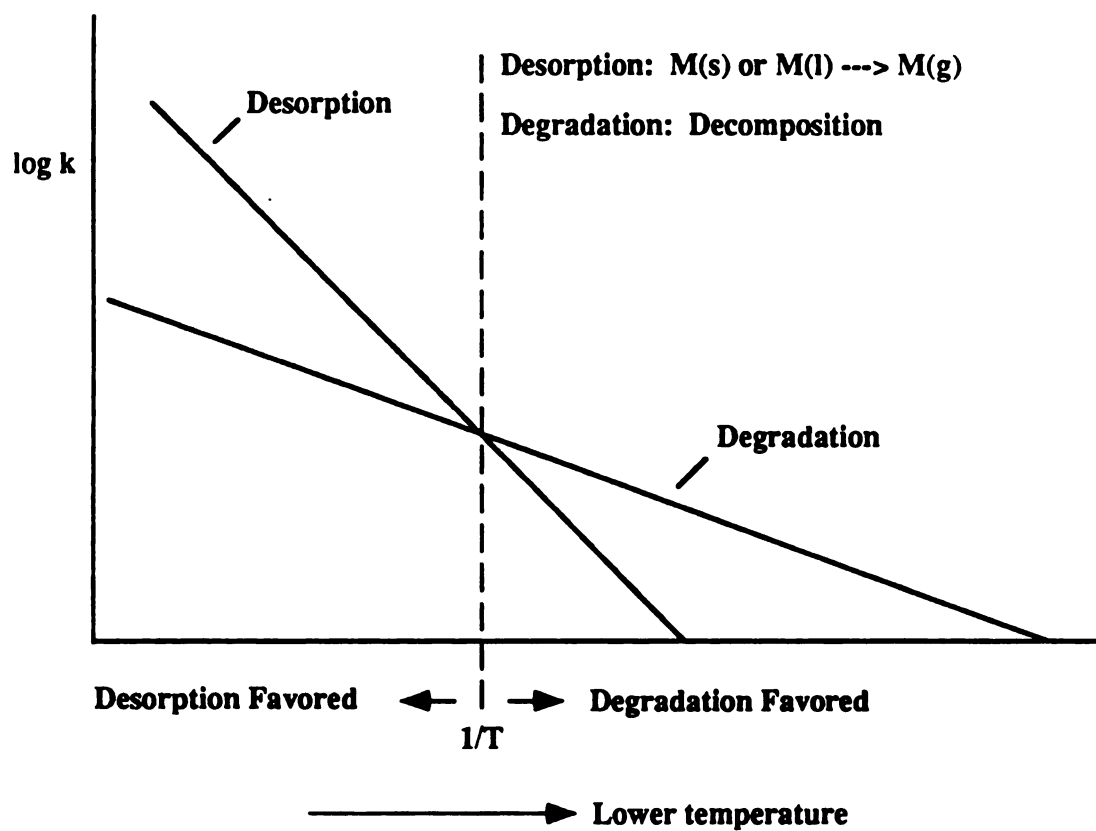
Because K^+ was used in K^+ IDS experiments to "sample" the neutral species in the gas phase, this technique was previously referred to as K^+ chemical ionization (K^+CI) [1] because the K^+ ions are simply used as reagent ions. Compared to the commonly used CI technique, this K^+CI was believed to be less dependent on the pressure of the systems.

It should be pointed out that the thermionic emitter (the K^+ bead) used in these experiments serves two purposes. First, it is used as the K^+ emitter, producing large fluxes of K^+ ions when heated. Second, it also serves to heat the analyte molecules on the sample holder radiatively, giving rise to thermal degradation and desorption. Because desorption and K^+ emission occurs simultaneously and in very close proximity (1 mm separation), K^+ attachment results.

B. Desorption vs. Degradation

The other process essential to the K^+ IDS technique is the transfer of the thermally labile compounds into the gas phase. The use of rapid heating to promote desorption of intact molecules over competitive decomposition reactions of thermally labile compounds was described by Friedman and coworkers [10] for the analysis of underivatized peptides. The enhancement of the volatility of a complex thermally-labile species due to rapid heating of the sample is based on a classical kinetic analysis of the competitive decomposition and vaporization processes.

In K^+ IDS experiments, with a compound such as glycylglycylglycine on the surface of the probe, a number of events occur as the temperature of the probe surface changes from room temperature to a final temperature of about 300 °C. If the surface is slowly heated, the compound will decompose and the more volatile decomposition products will vaporize. This is what occurs in pyrolysis-MS analysis [11]. However, on



R. J. Beuhler, E. Flanigan, L. J. Greene and L. Friedman, *J. Am. Chem. Soc.* 96, 3990 (1974)

Figure 2.3 Temperature Dependence of Desorption vs. Degradation

rapid heating, temperatures can be achieved above some critical temperature T_c , at which desorption rates are competitive with, or can exceed, decomposition rates. So it is possible to raise the temperature above this critical value before a substantial amount of the analyte is decomposed. This aspect of rapid heating, as shown in Figure 2.3, has been developed by Friedman [10]. In light of this, the evolution of neutrals in the gas phase above the emitter varies with time when the sample is heated. At an early stage of rapid heating, decomposition may dominate until T_c is reached. Then desorption of intact molecules may dominate the processes. Finally, long-lived species on the surface lead to further decomposition products. In K^+IDS experiments, these two processes are very competitive and important. One process provides structure information of analyte molecules and the other one provides molecular weight information.

As discussed above, there is a critical temperature for the desorption of any specific compound. However, this temperature for a given compound has never been determined. When K^+IDS experiments were performed in Bombick's work, the temperatures of both the thermal ionic emitter and the sample surface were the same since a single-filament probe was used. Due to the rapid heating and high temperature, both degradation and desorption occur. Therefore, intact molecules and their thermal degradation products are both detected.

When a two-filament probe was introduced by Daniel Kassel [5], the concept of rapid heating was challenged because the radiative heating utilized in the experiments was not expected to generate high heating rate and high final temperature. Karen Light realized the importance of these temperatures and experiments in the determination of these data were performed. It was found that, with a heating current of 3.0 A, the final temperature of the sample surface was around 300 °C (attained in 20 sec) and the heating rate was about 15 °C/sec. Nevertheless, spectra obtained from this probe were found to be very similar to those obtained from the single-filament probe.

Because the temperature dependence of thermal degradation and desorption are different, K^+ IDS spectra acquired at different times into the experiment have different degradation patterns and relative intensities. In K^+ IDS -MS, average spectra are frequently used. Therefore, K^+ IDS spectra provide information on both low temperature and higher temperature products, which are all related to the structure of the analyte molecules.

Since ions in a K^+ IDS spectrum are K^+ adducts of thermal degradation products, the interpretation of the spectrum must be based on the thermal degradation mechanism of the analyte. It was assumed that in such a short time in which thermal degradation could occur, only a few mechanisms may dominate. Of these, 1,2-eliminations were believed to be the most common [2]: thermal activation of a polar bond, accompanied by the shifting of a specific hydrogen, resulting in the formation of two stable molecules from one. This process usually requires little energy. My results, however, suggest that thermal decomposition with the formation of cyclic products could be a more important one, especially for peptides. In this case, H-shifts can be more reasonably attributed to the terminal hydrogens based on the experiments with deuterated peptides, which will be discussed in Chapter 4.

C. K^+ -Adduct Formation and Stabilization

It is believed that ions in K^+ IDS-MS are formed due to thermal degradation and desorption of neutral species followed by K^+ attachment to the gas-phase molecules. With the commonly used dual-filament probe, this is evidently true because the two filaments, K^+ emitter and sample holder, are spatially separated from each other (the original single-filament probe was not used for this dissertation work). Previous work with K^+CI [1], in addition to the results of ICR experiments [11] with K^+ adducts, suggest that K^+ rarely, if ever, induces fragmentation following attachment. Therefore, the peaks

in a K^+ IDS spectrum represent the statistical distribution of neutral thermal degradation products.

Because energy is released with adduct formation, adduct ions become excited once formed. Since little fragmentation was observed, adduct ions were believed to be stabilized somehow. In search for possible sources for such stabilization, Bombick found that the addition of a neutral collision gas into the ion source produced an increase in adduct formation for small analyte molecules. When N_2 was introduced into the ion source as a collision gas to a source pressure of approximately one torr, the detection limit for polyphenylether was lowered from 500 ng to 250 ng at a signal-to-noise ratio of five. This increase in adduct formation was used as the major evidence of adduct stabilization by a three-body collision process for nascent K^+ -adducts [9], a theory adopted by all of my predecessors.

However, this small decrease in detection limit by a large amount of collision gas demonstrated only a weak effect of collision-stabilization. For real K^+ IDS experiments, the pressure around the probe tip is calculated to be 10^{-3} torr under K^+ IDS condition, based on my calculations (see Appendix I for detailed calculations on ion source pressure and collision frequency). Such low pressure will not allow three-body collisions inside the ion source. Therefore, three-body collisions are not very likely to occur for nascent K^+ adducts.

In considering the stabilization of Li^+ adducts, Woodin and Beauchamp [12] proved that Li^+ attachment to an analyte molecule produced an excited complex that could be stabilized by the emission of an infrared photon. These biomolecular infrared radiative association reactions are assumed to be dominant stabilization mechanisms at very low pressures where the time between collisions is greater than 100 ms. This photo emission mechanism has gained popularity as a possible association mechanism for interstellar chemistry, but is unlikely to be responsible for the stabilization of the K^+

adduct ions formed in K^+IDS due to the short residence time inside the mass spectrometer.

As indicated above, K^+ adduct ions are excited with adduct formation. However, the energy release in adduct formation may not be large enough to induce any degradation, which may lead to K^+ detachment. In light of this, the nascent adducts may not be stabilized at all. Significant adduct ions may have dissociated back to K^+ ions before reaching the detector. The availability of the ions for detection is determined by the life times of the ions. If the adduct ion is not sufficiently stable, it cannot be detected. The response discrimination discussed in Chapter 5 - a previously undiscovered phenomenon in K^+IDS - may serve as an evidence that K^+ adducts formed in K^+IDS are not stabilized by collisions.

IV. MK^+ Stability Studies by Using a Directly Heated K^+IDS Probe

A. Characterization of a Novel Direct-Heating K^+IDS Probe

In order to make the K^+IDS probe more adjustable, a novel probe with direct-heating capability was designed and made based on the following consideration. (1) For the original two-filament probe in which samples on a sample holder are heated relatively slowly ($20\text{ }^\circ\text{C/sec}$), the heating rate varies from time to time, and from one probe to another due to the uncertainty in bead size, thickness, shape, composition, bead-sample separation, etc. So, whenever a different bead is made or after a bead is used for a while, the heating rate will change (2). The final temperature of the sample wire obtainable is only as low as $300\text{ }^\circ\text{C}$, and the heating rate is not so “rapid” as expected.

With the new probe, the sample holder can be powered to pass electric current. There are two advantages for this new probe (1). By adjusting the sample heating current, it is possible to adjust the desorption rate and thermal decomposition rate of the sample so both molecular weight and structural information can be obtained in a single

spectrum. This is especially true for highly thermally-labile compounds such as met-enkephalin, which produces only a weak molecular ion peak in a K^+ IDS spectrum (2). Very polar compounds can produce $(M+K)^+$ ions in K^+ IDS spectra when the sample is directly heated. Direct heating of the sample on the new probe can provide real “fast heating” rates which the normal probe cannot offer to desorb large molecules into the gas phase. In addition, this probe can also be operated as the original two-filament probe when the sample filament is not powered.

On the other hand, this probe also provides one problem. That is, the lifetime of a sample will become very short when direct heating is provided (much higher heating rate). With a quadrupole mass spectrometer, this may lead to a very skewed spectrum. Sometimes, no ions can be detected due to the short sample lifetimes.

Sample spectra of met-enkephalinamide (Figure 2.4) with two different probes were obtained. With the original probe the $(M+K)^+$ signal is weak. With the new probe the direct heating makes $[M+K]^+$ ions much more abundant. However, K^+ adducts of thermal degradation products from the direct heating probe is rare, thus structure information is lost. Because of this reason, K^+ IDS spectra of peptides in this dissertation were obtained by using the original two-filament probe.

B. MK^+ Stability Studied by Direct Heating

In previous K^+ IDS papers, it has been suggested that K^+ adducts formed are stabilized by collisions. No fragment ions will be generated from a K^+ adduct. For example, only $(M+K)^+$ ions are observed for many polymers. The rationale for this speculation is that nascent K^+ adduct ions can be collisionally stabilized in the ion source right after their formation by energy transfer in collision processes. It is assumed that the ion source pressure in a K^+ IDS experiment is so high that there are many collisions happening right after adduct formation so that the energy released during adduct formation will be transferred to other species, thus the K^+ -adducts are stabilized.

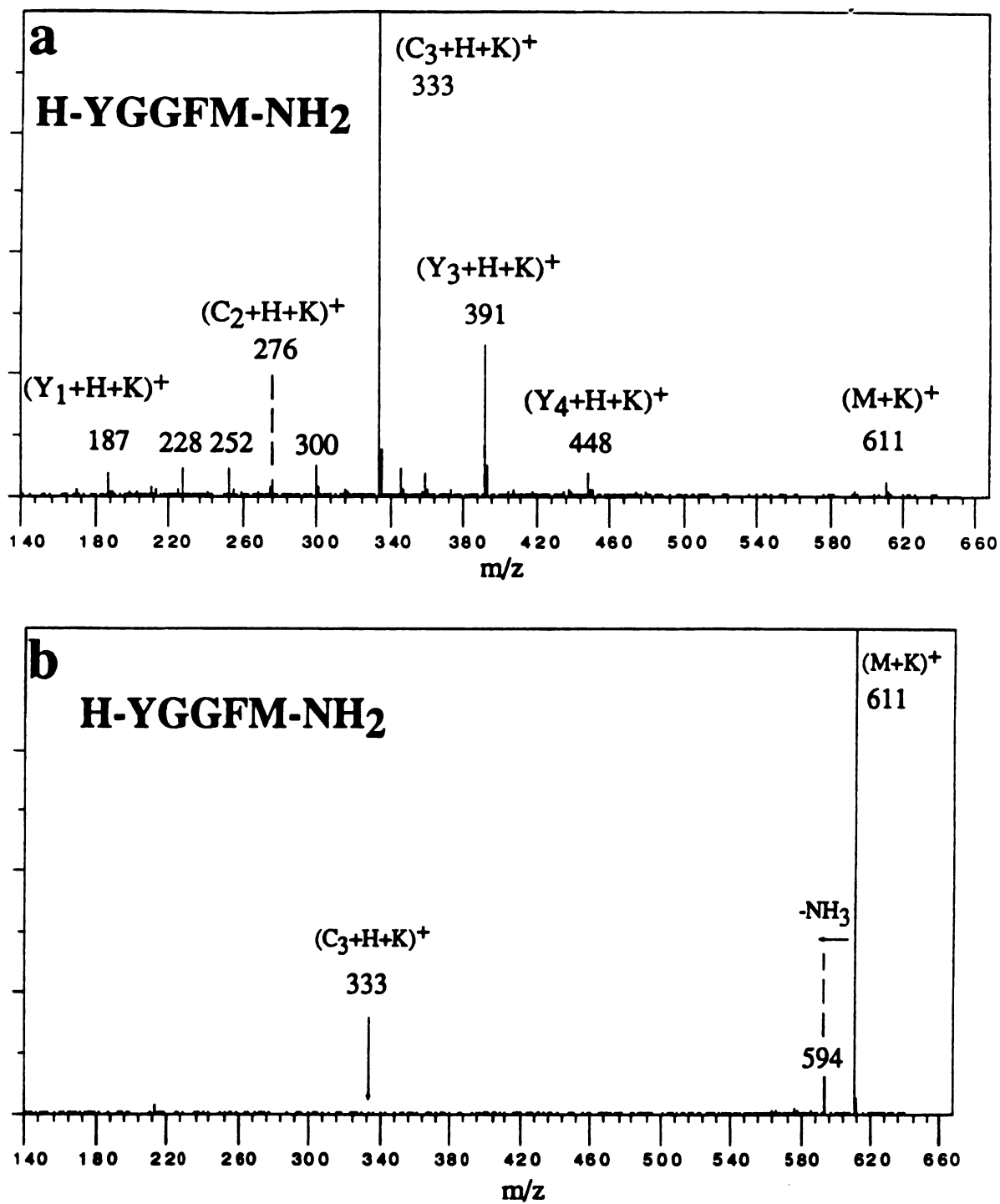


Figure 2.4 K^+ IDS spectra of H-YGGFM-NH₂: a) with the original probe, $I = 2.70$ A;
 b) with the new probe. $I(\text{sample}) = 2.0$ A, direct heating delay = 3 seconds.

The collision-stabilization theory can be very important if the assumption of high pressure in the ion source is correct. However, calculations on the source pressure show that the pressure, generated in a K^+IDS ion source with a typical run, falls in about 0.06 Pascal (10^{-3} to 10^{-4} torr), which leads to a conclusion that 90% of K^+ ions produced will not undergo collision even once (see Appendix I). Consequently, an adduct ion formed will have much less probability colliding with a neutral species.

Since collision stabilization theory is not very convincing, it is probable that no stabilization occurs after adduct formation. This is consistent with the observation of response discrimination that will be discussed in Chapter 5. Discrimination was found against small and cyclic compounds. The discrimination is a reflection of the stability difference of different adduct ions. In addition, the results from the study with mixed ionic emitters in Chapter 5 also confirm that there is significant K^+ detachment following adduct formation. Therefore, K^+ adducts are not stable due to K^+ detachment (short lifetimes). However, the lifetimes for such adducts cannot be estimated at the present time with confidence.

The stability of K^+ adducts should also be examined from the standpoint of fragmentation of K^+ adducts. This process is believed unlikely because the energy released during adduct formation is too small to induce such processes. The following experiments with direct heating will provide insights into the stability of K^+ adducts.

To study possible fragmentation of K^+ adducts (or stability of K^+ adducts), the relative abundance of $(M+K)^+$ and that of a possible fragment $(F+K)^+$ are monitored with a direct heating K^+IDS probe because a large abundance of $(M+K)^+$ can be produced for study. To circumvent the problem of short sample lifetime, the selected ion monitoring (SIM) mode is used in these experiments - multiple ions are monitored alternately at very short time intervals (50 milliseconds for each ion).

Table 2.1 shows an example of temperature dependence of thermal degradation of a peptide *H-YGGFL-OH*. For this peptide, the pseudo-molecular ion is at m/z 594, its

relative intensity in the mass spectrum is denoted as $I(594)$; the dominant fragment ion for this peptide is at m/z 374 - a K^+ adduct of (Y_3+H) whose relative intensity is denoted as $I(374)$. Current (A) is the direct heating current. The thermionic emitter was turned on first ($I = 2.65$ A) to produce K^+ ions. After five seconds of time delay (the radiative heating may have caused some degradation of the peptide), the power for the direct heating filament (the sample holder) was turned on to desorb samples on the filament. As the heating rate is increased, fewer degradation products are formed and more intact peptides are sampled.

Table 2.1 Degradation Vs. Desorption at Various Heating Rate			
Current (A)	$I(374)/I(594)$	% degradation*	# of scans**
0	20:1	95	120
1.0	1:1	50	8
2.0	1:3	25	4
2.5	1:6	15	2

*% Degradation = $I(374)/I(594)$. ** Number of scans that signal lasts.

If fragment ions $(Y_3+H+K)^+$ are mainly from $(M+K)^+$ ions - K^+ adduct ions of intact molecules, then the relative heating rate will not affect the relative ion abundances very much. Even at a very high heating rate - much more intact gas-phase molecules are formed, $I(374)/I(594)$ should stay almost the same. This is obviously not the case, as indicated by the data in the above table. Therefore, fragment ions are mainly from attachment of K^+ ions to thermal degradation products of neutral peptides. Fragmentation of K^+ adducts, is not significant, if any. Note in the data for experiments with large heating currents, $(Y_3+H+K)^+$ ions partly are from radiative heating in the first five seconds. Also, direct heating of the peptide can cause degradation to certain extent.

Therefore, all of the ion current for $(Y_3+H+K)^+$ may be from thermal degradation of neutral peptides.

References

1. Bombick D.; Pinkston, J. D.; Allison J. *Anal. Chem.* **1984**, *56*, 396-402.
2. Light, K.; Kassel, D. B.; Allison, J. *Biomed. Environ. Mass Spectrom.* **1989**, *18*, 177-184.
3. Bombick, D.; Allison, J. *Anal. Chem.* **1987**, *59*, 458-466.
4. Bombick, D.; Allison, J. *Anal. Chim Acta* **1988**, *208*, 99-116
5. Kassel, D. B.; Allison, J. *Biomed. Environ. Mass Spectrom.* **1988**, *17*, 221.
6. Rouse, J.; Allison, J. *J. Am. Soc. Mass Spectrom.* **1993**, *4*, 259-269.
7. Light, K., *Doctoral Dissertation*, Michigan State University, **1990**.
8. Blewett, J. P; Jones, E. J. *Phys. Rev.* **1936**, *50*, 464-468.
9. Bombick, D. *Doctoral Dissertation*, Michigan State University, **1986**.
10. Beuhler, R. J.; Flanigan, E; Greene, L. J.; Friedman L. *J. Am. Chem. Soc.* **1974**, *96*, 6.
11. Allison, J.; Ridge, D. P. *J. Am. Chem. Soc.* **1979**, *101*, 4998.

Chapter 3

Peptide Analysis by K⁺IDS Mass Spectrometry

I. Introduction

Since the advent of the K⁺IDS mass spectrometric technique, K⁺IDS has been used for the analysis of various organic compounds. Application of this technique for peptide analysis was of great interest to the members of Allison group. In the first paper [1], K⁺IDS spectra of three peptides, ranging from di- to tetra- peptides, were published. With the original single-filament probe, the spectra obtained seemed to be complicated, containing both K⁺ adducts and surface ionization products. The formation of the fragment ions were explained by the 1,2-elimination mechanism shown in Figure 3.1. However, an obvious ion series was not observed for either of the three peptides.

In another paper [2], a sample peptide, hexaglycine, was analyzed and an excellent mass spectrum was obtained. Dominant fragment ions were K⁺ adducts of thermal degradation products from the cleavage of amide bonds (peptide bonds) with the shift of a hydrogen atom. The cleavages of these peptide bonds were assumed to be a low-energy 1,2-elimination process. Based on group equivalent values, the energy required for the process was estimated to be - 5 kcal/mol, suggesting an exothermic process. This is unreasonably low because such processes are expected to be endothermic. The cleavages of CHR-NH bonds were also observed in the spectrum, but with much lower abundance. Cyclization processes were proposed for the formation of some of the ions.

1, 2 - Elimination mechanism

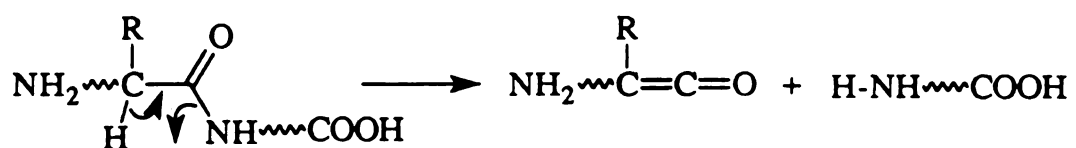


Figure 3.1 1, 2 - Elimination mechanism for the CO-NH bond cleavage of peptides.

The spectra in these papers demonstrated that K^+ IDS could be used for the analysis of peptides. However, obtaining a good spectrum requires a trial-and-error process because the spectrum of a peptide was highly dependent on the bias voltage set for the thermionic emitter/sample holder due to the single-filament design of the K^+ IDS probe.

In 1988, a two-filament probe was introduced for K^+ IDS experiments [3]. This probe, using radiative heating for both degradation and desorption, was reported to be 40 times more sensitive than the original one with one filament. Because the sample is no longer on the thermionic emitter, changes both on thermal degradation of peptides and ionization mechanisms might be expected. It was reported that the spectra for many compounds were almost exactly the same, as indicated in K. Light's dissertation [4]. Similar mechanisms may have been involved. However, no detailed research had been done on peptide analysis.

In this Chapter, the analysis of peptides with K^+ IDS, will be examined, the applicability of this technique to peptide sequencing is evaluated, and the advantages and limitations of K^+ IDS for peptide sequencing are discussed. The mechanisms for thermal degradation of peptides - a very important aspect of this technique, will be investigated in Chapter 4 in detail.

II. Experimental

Mass spectrometry: The K^+ IDS technique was performed on an HP 5985 GC/MS/DS quadrupole mass spectrometer. The K^+ IDS probe was a two-filament direct insertion probe. One filament is the thermionic emitter, producing K^+ ions in the gas phase. The other is the sample holder, on which sample is radiatively heated and desorbed. A detailed description of this probe is given in the K^+ IDS setup section in Chapter 2.

Chemicals: All peptides were purchased from Sigma Chemical Company, St. Louis, MO, and used without further purification. The samples were dissolved in methanol to a concentration of 10 $\mu\text{g}/\mu\text{l}$, or suspended in methanol. One to two microliters of solution were transferred to the sample filament. The sample was dried before being inserted into the mass spectrometer.

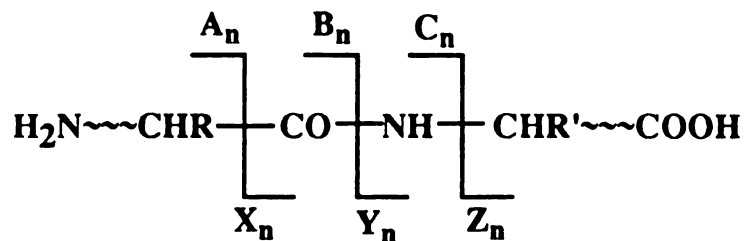
Peptide derivatization: N-terminally acetylated peptides such as Ac-VGVAPG-OH, were formed from the free peptide using acetic anhydride and a small amount of pyridine as a catalyst, by the procedure described by Knapp [5]. For peptide methyl esters such as H-VGVAPG-OCH₃, a 2N methanolic HCl was prepared first by slowly (dropwise) dissolving 20 μl of acetyl chloride into 100 μl of methanol. One mg of peptide was dissolved in 50 μl of the methanolic HCl. Five minutes after the reaction, the mixture was dried in a Speedvac(trademark) to remove the excess reagent and the residue re-dissolved in methanol. The mixture is dried because the HCl can corrode the rhenium wire (sample holder). (For N-acetylation and C-esterification at the same time, a procedure similar to that for N-acetylation was used. One milligram of a peptide was dissolved in a mixture of 50 μl of 10% of pyridine and 50 μl of acetic anhydride. The reaction requires two weeks for completion).

III. K⁺IDS Mass Spectra of Typical Peptides

A. Nomenclature of K⁺IDS Fragments

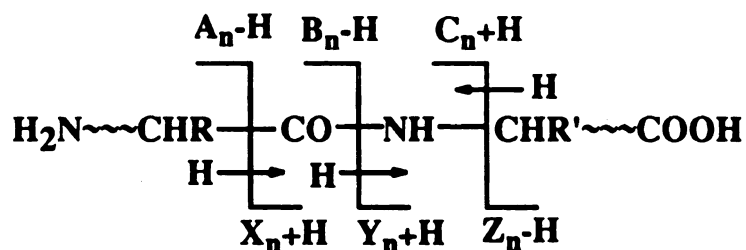
To precisely designate the neutral species and ions formed in K⁺IDS, a variation of the original Roepstorff nomenclature [6] is used. For a peptide NH₂~~~CHRCO-NH~~~COOH, if the interior amide bond cleaves, two fragments (radicals) will be formed. The N-terminal fragment, NH₂~~~CHRCO•, is called a B_n fragment and the C-terminal fragment, •NH~~~COOH, is called a Y_n fragment. The ions formed in the K⁺IDS experiment are K⁺-adducts of even-electron species. Skeletal bond cleavages are

A. Roepstorff Nomenclature* for Peptide Fragments



* P. Roepstorff and J. Fohlman, Biomed. Mass Spectrom. 11, 601(1984)

B. Nomenclature for Neutral Degradation Products



C. Nomenclature for Ions In K⁺IDS

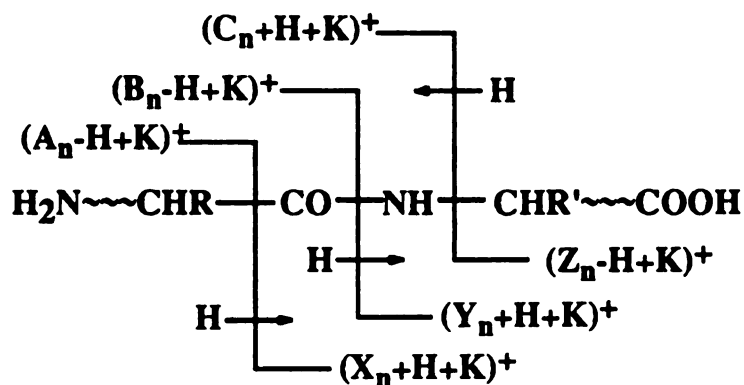


Figure 3.2 Nomenclature for peptide fragments and ions.

accompanied by a H-shift or an OH-shift in thermal degradation processes for peptides. Therefore, ionic designations such as $[Y_n+H+K]^+$, $[B_n-H+K]^+$, $[C_n+H+K]^+$, and $[B_n+OH+K]^+$ will be used, where n is the number of amino acid residues (or number of side chains) contained in that fragment. From this designation scheme, the m/z value of each ion under discussion is clearly defined. The details of the nomenclature scheme, indicating the types of ions observed (the types of thermal degradation products generated), are given in Figure 3.2. The K^+ adduct of each intact peptide will be designated as $[M+K]^+$.

In peptide chemistry, one letter designations are frequently used for amino acid residues. To designate a peptide completely, the H at the N-terminus and the OH at the C-terminus will be specifically indicated by a dash line (H- and -OH). To avoid confusion between histidine (H) and hydrogen (H), histidine is underlined as H whenever a confusion might occur.

With peptides of known amino acid sequence, m/z values of fragment ions can be calculated by using a commercial program named MacProMass 1.0. This program was designed for the calculating the m/z values of peptide fragments from protonated peptides. By making a slight change on the programmable termini, this program can be used to calculate the m/z values of K^+ IDS fragments. For example, the $(Y_n+H+K)^+$ ions in K^+ IDS are 38 mass unit heavier than the corresponding y (Y'') ions from FAB, setting-up a C terminus to -OK instead of -OH can give m/z values of the C-terminal fragments. By changing the N terminus from H- to K-, the m/z values of N-terminal fragments for K^+ IDS can be calculated.

B. Typical K^+ IDS Spectra of Peptides

In the K^+ IDS experiment, microgram quantities of an analyte are placed on a rhenium wire, and the temperature is increased from room temperature to approximately 300 °C in 10 seconds. The temperature is then held at this value until the sample is

depleted. During the experiment, K^+ ions attach to desorbed neutral molecules, the mass spectrometer is repetitively scanned, and a set of mass spectra is collected. For some samples, there is a time (temperature) dependence of the resulting mass spectra since each degradation process has a unique activation energy, which leads to the differences in the relative intensities of mass spectral peaks in different scan files. However, what is frequently observed is that a number of processes begin to occur at approximately the same temperature. This might be expected for peptides since, even though each amino acid residue has a unique side chain, peptides consist of only three types of skeletal bonds.

When the tetrapeptide H-FGGF-OH is rapidly heated, and K^+ ions are attached to molecular species that desorb into the gas phase, typical experimental results are shown in Figure 3.3a. As desorption and thermal degradation occur, spectra are obtained. The spectra collected are summed, and a single K^+ IDS spectrum is reported, which will provide information on the low-energy thermal-degradation processes. Note that, as the thermal degradation chemistry occurs, some of the peptide molecules desorb intact. A temperature is reached at which desorption and thermal degradation compete. If a peptide decomposes on the surface to two smaller molecules, they appear to desorb promptly rather than remain on the surface and decompose further. Thus, the experiment allows for the primary degradation processes to be investigated. Following such primary unimolecular processes, prompt desorption of thermal degradation products occurs because of the temperatures used.

The spectrum shown in Figure 3.3b is a typical K^+ IDS mass spectrum for a small peptide. All of the ions detected are K^+ -adducts. For example, the peak in the spectrum at m/z 465 represents a K^+ (39 Da) adduct of the intact analyte molecule (426 Da). The peak at m/z 261 represents a K^+ adduct of a thermal degradation product with a mass of 222 Daltons. A fragment of the peptide can be generated with this mass by cleaving the central amide bond, with one additional hydrogen atom, to yield (Y_2+H), which can also

Time Dependence of Spectra: *H*-FGGF-*OH*

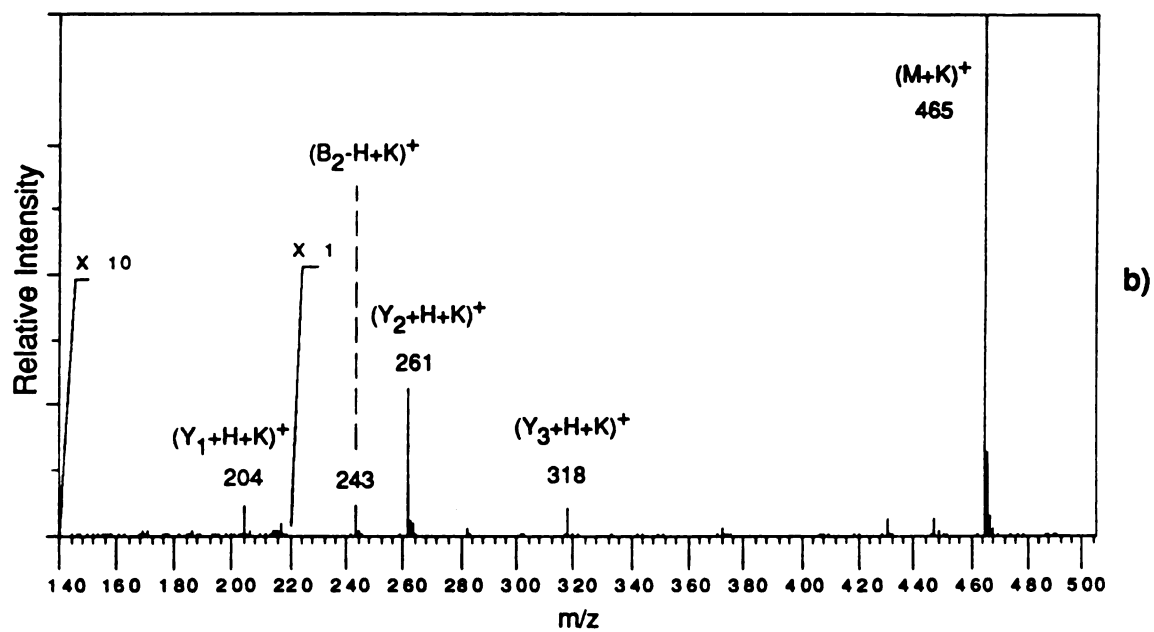
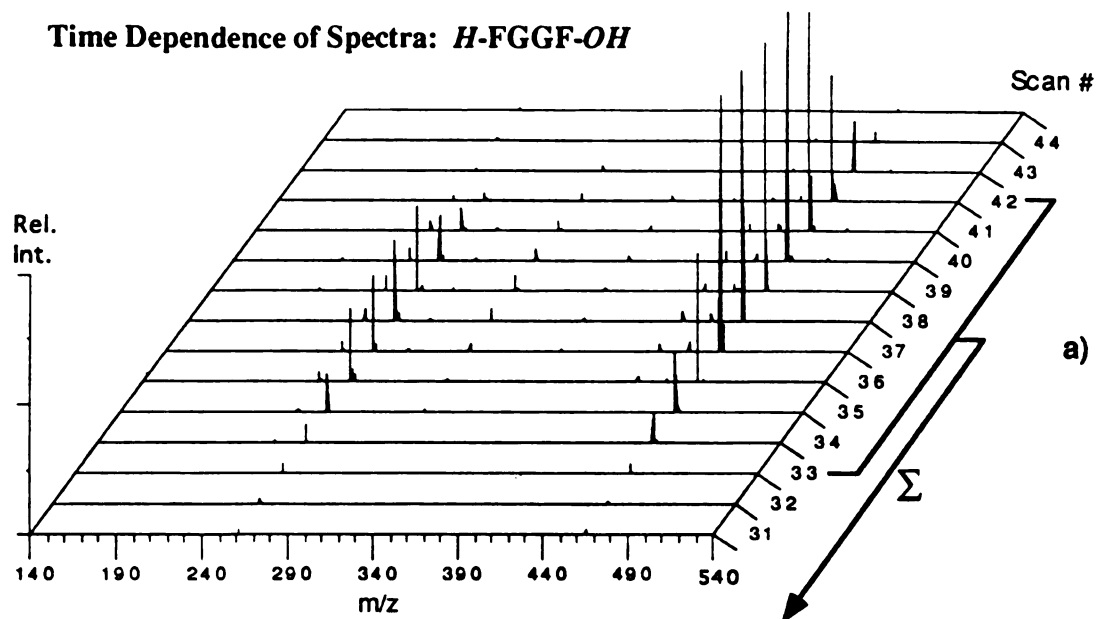


Figure 3.3 K^+ IDS mass spectra of *H*-FGGF-*OH*:

a) Temperature dependence; b) Average spectrum.

be written as H-GF-OH. Thus, the ions at m/z 261 are designated as $[Y_2+H+K]^+$ or $[H-GF-OH]K^+$. By correlating K^+ IDS mass spectra with the structures of many peptide analyte molecules, trends in the degradation chemistry become clear, and ionic designations become apparent. Note that the $[Y_n+H+K]^+$ ion series in the spectrum ($n=1-3$) provides information on the amino-acid sequence of the peptide and K^+ -adducts of the intact, desorbed peptide provide molecular weight information. Thus, K^+ IDS is a useful mass spectrometric method as well as a tool for understanding thermal degradation chemistry.

Figure 3.4 shows the K^+ IDS mass spectrum of H-VGVAPG-OH as a second example. Again, the spectrum shows that both the intact molecule and its thermal degradation products can be formed simultaneously. All of the ions observed are K^+ -adducts of closed-shell molecules that can be related to the parent molecule, formed by skeletal bond cleavages with accompanying hydrogen atom shifts. For this peptide, the ion series $(Y_n+H+K)^+$ is observed, which can be used to deduce the sequence of the peptide.

The spectra shown in Figure 3.3 and Figure 3.4 are typical of the K^+ IDS results in the following aspect: the dominant ions are K^+ adducts of degradation products that result from cleavage of amide bonds even though these bonds are the strongest skeletal bonds. While two neutral products, (Y_n+H) and (B_m-H) , are generated (simultaneously and in equal quantities) when an amide bond is broken, the $[Y_n+H+K]^+$ ions are more intense than the corresponding $[B_m-H+K]^+$ ions. This observation will be discussed in Chapter 4.

C. K^+ IDS Spectra of Polar Peptides and Dehydration Reactions

In K^+ IDS experiments, peptides with amino-acid side chains containing very polar functionalities have shown significant dehydration reactions. The major difference

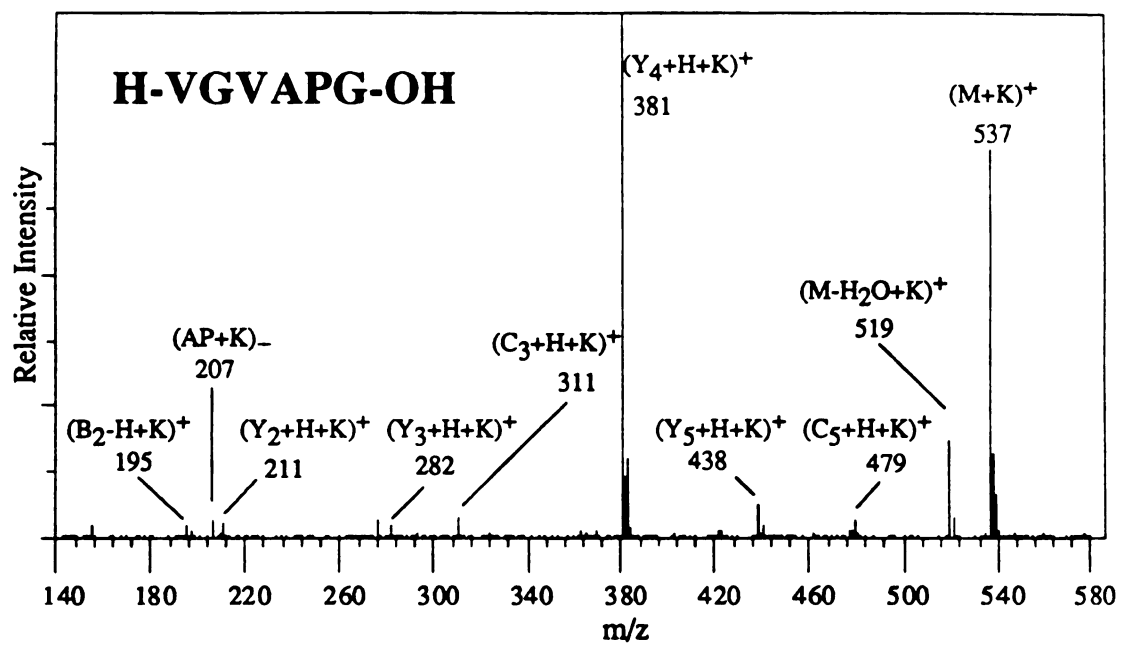


Figure 3.4 K^+ IDS mass spectrum of H-VGVAPG-OH.

the
n
c
g
-C
in
H.
fro
the
for
the
atta

between peptides containing alkyl, aromatic or H side chains and peptides with other side chains (more polar) lies in their polarities and chemical reactivities.

The high polarity of some side chains, such as a carboxyl group in glutamic acid, has direct consequences in the K^+IDS experiment. More polar peptides lead to stronger interactions between peptides, leading to stronger interactions between peptides and the sample-holder surface, greater vaporization energies and longer heating time before desorption. The extended heating-time before a peptide molecule can be desorbed while it acquires energy from heating, can lead to extensive thermal degradation such as skeletal bond cleavages as well as dehydration. Consequently, there are little or no intact $(M+K)^+$ ions detected for such peptides. When this occurs, only a few reactions will dominate and the resulting spectrum can provide only limited sequence information of a peptide.

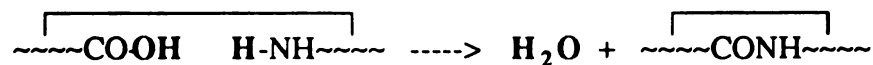
For peptides with OH-containing residues such as serine ($R = -CH_2OH$) and threonine [$R = -CH(OH)CH_3$], the side chains are very polar. Peptides containing these residues do not show much fragmentation (thermal degradation). This result, however, can not be explained at this time. With $-COOH$ and $-NH_2$ containing residues such as glutamic acid ($R = -CH_2CH_2COOH$), aspartic acid ($R = -CH_2COOH$) and lysine ($R = -CH_2CH_2CH_2CH_2NH_2$), dehydration frequently occurs to a significant extent, both for intact peptide molecules and for their thermal degradation products.

With these dehydration reactions, ions such as $(Y_n+H+K-H_2O)^+$ and $(M-H_2O+K)^+$ are formed. These dehydration ions such as $(Y_n+H+K-H_2O)^+$ ions may be from dehydration of regular $(Y_n+H+K)^+$ ions. They also can be formed directly from thermal degradation of $(M-H_2O+K)^+$ ions. It is generally believed that K^+ adducts formed do not produce fragments. Therefore, these ions are most likely the adducts of their corresponding degradation products. Dehydration probably occurs before K^+ attachment. The extent of dehydration varies with amino-acid composition of a peptide.

When a glutamic acid/aspartic acid residue is present in a peptide, the extent of dehydration increases significantly, as is the case in the spectrum of H-FLEEI-OH (Figure 3.5). This result suggests that carboxylic acid group on the side-chain is involved in the dehydration process. Frequently, this will generate ions such as $(Y_n-H_2O+K)^+$ ions, $(Y_n-H_2O-NH_3+K)^+$ ions, as well as dehydration of the pseudo-molecular ions, $(M-H_2O+K)^+$. It has been found that the shifting hydrogen in dehydration is from either the N-terminus or amide group (see Chapter 4 for details). Many other peptides, such as H-VGSE-OH, HCO-AGSE-OH and H-RKEVY-OH, show similar dehydration.

As mentioned above, dehydration from side-chain carboxyl groups is much easier than that from the C-terminus of a peptide. This is probably because these carboxyl groups can reach farther in various directions due to the longer side chains than the C-terminal one.

With lysine-containing peptides, such as H-PFGK-OH, significant dehydration products are also observed as shown in Figure 3.6. A series of dehydration ions such as $(Y_2-H_2O+K)^+$, $(Y_3-H_2O+K)^+$, $(M-H_2O+K)^+$ and $(M-2H_2O+K)^+$ are observed for this peptide. One plausible explanation for this dehydration process is that the shifting H is from the side-chain NH_2 . In the dehydration process, intramolecular dehydration occurs and forms a cyclic amide.



K^+ IDS spectra of other lysine-containing peptides such as H-TSK-OH and H-KHK-OH also show similar dehydration reactions. However, the loss of the second water molecule has not been explained. More data are needed to uncover the reason.

When a tyrosine residue is present in a peptide, dehydration generally increases though the extent varies for different peptides. For the peptides H-YGGFM-OH and H-

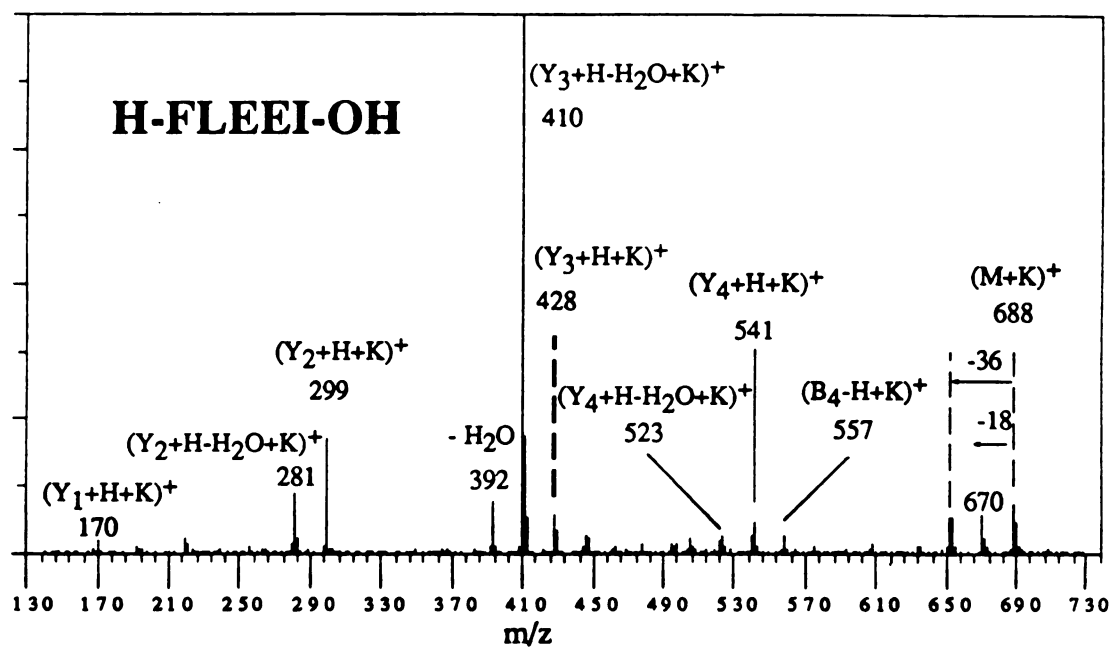


Figure 3.5 K^+ IDS mass spectrum of H-FLEEI-OH.

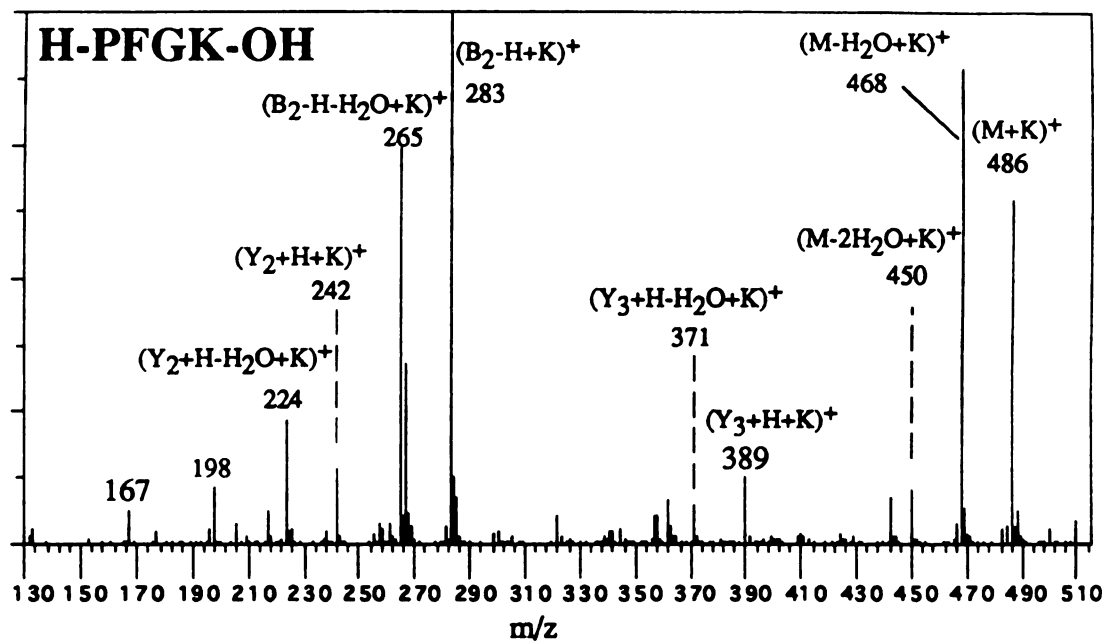


Figure 3.6 K^+ IDS mass spectrum of H-PFGK-OH.

FGGFM-OH, their K^+ IDS spectra are almost the same except that the former gives slightly more dehydration products. This indicates that the dehydration involves the tyrosine side chain, but is not very significant. For the peptide H-YGG-OH, however, K^+ IDS spectrum suggests a significant dehydration of the peptide. Because this peptide can be desorbed into the gas phase more easily than H-YGGFM-OH, due to its lower molecular weight (less heat will be absorbed before desorption), the dehydration must be position dependent. For H-YGG-OH, there is a favorable interaction between the C-terminal carboxyl group and the phenolic OH on the tyrosine side chain (or N-terminal NH_2) due to the closeness of the two functional groups. This leads to dehydration. For H-YGGFL-OH, however, these two groups are too far away for a similar reaction to occur.

Dehydration also occurs for peptide amides even though there are no carboxyl groups within such molecules. Obviously the reaction proceeds via a different mechanism. We postulate that the dehydration occurs most probably at the C-terminus involving the following rearrangement followed by a 1,2-elimination:



Other peptide amides such as H-YGGFL- NH_2 , H-GGFL- NH_2 , H-YPLG- NH_2 and t-BOC-WMDF- NH_2 have shown the same dehydration reactions.

When a peptide is too polar, a K^+ IDS spectrum may not provide information about either molecular weight or structure of the peptide because the molecules will be very difficult to desorb into the gas phase. In such a case, some decomposition will occur and the molecular ions will not be detected. For example, the peptide H-RKEVY-OH (Figure 3.7) gives only ions from the cleavages of the second amide bond from the N-terminus, forming (B₂-H) and (Y₃+H). No (M+K)⁺ ions are detected.

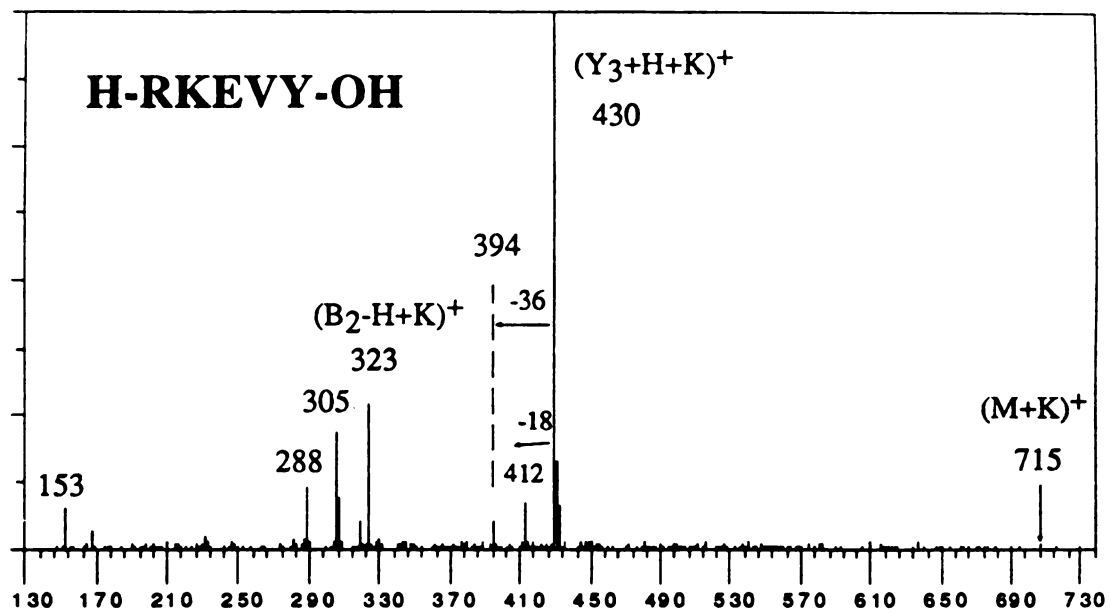


Figure 3.7 K⁺IDS mass spectrum of H-RKEVY-OH.

I

h

a

d

ie

c

((

3.

di

th

sin

du

is

cle.

pep

H-C

at m

addi

repr

small

D. K^+ IDS Spectra of Peptide Derivatives

1. Peptide Amides

Amidation is one of the most common transformations of peptides [7]. Therefore analysis of peptide amides is of great importance in biochemistry.

When a peptide is converted into a peptide amide, the K^+ IDS spectrum changes dramatically. For a regular peptide H-YGGFL-OH, the dominant ions are $(Y_n+H+K)^+$ ions, with $(Y_3+H+K)^+$ represented by the base peak of the spectrum. When the corresponding amide, H-YGGFL-NH₂, is analyzed, the dominant ions become $(C_n+H+K)^+$ ions and $(Y_n+H+K)^+$ ions, and the base peak represents $(C_3+H+K)^+$ (Figure 3.8).

These observations can be explained by a cyclization mechanism which will be discussed in Chapter 4. It has been observed that cyclization via the termini of peptides is the dominant reaction in thermal degradation of peptides.

For H-YGGFL-NH₂, cyclizations from both termini are competitive due to similar steric hindrance. The dominant cyclization from the C-terminus $(C_3+H+K)^+$ is due to the loss of cyclo-(FL) from the N-terminus. The weaker NH-CHR bond probably is the main reason why the cleavage forming $(C_3+H+K)^+$ is more favored than the cleavage forming $(Y_3+H+K)^+$.

The change of a peptide spectrum is not always so dramatic when a regular peptide is converted into a peptide amide. For example, the spectra of H-GGFL-OH and H-GGFL-NH₂ (Figure 3.9) are very similar except that $(Y_1+H+K)^+$ ions of the former at m/z 170 (weak) is replaced by $(C_2+H+K)^+$ ions of the latter at the same m/z value. In addition, the "apparent" isotopic peak at m/z 317 is not an isotopic peak; it actually represents a $(C_3+H+K)^+$ ion, which can be easily overlooked.

There are several possible reasons for this small change: 1. C_1 and C_2 are too small to respond well (see Chapter 5 for size discrimination). 2. Since the N-terminal

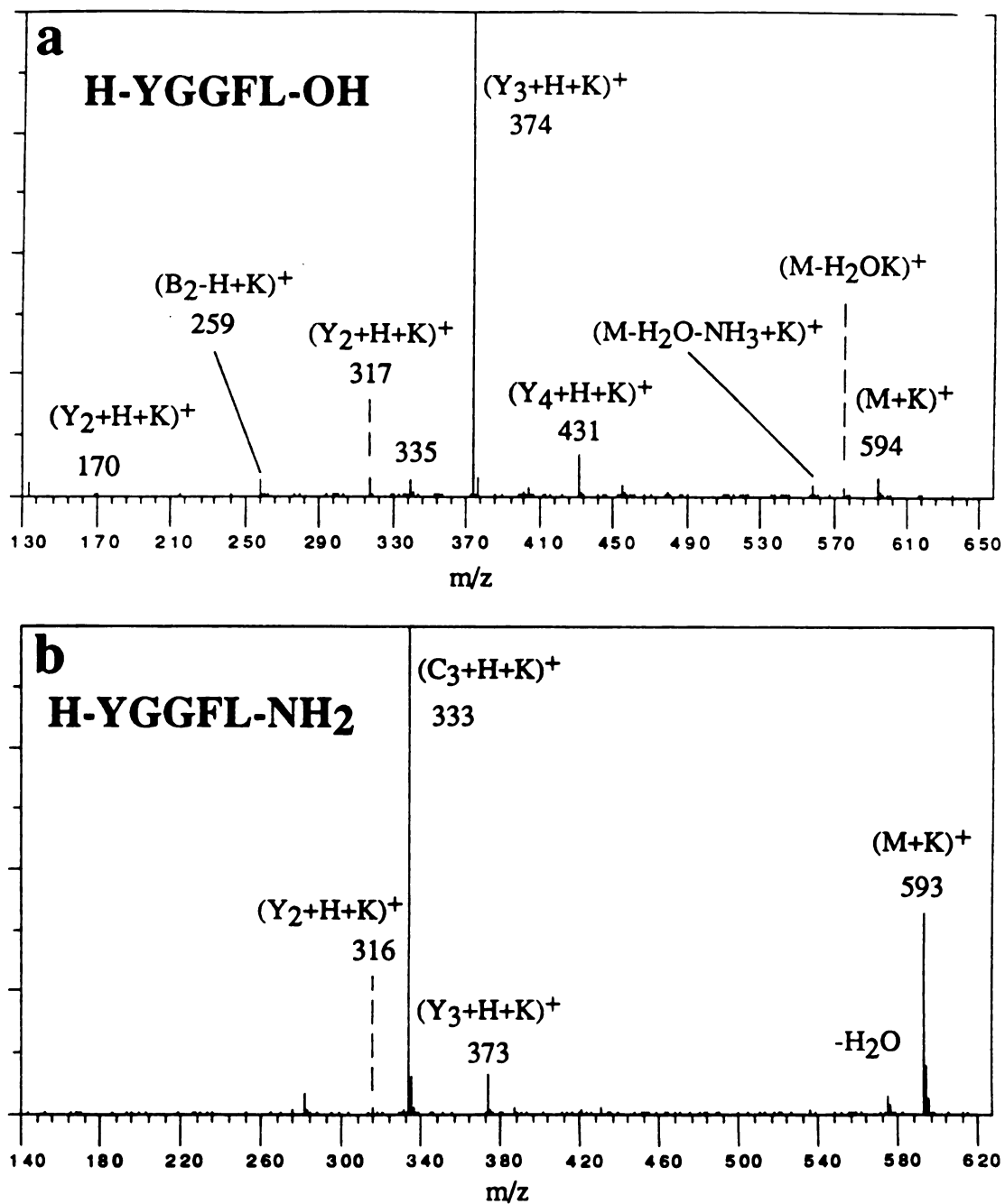


Figure 3.8 K⁺IDS mass spectra of: a) H-YGGFL-OH; b) H-YGGFL-NH₂.

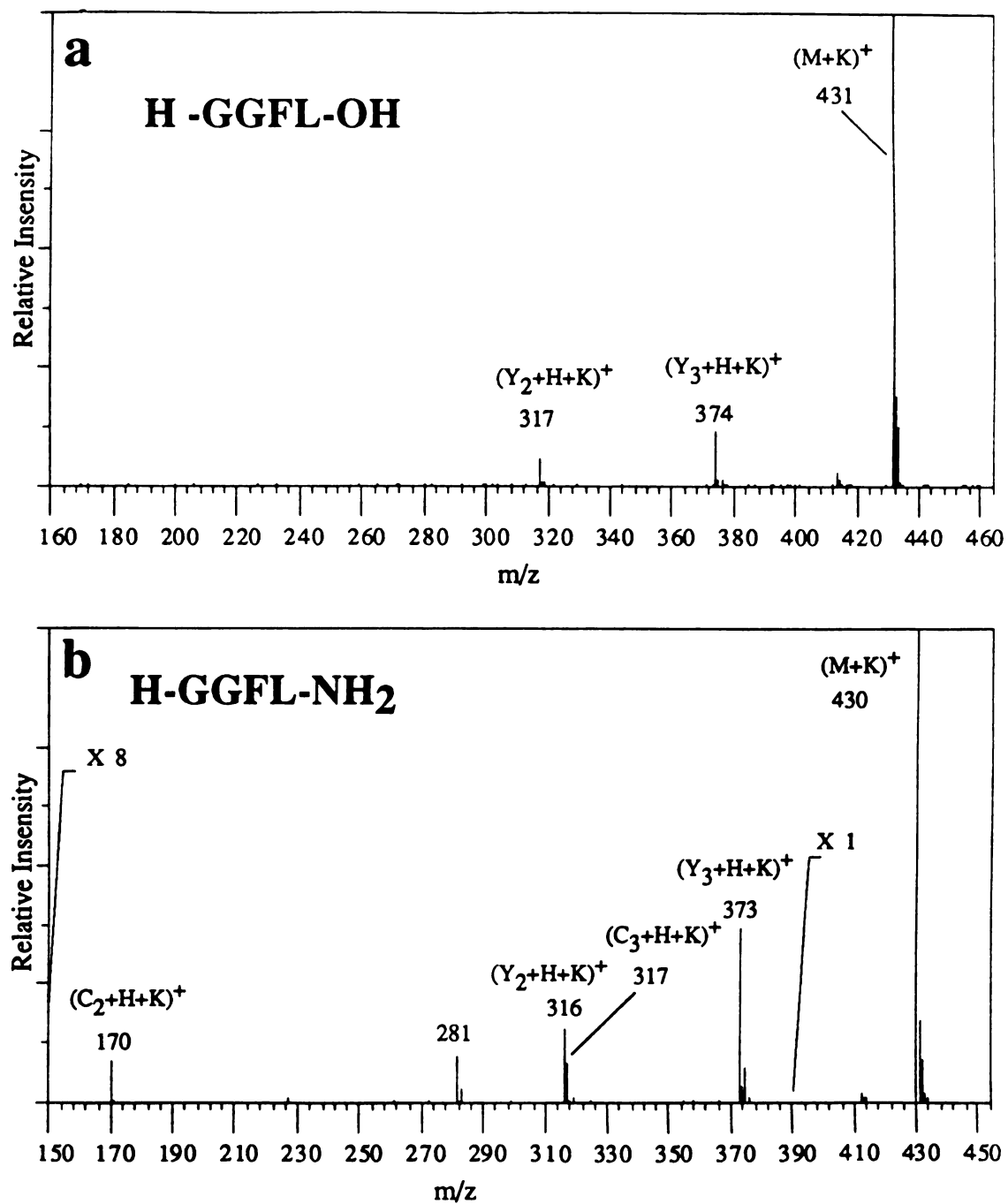


Figure 3.9 K^+ IDS mass spectra of: a) H-GGFL-OH; b) H-GGFL-NH₂.

glycine residues present such a small steric hindrance for cyclization from the N-terminus (see Chapter 4 for details), formation of (Y_n+H) is still favored.

2. N-terminally derivatized peptides

The structural analysis of N-terminal derivatives of peptides is of great interest to biochemistry. For example, N-acetylation is a common transformation of peptides for the N-terminal amines and amines at lysine side chains [7]; CBZ (Carbobenzoxy-: $C_6H_5CH_2-OCO-$) and t-BOC (N-tert-butoxycarbonyl: Me_3COCO-) are important N-terminal protection groups used in peptide synthesis.

When the N-terminus of a peptide such as H-VGVAPG-OH is blocked, by acetylation for example, the appearance of the spectrum changes dramatically. For the regular peptide, the dominant ions are $(Y_n+H+K)^+$ ion series. With the N-terminal derivatives of the peptide, these ions become very weak or absent. Instead, the dominant ion series become $(B_n+OH+K)^+$ ions (Figure 3.10). Because the only possible OH source is at the C-terminus of the peptide, these ions must be formed via cyclization from the C-terminus because the regular cyclization reaction from the N-terminus is blocked by the acetyl group.

N-terminally blocked peptides also produce $(C_n+H+K)^+$ ions, such as $(C_3+H+K)^+$, $(C_4+H+K)^+$ and $(C_5+H+K)^+$ ions in the above mentioned spectrum. The formation of these ions will be discussed in Chapter 4.

Similar spectra have been found for other N-terminally blocked peptides such as CBZ-GPGGPA-OH (Figure 11a), CBZ-GPFPL-OH (Figure 11b), t-BOC-PPPP-OH (Figure 11c), Ac-VGGFL-OH, Ac-YGGFL-OH, HCO-AGSE-OH. In addition to $(B_n+OH+K)^+$ and $(C_n+H+K)^+$ ions, other ions such as $(Y_n+H+K)^+$ ions are also observed, but with lower abundances.

It should be pointed out that the large N-terminal derivatives show characteristic neutral losses from the pseudo-molecular ions. Loss of $C_6H_5CH_2OH$ (-108) from MK^+

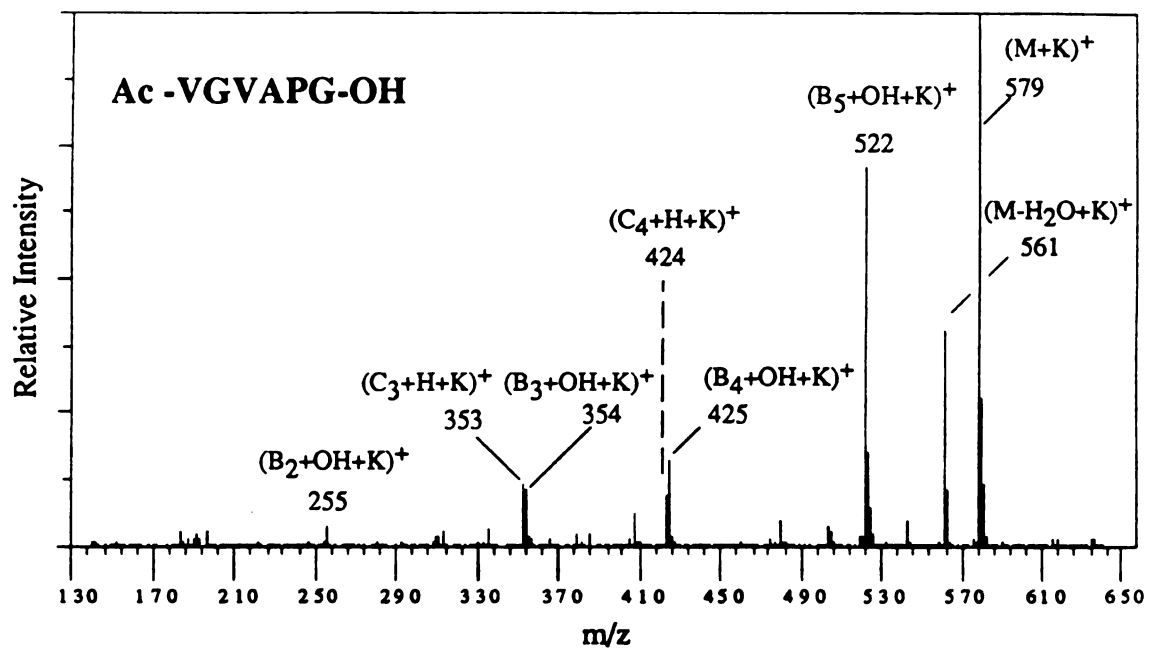


Figure 3.10 K^+ IDS mass spectrum of Ac-VGVAPG-OH.

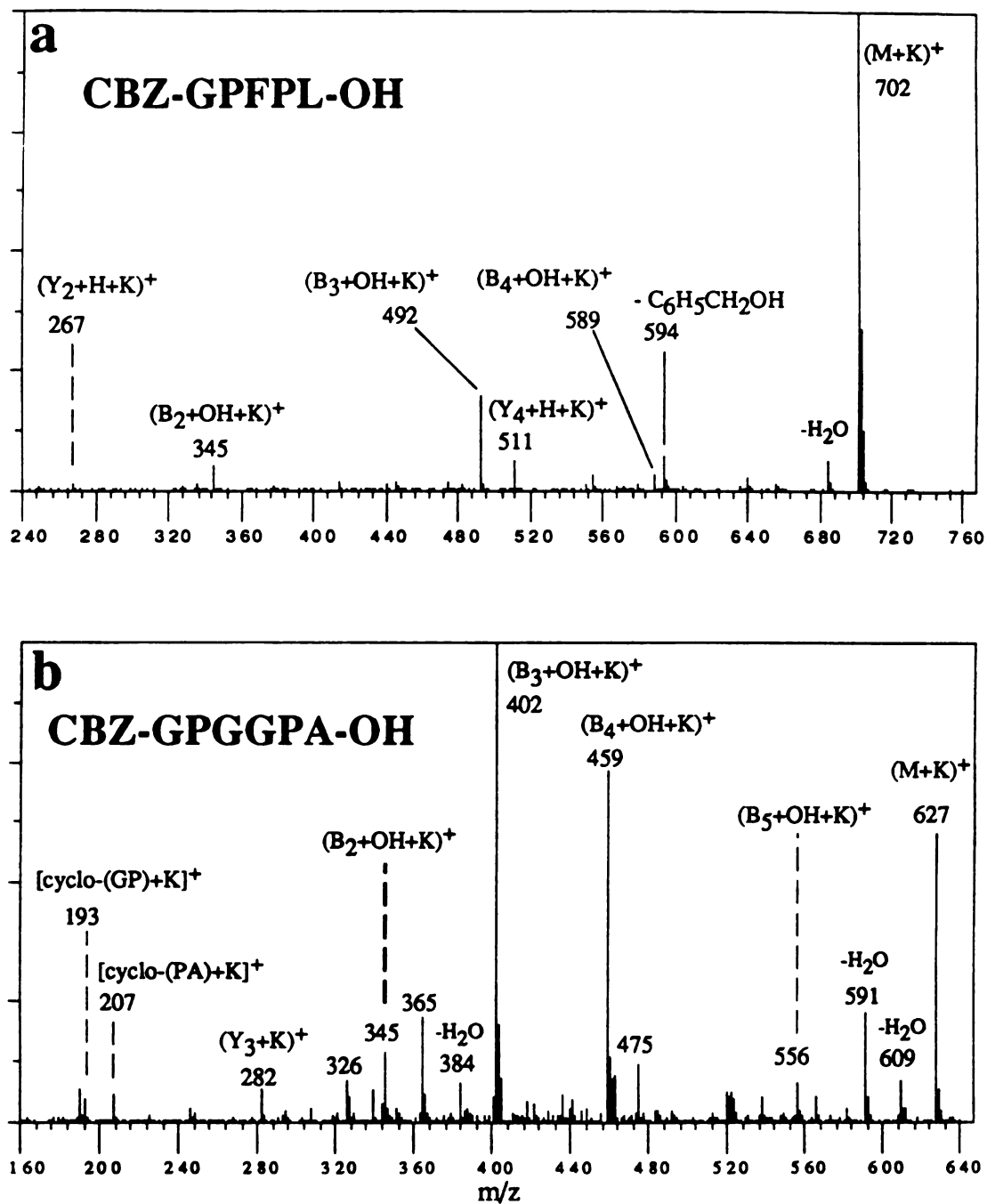


Figure 3.11 K⁺IDS mass spectra of: a) CBZ-GPFPL-OH; b) CBZ-GPGGPA-OH.

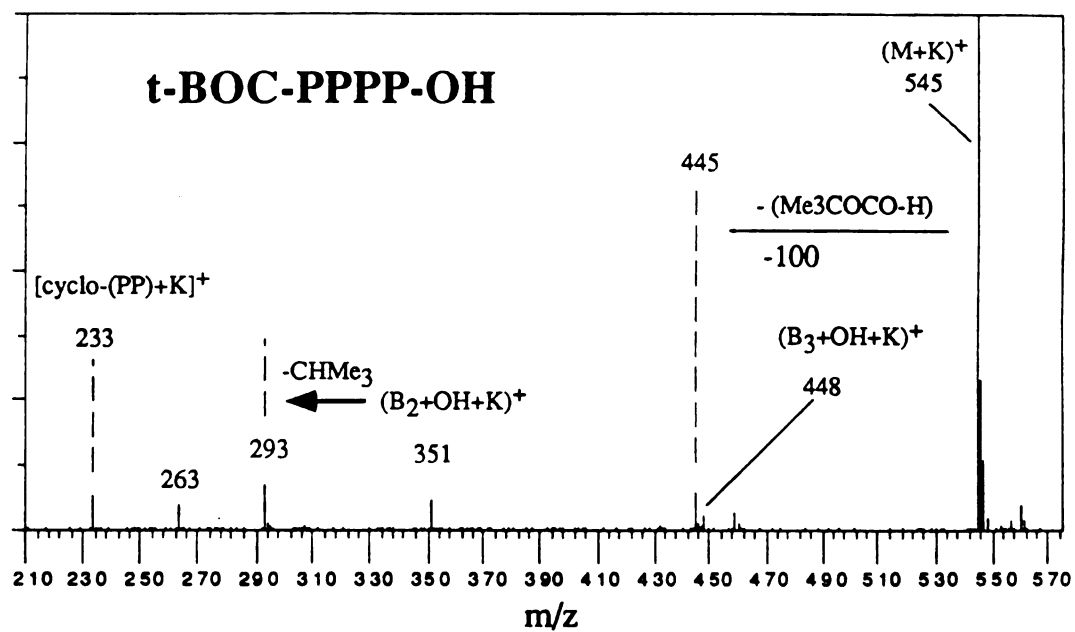


Figure 3.11c K^+ IDS spectrum of t-BOC-PPPP-OH.

has been found for CBZ derivatives of peptides; loss of 100 (t-BOC-1) from the MK^+ has been found for t-BOC derivatives. Therefore, neutral losses of 108 and 100 are indicative of CBZ and t-BOC derivatives, respectively (Figure 11a-c).

3. Peptides with C-terminal esterification

When the C-terminus of a peptide is blocked with a methyl ester group, the ion series from K^+IDS stay the same as for the underivatized one, with all $(Y_n+H+K)^+$ ions 14 mass units higher. This can be seen in the K^+IDS mass spectra of H-VGVAPG-OCH₃ and H-YGGFL-OCH₃ (Figure 3.12). This is because cyclization from the C-terminus of a peptide becomes even more difficult than in the case of an underivatized peptide while cyclization via the N-terminus remains the same. Also found is the common loss of methanol (-32) from the molecular species which is indicative of a methyl ester.

4. Peptide variants

H-YGGFL-OH and its derivatives, due to their commercial availability and low cost, were studied in the early stage of this research. With K^+IDS spectra of these peptide variants, the aromatic side chains ($R_Y = -CH_2C_6H_4OH$ and $R_F = -CH_2C_6H_5$) were suspected to be the major reason for the formation of the major ions such as $(Y_3+H+K)^+$. To test this speculation, two similar peptides, H-AGGFL-OH and

H-VGGFL-OH, were synthesized and their K^+IDS mass spectra were compared with that of H-YGGFL-OH.

When the first amino acid residue of peptides H-XGGFL-OH ($X = Y, A, V$) is changed from tyrosine (Y) to alanine (A) to valine (V), no obvious change in the spectra is observed (see Figure 3.8, Figure 3.13 and Figure 3.14). This result indicates that the size of the side chain of the first amino-acid at the N-terminus is not the reason why

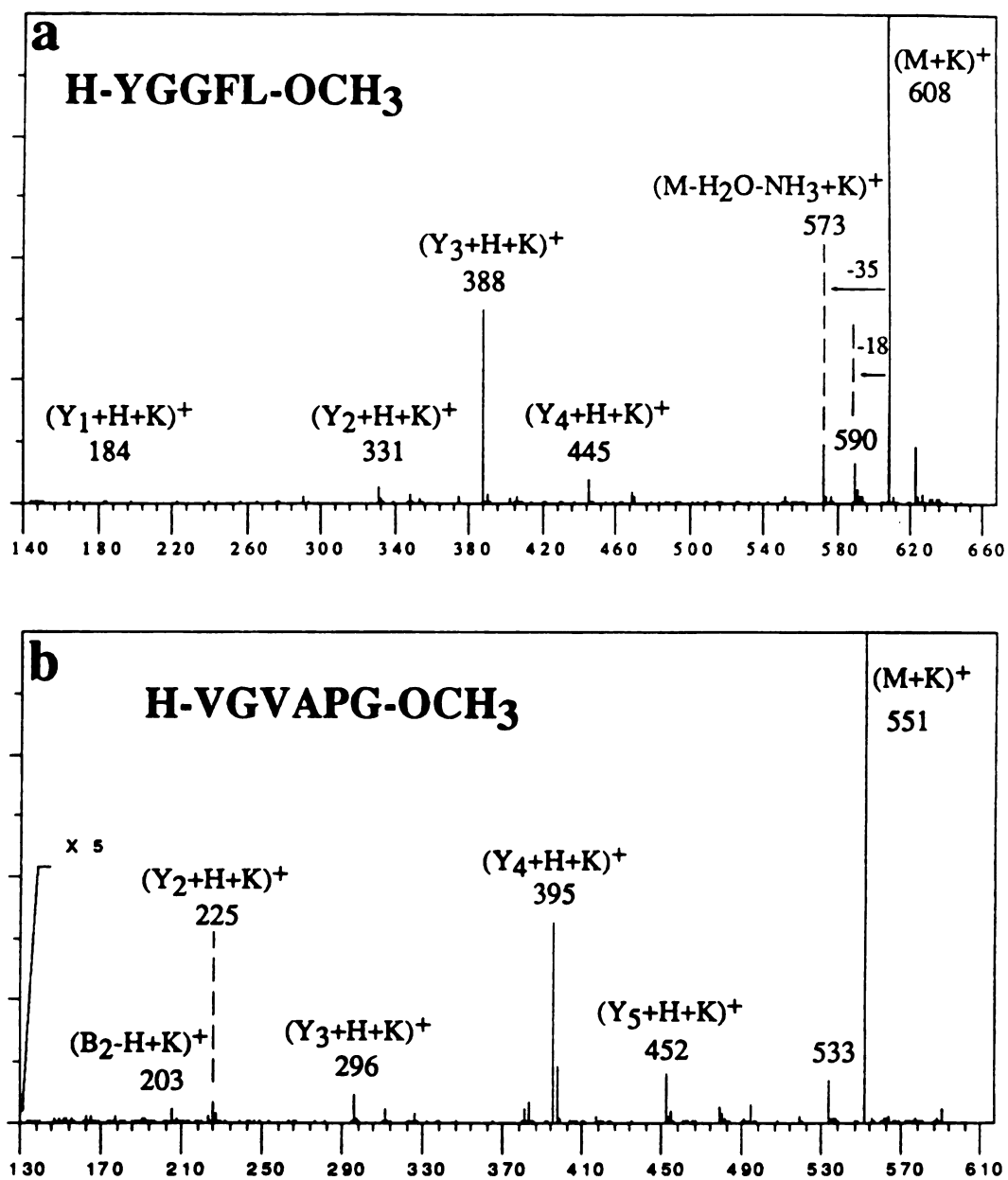


Figure 3.12 K⁺IDS mass spectra of: a) H-YGGFL-OCH₃; b) H-VGVAPG-OCH₃.

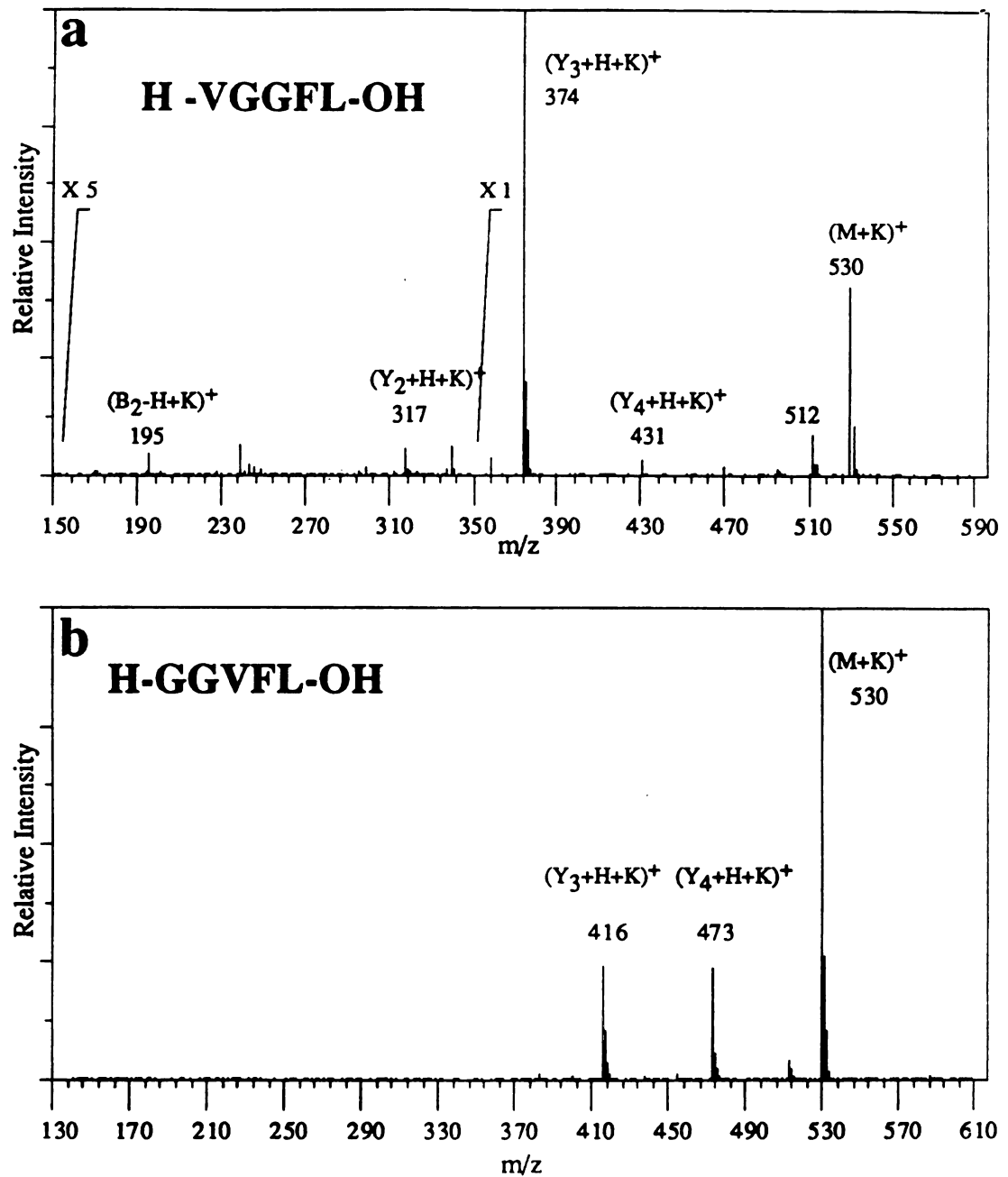


Figure 3.13 K^+ IDS mass spectra of: a) H-VGGFL-OH; b) H-GGVFL-OH.

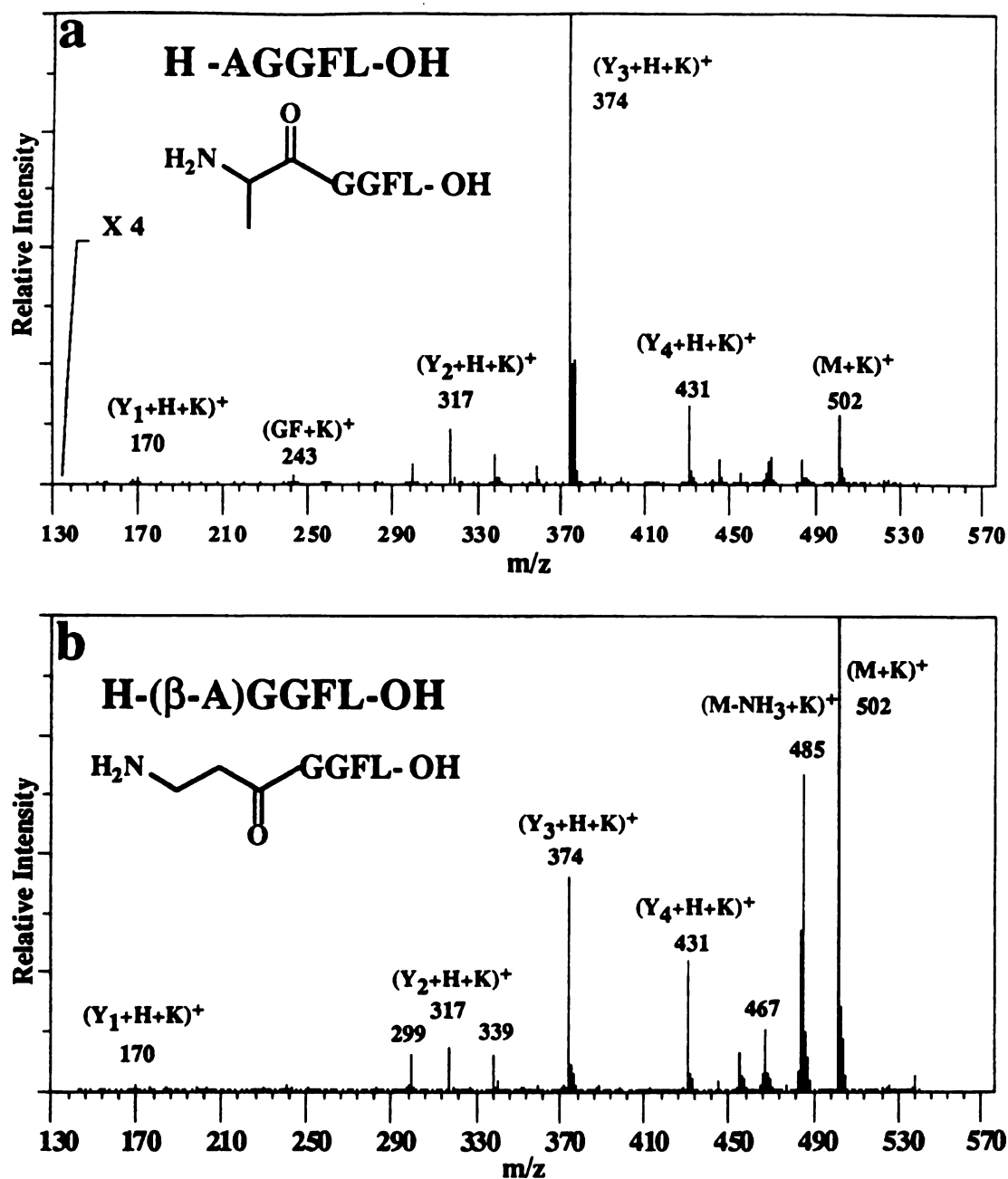


Figure 3.14 K⁺IDS mass spectra of: a) H-AGGFL-OH; b) H-(β-A)GGFL-OH.

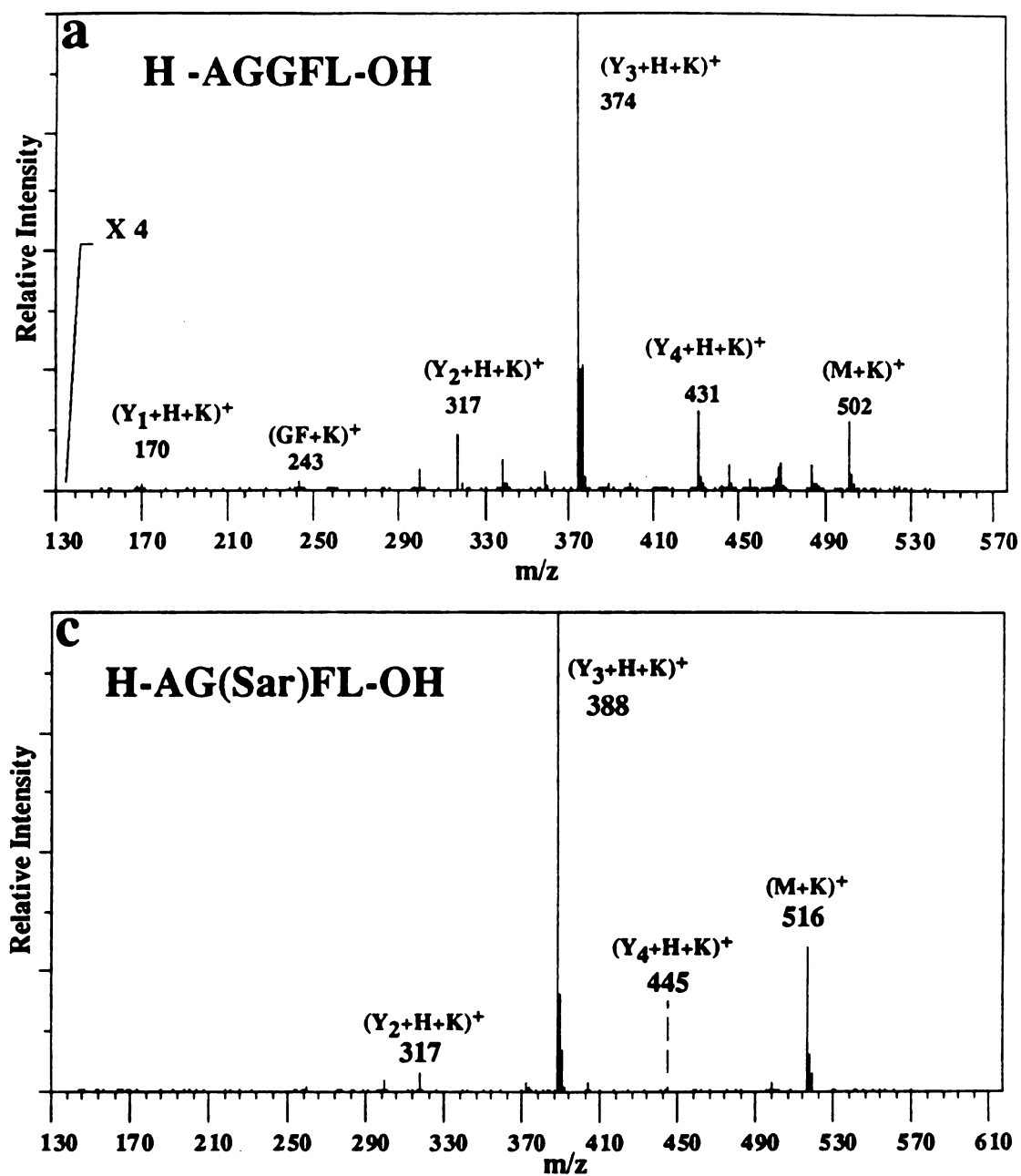


Figure 3.14 K⁺IDS spectra of: a) H-AGGFL-OH; c) H-AG(Sar)FL-OH.

cyclization occurs. It also may be concluded that aromatic side chains have nothing to do with the dominant cleavages which lead to the formation of the major ions.

Spectra of two peptides (Figure 3.13), H-VGGFL-OH and H-GGVFL-OH, with the same amino-acid composition but different sequences, were also examined. When the sequence of a peptide is changed (not the amino acid composition) as in this case, changes in the relative abundances of the same ion series are observed. For example, $(Y_4+H+K)^+$ is as abundant as $(Y_3+H+K)^+$ for H-GGVFL-OH. For H-VGGFL-OH, the $(Y_4+H+K)^+$ is much less abundant than $(Y_3+H+K)^+$ because the formation of the later is more favored. Similar reactions have been observed when the N-terminal amino acid is glycine. For example, with H-GGFL-OH and H-GPGG-OH, loss of the N-terminal glycine is also favored. Therefore, the presence of glycine at the N-terminus of a peptide may affect bond cleavages in thermal degradation of peptides.

Three peptide variants with the same sequence, but with simple modifications along the peptide chain, were studied. H-AGGFL-OH, H-(β -A)GGFL-OH and H-AG(Sar)FL-OH are the three peptides studied. The β -alanine residue ($NH_2CH_2CH_2COOH$) has its NH_2 at the β -position while the regular alanine has its NH_2 at the α -position. Sarcosine [$NH(CH_3)CH_2COOH$] is very similar to glycine (NH_2CH_2COOH) except that one of the N-terminal hydrogens is replaced by a methyl group. When a modification is made to the peptide skeletal bonds, the thermal degradation pattern may change. For example, when the N-terminal α -alanine is changed into β -alanine, the spectrum changes significantly in terms of relative intensities of all the ions (Figure 3.14). With α -alanine, $(Y_3+H+K)^+$ ions dominate the spectrum, indicating that there exists one dominant degradation reaction. With β -alanine, all ions formed are of comparable abundances, suggesting that there is no dominant reaction. Also the intense peak of $(M+K)^+$ indicates that this peptide is much more stable than the former due to the difference in amino group positions of the N-terminal amino acid residue.

No dramatic change has been noticed when one of the amide hydrogens was replaced by a methyl group (glycine to sarcosine). The spectra of two peptides, H-AGGFL-OH and H-AG(Sar)FL-OH, are comparable, with $(Y_3+H+K)^+$ dominant. This suggests that the N-terminus of a peptide affects more than amides on thermal degradation of peptides. However, the introduction of a methyl group does make the peptide more stable, and it changes the distribution of degradation products as well.

E. Internal ions from peptides.

In FAB-M/S, an internal ion is formed when two skeletal bonds are cleaved with the charge on the middle fragment. In K^+ IDS, internal ions are also observed, especially for proline-containing peptides. This is the same in K^+ IDS. The internal ions observed are shown in the following peptides.

<u>Peptide</u>	<u>Internal ions observed</u>
H-VGGFL-OH / H-YGGFL-OH	[cyclo-(GF)] K^+ at m/z 243
H-VGVAPG-OH	[cyclo-(AP)] K^+ at m/z 207
CBZ-GPGGPA-OH	[cyclo-(GP)] K^+ at m/z 195
t-BOC-PPPP-OH	[cyclo-(PP)] K^+ at m/z 233
CBZ-GPFPL-OH	[cyclo-(PF)] K^+ at m/z 283

The presence of these internal ions usually provides only very limited structural information and only can be used to confirm a partial sequence of a peptide.

IV. Peptide sequencing by K^+ IDS mass spectrometry

Peptide sequencing is one of the most successful applications of mass spectrometry. The success of peptide sequencing by mass spectrometry lies in the basic

structures of peptides, which contain repeating units of -NH-CHR-CO- with R different for different amino acids. Because of this property, peptides contain only three basic skeletal bonds: NH-CHR , CHR-CO and CO-NH . When consecutive ions from cleavages of the same type of bonds such as CO-NH bonds, the mass difference of these two ions reveals the mass of an amino acid residue, from which one amino acid residue is identified (For isomeric leucine and isoleucine or for isobaric glutamine and lysine, other ion series or derivatization have to be used for the differentiation). A complete set of such ions, therefore, can give a complete sequence of the peptide. If one ion series is not complete, only a partial sequence can be deduced from that ion series. Other ion series have to be identified to complete the missing sequence by overlapping the partial sequences deduced from each ion series. In favorable cases, a complete sequence can be finally determined.

The K^+IDS spectrum of a peptide H-YGGFL-OH (Figure 3.8a), for example, can be used to illustrate this technique. Because $(\text{Y}_n + \text{H} + \text{K})^+$ ions are the dominant ions for underivatized peptides, they will be used for the purpose of sequence analysis. The mass difference of the first few peaks from the molecular ion peaks is too small to correspond to any amino acid residue. The peak at m/z 431 is 163 mass units lower than the peak at m/z 594, indicating that the first amino acid is a tyrosine residue. The next major peak at m/z 374 is 57 mass units lower than the peak at m/z 431, indicating a glycine residue by difference. This process is repeated for peaks at m/z 374, 317 and 170; and a complete sequence is obtained for this peptide: H-YGGFL/I-OH . Note that isoleucine and leucine cannot be distinguished with this technique.

For real peptide sequencing, interpretation of a mass spectrum of a peptide is not always a trivial task. A mass spectrum can contain many incomplete ion series (including ion series from side chain fragments) and interpretation of a spectrum can be very slow. Computer programs [8-11] have been introduced to speed up such tedious processes and the best sequence fit can be obtained within a few minutes.

For peptide sequencing with K^+IDS , the most important ion series are $(Y_n+H+K)^+$ ion series for underivatized peptides, $(C_n+H+K)^+$ and $(Y_n+H+K)^+$ ion series for peptide amides, and $(B_n+OH+K)^+$ ion series for N-terminally derivatized peptides.

There are some advantages for the application of this technique for peptide analysis. It is easy to implement on any quadrupole instrument with a direct insertion probe. The technique is inexpensive to use. The instrument is simple. Obtaining a K^+IDS spectrum is very fast and the spectra are easy to interpret. All of the ions are from the analyte molecules since no matrix is used. However, the best application of K^+IDS analysis is still limited to peptide confirmation - both sequence and molecular weight - due to the limitations shown below.

There are some serious limitations for peptide sequencing by this K^+IDS technique. For di-peptides, no skeletal bond fragment ions can be observed due to fast desorption without skeletal bond cleavages. Frequently, the only fragment ion is from dehydration. For tri-peptides, sequencing could be difficult since peptides with low polarity may not degrade significantly before desorption. The ideal peptides for analysis by K^+IDS are tetra- to hepta- peptides. With larger ones, thermal degradation may dominate and it can be difficult to obtain molecular weight information. With large peptides or proteins, K^+IDS spectra can be very complicated, if obtainable. Figure 3.15 shows the spectrum of a peptide of 22 amino acid residues from a mass spectrometer with a mass range of 1000 Da. It can be seen that most of these peaks are not labeled because thermal degradation of this large molecule is too complicated.

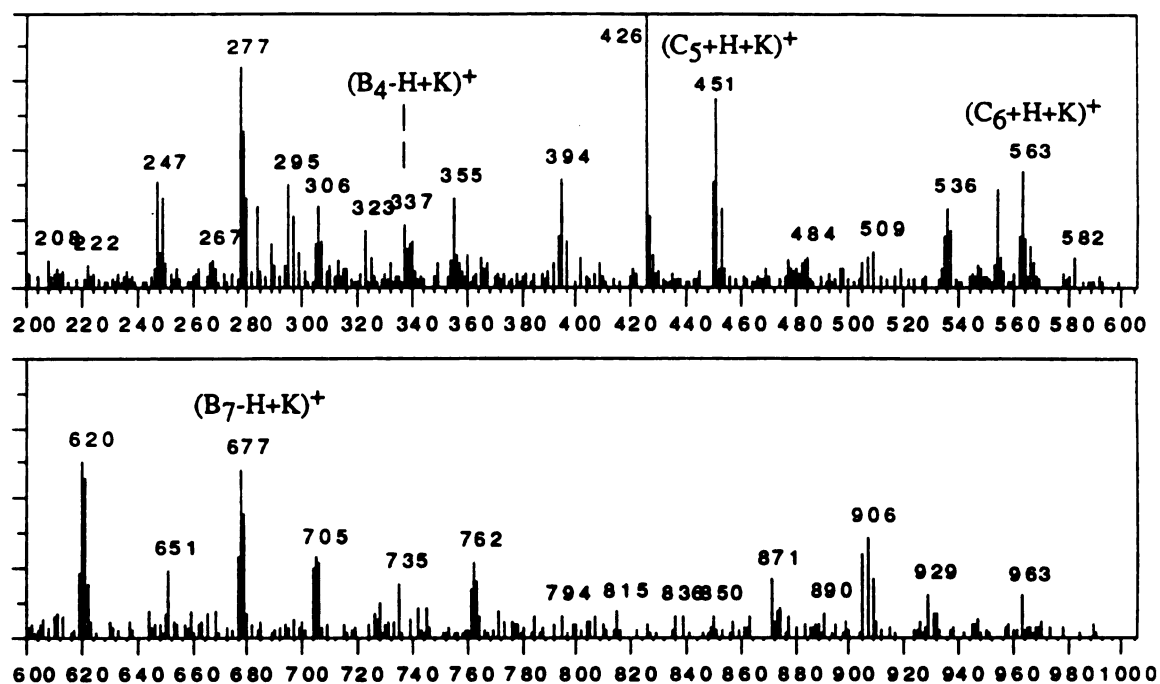


Figure 3.15 K⁺IDS mass spectrum of a 22mer peptide Melittin (MW 2846.7).

The sequence of the peptide is H-GIGAVLKVLTTTGLPALISWIKRKRQQ-NH₂.

References

1. Bombick D.; Pinkston, J. D.; Allison J. *Anal. Chem.* **1984**, 56, 396-402.
2. Bombick, D.; Allison, J. *Anal. Chem.* **1987**, 59, 458-466.
3. Kassel, D. B.; Allison, J. *Biomed. Environ. Mass Spectrom.* **1988**, 17, 221.
4. Light, K., *Doctoral Dissertation*, Michigan State University, **1990**.
5. Knapp, D. R. "Chemical Derivatization for Mass Spectrometry" in *Methods in Enzymology*, vol. 193, McCloskey, J. A., ed., Academic Press: San Diego, **1990**; pp 314-328.
6. Roepstorff, P.; Fohlmann, J. *Biomed. Mass Spectrom.* **1984**, 11, 601-601.
7. Stults, J. "Peptide Sequencing by Mass Spectrometry", in *Biomedical Application of Mass Spectrometry*, vol 34, Suelter, C. H.; J. T. Watson ; ed., Wiley: New York, **1990**; pp145-201.
8. Johnson, R. S.; Biemann, K. *Biomed. Environ. Mass Spectrom.* **1989**, 18, 945.
9. Alberth W.; Straub K. M.; Burlingame A. L.; *Anal. Chem.* **1982**, 54, 2029
10. Siegel, M. M.; Basuman, N. *Biomed. Environ. Mass Spectrom.* **1988**, 15, 333.
11. Sakurai, T.; Matsuo, T.; Matsda, H.; Katakuse, I. *Biomed. Mass Spectrom.* **1984**, 11, 396.

Chapter 4

The Characterization of the Primary Thermal Degradation Processes of Peptides

I. Introduction

The pyrolysis/thermal degradation of organic molecules is a process that has been used both for the production of chemicals and for analysis [1]. In the latter, mass spectrometry (MS) has been an important tool in characterizing products of pyrolysis (Py) of organic compounds, both directly in techniques such as in Py/MS, and with an additional separation step such as in Py/GC/MS. In pyrolysis studies, temperatures of 600-800°C are frequently used. The characterization of thermal degradation processes can be challenging since, under some conditions, primary degradation products decompose further and undergo subsequent chemistry, yielding complex mixtures of products. To date, little work has been reported on the thermal stability/thermal degradation of peptides in general; however information is available on the pyrolysis of small dipeptides and amino acids [2].

In this chapter, the K^+ IDS technique will be utilized for the characterization of the primary thermal degradation chemistry of peptides. The strength of the K^+ IDS technique is in the simplicity of both the experiment and the resulting mass spectra. Since each thermal degradation product gives one peak in the mass spectrum, K^+ IDS mass spectra reflect a "molecular weight distribution" of the thermal degradation products of the analyte molecules, which, in combination with analogous studies of derivatized and isotopically-labeled compounds, can be used for the study of unimolecular, condensed

phase thermal degradation chemistry. The approaches presented here are designed to provide insights into the structures of the thermal degradation products, and to demonstrate a unique and simple tool for characterizing thermal degradation processes for biomolecules, as well as other thermally-labile compounds.

Because of the importance of the process, which has been detailed in part II of Chapter 1, a thorough study has been conducted in this chapter. Deuterated peptides have been prepared to trace the source of the shifting hydrogen atoms. Derivatized peptides have been used to determine the roles of peptide termini in thermal degradation. Specifically designed peptides have been synthesized and used to test the proposed mechanisms. The effects of varieties of the termini of peptides and steric hindrance have been considered in thermal degradation. At the end of this chapter, thermodynamics and kinetics are used to support the proposed mechanisms.

II. Experimental Section

All mass spectrometric analyses were performed on an unmodified HP5985 GC/MS/DS quadrupole mass spectrometer with a mass range of 10-1,000 Daltons equipped with a modified direct insertion probe, similar to that reported previously by Röllgen et al. [3] and by Kassel and Allison [4]. The probe places two wire filaments into the ion source. One filament serves as the thermionic emitter, generating K^+ ions when resistively heated. The other filament serves as the sample holder from which the analyte molecules undergo thermal degradation and desorption. The sample holder is radiatively- heated from the ionic emitter or resistively heated with a separate power supply (direct heating). The analyte molecules and their degradation products are thermally desorbed from the sample holder and form adducts in the gas phase with the potassium ions emitted from the thermionic emitter.

The peptides H-GP-OH, H-GGFL-OH, cyclo-GP, H-YGGFL-OH, and H-FGGF-OH were obtained from the Sigma Chemical Co. , St. Louis, Missouri, and used without further purification. H-AGGFL-OH, H-(β -A)GGFL-OH (β -A is β alanine), H-VGGFL-OH, H-GGVFL-OH, H-VGVAPG-OH, H-VGVA α dPG-OH, H-V β dGV β dAPG-OH, and H-AF β d²LA-OH were synthesized in the laboratory of Dr. Phil Andrews at the University of Michigan. The three partially-deuterated peptides listed above, were synthesized with the corresponding deuterated amino acids as the starting materials. N-terminally acetylated peptides such as Ac-VGVAPG-OH, are formed from the free peptide using acetic anhydride and a small amount of pyridine as a catalyst, by the procedure described by Knapp [5].

All of the samples used in K⁺IDS experiments were dissolved or suspended in methanol to allow transfer of 1-2 μ l of sample onto the tip of the sample holder. The solvent was evaporated off before the probe was inserted into the mass spectrometer.

III. The Primary Thermal Degradation Processes of Peptides

The thermal degradation chemistry for peptides, involving skeletal bond cleavage with an accompanying hydrogen atom shift, had been proposed [6-7] to follow a 1,2 - elimination process, Figure 4.1. However, additional experimental results suggest an alternative mechanisms should be proposed because it cannot explain many experimental observations. A 1,2-elimination mechanism would suggest that the probabilities of cleavage of any of the amide bonds would be similar, since the process involves only amide bonds and adjacent H atoms. In our experiments, however, the rates for cleaving the various amide bonds differ dramatically throughout a single peptide, as well as from one peptide to another. Also, this mechanism cannot explain the formation of [C+H+K]⁺ ions, which are occasionally observed, since there is no hydrogen atom at the required position (on the carbonyl group) to participate the reaction.

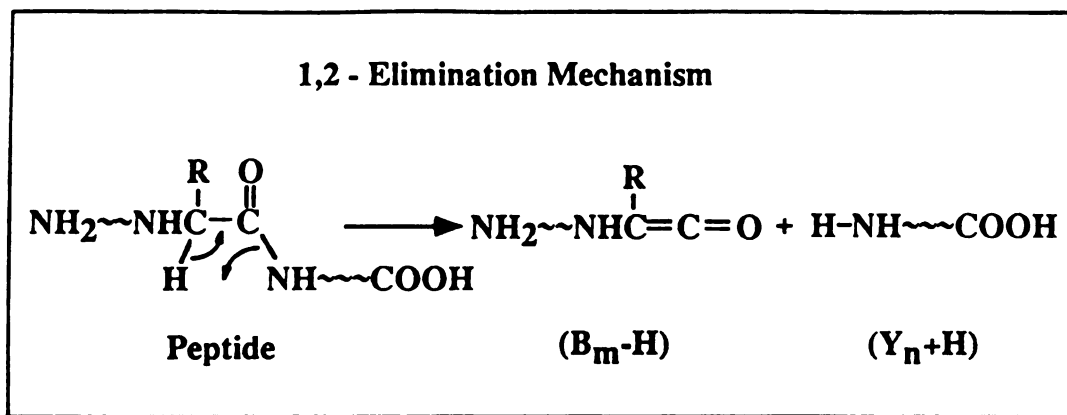


Figure 4.1 A schematic diagram for the 1,2 - elimination mechanism showing thermal degradation of peptides.

Because the 1,2-elimination mechanism is inconsistent with the experimental results for peptides, alternative degradation mechanisms were considered. Since H-shifts are frequently involved in the thermal degradation of peptides, as well as other thermally-labile molecules [6-7], determining the source of the shifting H is key to determining the mechanism. This can be done using deuterium labeling.

A. Deuterium-labeling Experiments

Two deuteration approaches for peptides have been successfully used. The first method involves deuterium exchange in a deuterated solvent such as CH_3OD and D_2O . Hydrogen atoms that are bound to the N-terminal nitrogen, amide nitrogens, and the C-terminal carboxylate group can be exchanged easily at room temperature within seconds. To demonstrate the utility of H/D exchange, consider the dipeptide H-GP-OH. When this small peptide is subjected to rapid heating, desorption of the intact molecule dominates. A fraction of the molecules dehydrate, and the (M-H $_2$ O) molecules desorb as well. The elimination of water from a peptide poses the same questions as the processes in which skeletal bonds cleave. To eliminate H $_2$ O, a C-OH bond cleaves with an accompanying H-shift. What is the source of the shifting hydrogen atom? Water elimination is analogous to the process that forms B- and Y-type products. With small dipeptides, skeletal bond fragmentation is usually a minor process relative to water elimination, thus they provide an opportunity for characterizing this particular process. Also, small peptides contain a relatively small number of exchangeable H atoms, and it is easier to approach 90+% H/D exchange.

If H-GP-OH is dissolved in D_2O , placed on the K^+IDS probe, and the experiment performed, the spectrum shown in Figure 4.2a is obtained. There are 3 exchangeable H atoms in this dipeptide. Complete exchange of these three H atoms yields a K^+ -adduct of the intact peptide at m/z 214. Those molecules undergoing

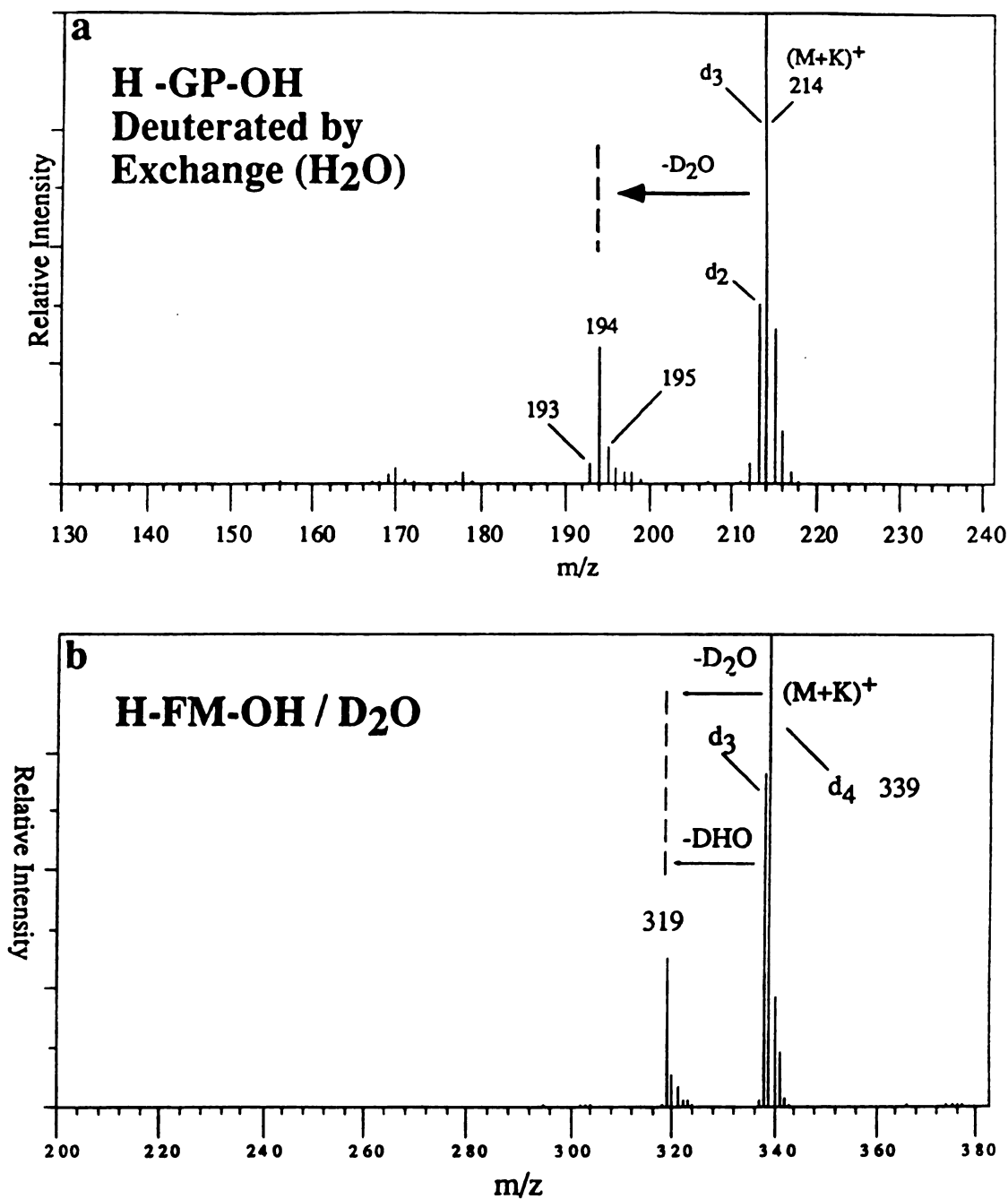
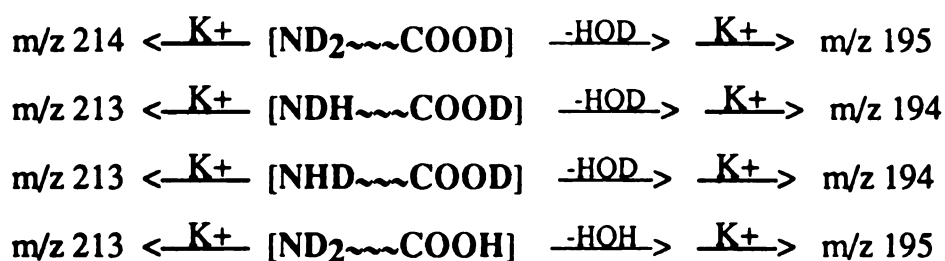


Figure 4.2 K^+ IDS mass spectra of: a) H-GP-OH that had been exposed to D_2O ;
b) H-FM-OH that had been exposed to D_2O .

incomplete exchange are represented by the peaks at lower m/z values. The distribution of the $[M+K]^+$ peaks indicates that 90% of the exchangeable H's have been replaced by deuterium atoms.

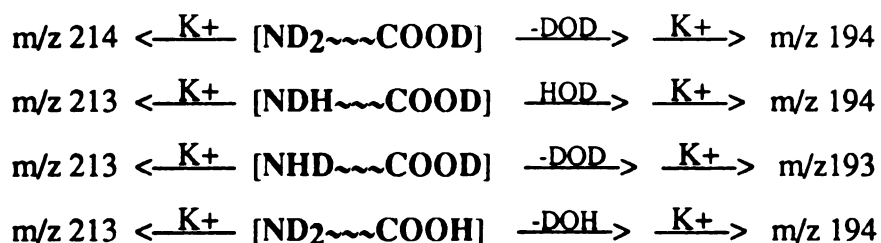
The dipeptide H-GP-OH has the elemental composition $C_7H_{12}N_2O_3$. The deuterated form that can be obtained via H/D exchange is $C_7H_9D_3N_2O_3$. In the spectrum of the deuterated dipeptide, the m/z value of the dominant peak representing the dehydration product is 194, which corresponds to $[C_7H_9D_1N_2O_2+K]^+$. The relationship of the isotopic variants for this species, relative to that for the $[M+K]^+$ ions is as follows. If the loss of H_2O , in the form of DHO or H_2O , goes through a 1,2- elimination process, the degradation will produce the following ions:



Each expression inside the brackets indicates the two termini of the deuterated peptide and the m/z value of the corresponding K^+ -adduct is on the left side of the expression. The abundance of the K^+ -adduct of the each deuterated variant reflects its relative abundance. When a water molecule is lost from the peptide molecule, the adduct formed will have the m/z value shown on the right side. If exchange of each candidate H atom occurs to approximately the same extent, and the water elimination occurs via a 1,2-elimination (involving a H atom close to the C-terminus) the expected ratio of m/z 194 to 195, based on statistical analysis, would be 1: 5, which is NOT in agreement with the experimental value of 4:1. The expected ratio of m/z 194 to 195 is calculated as follows: The relative quantities of the completely exchanged peptide H-GP-OH(d3) and the partially exchanged peptide H-GP-OH(d2) are 100 to 35 based on the intensity ratio of

their K^+ adducts at m/z 214 and 213. Based on the above chart, the expected ratio of m/z 194 to 195 should be $(35 \times 1/3) : (100 + 35 \times 2/3) \approx 1:5$. The experimental ratio of m/z 194 and 195 is based on the relative intensities of the peaks at these m/z values.

However, if the loss of $H_2O/HDO/D_2O$ is through a 1,6-elimination in which the shifting H atom is from the N-terminus (allowing for a D-shift from the opposite end of the molecule), the elimination would allow for the loss of D_2O , and would give the following ions:



The expected ratio of m/z 193 to 194 will be $(40 \times 1/3) : (100 + 40 \times 2/3) = 1:9$, which is in very good agreement with the experimental data (1:6). Simply, the spectrum suggests that most of the dipeptide molecules contain 3 deuterium atoms, and the water elimination involves the loss of D_2O . This can only happen via a cyclic intermediate. Therefore, the loss of H_2O in the thermal degradation of this dipeptide occurs via a 1,6-elimination process.

Analyses of another dipeptide H-FM-OH also give the same conclusion, as shown in Figure 4.2b. For this peptide, a greater exchange rate at the C-terminus $COOH$ is suggested based on the following: Because the completely exchanged peptide H-FM-OH (d_4) is more abundant than the partially deuterated peptide H-FM-OH(d_3), the dominant formation of ions at m/z 319 indicates a loss of D_2O molecule, which suggests that the dehydration process is a 1,3- or 1,6-elimination process. The weak ion intensity at m/z 318 thus suggests a dominant loss of DHO from H-FM-OH(d_3) with one exchangeable hydrogen undeuterated. Apparently if the undeuterated hydrogen is on the C-terminus

only, then the loss of DHO will be the only reaction for H-FM-OH(d3), which leads to no ion current at m/z 318. This is almost exactly true, suggesting that the undeuterated exchangeable hydrogen is at the C-terminus mostly. Therefore, the exchange rate at the C-terminus must be the greatest among the four exchangeable sites of the peptide. (Note: The peptide is assumed to be exchanged completely first. Inside the vacuum lock and the ion source, back exchanges occur due to the presence of trace amount of H₂O vapor.)

The H/D exchange in D₂O was also undertaken with larger peptides such as the hexapeptide H-VGVAPG-OH, which has seven exchangeable H atoms. The resulting K⁺IDS spectrum is shown in Figure 4.3b. The H/D isotopic variants of the [M+K]⁺ ion suggest extensive deuterium incorporation, with more than 87% of the exchangeable sites deuterated [For the molecular ions, there are three peaks representing the deuterated peptide adducts containing seven, six and five deuterium atoms, respectively. The relative intensities of these deuterated peptides are 90%, 100% and 70% respectively. Therefore, the percentage deuteration = $100 \times (90 \times 7 + 100 \times 6 + 70 \times 5) / (90 \times 7 + 100 \times 7 + 70 \times 7)$, in this case]. In this hexapeptide, the dominant ion is the [Y₄+H+K]⁺ species; resulting from cleavage of the amide bond with a H shift onto the C-terminal fragment. An analysis of the isotopic species shows that an exchangeable H shifts in the process, thus a D-shift is observed in this case as well. It cannot be unambiguously determined whether the source of this shifting D is the N-terminal amine group, or an amide nitrogen in the N-terminal fragment. However, it is important to note that the bond cleavage/H shift is not a 1,2-elimination reaction, so H's that are 3 or more skeletal atoms away must be involved in the chemistry.

The second way to prepare partially-deuterated peptides is to use partially-deuterated amino acids in the peptide synthesis. In this way, deuterium atoms can be placed on carbon atoms in the peptide skeleton as well as in side-chains. The following partially-deuterated peptides were synthesized for this study: H-VGVA^αdPG-OH, H-VGVA^β3dPG-OH, H-V^αdGV^αdAPG-OH, H-V^βdGV^βdAPG-OH and H-AF^β2LA-OH,

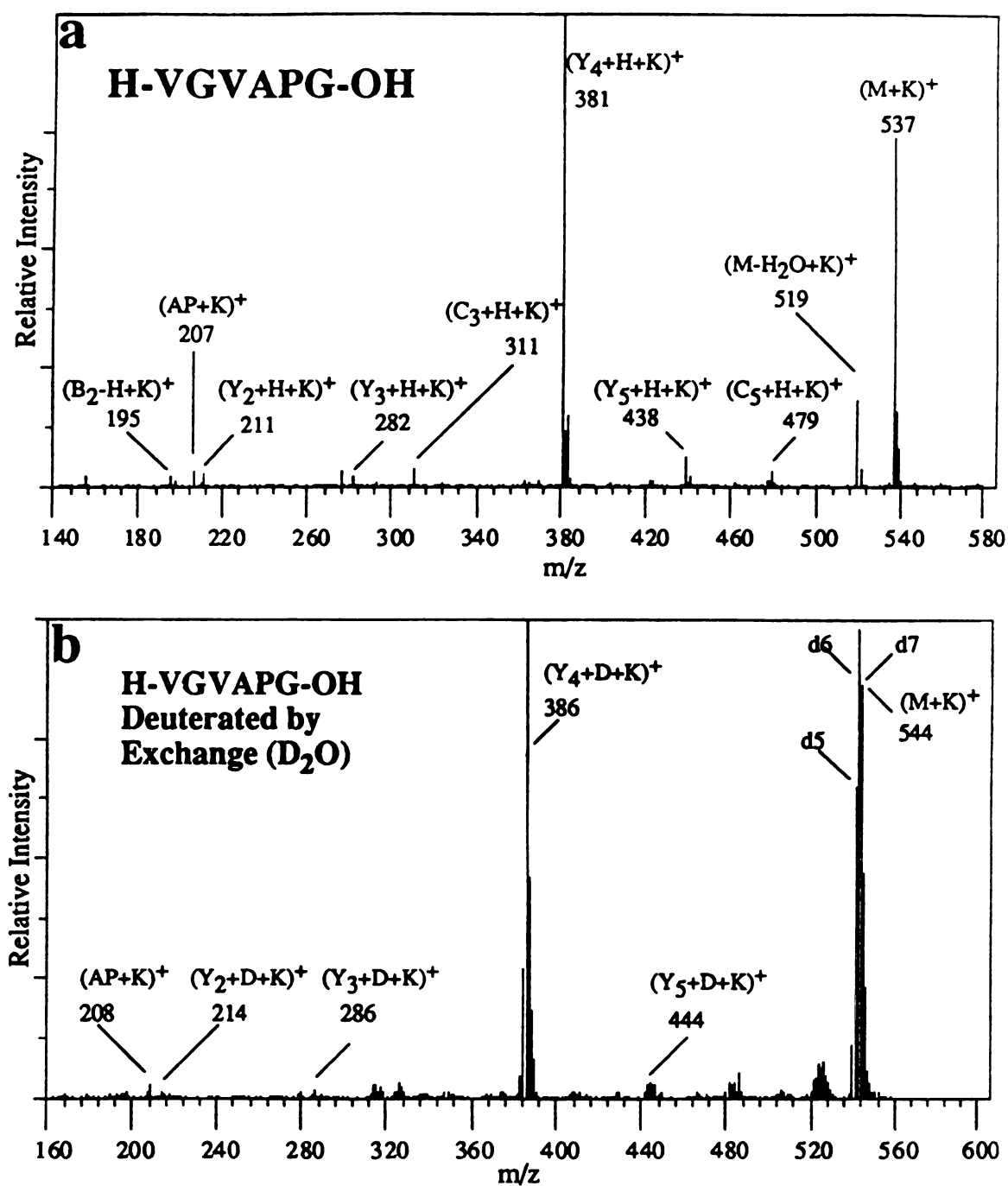


Figure 4.3 K^+ IDS mass spectra of: a) H-VGVAPG-OH; b) H-VGVAPG-OH exposed to D_2O (hydrogens bonded to N and O atoms are exchanged to deuteriums).

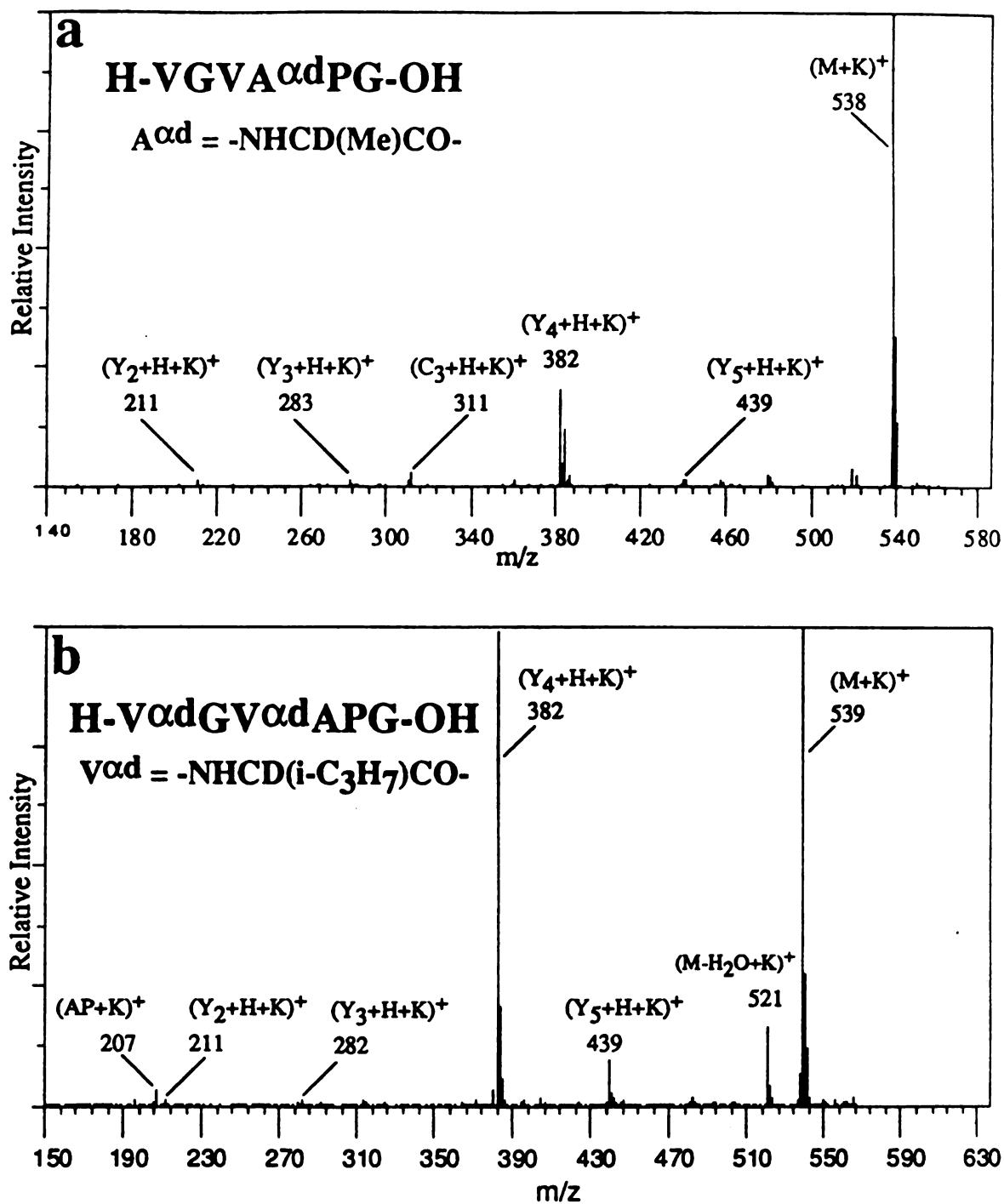


Figure 4.4 K^+ IDS mass spectra of: a) H-VGV α dPG-OH; b) H-V α dGV α dAPG-OH.

with α and β designating the deuterium position(s). In these peptides, some deuteriums are present on the backbone of the peptide chain such as $-\text{CDCH}_3$ - (in $\text{A}^{\alpha\text{d}}$), and others on the sidechains of the molecules such as $-\text{CD}_3$ (in $\text{A}^{\beta 3\text{d}}$) and $-\text{CD}(\text{CH}_3)_2$ (in the $\text{V}^{\beta\text{d}}$ residue).

The K^+IDS spectra of unlabeled H-VGVAPG-OH , as well as $\text{H-VGVA}^{\alpha\text{d}}\text{PG-OH}$, and $\text{H-V}^{\alpha\text{d}}\text{GV}^{\alpha\text{d}}\text{APG-OH}$ are shown in Figures 4.3a, Figure 4.4, respectively. The spectra show that the deuterium incorporation by synthetic methods is complete, and no reverse-exchange occurs. The results consistently show that, when Y-type ions are formed, H shifts only occur from nitrogen sites - amide groups and/or the N-terminus. The source of the shifting H atoms is not those H's that are bound to carbon atoms in the amino acid residues.

When these experiments are performed, the bond energy of the C-H bond cleaved is also considered. Since the C- βH bond in phenylalanine ($\text{R} = -\text{CH}_2\text{C}_6\text{H}_5$) is one of the lowest in peptides, the β -deuterated peptide $\text{H-AF}^{2\beta\text{d}}\text{LA-OH}$, was synthesized and the H-shift in this peptide was studied. Consistently, the same result was obtained - no H shifts from the side-chains occur.

All the experiments with deuterated peptides lead to the same conclusions. Such deuteration experiments alone, however, do not allow for definite determinations of the sources of the shifting H that accompanies skeletal bond cleavage to form the dominant degradation product, $(\text{Y}_n + \text{H})$. To complete the investigation, other variants of the peptides were characterized.

B. Peptide Derivatization - Evidence for Cyclization

As demonstrated above, a shifting hydrogen atom is not from α -carbons; it can only be from either amides or the N-terminus of a peptide. If the N-terminus of a peptide is blocked, then the only choice will be amides.

Insights were gained in the thermal degradation chemistry of small peptides via the N-acyl derivatives. When a peptide is N-acetylated, and there is no longer an amino group at the N-terminus, changes in the K^+ IDS mass spectra are observed. For the underivatized hexapeptide H-VGVAPG-OH, as shown in Figure 4.3a, the dominant ions observed in the K^+ IDS spectrum are the $[Y_n + H + K]^+$ ions, as has been previously discussed. When the N-terminus of H-VGVAPG-OH is blocked with an acetyl group forming CH_3CO -VGVAPG-OH, the dominant ions observed are no longer $[Y_n + H + K]^+$ ions. Instead, an unexpected series of ions of the type $[B_n + OH + K]^+$ and $[C_n + H + K]^+$ ions become dominant (see Figure 4.5). These observations suggest a scenario which is summarized in Figure 4.6. First, since there is such a dramatic change in the chemistry upon acylation when the N-terminal amino group is removed, then the thermal degradation chemistry for underivatized peptides that yields molecules of the type $(Y_n + H)$ must involve a H-shift from the N-terminus. When this group is removed, no Y-type products are formed. Second, if the Y-type products are formed via a H-shift from the N-terminus, then the secondary structure of the decomposing peptide is critical, and must involve a cyclic intermediate. When the N-terminal amine group that can participate in H-bonding is removed, products that appear to involve cyclic intermediates through H-bonding to the C-terminus are observed. It is readily apparent that -OH shifts accompanying the cleavage of skeletal bonds many atoms away occur through cyclic intermediates when the N-terminus is blocked. Thus, the peptides appear to react through cyclic conformations. The H-bonding involving the N-terminus usually dominates. However, if the N-terminus is blocked, the C-terminus participates in important secondary interactions. Third, if peptides undergo skeletal bond cleavages and H-shifts (or OH shifts) through cyclic intermediates, then one linear product and one cyclic product should be produced in each case. Note that the dominant $(Y_n + H)$ product is formed by elimination of a cyclic, six-membered ring dipeptide. Thus, the dominant cyclic intermediate involves a H-bond via an 8-membered ring. Also, when the N-

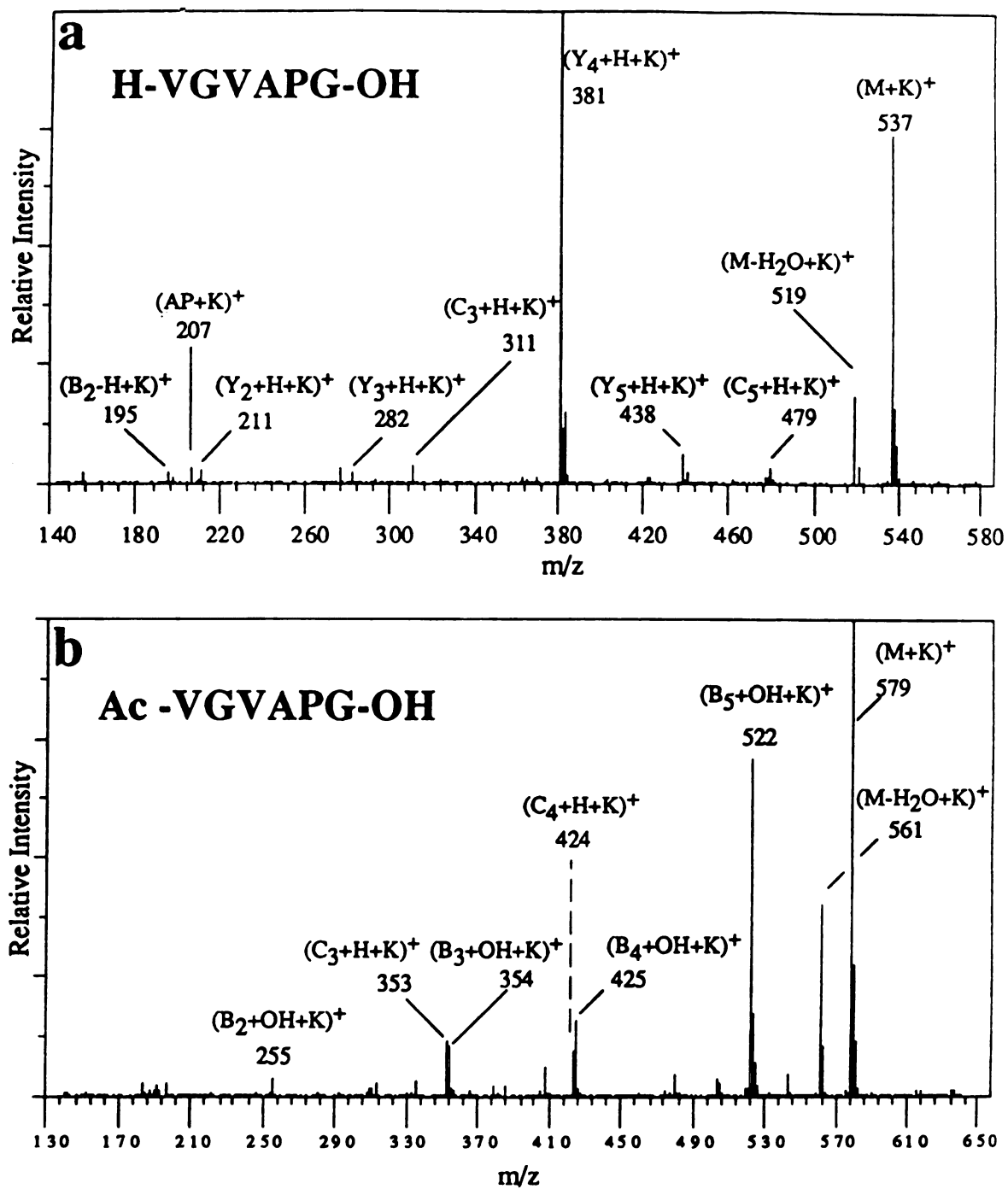


Figure 4.5 K^+ IDS mass spectra of: a) H-VGVAPG-OH; b) Ac-VGVAPG-OH.

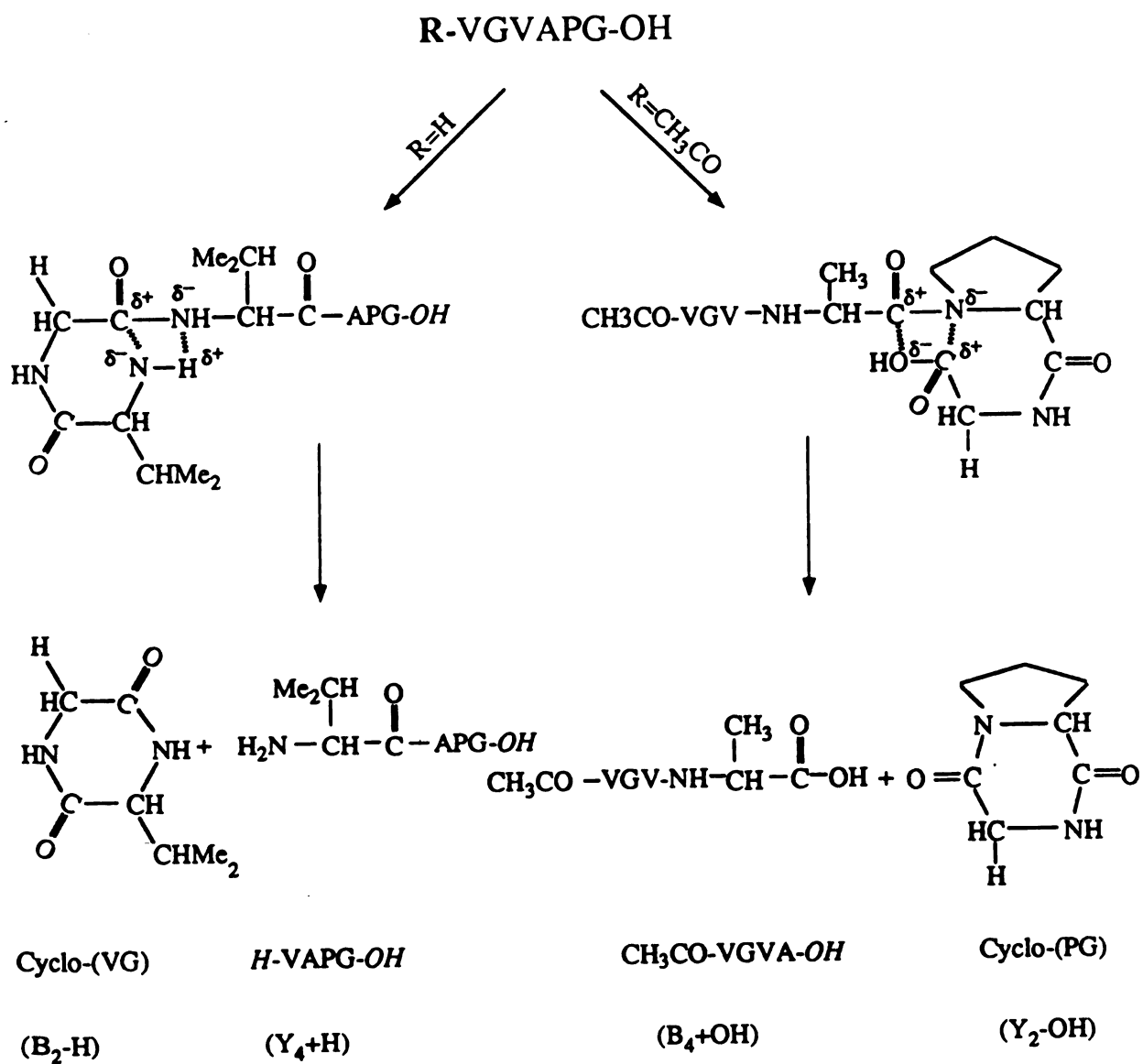


Figure 4.6 Thermal Degradation of Peptides: (H-VGVAPG-OH and Ac-VGVAPG-OH).

terminus is blocked, and cyclic intermediates involving the C-terminus form, the dominant (B_n+OH) product is formed by, again, elimination of a cyclic dipeptide. Thus, cyclic interactions that involve 6 and 8-membered rings simultaneously, as shown in Figure 4.6, form the dominant products.

Similar results from CBZ-derivatives (CBZ = carbobenzoxy- = $C_6H_5-CH_2OCO-$) such as CBZ-GPGGPA-OH, and t-BOC derivatives (t-BOC = tert-butoxycarbonyl = Me_3COCO-) such as t-BOC-PPPP-OH, were obtained (see Figure 3.11). All the results indicate that N-terminal derivatives blocks cyclizations from the N-termini and new ion series, $(B_n+OH+K)^+$ and $(C_n+H+K)^+$, characteristic of the peptide derivatives, are produced.

To further investigate the possibility of "remote" H-shifts via cyclic intermediates, the synthesis of peptides with other types of N-terminal modifications, for subsequent analysis by K^+ IDS, was pursued. Two forms of the amino acid alanine are available. In addition to the standard α -amino acid, $NH_2-CH(CH_3)COOH$, β -alanine is available, $NH_2-CH_2-CH_2-COOH$. The presence of β -alanine in a peptide will disrupt the normal sequence of the skeletal backbone ($-NH-CHR-CO-$). To investigate the influence of modifications of the N-terminus on thermal degradation, two peptides were synthesized, H-AGGFL-OH and H-(β -A)GGFL-OH, and their thermal degradation chemistries were compared. The resulting K^+ IDS spectra are shown in Figure 4.7. For H-AGGFL-OH (Figure 4.7a), formation of (Y_n+H) products dominate, with the $[Y_3+H+K]^+$ ion indicating that elimination of a cyclic dipeptide from the N-terminus is the dominating thermal degradation pathway. When the N-terminal residue is changed to β -alanine (Figure 4.7b), the spectrum changes substantially. Amide bond cleavages with accompanying H-shifts still occur, although they no longer dominate the desorbed products. Note that, if amide bond cleavages still involve H-shifts from the N-terminus, then the formation of (Y_n+H) products would involve the formation of 4-, 7-, 10-membered cyclic products. Apparently, none of these are as favored as the process that

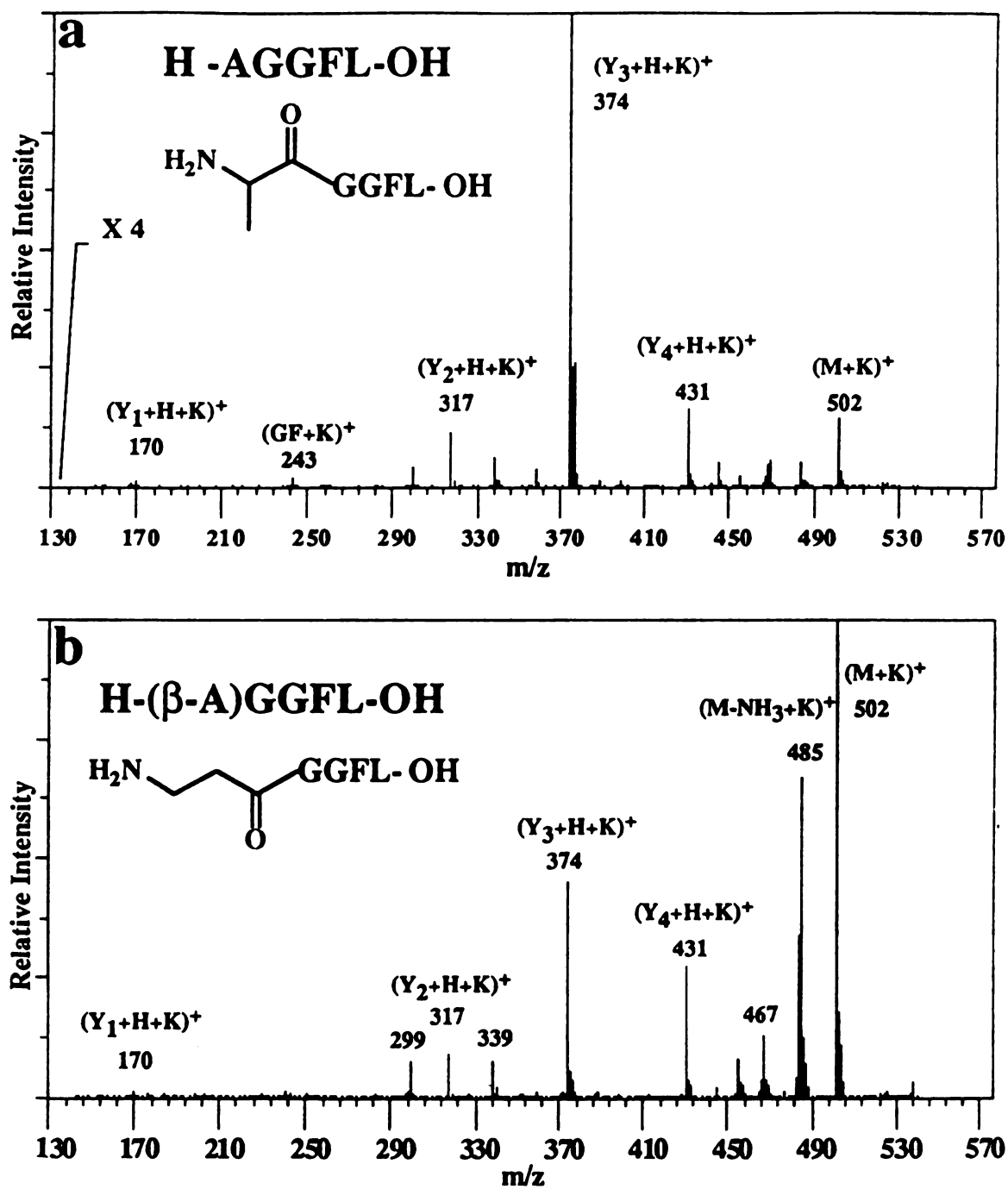


Figure 4.7 K⁺IDS mass spectra of: a) H-AGGFL-OH; b) H-(β-A)GGFL-OH.

forms a 6-membered cyclic dipeptide, which occurs for H-AGGFL-OH only. Also note that the ratio of thermal degradation to desorption of the intact molecule upon heating is smaller when β -A is at the N-terminus, leading to the $[M+K]^+$ ion as the base peak in Figure 4.7b. These changes in the spectrum when the N-terminal residue is modified in this way is consistent with the proposed importance of remote H-shifts from the N-terminus, accompanying skeletal bond cleavages throughout the peptide, and the importance of the formation of a cyclic product.

C. Termini, Sidechains and Steric Effects

It is clear from the above data that the primary, low-energy, thermal degradation chemistry of peptides involves cyclic intermediates and cyclic products. When the N-terminus of a peptide is not blocked, cyclization involves the shift of a H atom from the N-terminus; when the N-terminus is blocked, cyclization involves the C-terminal OH group. The N-bound H atoms at the termini of a peptide are, in part, most active in their participation in cyclic interactions because fewer steric obstacles are present, relative to those encountered by interior amide N-H groups.

If steric effects are important in the thermal degradation of peptides, the sizes of the sidechain of the amino acid residue at the termini may influence the distribution of thermal degradation products. Insights into one aspect of steric effects can be realized through the K^+ IDS spectra of the following series of peptides with various N-terminal residues: H-YGGFL-OH, H-VGGFL-OH, and H-AGGFL-OH. These are shown in Figure 4.8a-b and Figure 4.7a, respectively. When the N-terminal residue is Y, V or A, the spectra are essentially the same. The mechanism shown in Figure 4.6 for the free peptide dominates. Note in particular the ratio of the intensities of the ions representing $[Y_3+H+K]^+$ and $[Y_4+H+K]^+$, which are formed by eliminating neutrals containing 6- and 3-membered rings, respectively. Obviously, the former dominates. However, when the sidechain of the N-terminal residue is smaller, changes are observed. Figure 4.9b

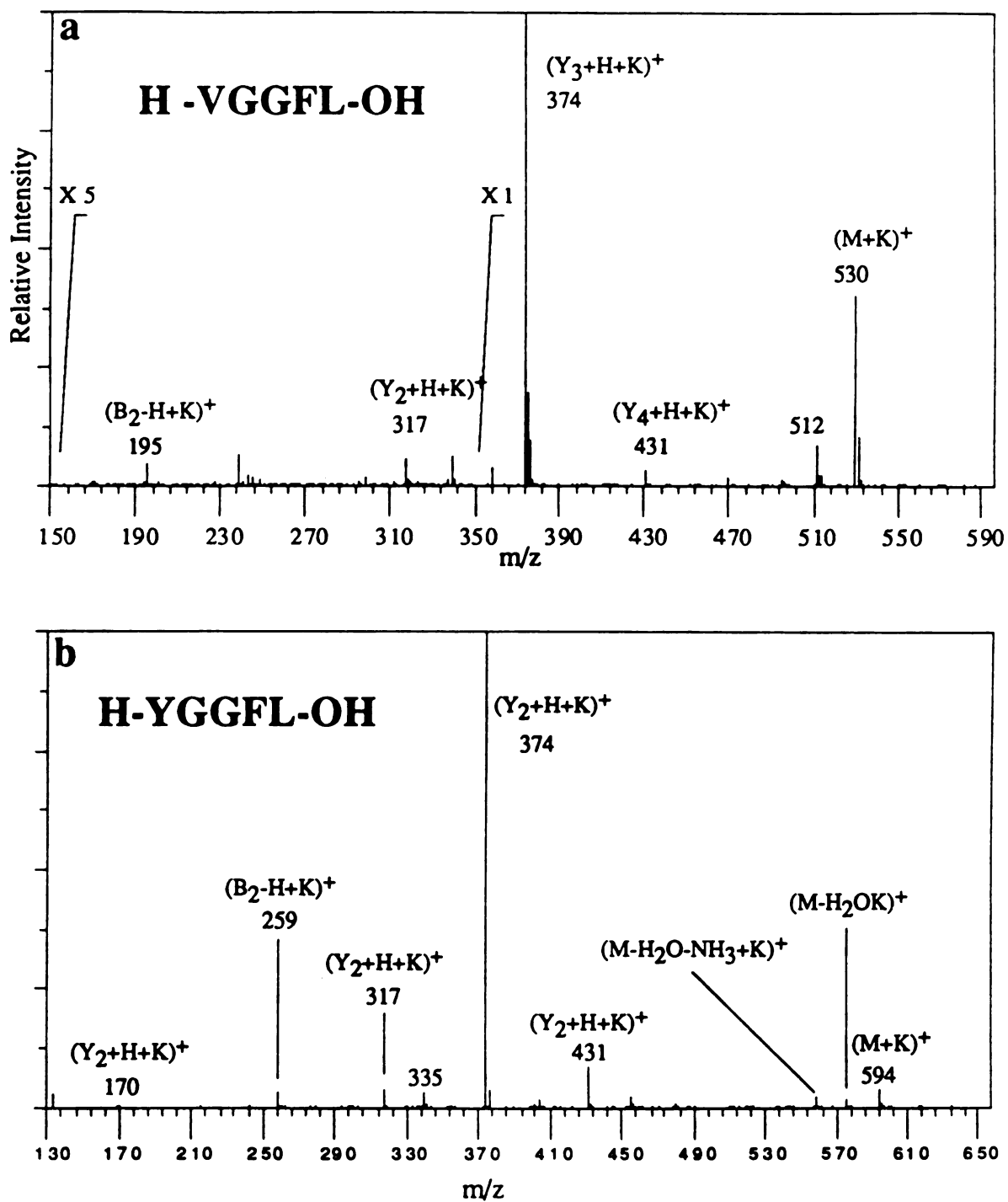


Figure 4.8 K^+ IDS mass spectra of: a) H-VGGFL-OH; b) H-YGGFL-OH.

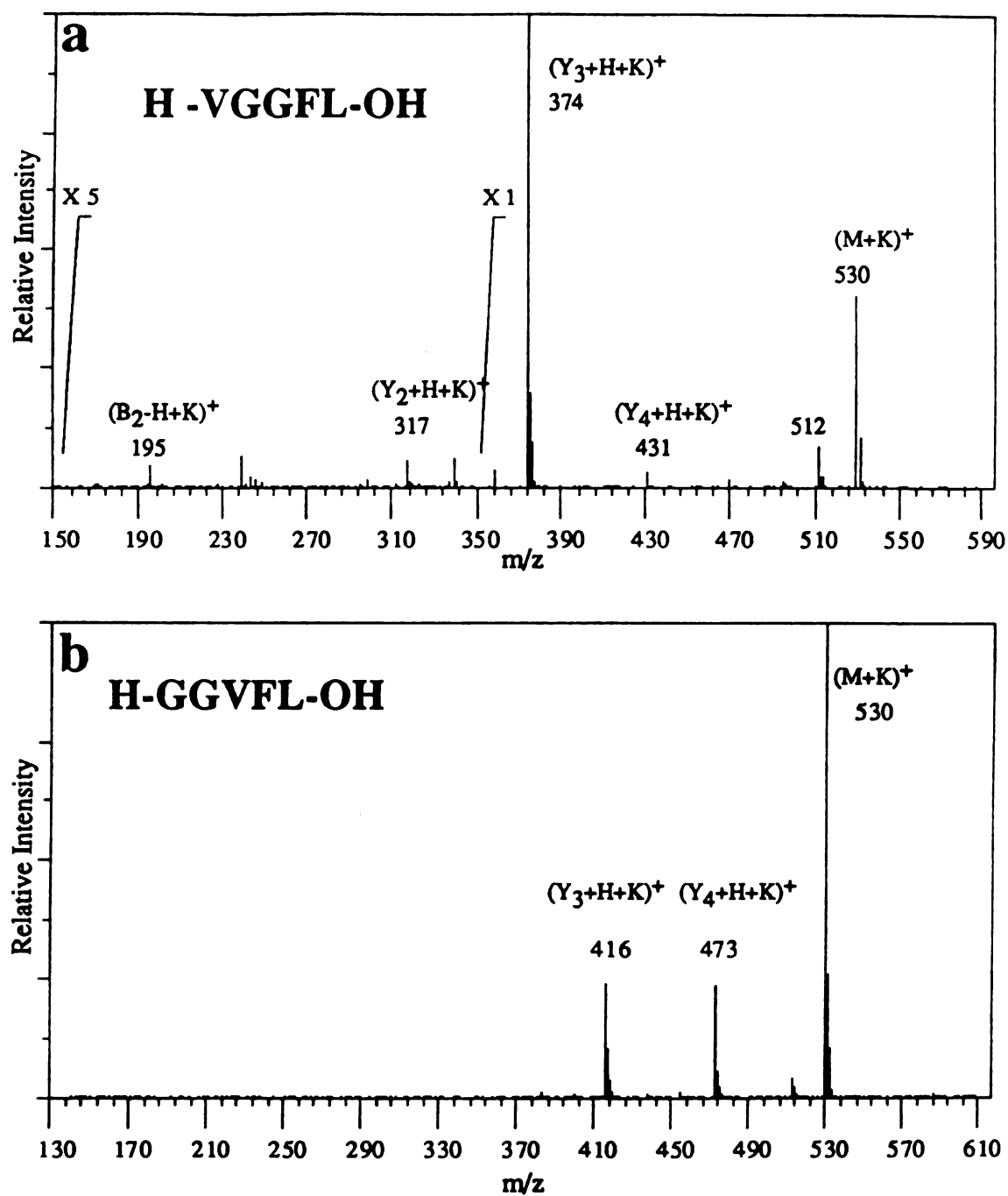


Figure 4.9 K^+ IDS mass spectra of: a) H-VGGFL-OH; b) H-GGVFL-OH.

shows the K^+ IDS spectrum of another pentapeptide, H-GGVFL-OH, in which the N-terminal glycine contains the smallest sidechain (least steric hindrance). The spectrum is very different. The relative probabilities of cleavages at various amide bonds change completely. In this case, the cleavage at the first amide bond is almost competitive with that at the 2nd amide bond. Apparently, the size of the sidechain in the N-terminal residue does have an influence on the distribution of the various cyclic intermediates, with the smallest cyclic intermediates being uncommon, unless the N-terminal residue is glycine. The same is observed in the spectrum of the tetrapeptide, H-GGFL-OH, where the N-terminal residue is again G. More peptide spectra will be useful to determine whether this effect is always observed for the N-terminal residues, and the precise secondary interactions that are involved in this "steric effect".

D. Thermodynamic aspects of the thermal degradation of small peptides

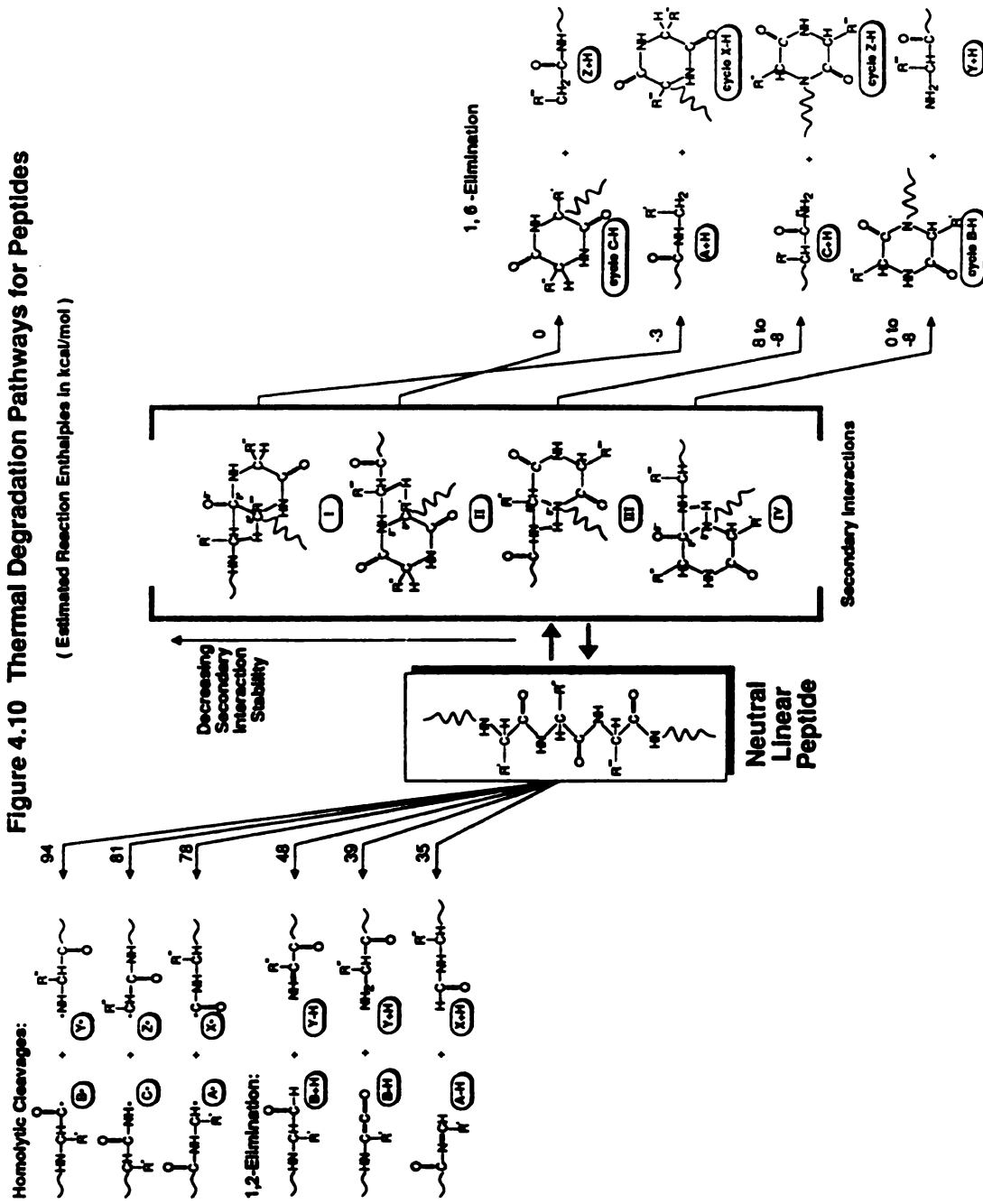
To better understand the mechanisms for the thermal degradation of peptides, thermodynamic aspects of the chemistry were considered. The experimental data presented here suggest that skeletal bond cleavages do not involve 1,2-elimination processes, but 1,n-elimination processes, where $n = 3, 6, 9$, etc. Is one energetically favored over the other?

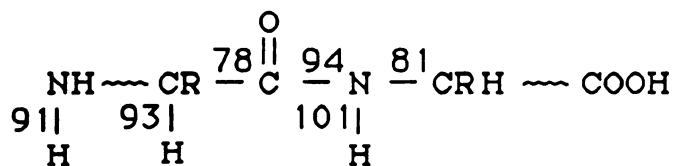
In all of the thermal degradation processes of peptide molecules that we have observed, two bonds are formed and two bonds are broken. The estimated reaction enthalpies for several possible processes are shown in Figure 4.10. To approximate the reaction enthalpies for some of the degradation processes shown, the dissociation energies of the bonds formed ($BDE(B_{f1})$ and $BDE(B_{f2})$) and bonds broken ($BDE(B_{b1})$ and $BDE(B_{b2})$) are considered, and the reaction enthalpies are estimated as follows:

$$\Delta H^\circ_{\text{rxn}} = BDE(B_{b1}) + BDE(B_{b2}) - BDE(B_{f1}) - BDE(B_{f2})$$

The bond dissociation energies (BDE's) that were used are shown below:

Figure 4.10 Thermal Degradation Pathways for Peptides





The bond dissociation energies for the three skeletal bonds of peptides were obtained from small molecules (see Appendix II for details), for which thermodynamic data are available[8]. For example, BDE(Y-X bond) is actually that for the molecule $\text{CH}_3\text{CO}-\text{NHCH}_3$. Values used for BDE (H-X), where $\text{X} = \text{NHR}, \text{NR}_2, \text{CHR}_2$, etc. were also extracted from available data on small molecules. The BDE for a N-H bond in the terminal amine group is that for a small primary amine.

Reaction enthalpies for 1,2-elimination reactions that are presented again represent those for smaller analogous systems, where sufficient thermochemical information is available. For example, the estimated reaction enthalpy for the highest energy 1,2-elimination, to form $\{(\text{B}+\text{H}) \text{ and } (\text{Y}-\text{H})\}$, represents the enthalpy for the process:

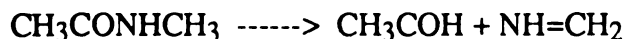


Figure 4.10 first points out that homolytic cleavage, involving the formation of two radicals, should not be expected since such reactions require much more energy than reactions in which the number of bonds broken is equal to the number of bonds formed, such as a 1,2-elimination. Products of simple homolytic cleavages are not observed under K^+IDS conditions. Lower energy 1, 2 - elimination reactions (requiring about 40 kcal/mol) also do not occur, as suggested by deuterium-labeling experiments. The lowest energy processes are those suggested on the right side of Figure 4.10, in which a cyclic and a linear product is formed in each case. Like 1,2-elimination reactions, these 1,6-eliminations involve the cleavage of two bonds and the formation of two bonds. However, the latter have approximate reaction enthalpies that are less than or equal to 0

kcal/mol. The differences in the two processes are fairly clear. In the 1,2-elimination, one of the bonds "formed" involves the conversion of a single bond to a double bond; double bonds have BDE's less than the sum of two single bond BDE's. Also, in a 1,2-elimination, the environment from which the H moves is different from that to which it moves. In contrast, consider the 1,6-elimination process shown in Figure 4.10 that yields (cyclo-C-H) and (Z+H). One C-N bond is broken while one is formed. Also a C-H bond is formed as a C-H bond is broken. Thus, of the mechanisms considered, the 1,6-elimination reactions represent the lowest energy pathways.

If the conversion of a peptide into two smaller peptides, one linear and one cyclic, is thermoneutral or exothermic, why are all not observed? Why does cleavage of one skeletal bond dominate? We suggest that the answer lies in a consideration of the intermediates through which the 1,6-elimination products are formed. These are also shown in Figure 4.10, and are arranged to suggest their relative stabilities. In Figure 4.10, intermediate IV is expected to be readily accessible. Dipole-dipole interactions will allow the molecule to align as shown, as a prelude to thermal degradation. In contrast, intermediate I would allow (cyclo-C-H) and (Z+H) species to be formed, however it is an unfavored, high-energy transition state. Its formation requires unlikely secondary interactions according to considerations of the partial charges on the atoms of the peptide backbone. Thus, the B- and Y-type thermal degradation products are most likely formed as shown in Figure 4.10 - they evolve from the most stable secondary structure, and the overall reaction enthalpy is lowest. (In this case, the estimated enthalpy range reflects differences between N-H bond dissociation energies for H's of either the N-terminal amino group or from an interior amide group.) The relative stabilities of the transition states determine, as usual, the reaction rates.

IV. CONCLUSION

K^+ IDS is shown here to be a useful technique for the mass spectrometric characterization of the thermal degradation chemistry of small peptides. In this chapter, one of the most important questions relevant to the technique have been answered, which allow spectra to be related to underlying thermal degradation processes.

The dominant skeletal bond cleavages in the thermal degradation of peptides occur most frequently at amide bonds. Cyclo-degradation was found to be the major process for thermal degradation of peptides. The formation of a cyclic product is favored because it is the lowest energy process; the dominant cyclization process is the one with the most stable transition state. For underivatized peptides, cyclization involves the N-terminus, the shifting H that accompanies skeletal bond cleavage is from the N-terminus. For N-terminally blocked peptides, cyclization from the N-terminus is hindered, and cyclization involving the C-terminus can occur. In this case, the shifting H or OH is from the C-terminus.

In this Chapter, we have reached a good understanding on thermal degradation of peptides. However, the much weaker $(B_n-H+K)^+$ signals than those of $(Y_n+H+K)^+$ in K^+ IDS spectra of peptides are still to be understood. In the following Chapter, the mechanisms for thermal degradation of peptides will be used for this purpose. The cyclic nature of (B_n-H) will be used in explaining why $(B_n-H+K)^+$ ions are not observed very often.

References

1. Irwin, W. J. *Analytical Pyrolysis: A Comprehensive Guide*; M. Dekker: New York, 1982; pp 3-44.
2. Irwin, W. J.; Slack, J. A. *Analyst* 1978, 103, 673-704.
3. Schmelzeisen-Redeker, G.; Giessmann, U.; Röllgen, F. W. *Org. Mass Spectrom.* 1985, 20, 305-309.
4. Light, K.; Kassel, D. B.; Allison, J. *Biomed. Environ. Mass Spectrom.* 1989, 18, 177-184.
5. Knapp, D. R. "Chemical Derivatization for Mass Spectrometry" in *Methods in Enzymology*, vol. 193, McCloskey, J. A., ed., Academic Press: San Diego, 1990; pp 314-328.
6. Bombick, D.; Allison, J. *Anal. Chem.* 1987, 59, 458-466.
7. Bombick D.; Pinkston, J. D.; Allison J. *Anal. Chem.* 1984, 56, 396-402.
8. Lias, S. G. ; Bartmess, J. E.; Liebman, J. F.; Holmes, J. L.; Levin, R. D.; Marlar, W. G. *J. Phys. Chem. Ref. Data*, 1988, 17, Suppl. No. 1.

Chapter 5

Response Discrimination In K^+ -Adduct Formation

I. Introduction

In K^+ IDS mass spectrometry, when a peptide molecule undergoes thermal degradation, two neutral species such as (Y_n+H) and (B_n-H) are formed and desorbed into the gas phase. Due to the stoichiometry of the reaction, the quantity of these two species (or the number density) are the same inside the ion source. These two gas-phase neutral species then react with K^+ ions generated from the K^+ thermionic emitter, forming K^+ -adducts.

As have been seen in K^+ IDS mass spectra, however, the peaks representing the $[B_m-H+K]^+$ ions are much less intense than those for the corresponding $[Y_n+H+K]^+$ ions. For example, the thermal degradation of the pentapeptide *H*-YGGFL-*OH* will produce $(Y_3 + H)$ and $(B_2 - H)$ in a 1:1 ratio. In the spectrum of *H*-YGGFL-*OH*, however, the abundance of $[Y_3+H+K]^+$ is 30 times as great as that of $[B_2-H+K]^+$. Why? What are the reasons for this observation? Is that because the (B_m-H) molecules are unstable? Is that because the volatility of the (B_m-H) molecules is not high enough? Or is that because of the poor stability of the $(B_m-H+K)^+$ ions?

For ion formation in K^+ IDS, three processes are involved - degradation, desorption, and "sampling" (adduct formation with K^+ ions). We have investigated the latter as the most likely source, i.e., that some discrimination exists in the adduct formation process. The nature of interactions between K^+ ions and neutral molecules is electrostatic, and should be sensitive to molecular size and structure, local dipole

moments within the molecule, and polarizability. The binding energies are relatively small, 20-40 kcal/mol [1-2], and adduct ions are presumably stabilized by emission of an infrared photon, or dissociate after some time period (K^+ detachment).

In this Chapter, response discrimination in K^+ IDS is investigated. The size and structure dependence of response is studied with peptides of different sizes and structures. The nature of discrimination will be studied by using mixed thermionic emitters. Results from this investigation are used to explain the general features of K^+ IDS spectra.

II. Experimental section

Preparation of mixed ionic emitters: A mixed thermionic emitter produces two or more different ions such as K^+ and Na^+ ions at the same time from the same emitter. To make these emitters, a regular K^+ ion emitter was made and conditioned first. For a K^+ and Na^+ ionic emitter, a small drop of Na_2CO_3 aqueous solution was added on the tip, air dried then put into the ion source for conditioning. The bead/emitter was conditioned by applying current gradually to 3.0 A, as is for a regular K^+ emitter. The emission of K^+ and Na^+ ions was examined to assure that the emission currents for K^+ and Na^+ are comparable. For a Cs^+ and K^+ emitter, a similar procedure was used. Instead of using Na_2CO_3 , Cs_2O was dissolved in water and a drop of the solution ($CsOH$) was applied to the thermionic emitter. This new bead was conditioned and emission of K^+ and Cs^+ ions were examined.

All peptides and amino acids were purchased from Sigma Chemical Co., St. Louis, MO., and were used without further purification. The samples were dissolved in water to concentrations of approximately $1\mu g/\mu l$. For peptide and amino acid mixtures, all components have roughly the same concentration of $1\mu g/\mu l$. One to two- μl aliquots of solution were transferred to the K^+ IDS sample-filament.

III. Binding Energies and Stabilities of K^+ -adducts

The interactions between K^+ ions and neutral molecules has been studied using high pressure mass spectrometry by Kebarle and his coworkers [1]. In their early study [1-2] on gas-phase solvation of alkali ions under equilibrium conditions, binding energies of K^+ ions with various organic and inorganic solvents were determined experimentally. Some of these data are listed in Table 5.1.

Table 5.1 Binding energies* and dipole moments of various molecules [1-2]

<u>M</u>	<u>$-\Delta H^\circ$(kcal/mol)</u>	<u>$-\Delta G^\circ$(kcal/mol)</u>	<u>Dipole moment (Debye)</u>
Me ₂ SO	35	25	3.9
DMA	31	24	3.81
DMF	31	23	3.9
Me ₂ CO	26	19	2.88
n-PrNH ₂	22	14	1.18
Pyridine	21	15	2.2
Me ₂ NH	20	13	1.0
MeNH ₂	19	13	1.29
Benzene	19	12	
NH ₃	18	12	1.47
H ₂ O	17	11	1.8

* For M- K^+ ions, binding energy = $-\Delta H^\circ_{rxn} (M + K^+ \rightarrow MK^+)$.

The data in Table 5.1, determined by using high-pressure mass spectrometry, have shown the following trends:

1. The greater the number of heteroatoms in a molecule, the greater the binding energy (for molecules with the same size). This clearly indicates that the K^+ in an K^+

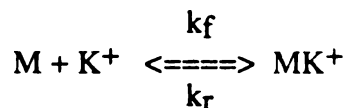
adduct ion is not bound to one specific atom. It must interact with many atoms within the neutral molecule.

2. The larger the size of a molecule, the greater the binding energy.

3. For a small molecule with one heteroatom, its K^+ ion affinity is about 10% of its proton affinity - a very weak binding. Therefore, if the excess energy of the adduct is large enough to cleave a bond within the adduct, K^+ detachment will most probably occur due to the weak binding.

Classical electrostatic calculations were performed by Clementi and his co-workers [3-5] for alkali metal adducts; the results were in good agreement with experimental measurements. Their calculations show that the bonding, particularly for the larger ions like K^+ , is almost purely electrostatic. For instance, the Mulliken population analysis [3-5] showed that a charge transfer of only 0.018, 0.013, and 0.004 electron from the water molecule to the Li^+ , Na^+ , and K^+ ions, respectively.

From these thermodynamic data, the formation constant for a K^+ -adduct of a compound with $\Delta G^\circ = -20$ kcal/mol, can be estimated to be around 10^{50} ($\log K = -\Delta G^\circ/RT$) at 300K. In condensed phases, this means that the K^+ -adducts formed will practically stay undissociated once formed, the reverse reaction rate is negligible compared with the forward reaction rate.



In the gas phase of a high vacuum system, as is the case in a K^+ IDS ion source, however, a large formation constant does not necessarily mean great stability because:

1. Formation constants are determined under equilibrium conditions. In a K^+ IDS ion source of a mass spectrometer, an equilibrium can never be achieved because high vacuum under K^+ IDS conditions leads to a very low number of collisions while a large number of collisions is required for equilibrium.

2. A small number of collisions leads to a low formation rate of K^+ -adducts, which leads to an even lower collision frequency with other species present in the ion source. In the formation of K^+ -adducts, energy is released, which is equal to the binding energy. Since there is no way for a newly formed K^+ -adduct to dissipate the energy released during their formation (through collisions or photon emission), the energy released may well be used to reverse the process.

3. Since the K^+ binding is the weakest "bond" in a K^+ -adduct -- 20% of a regular covalent bond, dissociation of K^+ -adducts will occur due to energy released during K^+ binding, and to lack of mechanisms for energy dissipation. Therefore, there is a lifetime for any K^+ -adduct formed. If the lifetime of a K^+ -adduct is shorter than its residence time inside the mass spectrometer (flight time from ion source to the exit of the quadrupoles - approximately 50 μs in the quadrupole mass spectrometer), the adduct ion will dissociate and will not be able to reach the detector. (In a solvent system, the situation is totally different. The energy released in the complexation process can be taken away very quickly by the large quantity of solvent molecules, and a newly formed molecule is thus stabilized). Therefore, K^+ adducts with long life-times will show greater response than those with shorter life-times.

So the questions are: In K^+ IDS experiments, what are the most important factors for a high yield of K^+ -adducts? What determines the lifetime of K^+ -adducts?

IV. Discrimination in the formation of K^+ -adducts

Since binding energies vary with the type and size of molecules, different thermal degradation products will have different binding energies. The difference in binding energy may lead to differences in K^+ IDS responses. Based on the above considerations, various compounds were studied for their K^+ -adduct formation and their relative responses in K^+ IDS experiments.

For a quadrupole mass spectrometer, ions with higher m/z values usually have lower transmission efficiencies. This is not considered in this study because the mass differences of the selected compounds are relatively small.

In this study, the following two important factors were considered: A) The size of neutral molecules; B) The structures of neutral molecules - linear or cyclic.

A. Size Discrimination

If small compounds such as amino acids are analyzed by K^+ IDS, desorption can be made to dominate. Thus, equimolar amounts of two amino acids (A and B) will yield equal numbers of desorbed molecules for subsequent attachment to available K^+ ions. If the peaks representing $[A+K]^+$ and $[B+K]^+$ are of differing intensities, this would indicate a response discrimination. The experiments in this section were designed to determine the extent of discrimination, if any.

Amino acid mixtures are used in this study because they are the basic constituents of peptides and because they can be the products from thermal degradation of peptides. They share the same chemical formula $NH_2CHRCOOH$, with R different for different amino acids. They do not show much chemical reactivity in K^+ IDS conditions, and the typical reaction is the direct attachment of a K^+ ion.

In the determination of response discrimination, proper quantitation is required. To do so, relative concentrations of different compounds should be known. For this purpose, a good solvent should be used and the best solvent for this study is water, in which many amino acids show good solubilities. Some amino acids were not studied in this work because of their poor solubilities in water.

Mixtures with two to five different amino-acids were used in this study and the relative responses were found to be very similar (Figures 5.1 - 5.3). For example, with a mixture of alanine and phenylalanine, the relative responses of phenylalanine to alanine

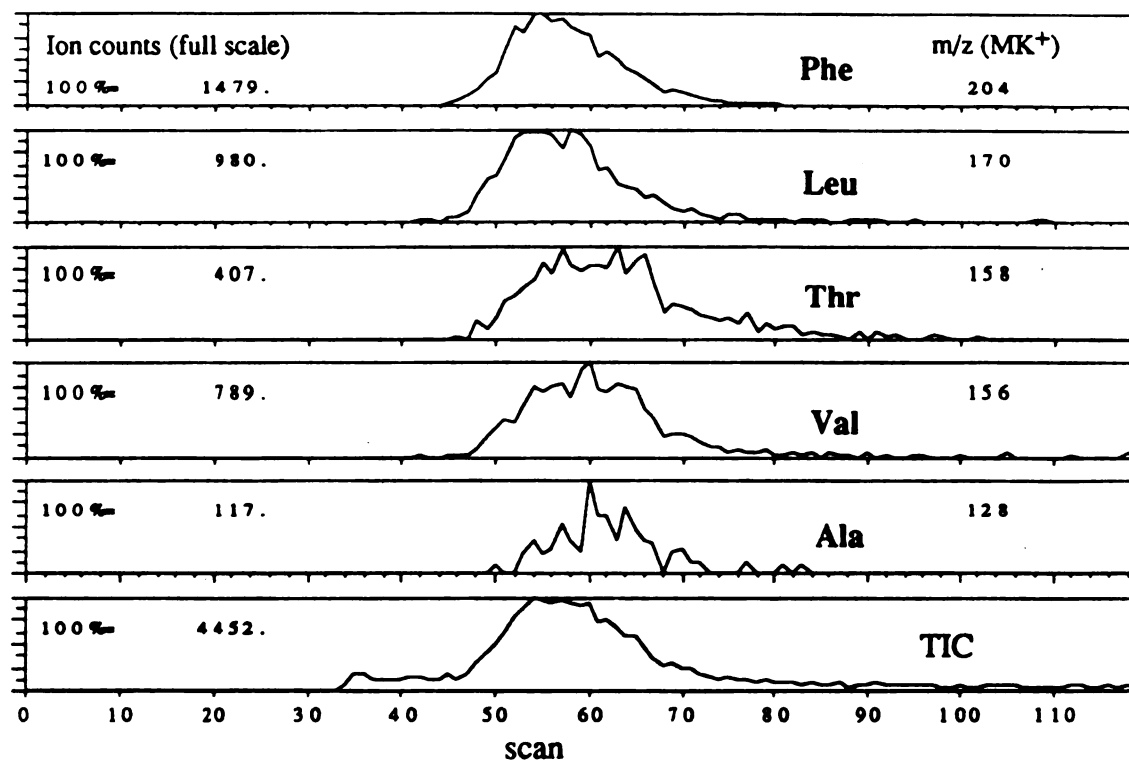


Figure 5.1 Relative responses of five amino acids (a mixture of alanine, valine, leucine, threonine and phenylalanine) in K⁺IDS.

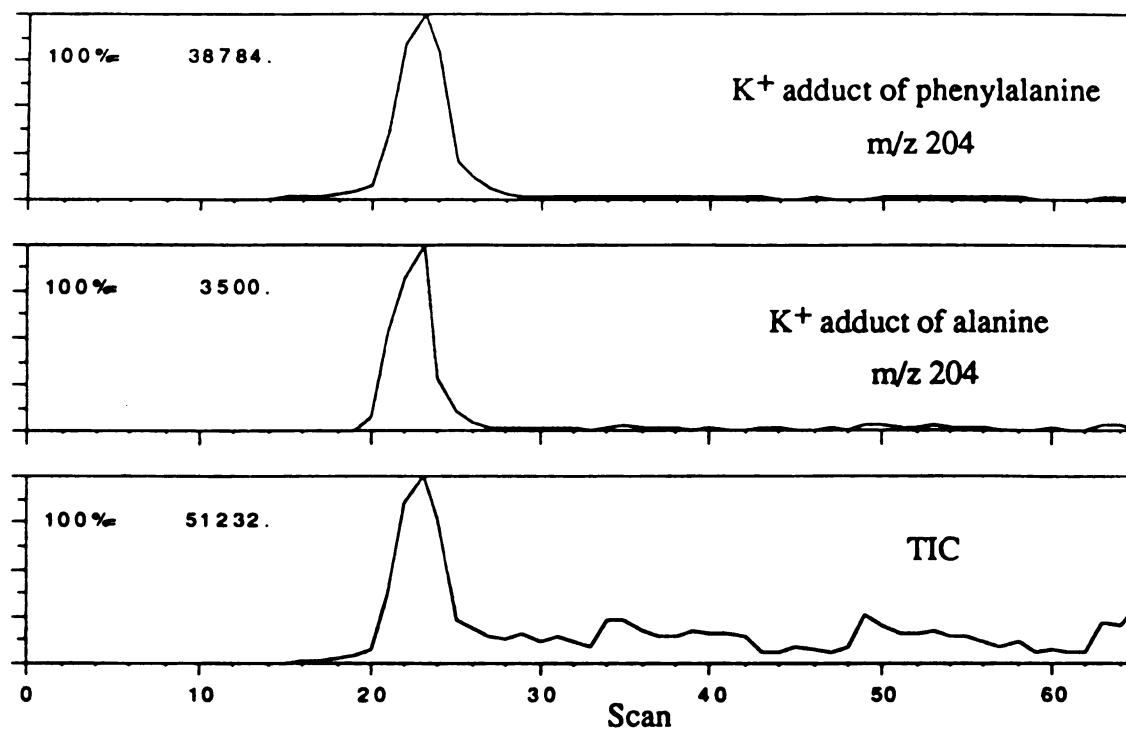


Figure 5.2 Relative responses of alanine and phenylalanine in K^+ IDS.

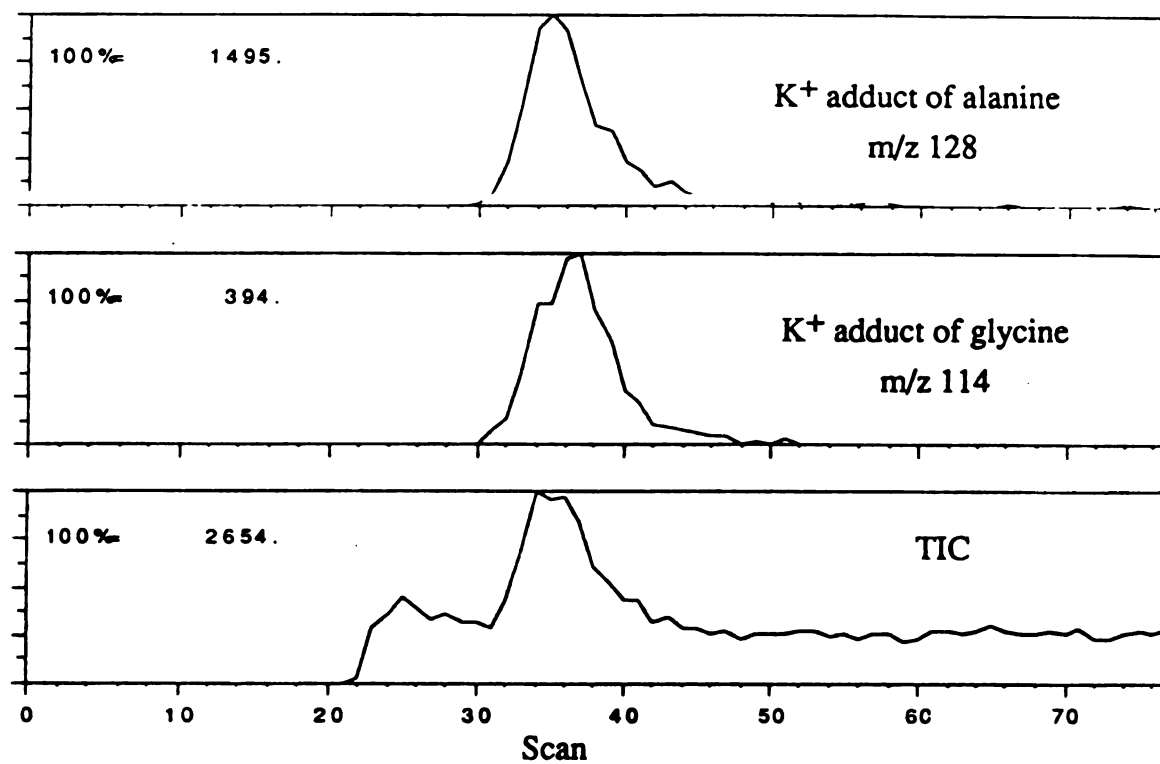


Figure 5.3 Relative responses of alanine and glycine in K⁺IDS.

were found to be 32 to 1 (Figure 5.2). With a mixture of five amino acids - alanine, threonine, valine, phenylalanine and leucine, the relative responses of phenylalanine to alanine were calculated to be 30 to 1 (Figure 5.1). This clearly indicates that there is no competitive processes occurring presumably because there are not many collisions in the gas-phase, which is consistent with our estimated low pressure shown in Appendix I. Note that equal mass of each amino acid was used for the mixtures. Therefore, the molecular mass of each amino acid should be considered when relative responses are calculated.

As shown in Figure 5.1, different amino acids have shown different responses to K^+ attachment. The smaller ones, such as glycine and alanine, have much lower response than the large ones, such as phenylalanine. For example, with a mixture of five amino acids - alanine, phenylalanine, leucine, threonine and valine, their relative responses are calculated to be alanine(Ala): phenylalanine(Phe): leucine(Leu): threonine(Thr): valine(Val) = 1: 32: 18: 8: 7, as shown in Figure 5.1. Glycine(Gly) has the lowest response to K^+ adduct formation among all amino acids: Ala: Gly = 6: 1. This is shown in Figure 5.3. The relative responses of some common amino acids are summarized in Table 5.2. In the table, the response for alanine is given a value of 1.

Table 5.2. Relative response factors, R_{rel} , for amino acids and small peptides

amino acids									
	Ala	Gly	Val	Thr	Ser	Met	Leu	Phe	Ile
R_{rel}	1	1/6	7	8	2	8	18	32	22
small peptides									
	Alaline	<i>H-A-A-OH</i>		<i>H-A-A-A-OH</i>		<i>H-A-A-A-A-OH</i>			
R_{rel}	1	10		100		200			

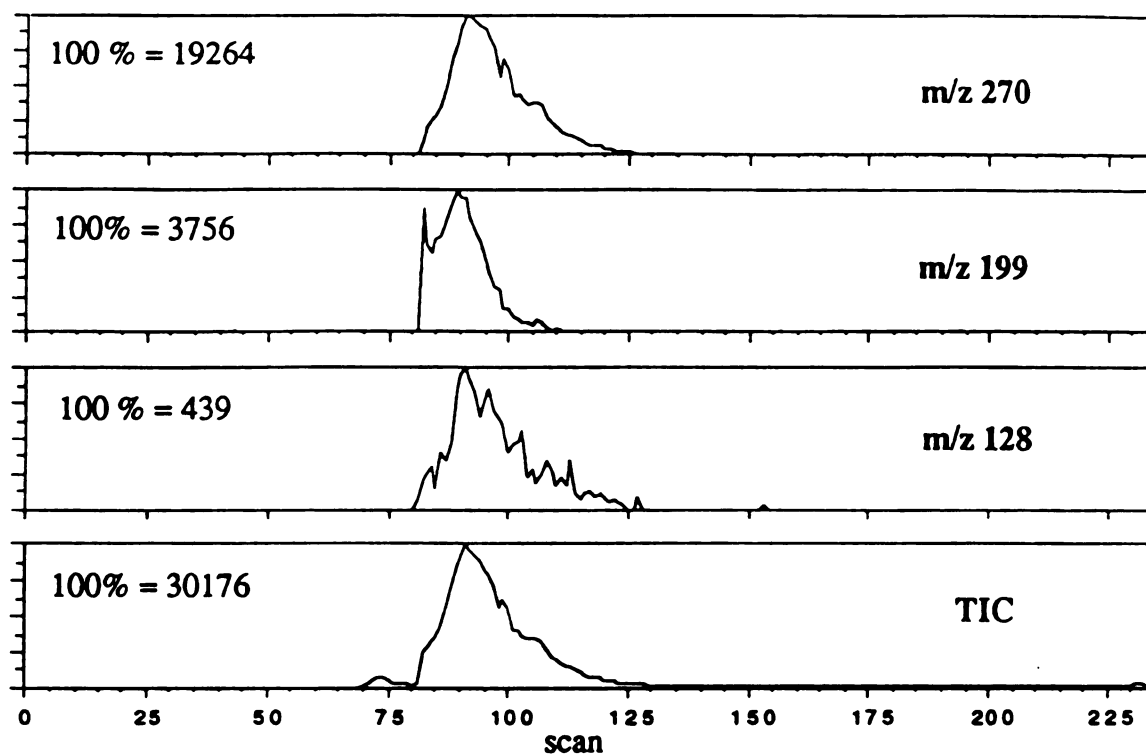


Figure 5.4 Responses of alanine, A-A and A-A-A at m/z 128, 199 & 270.

Generally the greater the size and polarizability, the greater the response - the trend is the same as binding energy trend observed by Kebarle and his coworkers [1-2]. For amino acids with the same size such as valine and threonine, the presence of heteroatoms can enhance the response due to the increased polarity. The responses of threonine and valine indicate that threonine is about 15% more sensitive than that of valine. Dipeptides usually have greater responses than amino acids, tripeptides usually have greater responses than dipeptides. As the size continues to increase, however, the response differences gradually level off. The results for a series of small peptides (Figure 5.4) are also listed in Table 5.2.

The observation of size discrimination can be attributed to the following factors:

1. The thermodynamic stability. The larger a neutral molecule, the more stable its K^+ -adduct because there are more atoms to redistribute the energy released during the adduct formation, and the longer its lifetime.
2. Collision frequency. Since K^+ ions can react with any organic molecules in gas phase, amino acids with larger sizes have greater collision frequency with K^+ ions. In other words, larger molecules have greater reaction rate, yielding a higher concentration of adduct ions in the gas phase.
3. Polarizability. The larger a molecule, the greater its polarizability, and the stronger its interaction with a charged K^+ . Heteroatoms give greater dipole moments to a molecule, thus give stronger charge-dipole interactions with K^+ ions, thus better stability.
4. Branching effect. H-AAA-OH and H-GGGG-OH have very similar molecular weight and size. However, the branched peptide H-AAA-OH (MW = 231) is found to be 4 times as sensitive as H-GGGG-OH (MW = 246), as shown in Figure 5.5.

Note that the relative response factor should be treated carefully. When an amino acid residue is added to a peptide molecule, the response may or may not increase significantly depending on the size of the original molecule. This statement can be illustrated by the following experimental data for the relative responses of an amino acid and five small peptides, assuming the relative response of phenylalanine (H-F-OH) is 1:

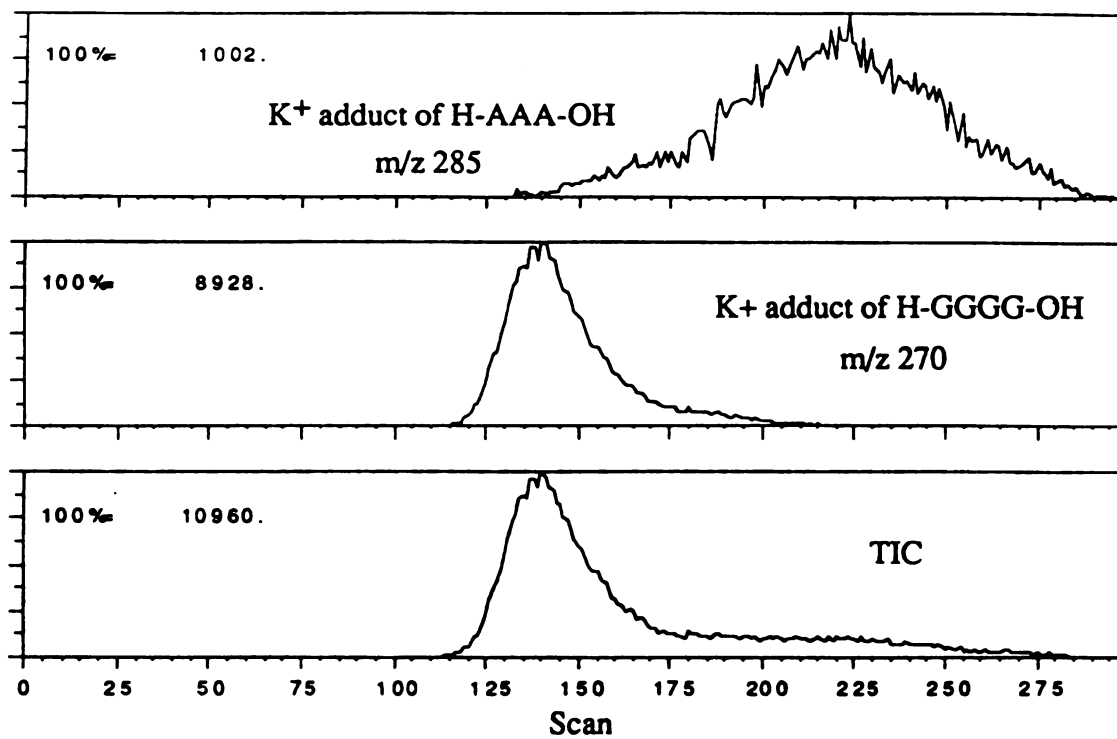


Figure 5.5 Relative responses of H-GGGG-OH and H-AAA-OH in K⁺IDS.

Compound	H-F-OH	H-FG-OH	H-FL-OH	H-GGF-OH	H-GFL-OH	H-AFLA-OH
R _{rel}	1	5	7	6	10	10

These data indicate that the response factor for the addition of each amino acid residue is not a constant. For example, from H-F-OH to H-GF-OH, the response increases by a factor of five; while from H-FL-OH to H-GFL-OH, the increase in response is $10/7 = 1.5$; From H-FG-OH to H-GGF-OH, there is no significant change in response at all. It appears that, as the size of a "large" peptide increases, the response of the peptides does not change significantly since the additional functionalities can not interact with K^+ ions, thus no further stabilization effect can be observed.

B. Structure Discrimination

In characterizing thermal degradation of peptides, we have found that some of the neutral species formed are cyclic and others are linear. It is natural to suspect that the structure of a molecule may affect its binding ability with K^+ ions because different structures can provide different interaction sites and interaction coordination. For instance, a neutral (B_n+H) molecule has a cyclic configuration and not all of its functional group can interact with K^+ efficiently to form a multidentate adduct at the same time. For a linear molecule, however, it can form such multidentate adducts more efficiently because of its lack of ring constraint (much more flexible).

This speculation was tested. If equimolar amounts of *H-GP-OH* and cyclo(-GP) are analyzed by K^+ IDS, the resulting spectra only contain the $[M+K]^+$ species of each. If the intensities of these two peaks are monitored, the results shown in Figure 5.6 are obtained. The time-dependent response reflects the desorption of the two species, and the relative responses clearly show that the linear form is "sampled" much more efficiently

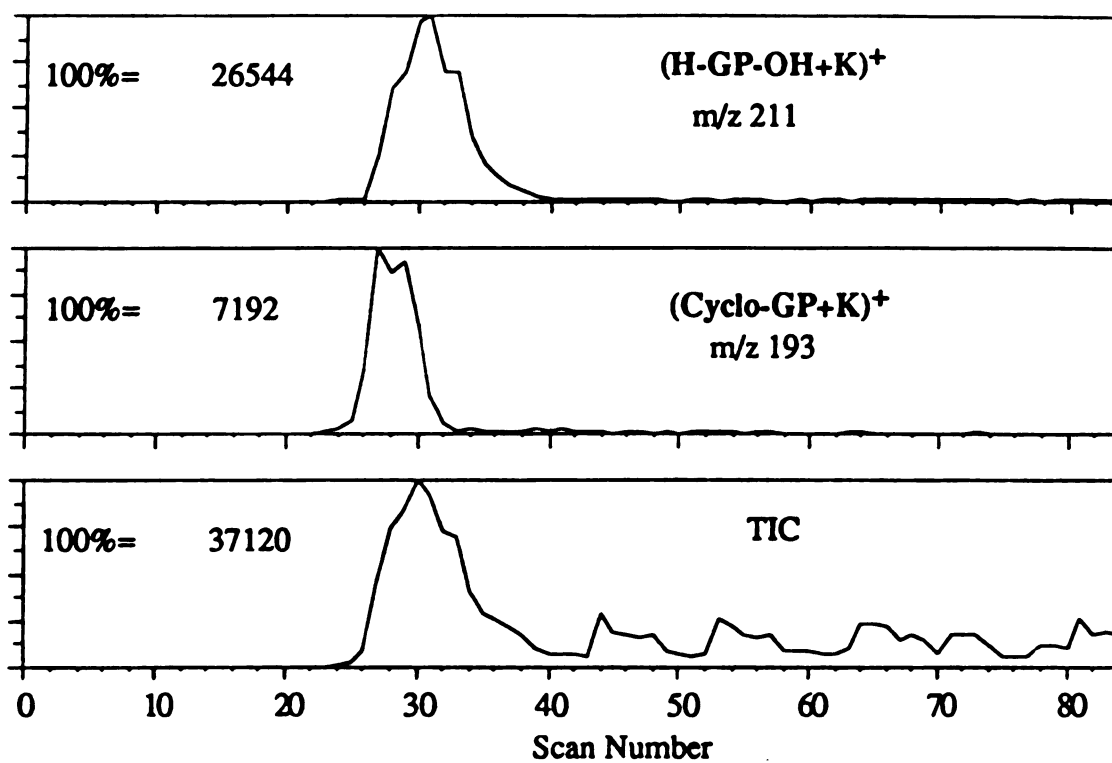


Figure 5.6 Mass chromatograms showing the relative responses of H-GP-OH and cyclo-(GP) in the K^+ IDS experiments.

than the cyclic form by K^+ ions - the response is 8 times larger for the linear form. It is reasonable to believe that a linear molecule can form a more stable multidentate complex with K^+ than can a constrained cyclic molecule, thus the results of these response studies are not unexpected.

C. Discrimination Studied By Thermal Degradation Of Tri- And Tetra-Peptides

The mass spectral data of tripeptides can be used to deduce the relative response factors of smaller peptides. Note here that skeletal bond cleavages are observed for these peptides and the formation of (B₂-H) and (Y₁+H) is observed.

For example, by comparing the responses from H-GGF-OH and H-FFF-OH, the response of cyclo-(FF) relative to cyclo-(GG) can be deduced. If "I" is used to represent the relative intensity of ions, then $I_1(\text{cyclo}(\text{FF})):I_1(\text{F}) = 36:3$ can be obtained from the spectrum of H-FFF-OH. From the spectrum of H-GGF-OH, $I_2(\text{cyclo}(\text{GG})):I_2(\text{F}) = 14:29$ can be obtained. Note that the subscript "1" and "2" indicate the data are from spectra 1 and 2, respectively.

$$I_1(\text{cyclo}(\text{FF})):I_1(\text{F})/I_2(\text{cyclo}(\text{GG})):I_2(\text{F}) = 36:3/14:29 = 25$$

$$I_1(\text{cyclo}(\text{FF})):I_1(\text{F})/I_2(\text{cyclo}(\text{GG})):I_2(\text{F}) = I(\text{cyclo}(\text{FF}))/I(\text{cyclo}(\text{GG}))$$

$$I(\text{cyclo}(\text{FF}))/I(\text{cyclo}(\text{GG})) = 25$$

This means that cyclo-(FF) is 25 times as sensitive as cyclo-(GG) to K^+ attachment. By the same method, the responses of amino acids can be obtained. For example, by comparing the spectra of H-GGG-OH and H-GGF-OH, the response of phenylalanine relative to glycine can be deduced.

The relative responses of linear and cyclic dipeptides can be deduced from a single tetra-peptide spectrum since the formation of a linear (Y₂+H) and a cyclic (B₂-H) commonly is the dominant reaction. However, loss of H₂O sometimes may complicate the situation (make the response for a linear molecule smaller than it should be). From the K^+ IDS mass spectra of H-FGGF-OH (Figure 3.3) and H-FGFG-OH, it was found that

the linear dipeptide H-FG-OH and H-GF-OH are five times more sensitive than its corresponding cyclic dipeptide cyclo-(FG) (without considering the loss of H₂O from (Y₂+H) to a cyclic (B₂-H)). In contrast, from the spectrum of H-PFGK-OH (Figure 3.6), the cyclo-(PF) is four times more sensitive than the linear H-GK-OH due to the large size difference of these two.

D. Discrimination against Weak Binding: Experiments with Mixed Ionic Emitters

From thermodynamic data, we have proposed that discrimination is due to the small binding energies between K⁺ ions and different neutral species in the gas-phase. To demonstrate this in K⁺IDS, experiments with mixed ionic emitters, which emit more than one type of alkaline metal ions, have been performed to show the efficiency of alkali metal ions in sampling the same gas-phase peptide/fragments. To be more specific, we have used two mixed ionic emitters: one containing Na⁺ and K⁺, and the other containing K⁺ and Cs⁺ ions. The results from peptides with these thermionic emitters are shown below.

1. Na⁺ and K⁺ ionic emitter

When a peptide such as H-VGGFL-OH is heated in an ion source equipped with a K⁺ and Na⁺ mixed emitter, thermal degradation and desorption occur, which is then followed by alkali metal ion (Na⁺ and K⁺) attachment. At any given time, neutral species are presented to both K⁺ ions and Na⁺ ions with equal concentration. Assuming there is no discrimination for sampling "large" neutral species for both K⁺ and Na⁺ ions - reasonable due to physical trapping, then the peak intensity ratio of (M+K)⁺ and (M+Na)⁺ will reflect the relative ion currents of K⁺ and Na⁺ ions inside the ion source. If there is no discrimination, for any given fragment F, the peak abundance ratio of

$(F+K)^+$ to $(F+Na)^+$ would be the same as that of $(M+K)^+$ to $(M+Na)^+$. The data shown below is for the peptide H-VGGFL-OH, which is obtained from Figure 5.7.

$$I(M+Na^+)/I(M+K^+) = 13/25 = 1/2$$

$$I(Y_3+H+Na^+)/I(Y_3+H+K^+) = 55/100 = 1/2$$

$$I(B_2-H+Na^+)/I(B_2-H+K^+) = 4/2 = 2/1$$

At the high-mass region of a spectrum, the large sizes of K^+ adducts of both (Y_3+H) and intact analyte molecules make the adducts relatively stable, thus no significant discrimination is observed. When the size becomes smaller, discrimination against the formation of K^+ adducts shows up. For example, the relative concentration of K^+ ions is twice that of Na^+ ions according to the adducts formed at the high mass region of the spectrum. If there is no difference in the binding energy between K^+ ions Na^+ ion, then $I(B_2-H+Na^+)/I(B_2-H+K^+)$ should be 1/2. In fact, the ratio is found to be 2/1. This observation indicates that there is a strong discrimination against the formation of K^+ adducts or the adduct ions with weaker binding energies.

2. K^+ and Cs^+ mixed ionic emitter

The same experiment is also performed for K^+ and Cs^+ mixed ionic emitter, with Cs^+ a weaker binding ion than K^+ ion. The data shown below is for H-VGGFL-OH, which is obtained from Figure 5.8.

$$I(M+Cs^+)/I(M+K^+) = 3/1$$

$$I(Y_3+H+Cs^+)/I(Y_3+H+K^+) = 1/1$$

In this experiment, the emission of Cs^+ ions is about four times that of K^+ ions. When a large neutral species such as a pentapeptide is attached to these ions, the large sizes of the peptides and multiple interaction sites make both the K^+ and Cs^+ adducts stable, little discrimination was seen, as is shown in the ion intensity ratio between Cs^+ adducts and K^+ adducts. When a smaller molecule such as the (Y_3+H) , a peptide, is attached by these ions, discrimination against the formation of Cs^+ adducts is seen. The yield of Cs^+

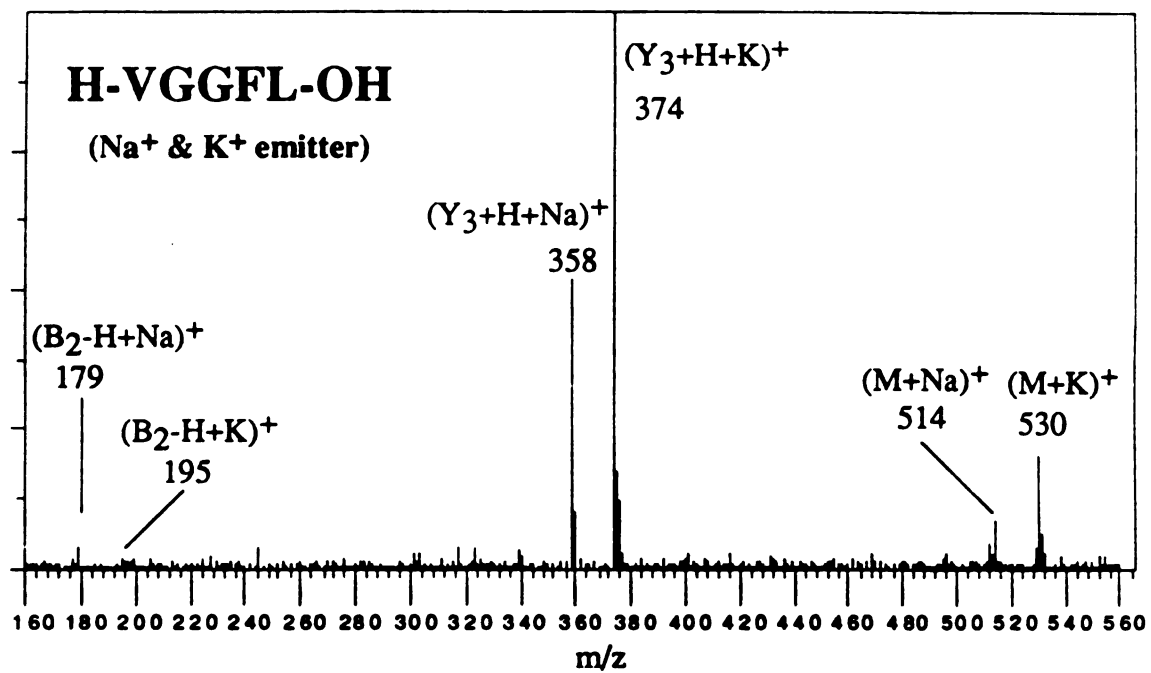


Figure 5.7 Relative responses of K⁺ and Na⁺ to a peptide H-VGGFL-OH and its thermal degradation products.

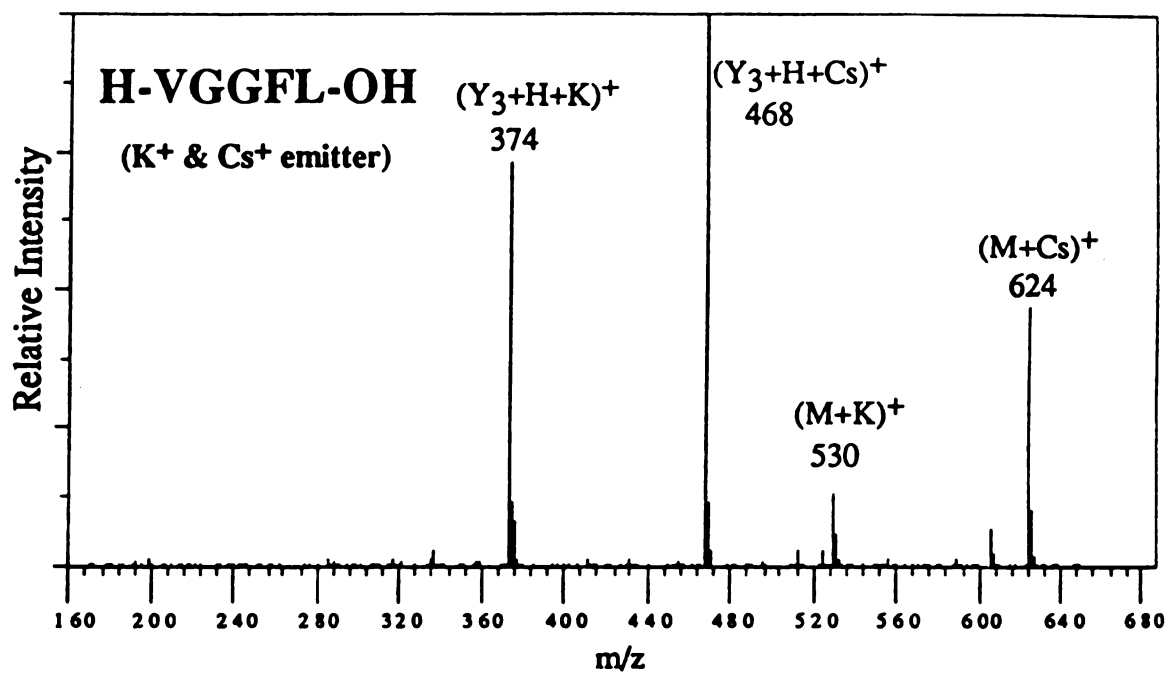


Figure 5.8 Responses of K⁺ and Cs⁺ to a peptide H-VGGFL-OH and its degradation products.

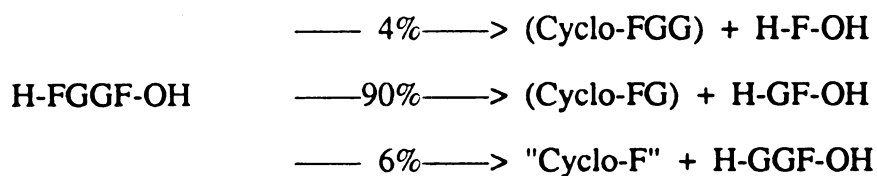
adducts is much smaller (only 30%) than that of K^+ adducts, as is demonstrated by the adduct ion abundance ratio.

E. Summary (Discrimination in Interpretation of K^+ IDS Spectra)

Based on the cyclization mechanism for thermal degradation and the subsequent discrimination in the K^+ adduct formation step against small molecules and against cyclic molecules, interpretation of K^+ IDS spectra of peptides becomes straightforward. Many important features of K^+ IDS spectra can be explained easily: 1. For underivatized peptides, $(Y_n+H+K)^+$ ions formed are linear while their corresponding $(B_n-H+K)^+$ ions are cyclic. The discrimination against cyclic molecules leads to the fact that the spectra of underivatized peptides are dominated by $(Y_n+H+K)^+$ ions while their corresponding $(B_n-H+K)^+$ ions are very weak. 2. For N-terminally blocked molecules such as N-acetylated peptides, the dominant ions are $(B_n+OH+K)^+$ ions and $(C_n+H+K)^+$ ions because these ions are linear while their corresponding ions are cyclic. 3. For molecules such as H-GGFL-OH, $(Y_n+H+K)^+$ ion abundance increase with their sizes due to size/volume effect. 4. The discrimination against peptides with cyclic structures provided us another evidence for the proposed cyclization mechanism.

In summary, the weak interactions between a K^+ ion and a neutral molecule leads to a finite lifetime for the nascent K^+ adducts. The limited lifetime is reflected in the response discrimination against smaller molecules and cyclic molecules, which give much weaker signals. The discrimination in K^+ IDS results in simple, easy-to-interpret spectra of underivatized peptides, which are dominated by $[Y_n + H + K]^+$ ions. The determination of the relative responses of amino acids and small peptides makes it much easier to interpret K^+ IDS spectra, and information regarding the probabilities of bond cleavages at different sites along a peptide backbone can be evaluated more accurately. For example, in Figure 3.3, the $[Y_2+H+K]^+$ peak is about five times as intense as the $[Y_3+H+K]^+$ peak, but this does not mean that the rate of bond cleavage at the second

amide bond from the N-terminus is five times that for the third amide bond, since there is a response discrimination against (Y₂+H). Since the response for (Y₃+H) is about five times that for (Y₂+H), the cleavage at the 2nd amide bond is estimated to occur at a rate 25 times that for the 3rd amide bond. For [Y₁+H+K]⁺, the peak is 80 times less intense than that for [Y₂+H+K]⁺, but cleavage of the 3rd amide bond from the N-terminus is only 16 times that of the second amide bond since the response favors (Y₂+H). Thus, relative response studies suggest that the data in Figure 1 reflects the following distribution of primary, low-energy thermal degradation products, as an example:



References

1. W. R. Davidson, P. Kebarle, *J. Am. Chem. Soc.* **1976**, 98, 6133-6138.
2. J. Sunner, P. Kebarle, *J. Am. Chem. Soc.* **1984**, 106, 6135.
3. Clementi, E.; Popkie, H.; *J. Chem. Phys.* **1972**, 57, 1077.
4. Kisenmacher, H.; Popkie, H.; Clementi, E. *J. Chem. Phys.* **1973**, 58, 1689.
5. Kisenmacher, H.; Popkie, H.; Clementi, E. *J. Chem. Phys.* **1974**, 59, 5892.

Chapter 6

Collision-Induced Dissociation of Deprotonated Peptides

I. Introduction

The determination of the amino acid sequence of peptides, by positive fast atom bombardment (FAB) mass spectrometry, is one of the best known applications of mass spectrometry, which has been well studied and well documented [1]. However, the application of negative ion FAB mass spectrometry to peptide analysis has, with notable exceptions, been used principally to detect $(M-H)^-$ ions. Recently, several research groups have studied the collision-induced dissociation (CID) of deprotonated tri-peptides and di-peptides [1-9]. It is becoming more clear now that MS/MS data from peptide negative ions can produce useful structural information, even though the fragmentation behavior of deprotonated peptides is little understood.

In this chapter, the fragmentation behavior of larger deprotonated peptides, is studied. In Bowie's early studies on the fragmentation of deprotonated peptides, only dipeptides and tripeptides were studied. Although their results provided some very useful information about the fragmentation of deprotonated peptides, especially side-chain specific fragmentations, the sizes of the peptides studied are not large enough to provide general rules for the fragmentation of deprotonated peptides. First, smaller deprotonated peptides usually give relatively more fragmentation because the internal energy deposited from collisional activation is much greater [10] and the energy can only be redistributed among a smaller number of atoms, generating various non-sequence ions. Secondly, some

reactions characteristic of larger molecules may not occur for smaller peptides due to smaller internal energy deposition. For example, C ions have not been frequently observed for dipeptides and tripeptides [1-10] while these ions are among the two dominant ion series observed for larger peptides [this work]. These ions provide additional information about the amino acid sequence of a peptide. Moreover, there is no obvious sequence-ion series for small peptides because their peptide chains are too short to generate large numbers of sequence-related ions. One relevant fact is that designations for sequence ions have not been used in these papers. Finally, there is a pressing need for a better understanding on the fragmentation of deprotonated peptides since deprotonated peptides, in some cases, can be more abundant than protonated peptides in an ion source, which can provide better sensitivities for MS and MS/MS analysis.

In this chapter, several important questions relevant to the fragmentation mechanisms of deprotonated peptides are addressed in detail. Those are: What is (are) the structure(s) of the deprotonated peptides from which all the fragments are derived? What are the dominant fragment ions from CID of deprotonated peptides? How are they most often formed?

To start with, general concept of tandem mass spectrometry and B/E linked scans will be introduced in section II. In section IV, the site of deprotonation for peptides will be investigated with deuterated peptides and derivatized peptides. Deprotonation in the gas-phase will be proposed and supported. In sections VI and VII, fragmentation of deprotonated peptides will be investigated. Charge-localized negative ions (peptide derivatives) are used. Other peptide derivatives and deuterated peptides are also used in exploring the fragmentation of deprotonated peptides. Mechanisms leading to the formation of the major ion series will be proposed. In section VIII, fragmentation of charge-localized peptides will be discussed. Mechanisms for the formation of fragment ions will be proposed. Ions formed in negative CID will be compared with ions formed in

positive mode. At the end of this chapter, the applicability of negative ion CID of deprotonated peptides for peptide sequencing will be discussed.

II. Tandem Mass Spectrometry

A. Introduction

When peptides are subjected to fast atom bombardment, protonated peptides are generated efficiently. These ions are chemically very stable and have little excess energy. As a result, not much fragmentation takes place and the signal consists mainly of the isotope cluster for $(M+H)^+$. Fragment ion abundances are generally ten times or more lower and the spectrum is, therefore, dominated by the signal for protonated peptides. Thus, such spectra contain little structure information beyond molecular weight.

As a result of lack of fragmentation and the accompanying lack of structural information, other methods were developed to induce cleavage of bonds. This can be achieved by transferring additional energy, sufficient to induce fragmentation of the stable molecular ion formed in the initial ionization process. Collision with a neutral gas is presently the most widely used, leading to collision-induced dissociation (CID). The selection of precursor ions and the subsequent mass analysis are achieved by tandem mass spectrometry (MS/MS). The precursor ions, generally $(M+H)^+$, in the first mass spectrometer (MS-1) are fragmented upon collision with inert atoms such as He, or some other energy transfer process, and the product ions (fragment ions) are recorded in the second mass spectrometer (MS-2). For MS/MS analysis, the ideal instruments are four-sector instruments such as JEOL HX110/HX110 with EBEB configuration with high resolution for both precursor ions and product ions, or triple quadrupole instruments (TSQ).

B. B/E Linked Scan

For the JEOL HX110 mass spectrometer (EB configuration)- the instrument used for this dissertation, however, MS/MS was achieved in a different manner named B/E linked scan. In this process (see ion flow diagram below), precursor ions, along with all other ions produced in the initial FAB process, collide with He gas in a collision cell located at the first field-free-region (1FFR) which is right in front of the electric sector, leading to collision-induced dissociation (CID). When the magnetic field strength (B) and the electric field strength (E) are scanned at the same time with B/E constant, it is called B/E linked scan. In a B/E linked scan, only ions with the same velocity as the precursor ions can pass through the two sectors, and be detected. Therefore, ions detected from a linked scan are from precursor ions with the same m/z values.

Ion source ----> 1FFR -----> E sector -----> B sector -----> Detector

When an ion F_1 is fragmented to form F_2 during collision with He, a small portion of the translational energy of F_1 (10 keV) is converted into internal energy (a few electron volts). Bonds cleave and fragments are formed. All fragments from the same precursor ions will travel with practically the same velocity as its precursor ions.

For singly charged ions to pass to the detector, they have to follow the equations:

$$eE = mv^2/R_e$$

$$eB = mv/R_m$$

Where E is the electric field strength, B is the magnetic field strength, R_e is the radius of the electric sector, R_m is the radius of the magnetic sector, v is the velocity of ions, m is the mass of ions, e is the charge on a single electron.

For a precursor ion F_1 (mass m_1) and its product ion F_2 (mass m_2), both with the same velocity, to pass the electric sector, they must obey the following equations:

$$eE_1 = m_1 v^2 / R_e$$

$$eE_2 = m_2 v^2 / R_e$$

Thus $E_1/E_2 = m_1/m_2$. If E_1 is set for passing the precursor ion F_1 , then the product ion F_2 can pass the electric sector by lowering the electric field strength to E_2 in proportion to its mass reduction from m_1 to m_2 .

For the same ions to pass the second sector (magnetic sector), they must follow the following equations:

$$eB_1 = m_1 v / R_m$$

$$eB_2 = m_2 v / R_m$$

Hence $B_1/B_2 = m_1/m_2$. By lowering the magnetic field strength proportionally, a product ion can pass the magnetic sector being detected.

When B and E are lowered at the same time with the same proportionality, a fragment ion can pass both detectors being detected and the mass of the fragment ions (product ions) is directly proportional to the electric and magnetic strength. This can be seen by combining the above results: $E_1/E_2 = m_1/m_2 = B_1/B_2$ and $B_1/E_1 = B_2/E_2 = \text{constant}$. By scanning B and E with B/E constant (linked scan), all ions detected are from the same precursor ions.

For a precursor ion to pass both sectors, the above two equations can be rearranged into $B/E = R_e/(vR_m) = K/v$. So the B/E ratio is a velocity-related constant for a given spectrometer. When the instrument is operated in this mode, it can be used as a velocity selector - only ions with the same velocity as the precursor ions can pass both sectors being detected. At the beginning of a B/E linked scan, the B/E ratio is adjusted to pass selected precursor ions by the computer control system, based on calibration of the instrument.

For B/E linked scans with the JEOL HX 110, the resolution for precursor ion selection is not very high, 0.5% about a preset mass. Generally ions within a few mass units of the precursor ions will be selected. However, this inaccuracy in precursor ion selection does not affect the appearance of a spectrum very much. For example, the $(M-H)^-$ for H-VGGFL-OH is at m/z 490.2. The B/E linked scans were performed at m/z at 490.2, 489.2 and 491.2 for this peptide. The spectra (Figure 6.1a-c) were obtained and compared. It is found that the three spectra are almost exactly the same, except that the one at $(M-H)^-$ (490.2) has better signal/noise ratio and greater totally ion current. This observation indicates that the CID spectrum for a compound would be acceptable if the preset m/z values is within a mass unit from the m/z value of MH^+ or $(M-H)^-$ ions.

III. Experimental Section

Mass spectrometry: Ions were produced with 6 keV beam of fast Xenon atoms in a JEOL HX-110 double-focusing mass spectrometer operated in the negative ion mode. The accelerating voltage was 10 kV and the resolution was set at 1000 (10% valley). Glycerol was the liquid matrix chosen to obtain all spectra because it generates spectra with the best signal-to-background value for all of the peptides studied. For CID-MS/MS, helium was used as the collision gas in a cell located in the first field-free region. The helium pressure was adjusted to reduce the abundance of the precursor ions by 30%. A JEOL DA-5000 data system generated linked scans at constant B/E. With CID experiments at a resolution of 1000, a main slit setting at 3000 resolution will produce much better resolved CID spectra. This setting is thus recommended and used for CID-B/E linked scans.

Chemicals: The peptides H-VGVAPG-OH, H-YGGFL-OH, H-YGGFL-NH₂, and t-BOC-PPPP-OH were purchased from the Sigma Chemical Co., St. Louis, Missouri, and used without further purification. Aminomethanesulfonic acid, aminoethanesulfonic acid and aminobenzenesulfonic acid were purchased from Fluka Chemical Corp.,

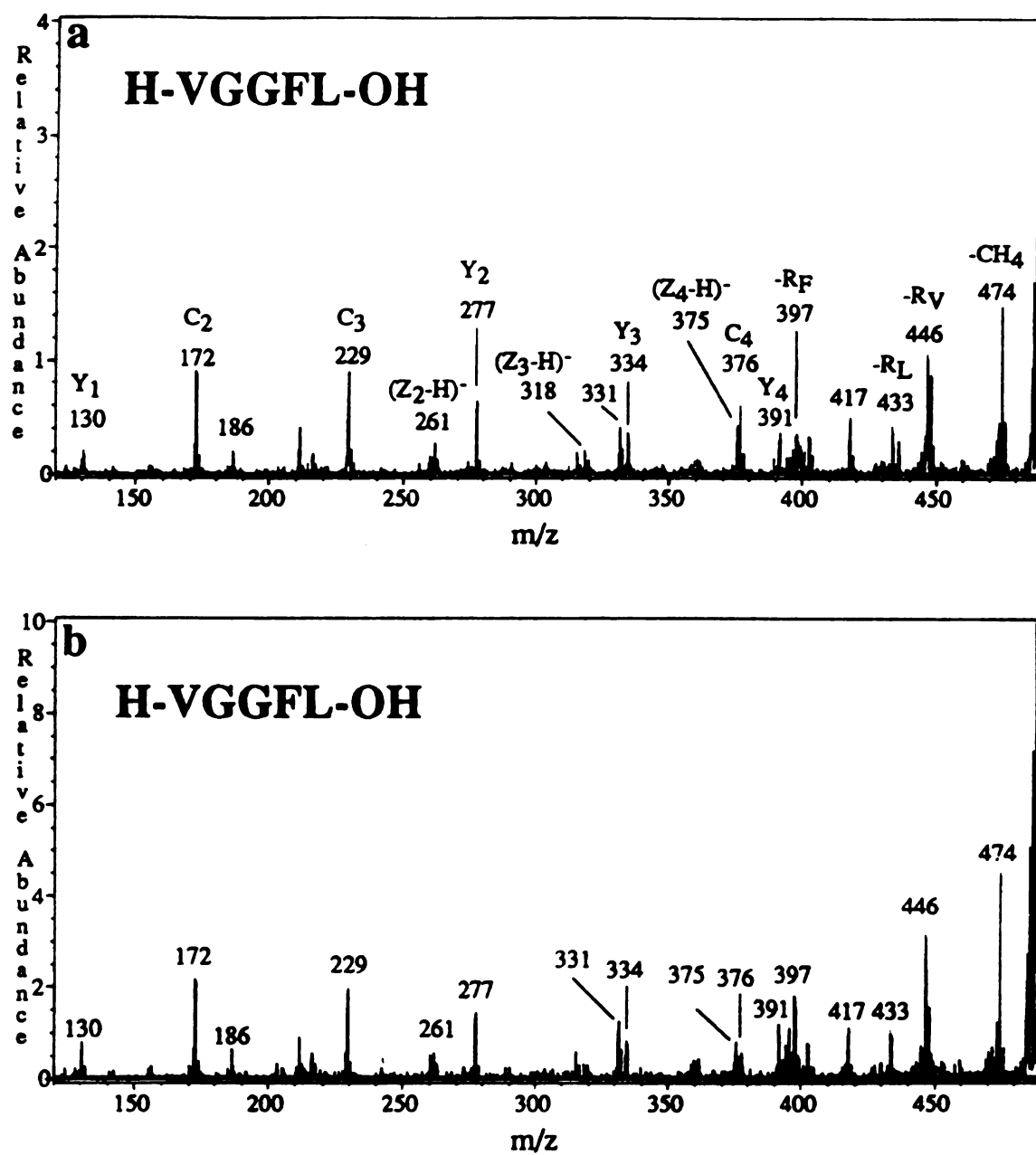


Figure 6.1 CID-B/E linked scan spectra for H-VGGFL-OH with precursors set at:
a) m/z 490.2, (M-H)⁻; b) m/z 489.2.

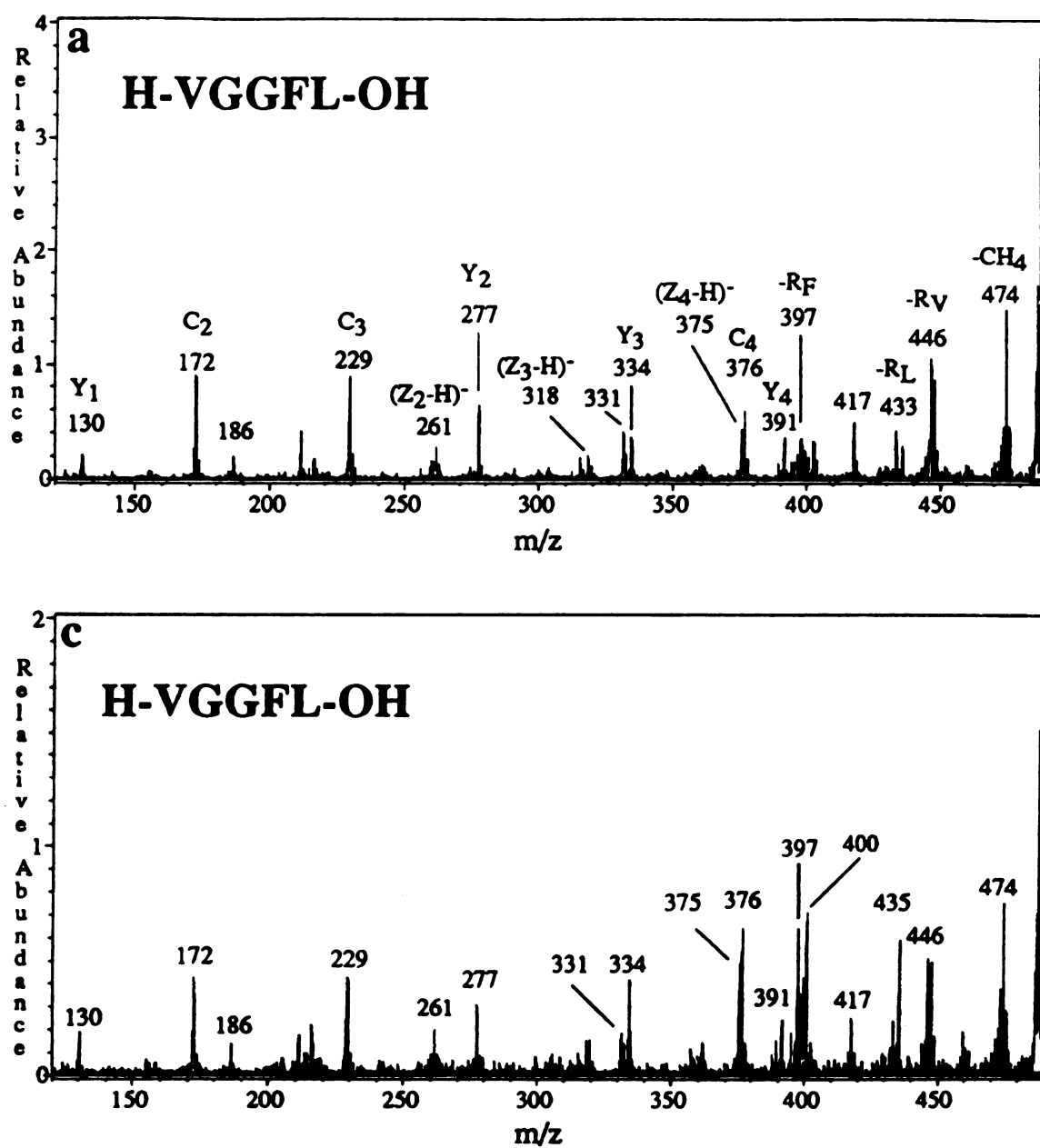


Figure 6.1 CID-B/E linked scan spectra for H-VGGFL-OH with precursors at:
a) m/z 490.2, (M-H)⁻; c) m/z 491.2.

Ronkonkoma, New York. H-AGGFL-OH, H-V α ^dGV α ^dAPG-OH, H-VGV α ^dAPG-OH, H-VGGFL-OH were synthesized in the laboratory at the University of Michigan. All other derivatization reagents were also purchased from Sigma Chemical Company without further purification.

Peptide derivatives (C-terminal esterification and N-terminal acetylation): N-terminally acetylated peptides such as Ac-VGVAPG-OH and Ac-AGGFL-OH, are formed from the free peptide using acetic anhydride, with a small amount of pyridine as a catalyst. The C-terminal methyl ester derivatives of peptides, such as H-VGVAPG-OCH₃ and H-AGGFL-OH, were formed from the free peptide using methanolic HCl. Detailed procedures have been described by Knapp [11]. For peptides with both termini blocked such as Ac-VGVAPG-OCH₃, equal volumes of acetic anhydride and 10% of pyridine methanol solution was added to the free peptide. The mixture was allowed to stand at room temperature for 15 minutes (longer time for higher yield). All of the reaction mixtures were dried on a Speedvac to evaporate all derivatizing reagents. This procedure also helps eliminate acid-catalyzed hydrolysis if the derivatives are prepared for later use.

Deuterated peptide methyl ester (peptide-OCD₃) was prepared as follows. A procedure very similar to the above was used. However, CD₃OD instead of CH₃OH, was used to prepare the hydrogen chloride methanol solution. The reaction mixture was dried on a speedvac. During this reaction, exchangeable hydrogen atoms of a peptide (NH₂-, -NH-, -COOH)- will exchange with the -OD deuterium of CD₃OD. To make the derivative deuterated only on the methyl ester moiety, back exchange with water was used. 50 μ l of water was added to the dried vial and the solution was dried on a Speedvac. This back-exchange procedure was repeated three times and the resulting residue re-dissolved in water for use. It is advisable not to use methanol for either back-exchange solvent or solvent for the product because the transesterification reaction, which occurs easily, can lead to a mixture of esters.

For peptide sulfonic-acid derivatives, the corresponding amino sulfonic acids such as aminomethanesulfonic acid (AMSA), aminoethanesulfonic acid (AESA) and aminobenzenesulfonic acid (ABSA) were used as the derivatizing reagents. They are coupled to the C-termini of peptides by using 1-ethyl-3-(dimethylaminopropyl) carbodiimide (EDC) as the coupling reagent in a pyridine-pyridinium chloride buffer solution of pH 6.

For peptide phosphonic acid derivatives, the corresponding aminophosphonic acids such as aminomethanephosphonic acid (AMPA), 2-aminoethanephosphonic acid (2-AEPA), 3-aminopropanephosphonic acid (1-APPA), 1-aminopropanephosphonic acid (3-APPA), 2-aminoethanephosphate (2-AEPO₄), 6-aminohexanephosphate (6-AHPO₄), were used as the derivatizing reagents. The same procedure as above was used.

For N-terminal derivatives such as sulfobenzoic acid ($\text{SBA} = \text{HO}_3\text{S}-\text{C}_6\text{H}_4-\text{CO}-$) derivatives of peptides, coupling with the above method gives rise to very low yield. The efficiency of the coupling can be improved by adding N-hydroxysuccinamide (NHS) at a higher pH buffer solution (N-morpholine-ethanesulfonic acid buffer at pH 6.5), as described recently by Sehgal and Vijay [12]. When a strongly acidic derivatizing reagent such as SBA is used, its pH value should be adjusted before the coupling reaction to assure proper reaction pH value. Otherwise, the buffer solution can not keep the pH value of the solution within the desired pH range with the addition of SBA. In our experiment, the SBA aqueous solution (pH \approx 2) is neutralized to about pH 6 before it was used. A reaction time of five hours or longer is usually required to achieve high yield.

IV. Deprotonation of Peptides

A. Deprotonation in the gas-phase or the liquid-phase?

When peptides are bombarded with fast atoms, they may be deprotonated in the liquid-phase or the gas-phase, as shown in Figure 6.2. In the case I, a deprotonated peptide is formed in the liquid phase due to acid-base equilibrium, this preformed ion is then desorbed directly from the liquid phase to the gas phase. According to this model, peptides with high liquid-phase acidity will have much higher efficiency in deprotonation thus will be more sensitive to MS analysis. In other words, a non-ionic species will have much lower efficiency of deprotonation or no deprotonation at all. In the second case, a peptide molecule is desorbed as a neutral into the gas phase; this neutral gas-phase molecule is then deprotonated by a deprotonated glycerol molecule via gas-phase ion-molecule reactions.

To test these desorption/ionization models, the responses of H-VGGFL-OH and its various derivatives were made and tested, each with different ionization efficiencies in the condensed phase such as glycerol matrix. For these compounds in a polar matrix such as glycerol, H-VGGFL-OH is considered zwitterionic due to the acid-base properties of the termini; Ac-VGGFL-OH is slightly acidic due to its C-terminal carboxylic acid group; SBA-VGGFL-OH is very acidic due to the strong acidic group (sulfonic acid group -SO₃H) at the N-terminus and the carboxylic acid group at the C-terminus; H-VGGFL-OCH₃ is non-ionic. If equal molar amounts of the peptide and their derivatives are bombarded with fast atoms in a polar matrix such as glycerol, different ion currents of (M-H)⁻ from these compounds will be obtained. If the response, the ion current from (M-H)⁻ of H-VGGFL-OH, is defined as 1, the relative response of a derivative can be obtained from the (M-H)⁻ current ratio of the derivative and the peptide. The responses of these compounds in formation of deprotonated molecules are listed in Table 6.1.

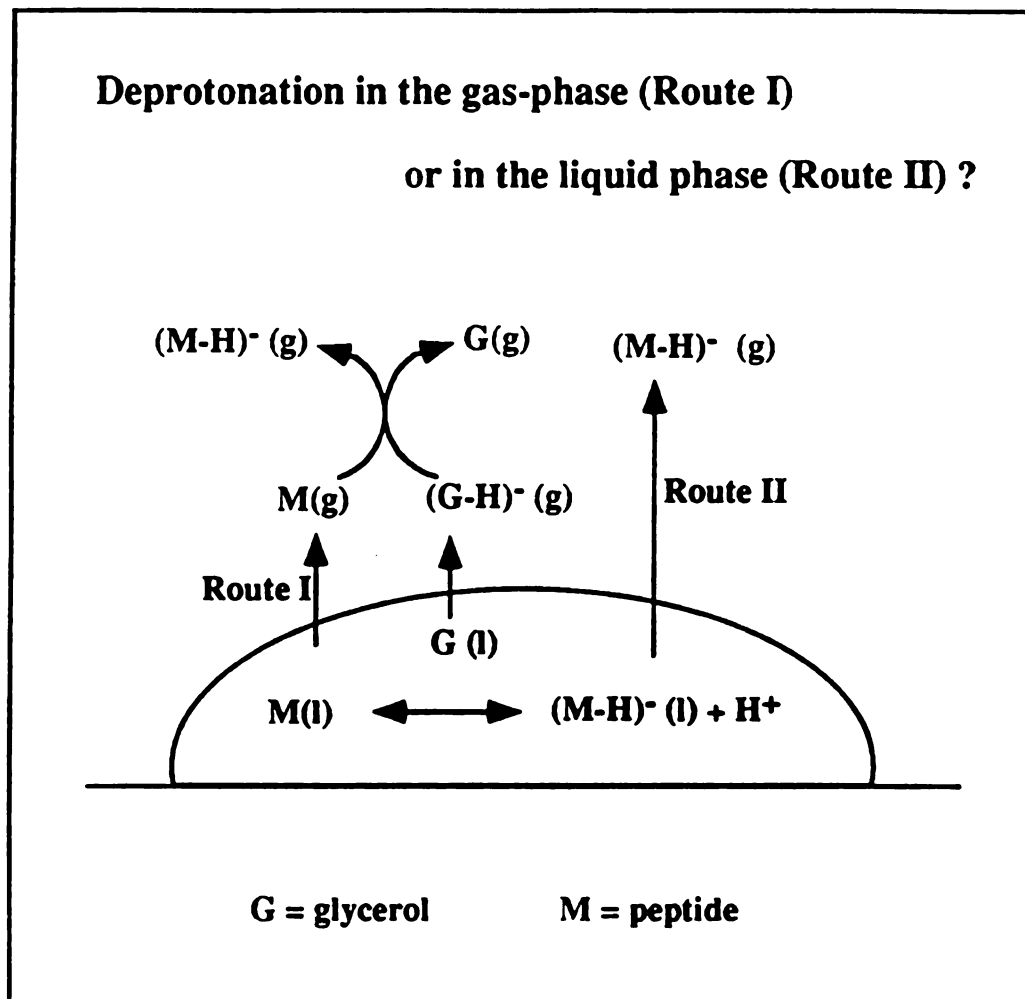


Figure 6.2 Deprotonation of peptides in glycerol matrix with FAB.

Table 6.1 Negative ion FAB responses of a peptide and its derivatives

<u>Peptide</u>	<u>Charge state in matrix</u>	<u>Relative Response</u>
H-VGGFL-OH	zwitterionic	1
Ac-VGGFL-OH	Ac-VGGFL-O ⁻ or neutral	1
SBA-VGGFL-OH	⁻ O ₃ S-C ₆ H ₄ -CO-VGGFL-OH	0.4
H-VGGFL-OCH ₃	neutral (non-ionic)	0.7

All the derivatives give responses smaller than that of H-VGGFL-OH. These observations lead to at least two conclusions: 1. It is not necessary to have preformed ions in the liquid-phase to produce gas-phase deprotonated ions. The spectra of H-VGGFL-OCH₃ and H-VGGFL-OH make it very clear. This comparison, however, does suggest that the C-terminus of a peptide is an important site of deprotonation. 2. Preformation of deprotonated peptides in the liquid phase does not enhance the number of gas phase deprotonated molecules. The responses of the two peptide derivatives, Ac-VGGFL-OH and SBA-VGGFL-OH, are clear evidences. 3. Therefore, deprotonation in the liquid-phase is not the mechanism for the formation of gas-phase deprotonated peptides.

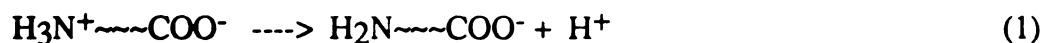
Note here there are many factors that could contribute to the change of responses. For example, derivatization changes the solubility, and surface activity of a peptide (in a specific matrix) which leads to a change in FAB response/(M-H)⁻ intensity. However, the effect of these factors can not be fully evaluated at this time. (The important point here is that, if the liquid-phase mechanism, RCOO⁻ (l) ----> RCOO⁻ (g), does not occur, then we don't know from where the H⁺ is lost. It could be -CHR-, -NH-, or -COOH).

1. Are peptides desorbed in zwitterionic form or in neutral form?

Peptides in aqueous solution are believed to be in a zwitterionic form. In a very polar matrix such as the commonly used glycerol, a peptide dissolved in it should also exist in a zwitterionic form.

When fast atoms (3 keV) bombard peptides in glycerol, it is our belief that only non-zwitterionic form of peptides are considered to be desorbed and deprotonated. First, non-ionic forms of peptides have much less interaction with the polar matrix such as glycerol and requires less energy for desorption, thus are preferentially deprotonated over the zwitterionic form. In addition, the high stability of $(M-H)^-$ ions from negative FAB-MS and MH^+ in positive mode, demonstrated by the intense peaks in the mass spectra, suggest that peptides are desorbed into the gas phase in a non-zwitterionic form. Otherwise, deprotonation or protonation alone in the gas phase will release a lot of energy ($\approx 160 \text{ kcal/mol} = 7 \text{ eV}$) in addition to the energy obtained from fast atom bombardment. This energy is far greater than the average internal energy deposition from collision activation, and is enough to induce high-energy fragmentations such as homolytic cleavages.

The energy released for the deprotonation of a peptide in zwitterionic form can be estimated as follows:



$$\Delta H^\circ (1) = -PA (H_2N \sim \sim \sim COO^-) \approx -PA (H_2N-C_2H_5) = -885 \text{ kJ/mol}$$



$$\Delta H^\circ (2) \approx -\Delta H^\circ \text{ acid } (C_3H_7O-H) = -1571 \text{ kJ/mol}$$

Combining the above two equations will result in equation (3):

$$(1) + (2) = (3):$$



$$\Delta H^\circ (3) = \Delta H^\circ (1) + \Delta H^\circ (2)$$

$$\begin{aligned} &\approx -1571 - (-885) = -686 \text{ kJ/mol} \\ &= -160 \text{ kcal/mol} \end{aligned}$$

This means that the deprotonation process is very exothermic if such a process occurs. However, no significant fragment ions are observed from regular FAB spectra, indicating that peptides are desorbed into the gas phase in non-zwitterionic forms.

It should be noted that some fragments from relatively high-energy processes are observed with FAB bombardment. For example, metastable spectra of $(M-H)^-$ of peptides frequently produces $(Z_n-H)^-$ ions which are supposed to be ionic radicals (negative distonic ions). The late formation of these ions may suggest that the excess energy obtained from FAB and from deprotonation is only slightly greater than the bond energy of NH-CHR (~ 80 kcal/mol), much less than the number shown above, indicating that the desorbed species is not in the form of zwitterionic form.

2. Thermodynamic support for gas-phase deprotonation

When the $(M-H)^-$ of a peptide H-VGGFL-OH is subjected to CID, the ion currents from fragment ions of both termini are about the same (Figure 6.1a). When AMSA is coupled to the C-terminus of a peptide such as H-VGGFL-OH, ion current from the C-terminus is far greater than that from the N-terminus (Figure 6.3a), indicating a significant charge-localization at the C-terminus of the peptide. When a ABSA derivative is analyzed, the charge localization effect is even more effective (see Figure 6.3b) because all fragment ions are C-terminal ions. Is it the change of gas-phase acidity or the change of the liquid-phase acidity that makes the difference?

Apparently, liquid phase deprotonation can not explain it because both the peptide and the derivatives are considered as zwitterionic molecules. No preformed $(M-H)^-$ (I) is present in the polar matrix such as glycerol.

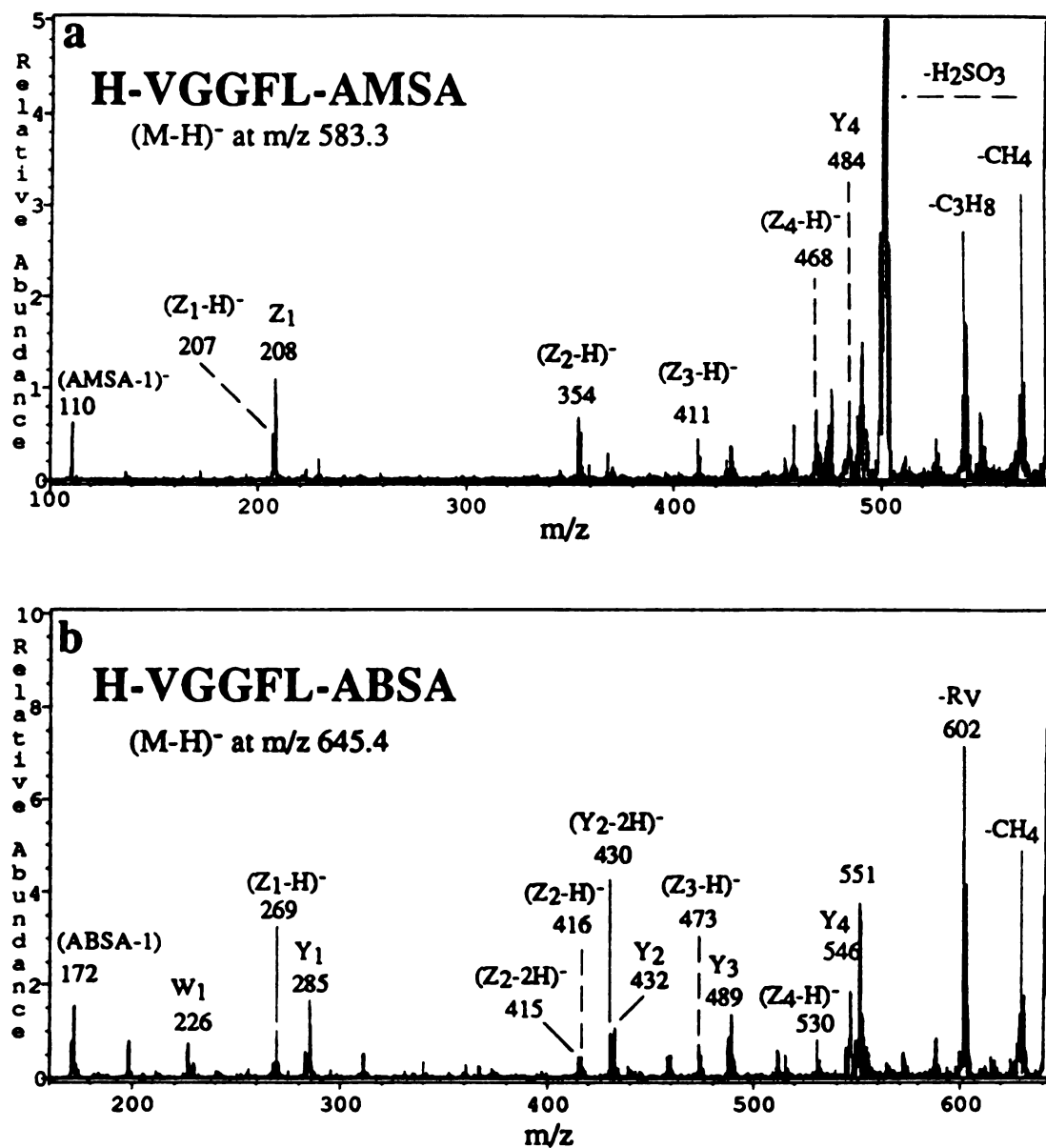


Figure 6.3 CID-B/E linked scan spectra of deprotonated peptides (derivatives):
a) H-VGGFL-AMSA; b) H-VGGFL-ABSA.

Consider gas-phase deprotonation. Since sulfonic acid is more acidic than carboxylic acid in the gas phase, thus the former (equation 4) is much more competitive than carboxylic acid group (equation 5) in deprotonation.



Therefore, charge-localization is observed at the sulfonic acid group. Charge-localization is indicated by the fact that only C-terminal ions are observed for ABSA derivatives.

With gas-phase deprotonation theory, the difference of CID spectra between ABSA derivatives and AMSA/AESA derivatives can be explained. The difference lies in their gas phase acidities. Even though the gas-phase acidity data for these derivatizing reagents are not available, the following data can provide insights into the effect of aromatic functionality on gas-phase acidity.

$$\Delta G^\circ_{\text{acid}} (\text{CH}_3\text{COOH}) = 1429 \text{ kJ/mol}$$

$$\Delta G^\circ_{\text{acid}} (\text{C}_6\text{H}_5\text{COOH}) = 1388 \text{ kJ/mol}$$

The introduction of the benzene ring reduces the gas-phase acidity by $40 \text{ kJ/mol} \approx 10 \text{ kcal/mol}$, which makes $\text{C}_6\text{H}_5\text{COOH}$ more favored in deprotonation than CH_3COOH . If this is the same for the sulfonic acid analog, which should be a fair statement, then ABSA with a benzene ring should be favored in deprotonation than AMSA/AESA. Therefore, in the gas-phase deprotonation reaction, ABSA derivatives are seen deprotonated more at the SO_3H group than AMSA/AESA derivatives. Because of this, ABSA has a stronger charge-localization effect than its aliphatic analogs. In summary, the results from charge-localization experiments support the gas-phase deprotonation mechanism.

B. The Site of Deprotonation of Peptides

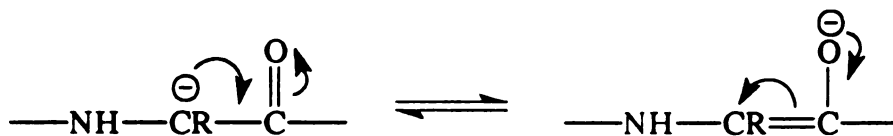
In early papers [1-10], the deprotonation site was assumed to be at the C-terminus of a peptide. The argument for this is based on the following gas-phase acidity data (amide -NH- was not considered in these paper), with the underlined H considered. Note that the gas-phase acidity of glycerol is considered because it is the most commonly used matrix for peptide analysis.

$$\Delta G^{\circ}_{\text{acid}}(\text{peptide } \text{CHR}) \approx \Delta G^{\circ}_{\text{acid}}(\text{CH}_3\text{COOH}) = 1518 \text{ Kcal/mol}$$

$$\Delta G^{\circ}_{\text{acid}}(\text{peptide } \text{COOH}) \approx \Delta G^{\circ}_{\text{acid}}(\text{CH}_3\text{COOH}) = 1429 \text{ Kcal/mol}$$

$$\Delta G^{\circ}_{\text{acid}}(\text{glycerol } \text{OH}) \approx \Delta G^{\circ}_{\text{acid}}(\text{C}_3\text{H}_7\text{OH}) = 1566 \text{ Kcal/mol.}$$

However, the reference data cited are not very convincing because acetic acid is quite different from amino acids, and because the α -hydrogens in a peptide (except for the N terminal one) are also dramatically different from the α -hydrogen in acetic acid. The presence of a amide group (-CONH- in a peptide) can make the deprotonation of the α -hydrogen atom much easier. In addition, with the deprotonation of an α -hydrogen, the negative charge will be stabilized by two electron withdrawing groups (-NH⁻CR-CO-) and two resonance structures:



This argument can be easily supported by comparing the following gas-phase acidity data with those shown above:

$$\Delta G^{\circ}_{\text{acid}}(-\text{CONHCHRCONH-}) \approx \Delta G^{\circ}_{\text{acid}}(\text{CH}_3\text{COOCH}_2\text{COCH}_3) = 1440 \text{ Kcal/mol}$$

$$\Delta G^{\circ}_{\text{acid}}(\text{NH}_2\text{CH}_2\text{COOH}) = 1401 \text{ Kcal/mol.}$$

The small difference between these two values suggest there may be significant deprotonation at α -carbon positions.

Table 6.2 compiles a list of gas-phase acidity data for the most common functional groups in peptides, with the gas-phase acidity value of a commonly used matrix glycerol.

Table 6.2 Gas-phase acidity of various functionality in peptides

<u>Deprotonation site</u>	<u>$\Delta G^\circ_{\text{acid}}$ (kJ/mole)</u>	<u>Reference Compound</u>
N-terminus	1640	CH ₃ CH ₂ NH ₂
-COOCH ₃	1610	HCOOCH ₃
Glycerol	1550	CH₃CH₂OH
CH ₃ CO-	1520	CH ₃ COOH
amide NH	1480	CH ₃ CONH ₂
-CHR-	1440	CH ₃ COOCH ₂ COCH ₃
C-terminus	1400	NH ₂ CH ₂ COOH

If the gas-phase acidity of a functional group is greater than that of glycerol, energetically it can not be deprotonated by deprotonated glycerol. If the gas-phase acidity value of a functional group is smaller than that of the glycerol, then it can be deprotonated by glycerol. Based on the data in Table 6.2, deprotonation can occur at the C-terminus, the amides and the α -carbons of a peptide because the $\Delta G^\circ_{\text{acid}}$ [13] values for these sites are smaller than that for glycerol.

It should be noted that deprotonation at side chains of some amino acids, such as glutamic acid, aspartic acid and cysteine, tyrosine, histidine and tryptophan, can be significant if present. However, deprotonation at these positions usually does not generate significant sequence ions, thus they were not studied in this work. The discussion below will be focused on the deprotonation along peptide backbone structures.

1. Does deprotonation occur at α -carbon position?

The N-terminus of a peptide is the least likely site of deprotonation. The high free energy required for the deprotonation makes it the least favored considering that deprotonation at many other sites are much more favored energetically.

Deprotonation at the C-terminus is assumed to be the most probable from other's work [2-8] due to its high gas-phase acidity. In addition to this site, are there any other sites of peptides showing significant deprotonation at fast atom bombardment?

To determine the site of deprotonation, deuterium-labeled peptides were used. Since deuterium exchange reactions are rarely complete, peptides with deuterium incorporated at α -carbon positions were synthesized and used in our study to assure high purity of deuterated peptides.

The FAB spectra of Ac-glycine- α d₂ (CH₃CONHCD₂COOH), H-VGVAPG-OH, H-VGVA α dPG-OH and H-V α dGV α dAPG-OH, H-AF β d₂LA-OH were obtained; the relative intensities of (M-H)⁻ and (M-2H)⁻/(M-D)⁻ ions are listed in Table 6.3. It should be pointed here that the purity of these deuterated peptides have been examined in these experiments.

Table 6.3 Relative intensities of (M-1)⁻ and (M-2)⁻ * ions for (deuterated) peptides

Peptide	Rel. Int. (M-H) ⁻	Rel. Int. (M-2H) ⁻ /(M-D) ⁻
H-VGVAPG-OH	100	5
H-VGVA α dPG-OH	100	5
H-V α dGV α dAPG-OH	100	5
CH ₃ CO-NHCD ₂ COOH	100	5

*Note: (M-1)⁻ = (M-H)⁻; (M-2)⁻ = (M-2H)⁻ and/or (M-D)⁻

The data in the above Table indicate that there is no change in the relative intensity of (M-H)⁻ and (M-2H)⁻/(M-D)⁻ ions. Therefore, there is no noticeable deprotonation at the

α -carbon positions (-CHR-) to the carbonyl group. Deprotonation of α -carbon positions in underivatized peptides does not occur for regular peptides.

2. Does deprotonation occur at amides or at α -carbon?

To answer this question, consider the other two potential sites of deprotonation besides the C-terminus of a peptide. Gas-phase acidity data suggest that deprotonation can occur at both the amide position and the α -carbon position, with the latter favored. In FAB experiments, which one is dominant?

To determine the deprotonation of amide and α -carbon positions, experiments with C-terminally blocked and α -deuterated peptides, such as H-VGVA α ^dPG-OCH₃ and H-V α ^dHGV α ^dAPG-OCH₃, were used, and the data for (M-H)⁻ and (M-2H)⁻/(M-D)⁻ were compared with that for H-VGVAPG-OCH₃ (see Table 6.4). In this process, the (M-2H)⁻ ion, which has the same m/z value as the (M-D)⁻ ion, has been taken into account; the intensity of (M-2H)⁻ ions for the undeuterated peptide is subtracted from that of the (M-2)⁻ ions [(M-2H)⁻ and/or (M-D)⁻ ions] for the deuterated analogs since it appears in the negative ion FAB-MS spectrum of every compound.

To exclude possible deprotonation at the methyl ester moiety, deuterated methyl ester, H-VGVAPG-OCD₃, was synthesized and examined by mass spectrometry (Table 6.4). It is found that there is no deprotonation at the methyl ester moiety of the derivatized peptides. Therefore, esterification is an effective method in blocking the C-terminus of a peptide without introducing new sites of deprotonation.

Based on Table 6.4, it is concluded that there is no removal of α -hydrogens (of -CHR- groups) for peptides in these experiments. Therefore, deprotonation of amides is much easier than that of α -carbon positions in FAB-MS experiments. The sites of deprotonation, along a peptide chain, are the C-terminal carboxyl group and the amide groups. However, it is NOT clear yet to what extents deprotonation occurs at each of these positions.

Table 6.4 Relative intensities of (M-1)⁻ and (M-2)⁻ ions for (deuterated) peptide esters

Peptide	Rel. Int. (M-H) ⁻	Rel. Int. (M-2H) ⁻ /(M-D) ⁻
H-VGVAPG-OCH ₃	100	5
H-VGVA ^α dPG-OCH ₃	100	5
H-V ^α dGV ^α dAPG-OCH ₃	100	5
H-VGVAPG-OCD ₃	100	5

3. Why is deprotonation of amides favored over that of α-carbon positions?

As stated above, thermodynamic data suggest that deprotonation of α-carbon positions (-CHR-) is favored compared to that of amide hydrogen. However, experimental results indicate that the expected deprotonation of α-hydrogen does not occur. Instead, deprotonation of amides is favored. Why?

One possible explanation is that the deprotonation kinetics dictates the sites of deprotonation because the deprotonation process is very short in time. For deprotonation at these two potential sites, the one with a faster deprotonation rate will dictate the site of deprotonation while the rates of these reactions are determined by the stability of their transition states.

To understand the stability of the two transition states in Figure 6.4, consider the polarity difference between C-H and O-H/N-H bonds. Due to the difference in electronegativity among C, H, N and O atoms, C-H is basically a non-polar bond while O-H and N-H are strong polar bonds. For reaction I in Figure 6.4, the strong charge-dipole (N-H) interaction with a charged oxygen atom of deprotonated glycerol stabilizes the intermediate/transition state, which leads to the deprotonation. In reaction II, however, there is no such strong interactions (C-H is practically a non-polar bond) present, thus the

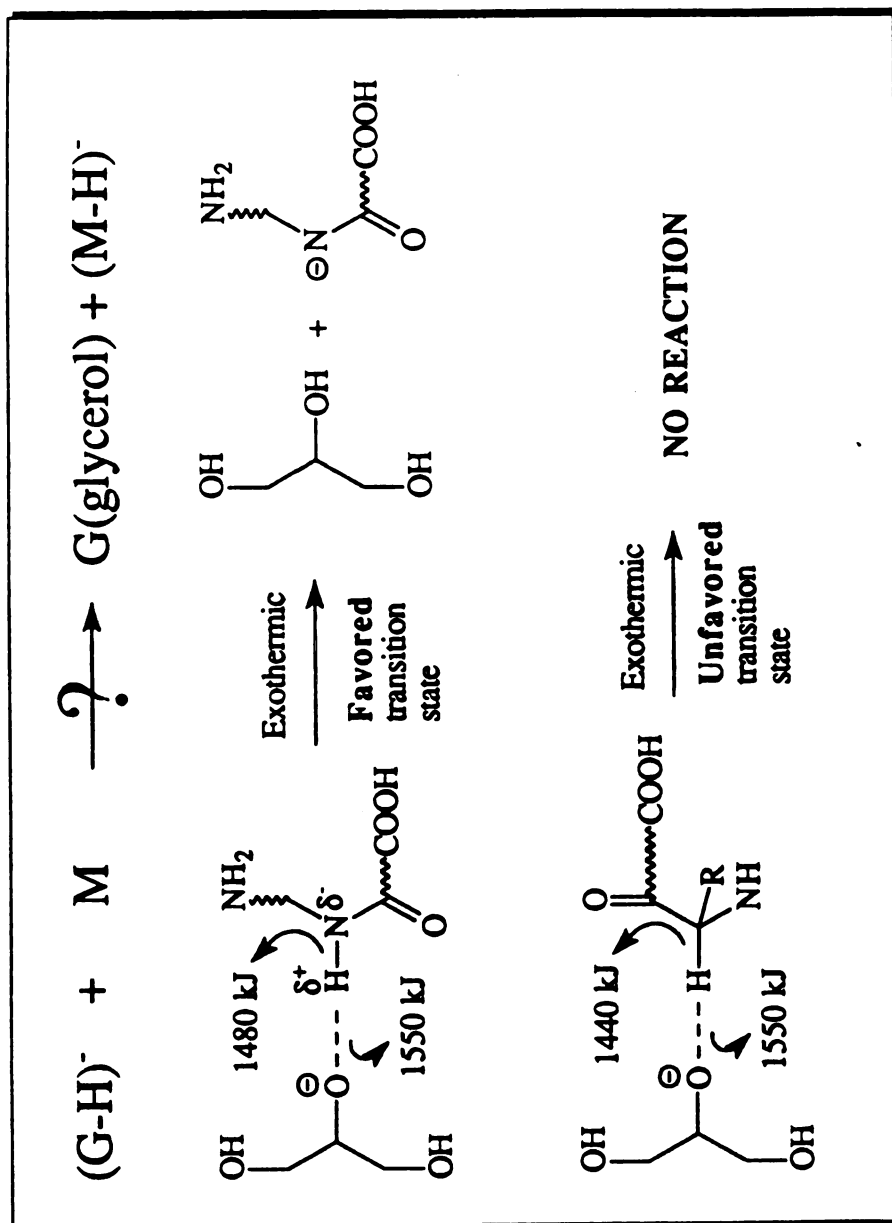


Figure 6.4 Kinetic reasoning for favored deprotonation of amides over that of α -carbon positions.

intermediate/transition state is not stabilized. Therefore, deprotonation at the α -carbon position is not observed. In summary, deprotonation requires a favorable transition state; and the reaction with stable transition states will dominate.

4. Charge-localization: Evidence for amide deprotonation

As can be seen from above experiments, deprotonation can occur at amides and the C-terminal carboxyl group. Is deprotonation at amides significant compared to that at the C-terminus? If deprotonation occurs only at the C-terminus of a peptide - that is, when charge is localized at the C-terminus of a peptide, what ions can be generated from CID of the charge-localized peptides?

To make C-terminally charge-localized peptides, peptide derivatives were made with sulfonic acid groups at the C-terminus. As shown in the spectra of H-VGGFL-OH and its derivatives in Figure 6.1a, the dominant ions for the underivatized peptides are C ions and Y ions, in about equal abundance. The dominant ions from H-VGGFL-AMSA (Figure 6.3a) are C-terminal ions while N-terminal ions are rare and weak. For H-VGGFL-ABSA (Figure 6.3b), there is no N-terminal ions, and all fragment ions are from the C-terminus. These spectra clearly indicate that C-terminally deprotonated peptides can generate only C-terminal ions!

Similar experiments were performed for N-terminally charge-localized peptides. When a sulfobenzoic acid group is coupled to the N-terminus of a peptide such as H-VGGFL-OH, charge will be localized at the N-terminus in this form, $^{-}\text{O}_3\text{S}-\text{C}_6\text{H}_4-\text{CO}-\text{VGGFL-OH}$. When this ion was subjected to CID, it was found that all ions generated were N-terminal ions (Figure 6.5), such as $(\text{A}_n-2\text{H})^{-}$, $(\text{B}_n-\text{H}+\text{OH})^{-}$. For a regular peptide, these ions are not observed. These results suggest that N-terminally deprotonated peptides generate only N-terminal ions. It also confirms that N-terminus of a peptide is not the site of deprotonation.

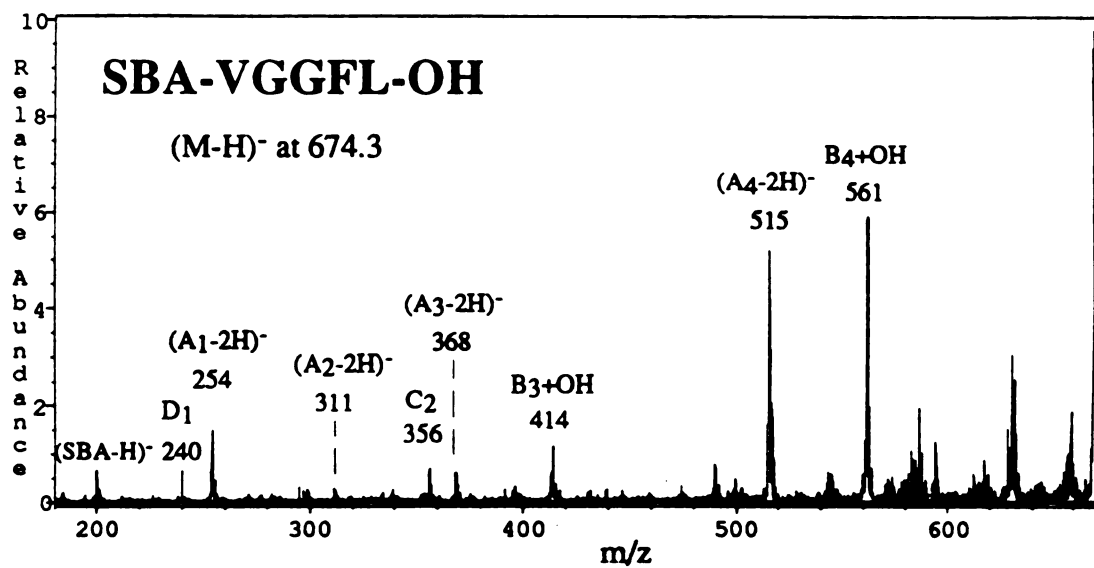


Figure 6.5 CID-B/E linked scan mass spectrum of a deprotonated peptide SBA-VGGFL-OH.

For a regular peptide, if deprotonation occurs at the C-terminus, as was stated in other's work [2-8], then N-terminal ions will not be seen in CID spectrum of that deprotonated peptide, as suggested by experiments with the above charge-localized peptides. In fact, both C-terminal and N-terminal ions are observed for CID of regular deprotonated peptides in about the same abundance. Therefore, there must be significant deprotonation at amide sites from which both C-terminal and N-terminal ions can be formed. The total fragment ion current from amide-deprotonated peptides is greater than that from C-terminally deprotonated peptides.

5. Final comments on the site of deprotonation

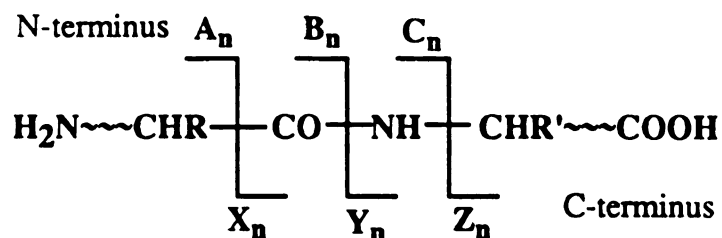
In explaining the backbone cleavage of deprotonated di-peptides and tri-peptides, rearrangement following deprotonation at the C-terminus of a peptide has been proposed [1] to explain the formation of Y ions. Our experimental results suggest, however, that there is a significant deprotonation at amides that is responsible for the formation of both N-terminal ions and C-terminal ions. Deprotonation at amides produces more sequence ions (C ions at least) than C-terminally deprotonated peptides.

V. Fragment Ions from CID-MS/MS spectra of Deprotonated Peptides.

A. Nomenclature

To designate negative ions precisely, the original Roepstorff nomenclature scheme [14] will be used, as is shown in Figure 6.6. A_n , B_n , C_n , X_n , Y_n and Z_n are used to represent the fragment formed at specific skeletal bond and terminus, where the subscript n represents number of side chains contained in a fragment. If a hydrogen atom is removed from a fragment, it is labeled by "-H". For example, $(Z_n-H)^-$ represents an anion that is one mass unit short of a regular Z_n fragment.

a) Roepstorff nomenclature [14] for peptide fragments



b) Common fragment ions from CID of deprotonated peptides

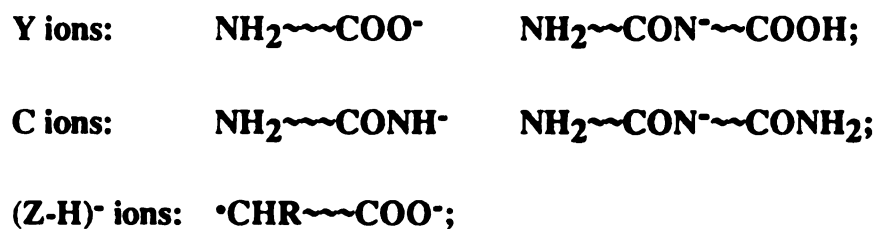


Figure 6.6 a) Roepstorff nomenclature for peptide fragments;
 b) Common fragment ions from deprotonated peptides.

When the amide bond of a neutral peptide, $\text{NH}_2\sim\sim\text{CO-NH}\sim\sim\text{COOH}$, is cleaved, two neutral fragments (radicals) are formed. The N-terminal fragment, $\text{NH}_2\sim\sim\text{CO}\cdot$, is called B_n fragment, and the C-terminal fragment, $\cdot\text{NH}\sim\sim\text{COOH}$, is called Y_n fragment. For a Y_n anion from CID of deprotonated peptides, the mass of a Y_n ion is practically equal to the mass of the Y_n neutral fragment, differing only by the mass of an electron. Note that Y_n ions can be formed in many different ways and their structures can be different.

It should be noted that the mass of a Y_n in negative mode is different from the mass of a y_n in positive mode. In positive mode, a y_n is a short-hand expression for a $(\text{Y}_n+2\text{H})^+$, which is two mass unit heavier than the Y_n anion from negative mode.

Besides the ions from skeletal bond cleavages, there are a few ions from sidechain cleavages that need to be clarified. The most important ions of this type are D_n ions and W_n ions, which are also two mass unit lower than the corresponding d_n and w_n ions in positive mode. D_n ions can be considered formed from their corresponding $(\text{A}_n\text{-H})^-$ ions [$\text{D}_n = (\text{A}_n\text{-H})^- - \text{R}$], and W_n ions can be considered formed from their corresponding $(\text{Z}_n\text{-H})^-$ ions [$\text{W}_n = (\text{Z}_n\text{-H})^- - \text{R}$].

Fragmentation in negative mode is more complicated than that in positive mode. In positive mode, a peak is frequently accompanied by only the isotopic peaks. In negative ions, however, peak clusters are always observed, especially for ions at high mass region of a spectrum. This complication sometimes makes ion assignment difficult; experiments with deuterated peptides are also less effective than those for positive ions.

B. Common fragment ion series

i) The most common fragment ions are Y_n ions, C_n ions and $(\text{Z}_n\text{-H})^-$ ions (Figure 6.1a - the spectrum of H-VGGFL-OH). The latter two have not been encountered in the study of smaller peptides such as di- and tri- peptides. Dehydration products of these ions,

and fragments of these ions from specific side-chain loss such as loss of CH_2O from serine [1] are also observed.

ii) $(\text{A}_n-2\text{H})^-$, $(\text{B}_n-2\text{H})^-$, $(\text{X}_n-2\text{H})^-$ ion series are usually not very abundant in negative FAB spectra, except for those at the high mass end and those with cleavages around aromatic side chains. However, if more acidic side chains (Asp and Glu) are at or near the N-terminus of a peptide, $(\text{A}_n-\text{H})^-$ and $(\text{A}_n-2\text{H})^-$ ions can become fairly abundant. When a charge is localized at the N-terminus of a peptide, $(\text{A}_n-\text{H})^-$ become one dominant ion series (Figure 6.5).

iii) $(\text{Z}_n-\text{H})^-$ and $(\text{A}_n-\text{H})^-$ ion series are the only two groups that are not two mass units lower than their positive ion counterparts.

iv) When a charge is localized at the N-terminus of a peptide, or when a proline residue is close to the C-terminus of a peptide, $(\text{B}_n+\text{O})^-$ ions/ $(\text{B}_n-\text{H}+\text{OH})^-$ ions are formed at the high mass region of a peptide spectrum (Figure 6.7).

C. Ion Structure and Stability

In the fragmentation of deprotonated peptides, Y ions and C ions are the most frequently observed. To understand the formation and their relative abundances, it is necessary to consider the structures of these ions and structure-stability relationships.

When a peptide is deprotonated at the C-terminus or amides, these deprotonated peptides will all have resonance structures, which stabilize fragment ions formed in the CID of deprotonated peptides. Fragments with resonance structures will generate much more intense peaks in a mass spectrum. In a later part of this work, this assumption is successfully used to explain the relative intensities of various ion series in deprotonated peptides.

One of the most important ion series is the Y_n ions and the following is the possible structures of these ions:



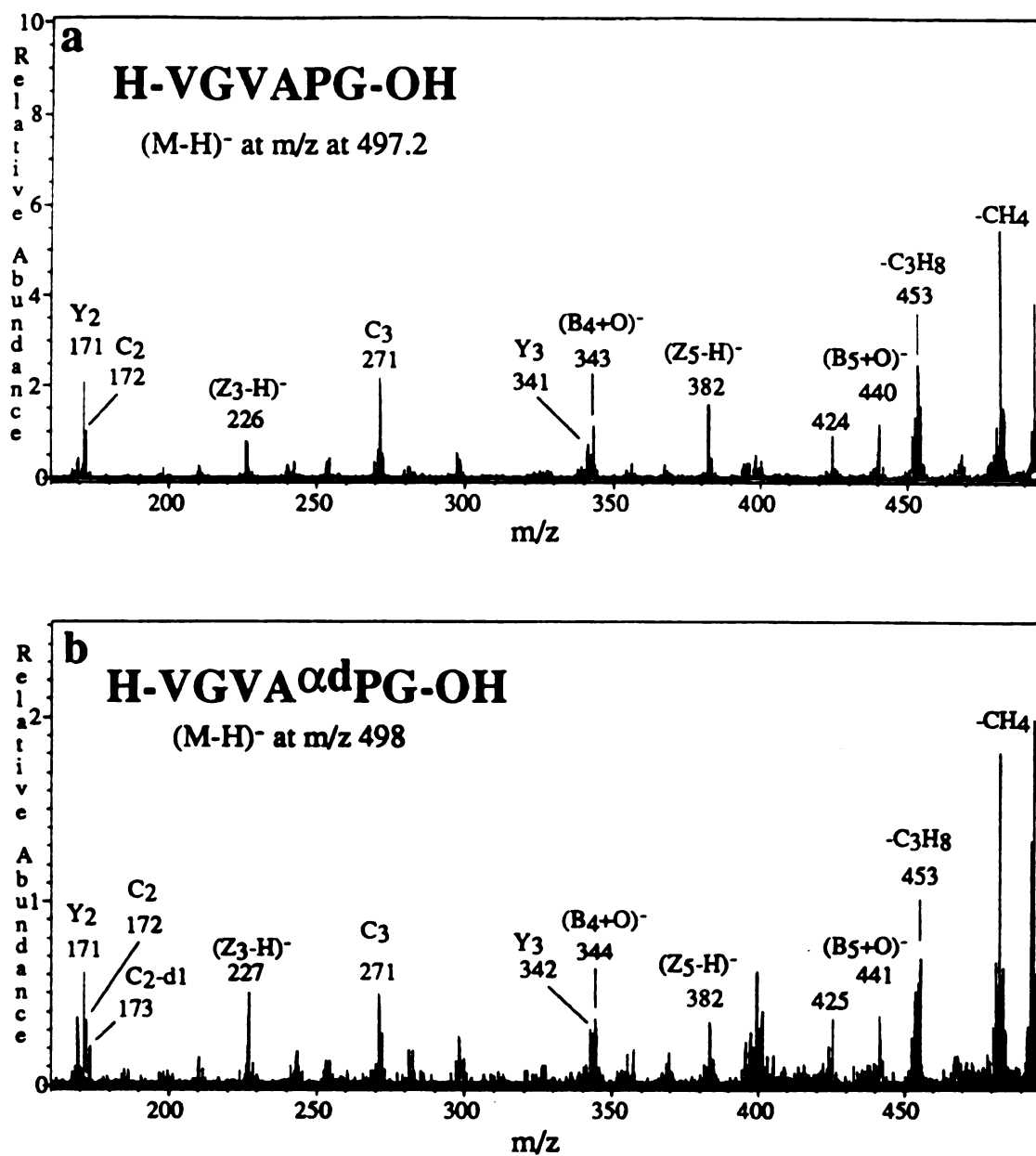


Figure 6.7 CID-B/E linked scan mass spectra of deprotonated peptides:

a) H-VGVAPG-OH; b) H-VGVA^αdPG-OH.

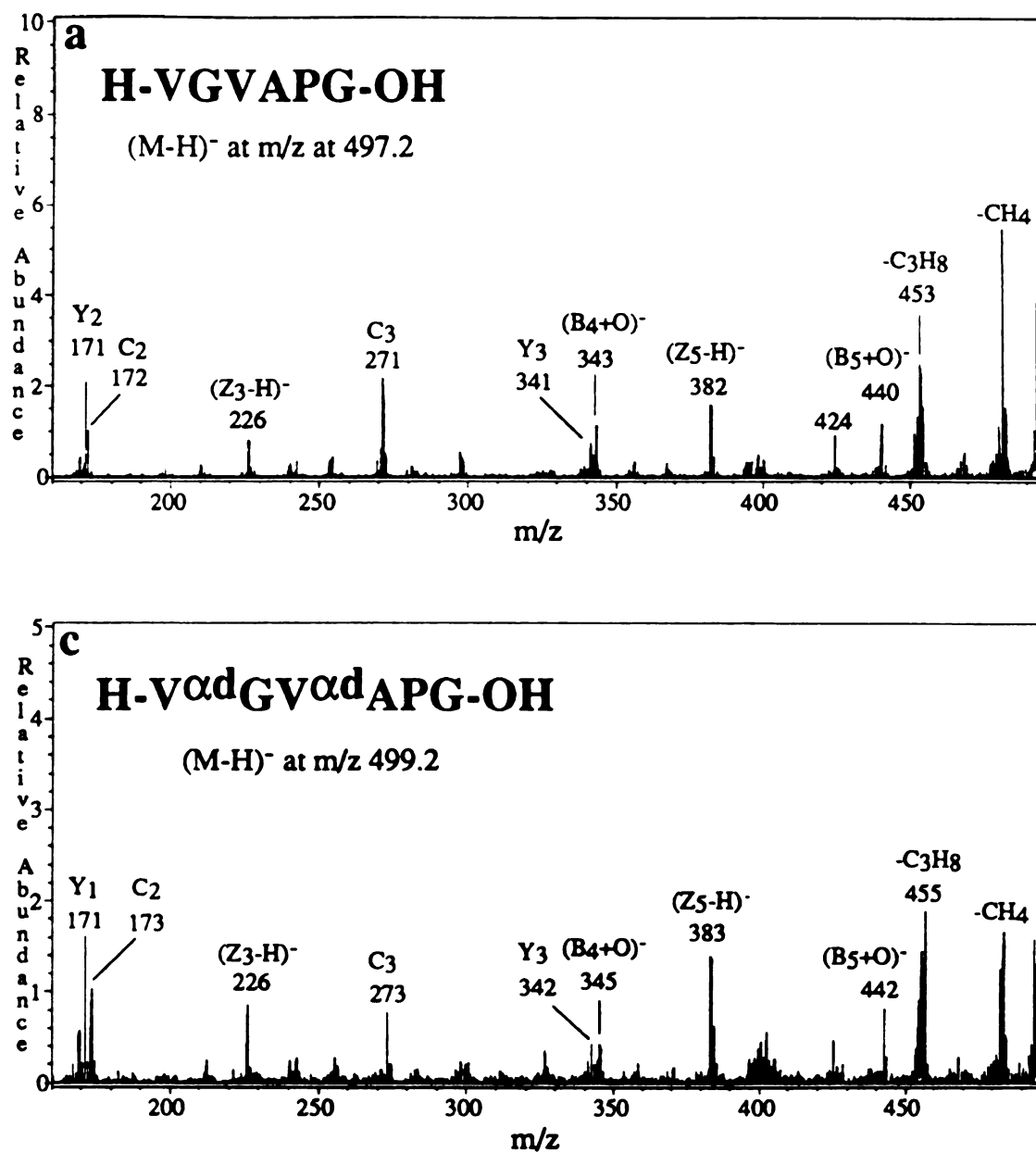
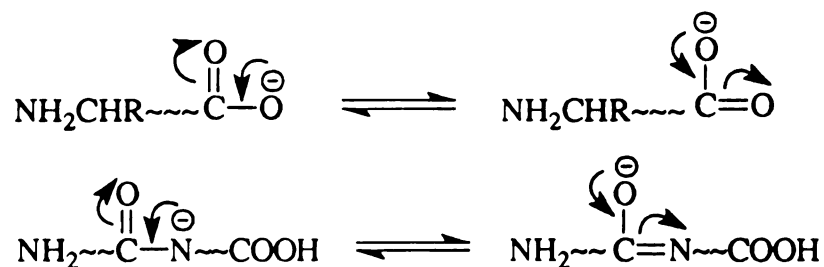


Figure 6.7 CID-B/E linked scan mass spectra of deprotonated peptides:

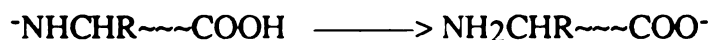
a) H-VGVAPG-OH; c) H-VαdGVαdAPG-OH.



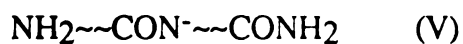
From the structures of these ions, it is easy to see that the last two structures are more stable because they have resonant structures. Therefore these structures are most probably the structures of Y ions formed in CID experiments.



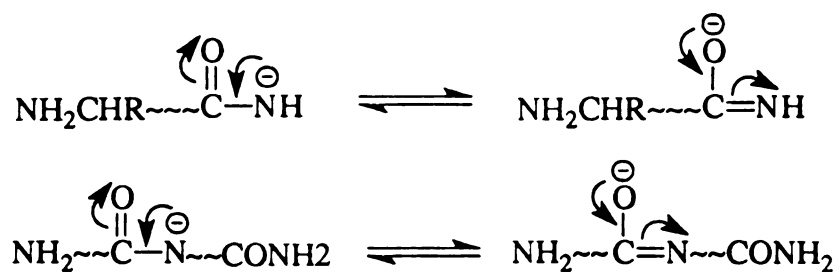
Structure I is less stable due to the lack of a resonance structure. However, this structure can rearrange to a much more stable form easily via the following reaction (a very exothermic reaction with $\Delta G^\circ \approx -60$ kcal/mol), especially when the ion is not very large:



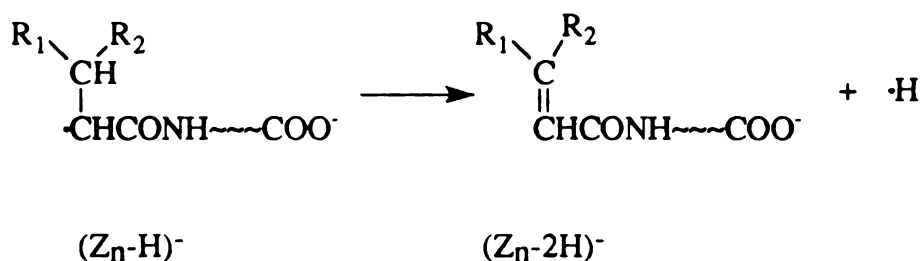
The other most important ion series from CID of deprotonated peptides is the C-ions and the following is a list of their possible structures:



Note here that the first two structures are more stable because they have the following resonance structures.



For Z-type of ions, the most commonly seen are $(Z_n\text{-H})^-$ and $(Z_n\text{-2H})^-$, with the former frequently more abundant. The $(Z_n\text{-H})^-$ ions are probably formed via homolytic cleavage of C-terminally deprotonated peptides.



VI. Mechanisms for the Fragmentation of Deprotonated Peptides

In the study of ion fragmentation chemistry, two approaches have been frequently used. One of them is through the use of deuterium-labeled compounds to trace the shift of a hydrogen atom when it is involved. The other common method is by controlled derivatization such as derivatizing specific functionality to examine the role of that functionalities in the fragmentation of a specific compound [11]. In this work, both deuterated peptides and derivatized peptides will be used to study the CID behavior of deprotonated peptides.

A. H-Shift: Mechanistic Study by Using Deuterated Peptides

Mechanisms regarding the formation of some common ions involving the shift of hydrogen atoms, from CID of deprotonated di- and tri- peptides, have been proposed in the literature[1-10]. In these studies, deuterated peptides from deuterium/hydrogen exchange have been prepared. It has been reported that, for all dipeptides studied [1], the shift of α -hydrogen was observed.

In this study, partially deuterated larger peptides, with deuteriums at specific α -carbon positions, were used and the CID spectra of these deprotonated peptides were obtained. From the CID spectra of H-VGVAPG-OH, H-VGVA α dPG-OH and H-V α dHGV α dAPG-OH (Table 6.5 and Figure 6.7a-c), it was found that shifting of deuterium did not occur in the formation of Y_n ions. In the formation of C ions, most of them are formed without α -hydrogen shift being observed. However, an α -hydrogen shift does occur to a small extent (30% in the case of H-VGVA α dPG-OH), four atoms away from the deprotonated amide nitrogen. Therefore, the formation of Y_n ions does not involve the shift of α -hydrogens. However, there are at least two ways that C ions can be formed via one of which there is an α -hydrogen shift.

Table 6.5 Ions from peptides and their deuterated analogs

Peptide	m/z(C ₂)	m/z(Y ₃)	m/z(Y ₄)	m/z(Y ₂)
H-VGVAPG-OH (I)	172	242	398	171
H-V α dGV α dAPG-OH (II)	173	242	399	171
H-VGVA α dPG-OH (III)	172/173	243	399	171
Deuterium-shift ?	no/yes	no	no	no

Note that the changes in the m/z values of the same ions from different peptides above (for example C₂ of peptides I and II are at m/z 172 and 173, respectively) are not due to the shift of deuteriums except for C₂ of peptide III.

This observation carries a very important message. First, the formation of either Y_n ions or C_n ions is not from a 1,2 - elimination process. Secondly, fragmentation of larger peptides is different from that of dipeptides. In early papers on dipeptides [1], it was found that the formation of Y_n ions involved the shifting of an α -hydrogen atom to the deprotonated C-terminus. This is clearly not the case in this study.

Since present mechanisms can not explain all the observations in CID spectra of deprotonated peptides, alternative mechanisms have to be proposed.

B. CID Fragments from Derivatized and Underivatized Peptides

In fragmentation of deprotonated peptides, we believe that the site of deprotonation plays an important role. To determine the effect of deprotonation sites on fragment ion series, various peptide derivatives, as listed below, were made with expected deprotonation at different sites:

<u>Sample peptide</u>	<u>Deprotonation site</u>	<u>Fragment ions</u>
H-V/AGGFL-OH	C-terminus and amides	Y_n & C_n ions
Ac-VGGFL-OH	C-terminus and amides	Y_n & C_n ions
H-VGGFL-ABSA	C-terminus	C-terminal ions only
H-AGGFL-OCH ₃	Amides	C_n ions and Y_n ions
SBA-AGGFL-OH	N-terminus	$(A_n-2H)^-$ & $(B_n+O)^-$

a) **Regular peptides:** With these peptides, the most dominant fragment ions are C ions and Y ions (as shown in Figure 6.1a and 6.7a). There are also some other ions, however with much lower abundances. With N-terminal acetylated peptides, the fragment ions and their relative abundance are about the same, suggesting that the N-terminus is not very reactive in fragmentation of deprotonated peptides.

It should be pointed out, for small peptides such as di- and tri-peptides, C ions were not observed very often from CID of $(M-H)^-$. For larger peptides as was the case in this study, C ions have been found to be one of the most important ions. This clearly indicates that the effect of size on fragmentation because the size of a precursor ion affects the energy deposition and the energy distribution. Note here that the center-of-mass energy E_{com} - maximum amount of energy that can be obtained from collision is approximately inversely proportional to the mass of the precursor ion. ($E_{com} = [M_{He}/(M_{He}+M_p)] \times E_p$, where E_p is the translational energy of $(M-H)^-$ ion, M_p is the mass of the $(M-H)^-$, M_{He} is the mass of the collision gas He.)

b) Amide-deprotonated peptides: When the C-terminus of a peptide is blocked methyl ester, the deprotonation sites along the peptide backbone can only be amide nitrogens. As shown in Figure 6.8a-b, both C ion and Y ions are observed for the peptides H-VGGFL-OCH₃ and Ac-VGGFL-OCH₃. However, Y ions are suppressed more. This result clearly indicates that amide deprotonated peptides can produce both C ions and Y ions.

The ion series from amide deprotonated peptides indicates that amide deprotonated peptides barely produce Y ions. The suppression of Y ions, in the form of $-NHCHR \sim \sim \sim COOCH_3$, is related to the lack of a resonance structure, and thus they are less stable than their corresponding C ions (see part C of section V).

It should also be noted that the abundances for C ions are not as high as those from the regular peptides, indicating that the C-terminus of a peptide contributes to the formation of C ions via a H-shift from the C-terminus to deprotonation sites.

c) When the C-terminus of a peptide is made to be a very acidic moiety such as aminobenzenesulfonic acid moiety (ABSA = $-NHC_6H_4SO_3H$), the C-terminus of the peptide derivative will be the site of deprotonation and only C-terminal ions, dominantly Y ions and $(Z-H)^-$ ions (Figure 6.3), are observed. This observation clearly indicates that C-terminally deprotonated peptides can not produce the C ions. Therefore, there must be

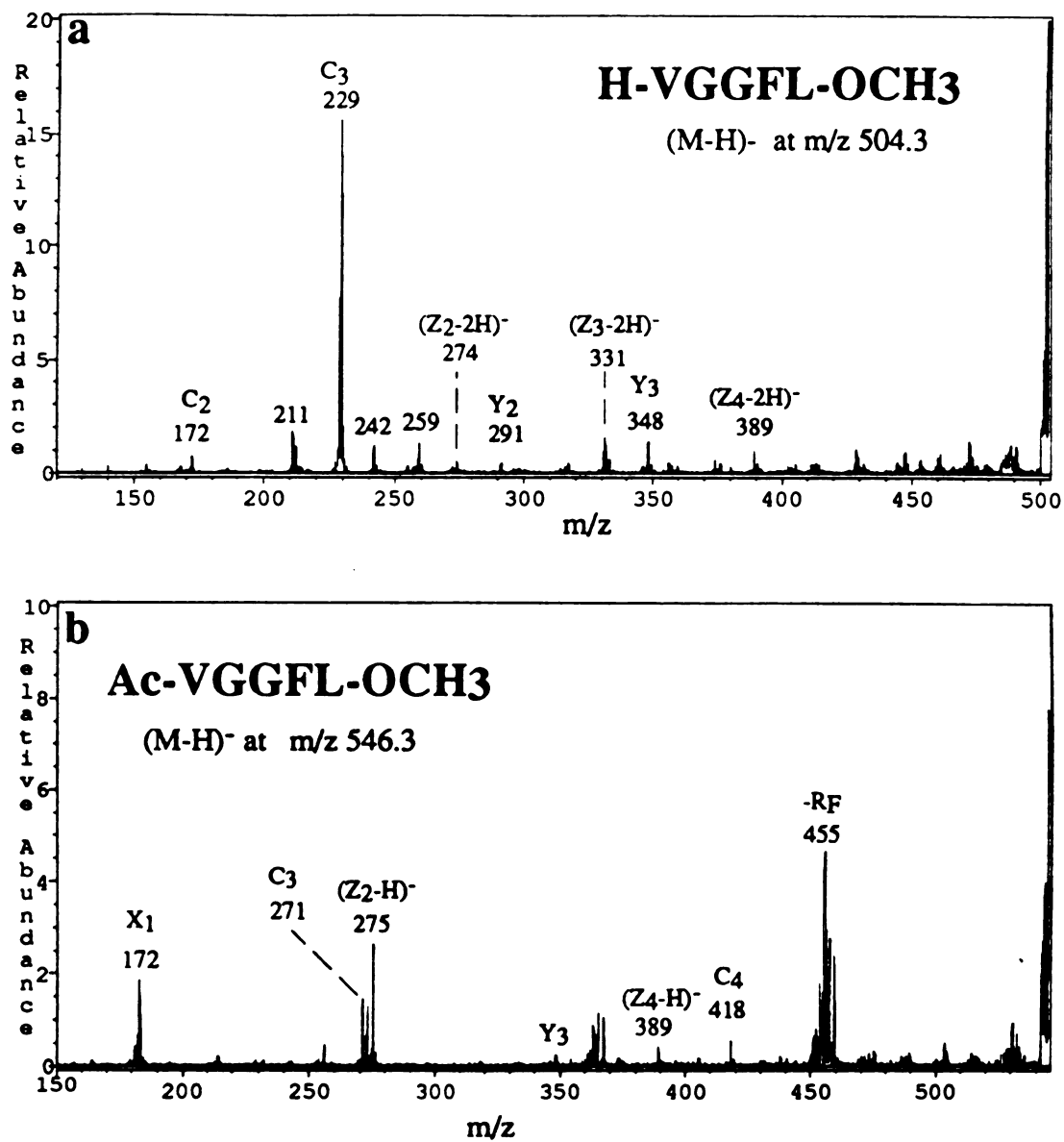


Figure 6.8 CID-B/E linked scan spectra of deprotonated peptides (derivatives):
a) H-VGGFL-OCH₃; b) Ac-VGGFL-OCH₃.

significant deprotonation at the amide sites which are responsible for the formation of C ions.

When the N-terminus of a peptide is attached to a very acidic moiety such as sulfobenzoic acid moiety (SBA = $\text{HO}_3\text{S}-\text{C}_6\text{H}_4-\text{CO}-$), the deprotonation site will be at the N-terminus of the peptide derivative. As shown in Figure 6.5, the dominant ions are N-terminal ions such as $(\text{A}_n-2\text{H})^-$ and $(\text{B}_n-\text{H}+\text{OH})^-$ ions. In the spectra of regular peptides, this ions are rarely seen, consistent with the gas-phase acidity data which suggest that the N-terminus of a peptide is not the site of deprotonation for regular peptides.

VII. Mechanisms: The Formation of Major Fragment Ions

A. Ions from Amide-Deprotonated Peptides

1,3 - Elimination mechanisms: When $(\text{M}-\text{H})^-$ ions of n-mer peptides are subjected to high-energy collisions with He, the Y_{n-1} and C_{n-1} ions are most frequently observed. These ions can be formed only via two mechanisms shown in Figure 6.9. Both are 1,3 - elimination reactions, with one charge-induced and the other charge-remote. Fragmentation in Figure 6.9a is more favored than that in Figure 6.9b because charge-dipole interactions in Figure 6.9a is more favored than those in Figure 6.9b.

In Figure 6.9a, a H-shift occurs from one of the two termini. Based on this mechanism, it is reasonable to believe that the following fragmentation reaction in Figure 6.10 can also occur. In this mechanism, a H-shift is from an adjacent amide NH. These reactions can be classified as a 1,3 - elimination reactions.

Displacement - reaction mechanisms: C ions and Y ions can also be formed via a displacement reaction without a H-shift, as is shown in Figure 6.11. In this

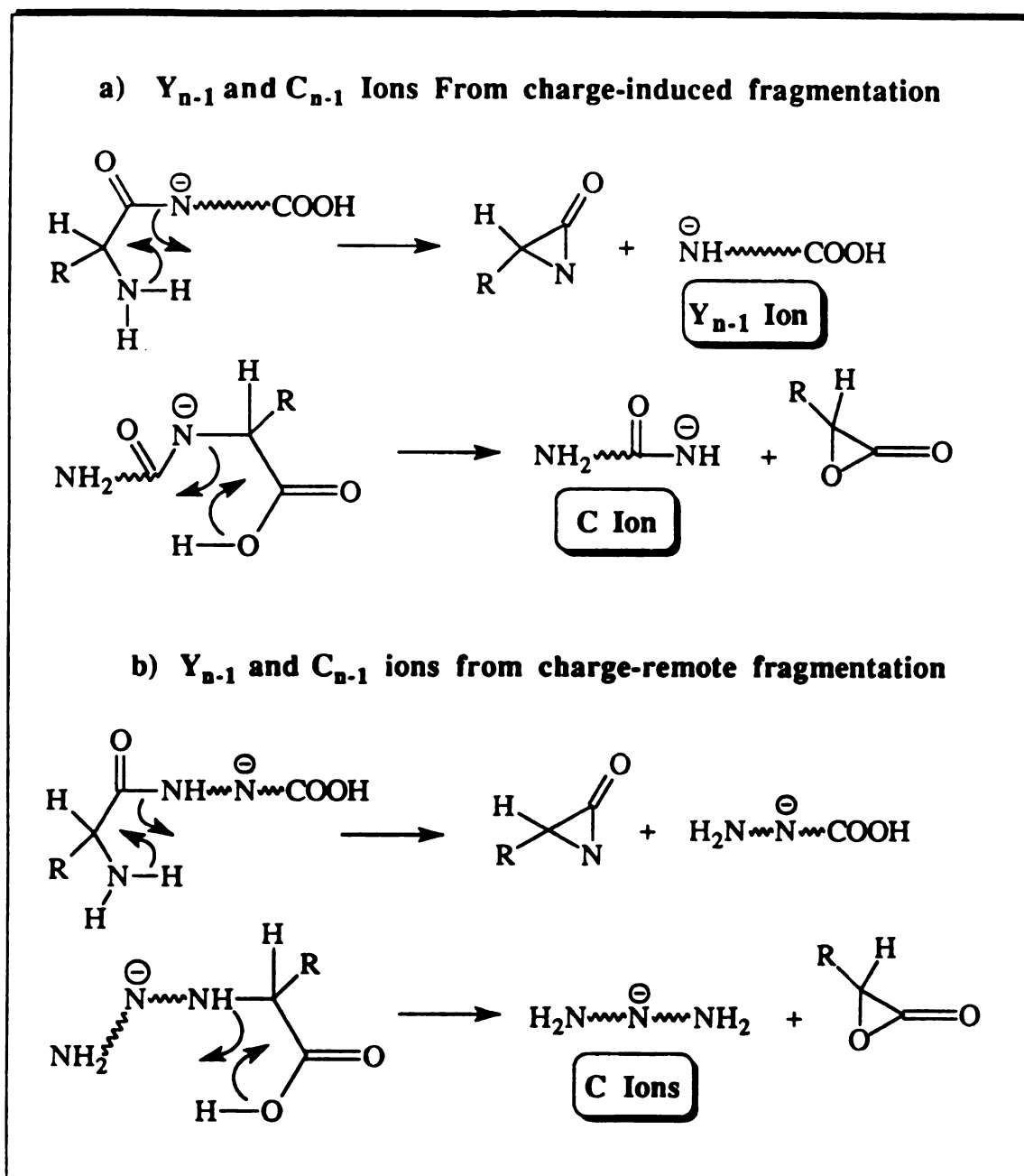


Figure 6.9 The formation of Y_{n-1} and C_{n-1} ions via 1,3 - elimination mechanisms.

a) Charge-induced fragmentation; b) Charge-remote fragmentation.

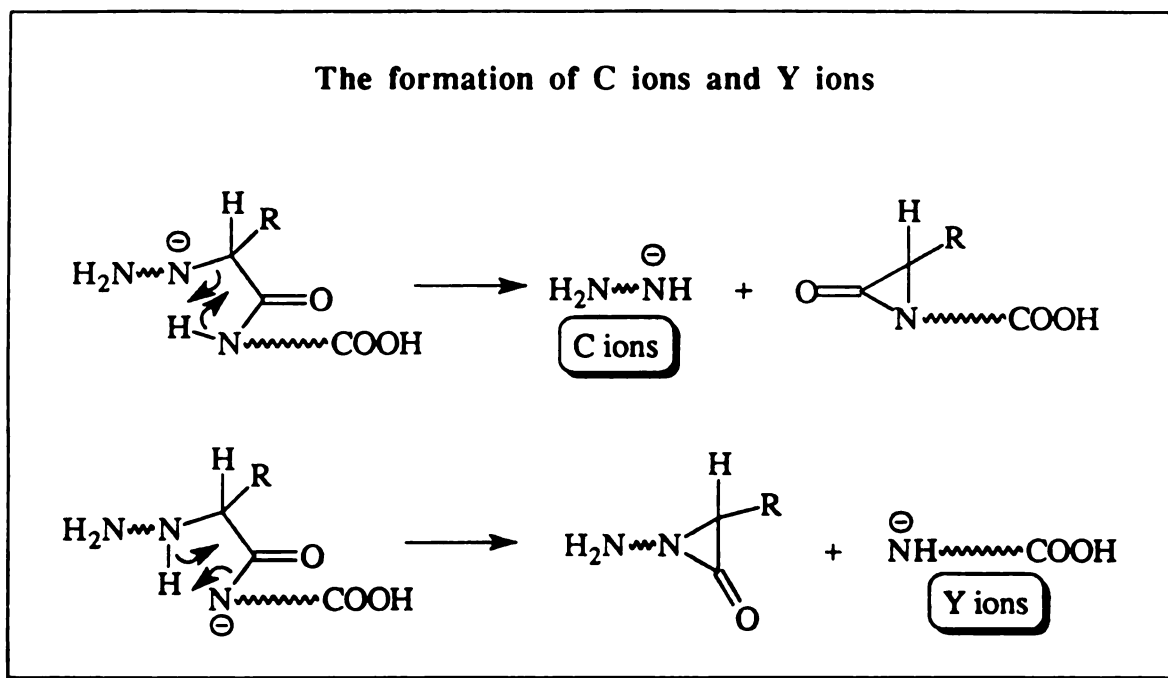


Figure 6.10 The formation of Y and C ions via 1,3 - elimination reactions
(Charge - induced fragmentation)

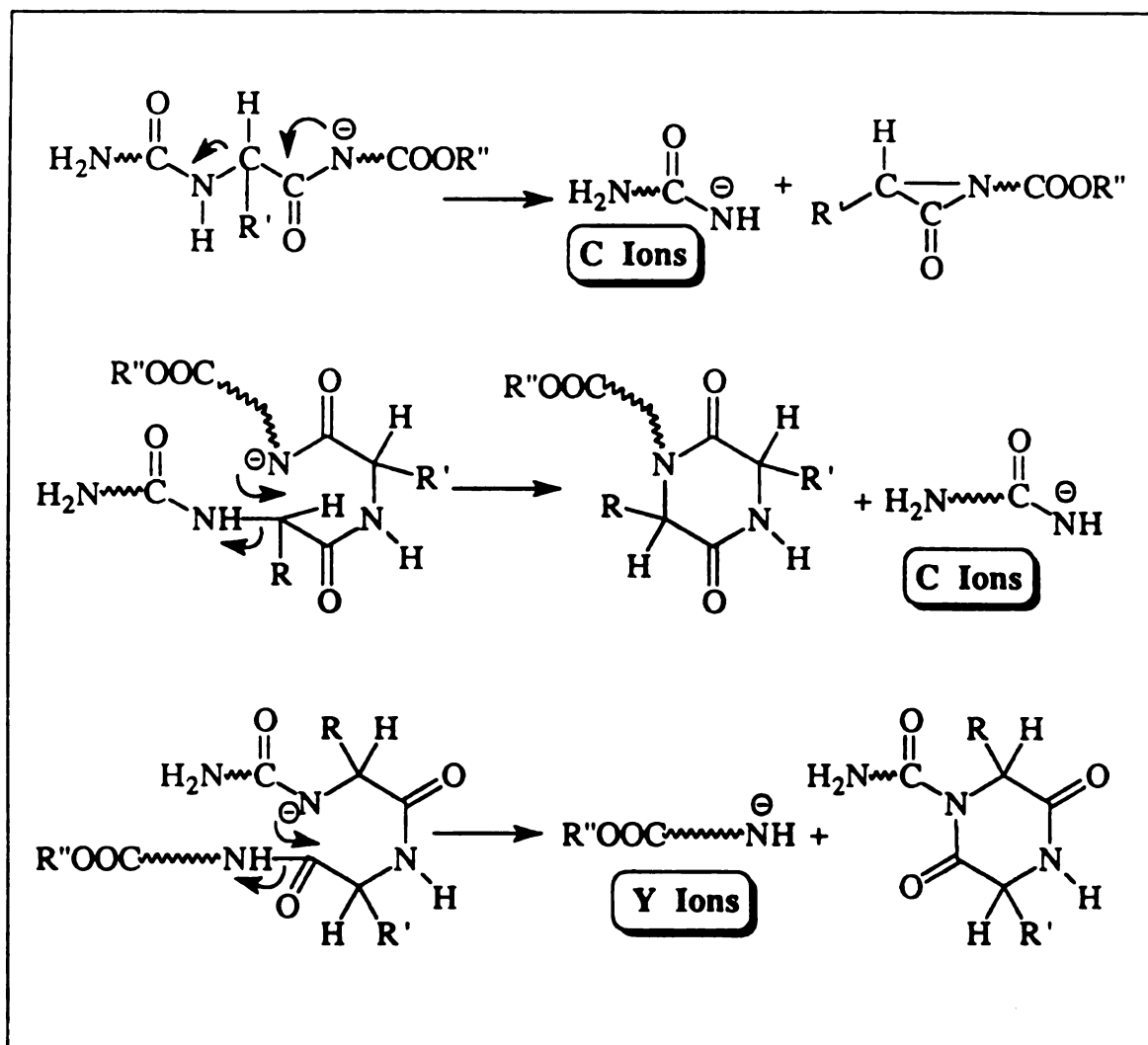
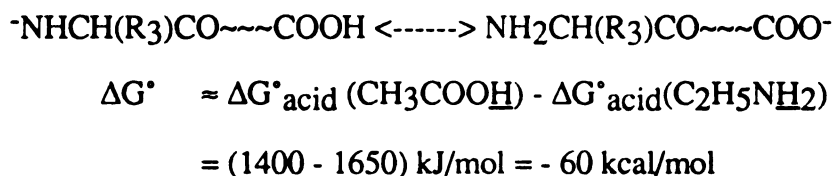


Figure 6.11 C_n ions and Y_n ions from displacement reactions.

mechanism, only electron-pair-shifts are involved. Because of this, steric hindrance for such processes are small thus such processes may be significant.

The above reaction mechanisms can easily explain many experimental facts. First, they can explain the fact that the relative intensities of Y ions and C ions are about the same for underivatized peptides. The reason is that the formation mechanisms for these ions are exactly the same. Even though the C ions thus formed are more stable due to their resonant structures, the following rearrangement reaction (very exothermic reaction!) can proceed to stabilize the Y ions thus formed, especially when the ions formed are not very large (so the termini of the ion will more probably interact with each other):



In the gas-phase of a high vacuum, different parts of a large molecule tend to interact with each other due to charge-dipole, dipole-dipole interactions (and van de Waal force), leading to folding of ions/molecules in the gas phase. Because of these interactions, this exothermic reaction is very likely to occur. So even though the Y ions formed initially do not appear very stable, this rearrangement reaction can give much more stable species.

Secondly, this mechanism can explain the relative intensities of C ions and Y ions when the C-terminus of a peptide is transformed into a methyl ester. It was observed that esterification severely suppressed the formation of Y ions. This is because the above rearrangement reaction can not occur to stabilize the Y ions thus formed. The poor stability of the Y ions (due to the lack of resonance structures) will suppress their formation. Thus the C ions formed with resonance structures will be much more abundant than Y ions.

Supporting evidence for the displacement mechanism is the spectral difference between the negative ion FAB-CID-B/E linked scan spectra of H-YGGFL-OH and H-YGGFL-NH₂. When the C-terminus is a carboxylic acid, the intensity ratio of C₂ to C₃ is

3:1 (Figure 6.12a). However, when the C-terminus is an amide, the ratio become 1:3 (Figure 12b). This change occurs because the displacement reaction via the C-terminus is sterically the most favored site thus reaction via the C-terminus is favored. Since 6-membered ring structure is generally the most stable, loss of a 6-membered neutral species and the formation of C₃ is the most favored (Figure 6.13). Note here that the C-terminus is certainly not the only site for deprotonation, but fragment ions from deprotonation site other than the C-terminus should be less abundant because fragmentation of these deprotonated peptides will present more steric hindrance. Note here this case is almost exactly the same as when it occurred in thermal degradation of peptides and peptide amides [15] (also see Chapter 3 for detail).

1,4 - Elimination: As seen in the experiments with deuterated peptides, part of the C ions formed does involve shift of α -hydrogen atoms, four atoms away from the cleavage site. To explain the formation of these ions, a six-membered ring intermediate is proposed and a α -hydrogen is transferred to the deprotonated amide nitrogen atom (Figure 6.14). This mechanism suggests that a deprotonated amide nitrogen atom can deprotonate an α -carbon position (-CHR-) when enough energy is supplied ($\Delta G^\circ = \Delta G^\circ_{\text{acid}}(-\text{CONH-}) - \Delta G^\circ_{\text{acid}}(-\text{CHR-}) \approx 10 \text{ kcal/mol}$, see section III). Another possibility is that the shifting hydrogen goes to a non-deprotonated amide, forming a C ions such as $\text{NH}_2\sim\sim\sim\text{CON}^-\sim\sim\sim\text{NH}_2$, by the same mechanism.

B. Ions from C-terminally deprotonated peptides

If the C-terminus of a peptide is the site of deprotonation, then the charge is fixed at the C-terminus and the situation will be the same as the sulfonic acid derivatives discussed earlier in this article. As can be seen in Figure 6.3b, all ions from the C-terminally deprotonated peptides are C-terminal ions. N-terminal ions can not be produced from the

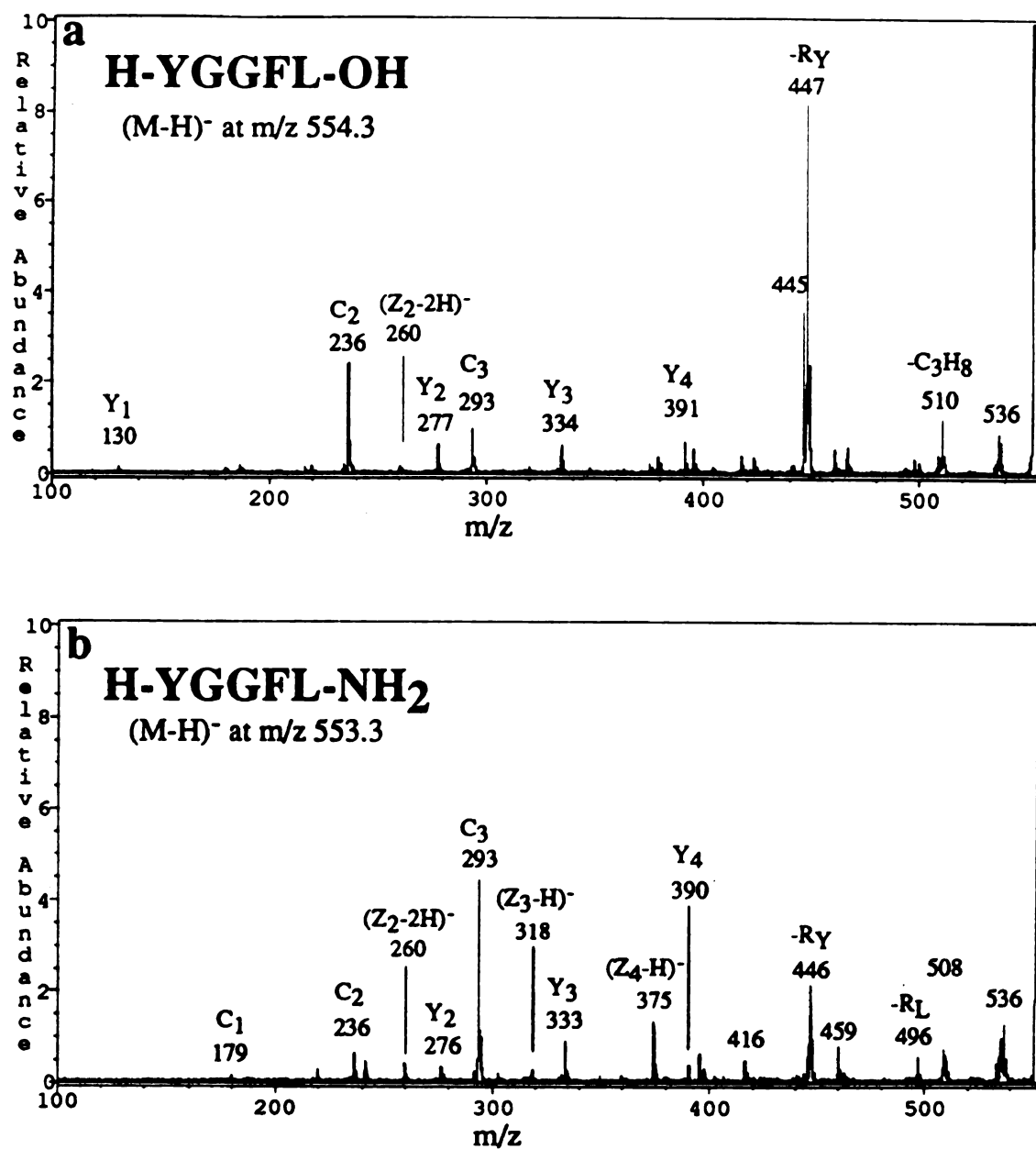


Figure 6.12 CID-B/E linked scan mass spectra of (M-H)⁻ ions of:
a) H-YGGFL-OH; b) H-YGGFL-NH₂.

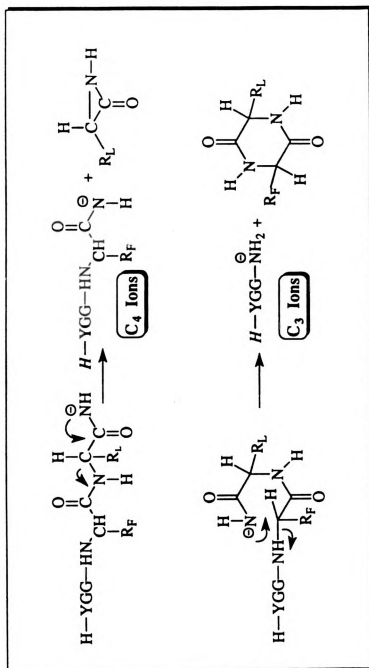


Figure 6.13 The formation of C ions from C-terminally-deprotonated peptide amides.

(H-YGGFL-NH₂ as an example)

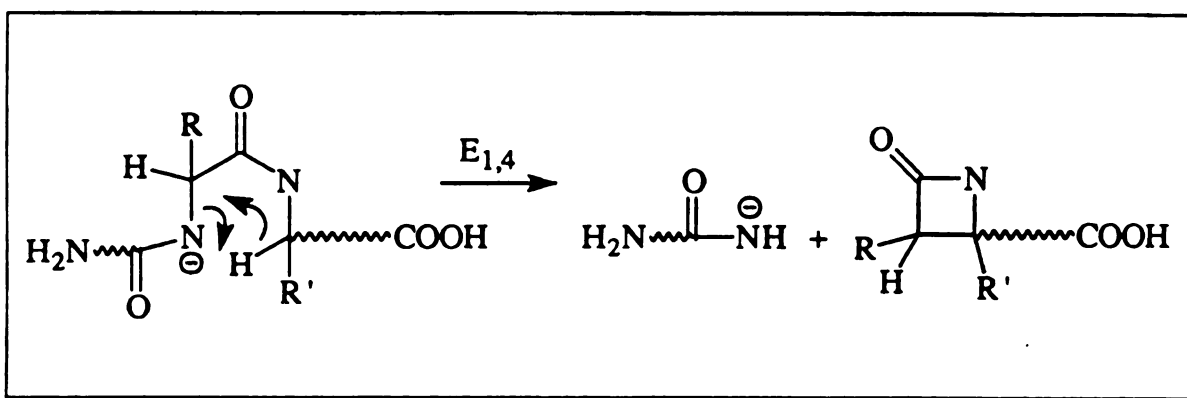


Figure 6.14 The formation of C_n ions via a 1,4 - elimination mechanism.

C-terminally deprotonated peptides. So only Y and (Z-H)⁻ ions are derived from these charged species.

To form a Y_n ion from a C-terminally deprotonated peptide, shifting of a hydrogen atom from the N-terminal side of the cleavage site must have occurred because C-terminally fixed-charge peptides showed abundant Y ions. This process may proceed via a 1,2-elimination mechanism or via cyclization from the N-terminus or amides. Since the charge is fixed at the C terminus of the peptide, this will be a charge-remote process and steric hindrance at related sites should be very important, as is demonstrated in the thermal degradation of peptides. However, this process may take more time to occur since the reaction is a charge-remote process.

From the CID Spectra of H-VGVAPG-OH, H-VGVA^{αd}PG-OH/OCH₃ and H-V^{αd}HGV^{αd}APG-OH/OCH₃, shifting of α-hydrogens are not observed. This indicates that the 1,2 - elimination process does not occur on the time scale of the experiment. Therefore, cyclization is the fragmentation mechanism (see Figure 6.15). Is the shifting hydrogen from the N-terminus? This is most probable for the loss of small cyclic neutral molecules. To form larger neutral cyclic molecules, a H-shift from amides is probably the best choice. Note in this process, cyclization is not charge induced, it is a remote-site process. In the gas phase, the spontaneous folding in minimizing the surface tension may help speed up these reactions.

VIII. Fragmentation of charge-localized peptides

A. Charge-localization on peptides

In mass spectrometry, fragment ions are believed to be from fragmentation of the corresponding molecular ions. In electron impact (EI) ionization, odd-electron molecular ions are formed because an analyte molecule either gains or loses one electron. Fragmentation of these ions are frequently driven by the radical. With softer ionization

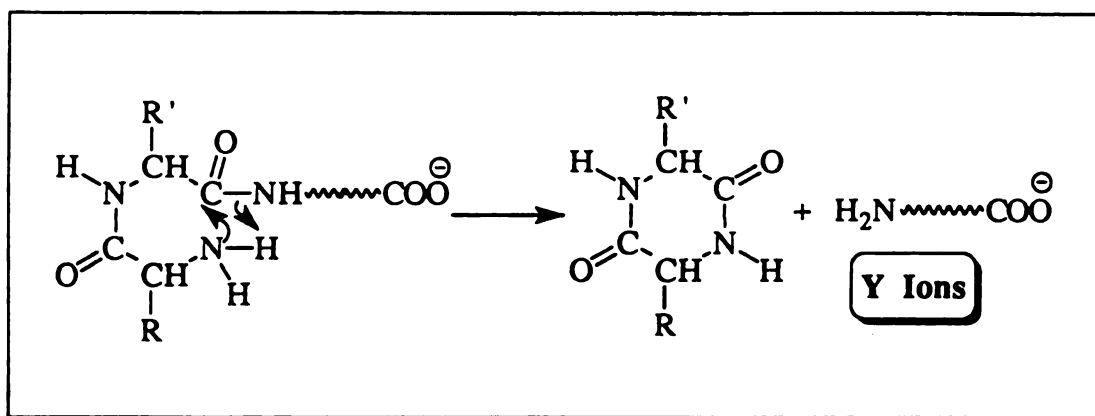


Figure 6.15 The formation of Y ions from charge-remote processes such as $E_{1,6}$ reactions shown here.

techniques such as FAB, even electron ions are formed. For example, molecular ions formed in FAB are MH^+ or $(M-H)^-$, by gaining or losing a proton. When these ions are forced/induced to fragment, fragmentation is considered to be driven by the charge - namely charge-induced fragmentation. Following the protonation or deprotonation process, not only the protonation site and its adjacent atoms have the greatest changes in electron density, but also it is the deprotonation site that is affected first and most by the energy release during a protonation process {Deprotonation of peptides for example, $\Delta G^* \approx \Delta G^*_{\text{acid}}(\text{CH}_3\text{COOH}) - \Delta G^*_{\text{acid}}(\text{glycerol-OH}) = (1400 - 1550) \text{ kJ/mol} = 35 \text{ kcal/mol}$)} Both processes make the bonds at and near the deprotonation sites the easiest to cleave. Therefore, the charge site (protonation or deprotonation site) within a molecule is crucial to the formation of fragment ions.

When protonated or deprotonated peptides are formed from fast atom bombardment, a charge site-the protonation/deprotonation site, is not at a single position. In positive mode, the charge site is determined by the most basic sites present in a peptide molecule such as that at an arginine side chain. To be more precise, protonation occurs with a statistical distribution such that the most basic site is protonated preferentially. In negative ion mode, the most acidic site is most probably the site of deprotonation. Still the deprotonated peptides $(M-H)^-$ exist as a collection of isomers with a proton removed from various sites within the molecules. Therefore, the peak representing $(M-H)^-$ does NOT represent a single chemical species. For $(M-H)^-$ ions, different ions may have different deprotonation sites. Ions with different charge sites may have different fragmentation patterns.

Since charge site is important in the fragmentation of protonated or deprotonated molecules, efforts have been made in previous research to put a charge at a fixed site in a molecule, by making charged derivatives, mainly to control/direct the fragmentation of MH^+ of the analyte molecules [16-19]. Charge-localization in positive ion mode was also proposed to provide a way of differentiating leucine and isoleucine in peptide sequencing

by Biemann and his coworkers [18-19]. It has been noticed that d_n ions or w_n ions in positive ion mode, formed from specific side-chain cleavages necessary for the differentiation, can only occur when charge is at or very close to either termini of a peptide [19]. Recently, Wagner et al. [20] used triphenylphosphonium (TPP) derivatives to achieve a different purpose. Charge localization was used to enhance the response of a peptide in FAB by charge localization and surface activity enhancement, in addition to improved fragmentation.

Charge-localization for positive ions are frequently achieved by attaching tertiary ammonium or phosphonium groups at or near either terminus of a peptide. References for the synthesis of these derivatives can be found in a recently work by Biemann and his coworker [21].

Charge-localization for peptide negative ions has not been reported previously. However, W. J. Griffiths and coworkers [22] used a series of aminosulphonic acid derivatives to improve the fragmentation of bile acids via charge-remote fragmentation. In this study, amino-sulphonic acids and aminophosphonic acids have been used as the derivatization reagents for charge localization on peptides.

B. Fragmentation of Deprotonated Peptides with Charge-localization.

A list of amino-sulfonic and amino-phosphonic acids, as described in the experimental section, have been used for derivatization reagents for charge-localization. Three peptides, H-VGGFL-OH, H-YGGFL-OH and H-AG(Sar)FL-OH, have been derivatized with the procedures described in the experimental section. The CID (including contribution from metastable ions) spectra were obtained.

Based on CID/metastable spectra of these peptide derivatives, sulphonic acid derivatives have shown better charge-localization effect than phosphonic acid derivatives. Among sulphonic acid derivatives, aminobenzenesulphonic-acids gives the best results for charge localization. For example, when the C-terminus of a peptide is derivatized by

AMSA and AESA (Figure 6.3), the dominant ions are C-terminal ions, indicating a fairly strong charge-localization efficiency. However, a few N-terminal ions such as C_3 , with low abundances, are always observed, suggesting an incomplete charge-localization (e.g. some peptide molecules are deprotonated at sites other than the C-terminus in this case, which leads to the formation of C_3 ions). When the C-terminus of a peptide is derivatized with ABSA, all ions observed are C-terminal ions (Figure 6.3b), indicating a complete charge-localization at the C-terminus.

Fragment ions from these three sulphonic acid derivatives are not exactly the same. AMSA derivatives produce mainly $(Z-H)^-$ ions and Z ions (uncommon!), and little Y ions and W ions are observed (Figure 6.3a). With AESA derivatives, major ions are almost exactly the same as those for AMSA derivatives. With ABSA derivatives, the ions are mainly Y ions, $(Z-H)^-$ ions, and W ions (corresponding negative counterparts of w_n in positive mode).

(It should be noted that CID spectra provide more fragment ions than metastable spectra. For these peptide derivatives, W ions and $(Y-2H)^-$ ions are enhanced with collisional activation.)

Charge-localization at the N-terminus of a peptide was also studied. The CID spectrum of SBA-VGGFL-OH clearly indicate a complete charge-localization (Figure 6.5). The dominant ions are found to be $(A_n-2H)^-$ ions, $(B_n-H+OH)^-$ ion - all N-terminal ions. Therefore, benzenesulfonic acids moiety can be used effectively to fix/localize a negative charge on peptides.

1. Fragment Ions from C-terminally Charge-localized Peptides

The major ions from C-terminally charge-localized peptides are Y ions, $(Z_n-H)^-$ ions, $(Y_n-2H)^-$ ions, and sometimes W ions.

(Z_n-H)⁻ ions: These ions appear in CID/metastable spectra of charge-localized peptides, regular peptides, even in C-terminally blocked peptides (sometimes). (Z_n-H)⁻ ions must be in the form of radicals also (•CHRCO----COO⁻). Their formation can be best described as homolytic cleavages of NH-CHR bonds from C-terminally deprotonated peptides (equation 6), or peptides with deprotonation sites (amides) near the C-terminus (equation 7).



(M-H)⁻

(Z_n-H)⁻

(Z-2H)⁻ ions: It is the radical nature of (Z-H)⁻ ions that probably leads to the formation of (Z-2H)⁻ ions by loss of H atom from the sidechain (equation 8, R = -CHR'R'').

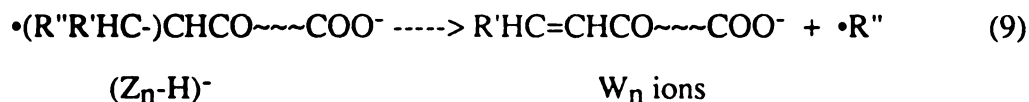


(Z_n-H)⁻

(Z_n-2H)⁻

Therefore, glycine may not form (Z_n-2H)⁻ ions due to its lack of side chain atoms. This is confirmed by the spectra of H-VGGFL-OH and H-VGGFL-ABSA. For (Z₃-H)⁻ and (Z₄-H)⁻, there is no corresponding (Z-2H)⁻ ions observed because of the presence of glycine residue at the cleavage sites. (Z₂-2H)⁻ IS observed because a phenyl alanine side chain is at the cleavage site.

W Ions: The radical nature of (Z_n-H)⁻ ions also lead to the formation of specific sidechain losses forming W ions (equation 9). Due to the stable structure of products - alkene in conjugation with a carbonyl group, this reaction is favored.

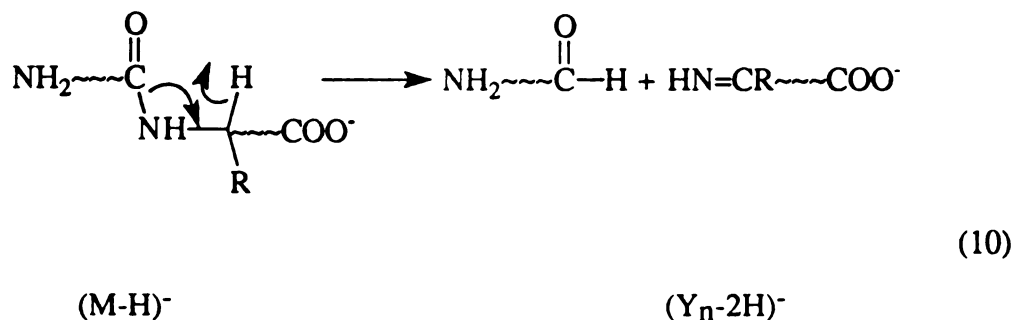


The significance is that this ion series can be used to differentiate isomeric leucine and isoleucine. For leucine and isoleucine, the side-chain loss is $-\text{CH}(\text{CH}_3)_2$ and $-\text{CH}_2\text{CH}_3$ respectively, which provides the basis for mass differentiation.

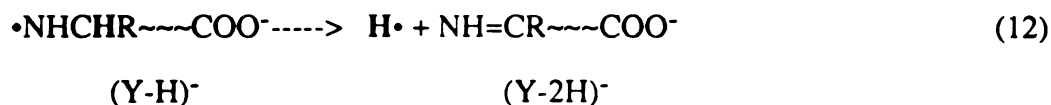
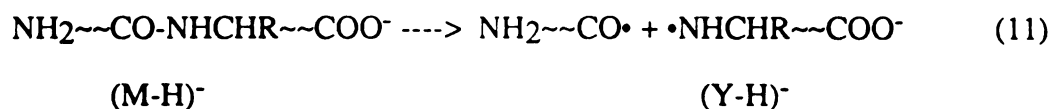
Z_n Ions: Z_n ions are observed with AMSA and AESA derivatives of peptides (Figure 6.3). Since the charge of such a derivative is localized at the C-terminus, a hydrogen atom must shift from the N-terminal side to the C-terminal side of the cleavage site via reactions such as 1,3-elimination. However, the source of the shifting hydrogen has not been studied.

Y Ions: For charge-localized peptides, a hydrogen shift is involved, and the shifting hydrogen must be from either the amides or the N-terminus of a peptide, as is shown for C-terminally deprotonated peptides (1,3-elimination mechanism).

(Y-2) ions. A hydrogen shift away from the C-terminal side of the peptide must be involved. Therefore, H shifts from CHR must be involved (equation 10).



Another possibility is that this ion series is formed from (Y-H)⁻ ions (equation 11), followed by ejection of a hydrogen atom (equation 12).



According to Wagner [23], the following charge remote fragmentation can occur for charge-localized peptides in positive mode because it is very similar to an reaction (equation 13) observed by Gross and coworkers [24]:

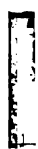
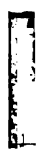
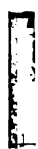
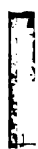


With charge-localized peptides, the ions in positive mode will be (B-2H)⁺ and (Y-2H)⁺ respectively. If this mechanism is true for the (Y-2H)⁻ formed in CID of negative charge-localized peptides, then the corresponding (B-2H)⁻ ions should be observed when a N-terminally charge-localized peptide is used. However, such (B-2H)⁻ ions have not been observed in the spectrum of SBA-VGGFL-OH. These results suggest that the above reaction VIII is not the reaction that occurred.

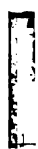
2. Fragment ions of N-terminal charge-localized peptides

The major ions from N-terminally charge-localized peptides are (A_n-2H)⁻, (A-H)⁻ ions and (B_n-H+OH)⁻ ions. The latter are also formed when proline is present at or near the C-terminus of a peptide, such is the case in H-VGVAPG-OH.

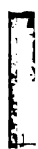
Abstract

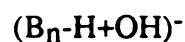


Abstract

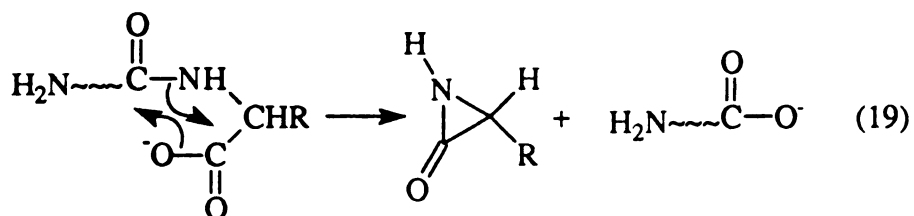


Abstract





0 11



IX. The Applicability of CID of Deprotonated Peptides for Peptide Sequencing

A. Peptide sequencing with CID-MS/MS of Negative Ions

Peptide sequencing by CID-MS/MS in positive mode has been demonstrated to be one of the most successful applications of mass spectrometry [25-27]. In negative mode, however, detailed studies on CID-MS/MS have been extended only to di- and tri-peptides before this dissertation work [1].

As has been demonstrated in the preceding sections of this Chapter, the dominant ions from CID spectra of deprotonated peptides are usually C_n ions, Y_n and $(Z_n-H)^-$ ions. These ion series, derived from skeletal bond cleavages of a peptide, contain important information of amino acid sequence of the peptide. With one complete ion series or more partial ion series identified, the sequence of a peptide can be deduced.

One of the most important approaches for sequencing starts by calculating the mass difference between the $(M-H)^-$ ion and any fragment ion that could correspond to loss of one residue, for example between $(M-H)^-$ and $(M-H)^--71$. Those with mass differences that exactly match a residue mass (e.g. 71 = alanine) are candidates for Y_{n-1} ion. There will likely be several of these, especially for larger peptides. For each of these Y_{n-1} candidates, one search for the next residue mass that could correspond to Y_{n-2} . For example, if there were peaks corresponding to $(M-H)^-$, $(M-H)^--71$, $(M-H)^--71-97$, and so on, the mass differences could correspond to Ala, Pro, and so forth. These data then suggest a sequence starting at the N-terminus of Ala-Pro- Constructing a tree diagram makes it easy to keep track of the candidate sequences. The best candidate(s) are those for which the data produce the longest sequence. A check of the validity of Y ion assignment is the identification of $(Z-H)^-$ and $(Z-2H)^-$ ions, which would appear 16 and 17 mass units lower in mass, respectively, than the corresponding Y ion. Ideally, there will be a

complete Y_n series that provide the entire sequence. More likely, there will be several partial sequences.

When Y series is absent or weak, $(Z_n-H)^-$ ion series should be checked starting at $(M-H)^--16$. A peak at $(M-H)^--16-71$ may suggest a $(Z_{n-1}-H)^-$ ion and the sequence starting at the N-terminus of Ala- ..., and so forth.

After finding the possible Y ion series, one should look for N-terminal fragments. The C ions start one mass unit below the $(M-H)^-$ ion mass. Search for peaks corresponding to $(M-H)^- - (1+\text{residue})$; this peak correspond to C_{n-1} ion. As with Y_{n-1} ion, search for residue mass losses from the C_{n-1} candidate(s) until one or more of a long C-ion series are found.

For example, the spectrum of H-VGGFL-OH (Figure 6.1a) as an "unknown" can be analyzed as follows: The identities of the peaks in the above spectrum should be identified first. For Y ions, the following series can be found: 490 --> 391 (-99 = Val)--> 334 (-57 = Gly) --> 277 (-57 = Gly) --> 130 (-147 = Phe), which suggests a partial sequence starting at the N-terminus of VGGF- (the next one may be Leu/Ile, to be confirmed). For C ion series, start at $490-1 = 489$, $489 \rightarrow 376$ (-113 = Leu/Ile) --> 229 (-147 = Phe) --> 172 (-57 = Gly), suggest a sequence starting at the N-terminus of -GFL/I. Therefore, the C_n and Y_n ion series can provide enough information to deduce the "unknown" sequence of this peptide, which is found to be V-G-G-F-L/I. Note that the leucine and isoleucine can not be differentiated in this specific case (They can be distinguished by charge-localization, which will be shown below.)

In peptide sequencing, ions from sidechain cleavages of a deprotonated peptide should always be checked first. These ions appear at the high mass region of CID spectra of deprotonated peptides, and provide important information about the presence of amino-acid residues. For example, peaks at m/z values of 91, 92 and 93 mass unit lower than the deprotonated peptides indicate the presence of a phenylalanine(s). Peaks at m/z values of 57 and 58 lower than the deprotonated peptides indicate the presence of leucine/isoleucine.

Dominant cleavages can occur for sidechains such as those of threonine and serine, which can be identified easily by neutral losses of 44 and 30, respectively, as demonstrated in the spectra of H-VHLTEVEK-OH (Figure 6.16) and H-RPPGFSPF-OH (Figure 6.17). The presence of these sidechains is obvious because it frequently produces a neutral loss current much higher than any other ions. The dominant loss of a sidechain can also occur for fragment ions. As is the case for the spectrum of H-RPPGFSPF-OH (Figure 6.17), in which the ion current from Y-30 (CH_2O ; 30u) is almost as large as that from C_n ions. Such ion series may be used to determine the position of these amino acid residues.

Charge-localized peptides (negatively charged) can be easily prepared for the purpose of peptide sequencing when needed. Fragment ions from a charge-localized peptide give simpler spectrum because these ions are either N-terminal or C-terminal ions. For example, H-VGGFL-ABSA produces almost exclusively Y ions and $(\text{Z}_n\text{-H})^-$ ions, which simplifies spectral interpretation. In addition, sidechain specific ions such as W and D ions are obtainable in CID of deprotonated peptides, especially for charge-localized peptides (see Figure 6.3b). The presence of these ions can be used to differentiate isomeric leucine and isoleucine residues. Charge localization with sulphonic derivatives such as ABSA and SBA derivatives can be served for these purposes. For example, the D_1 ions from H-VGGFL-ABSA indicates that the C-terminal amino-acid residue is leucine instead of isoleucine.

Although CID spectra of deprotonated peptides can provide structural information of peptides, there are several serious limitations for the purpose of peptide sequencing when it is compared to the corresponding positive mode.

1. The sensitivity in negative mode is usually much less than that in positive mode. Even when the production of precursor ion is more efficient than that in positive mode, the quality of CID spectra is also not as good. The reasons for this poor sensitivity will be discussed in section II of this Chapter.

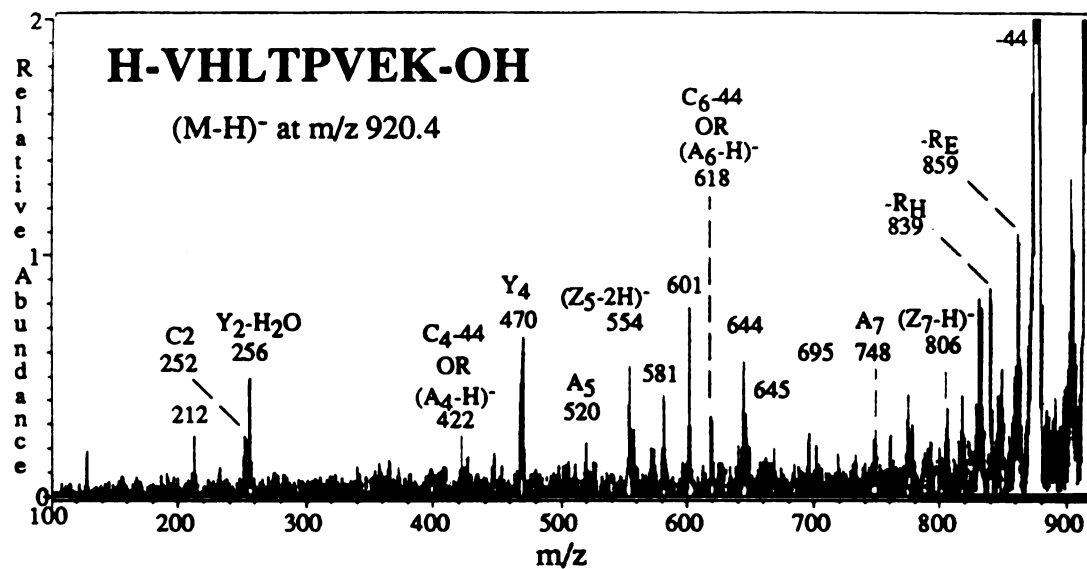


Figure 6.16 CID-B/E linked scan mass spectrum of a deprotonated peptide H-VHLTEVEK-OH.

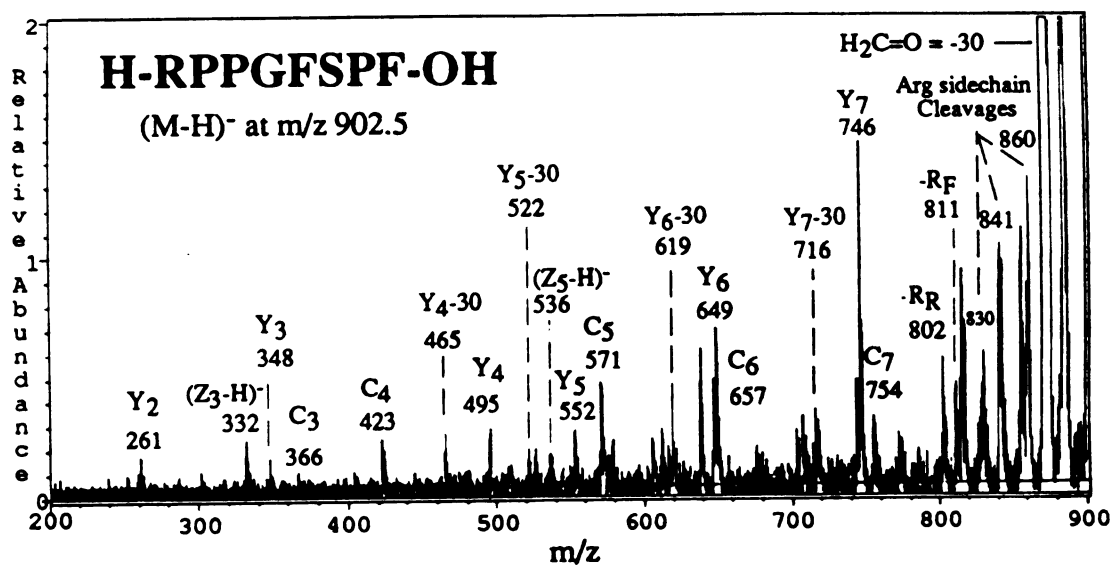


Figure 6.17 CID-B/E linked scan mass spectrum of a deprotonated peptide H-RPPGFSPF-OH.

2. In positive mode, immonium ions ($\text{CHR}=\text{NH}^+$) in the low-mass region of a spectrum provide very important information of the amino acid constituents - the presence or absence of some amino acid residues. In negative mode, such information is not available because no corresponding ions are formed.

3. In positive mode, the high-mass region of a CID spectrum provides important information about the presence or absence of an amino acid residue due to specific side-chain losses. The neutral losses are very specific and peaks corresponding to these are unique for each amino-acid residue. In negative mode, side-chain losses still occur, but with much more complication. When the side chain of a leucine residue cleaves, there are many ways by which the cleavages may occur. For example, loss of the whole side chain $[-\text{C}_4\text{H}_9 = -57]$ is observed. Loss of 58 is also observed in about the same abundance, loss of 56 is also observed. Loss of 16 (CH_4), 44 (C_3H_8), 15 (CH_3) and 43 (C_3H_7) can also occur for this amino acid residue. These non-unique cleavages can be very confusing, as can be seen from the spectrum of H-FLEEI-OH (Figure 6.18). For instance, if both valine and leucine residues are present in a peptide (Figure 6.1a - the spectrum of H-VGGFL-OH), the spectrum can not suggest the presence of valine because leucine also give some sidechain losses which are common for valine.

4. Sidechain cleavages of some amino acid residues such as threonine and serine can be so dominant that peptides containing one of these residues may produce spectra dominated by the specific cleavages [Figure 6.17 - the spectrum of H-RPPGFSPF-OH, and Figure 6.16 - the spectrum of H-VHLTPVEK-H]. For serine and threonine, the dominant losses are -30 ($\text{CH}_2=\text{O}$; 30u) and -44 [$\text{CH}_3\text{CH}=\text{O}$; 44u]. The dominant cleavages lead to the decrease in the total ion current of other fragment ions, which reduces the structural information that is available for peptides without such sidechains. In addition, these specific losses extend to fragment ions also, making sequencing more complicated.

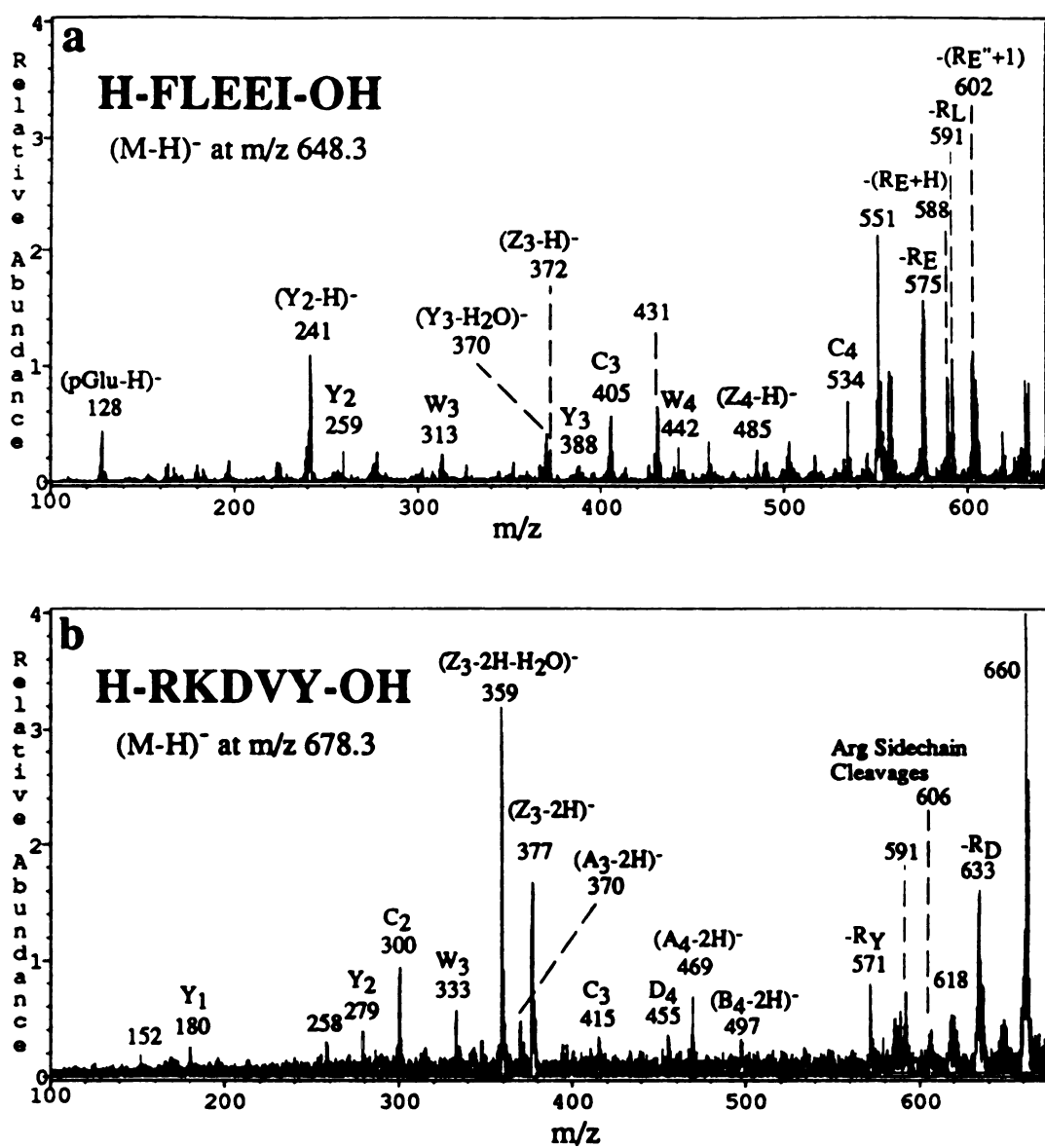


Figure 6.18 CID-B/E linked scan mass spectra of deprotonated peptides:

a) H-FLEEI-OH; b) H-RKDVY-OH.

The presence of such residues, however, does not always produce the dominant cleavages. This can be seen from the CID spectrum of H-WAGGDASGE-OH (Figure 6.19).

5. Ion series can be very sensitive to changes in deprotonation sites. For example, esterification of a peptide may cause dramatic changes in total ion current. When sites such as carboxyl groups are blocked, ion current will decrease.

6. As is the case in positive mode, sequence ions are not always complete, especially for large peptides. It is also observed that small fragments are not observed for relatively large peptides, as is the case for H-RVYIHPF-OH (Figure 6.20).

B. Why is negative mode not favorable?

1. The poor sensitivity

The poor sensitivity of negative mass spectrometry (not with NCI or EC-NCI) has been recognized for many years. The sensitivity of regular FAB in negative mode is found to be about 100 times lower than that in positive mode. The efficiency of fragmentation of $(M-H)^-$ in CID-MS/MS is also much less than that of $(M+H)^+$. With experiments on a JOEL HX 110 instrument, with full scale of precursor ion beam, positive mode produces signal at 50% level while negative mode produces signals usually around 2% levels. What are the reasons?

The above observations can be answered partly by the low electron affinity values which lead to low efficiency for the production of $(G-H)^-$ (g) and $(M-H)^-$ (g) ions due to their poor stability.

The production of $(G-H)^-$ ions: With gas-phase ionization mechanism, deprotonation of peptides occurs due to the following reaction:

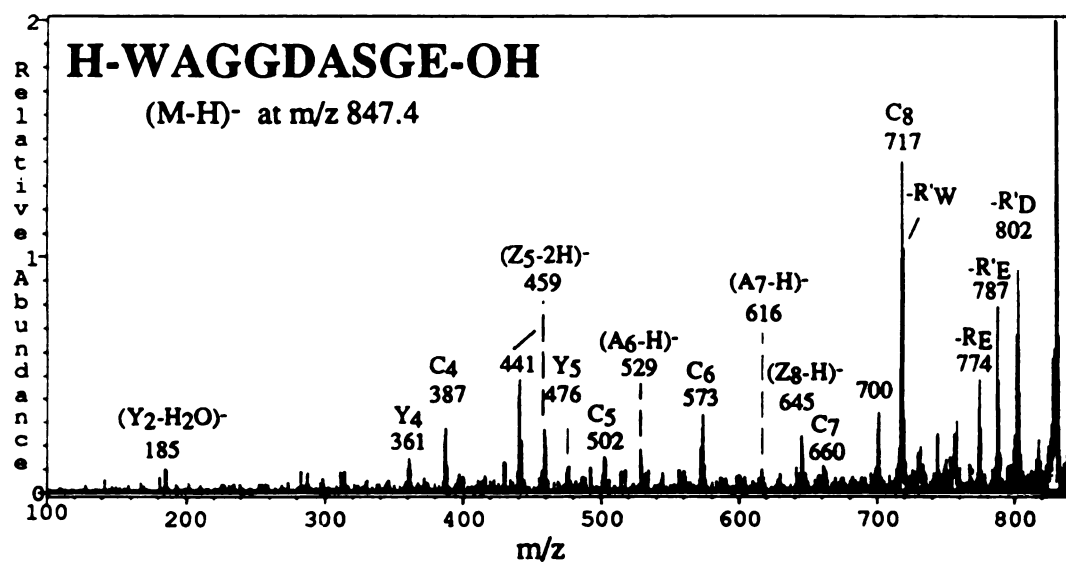


Figure 6.19 CID-B/E linked scan spectrum of (M-H)⁻ of H-WAGGDASGE-OH.

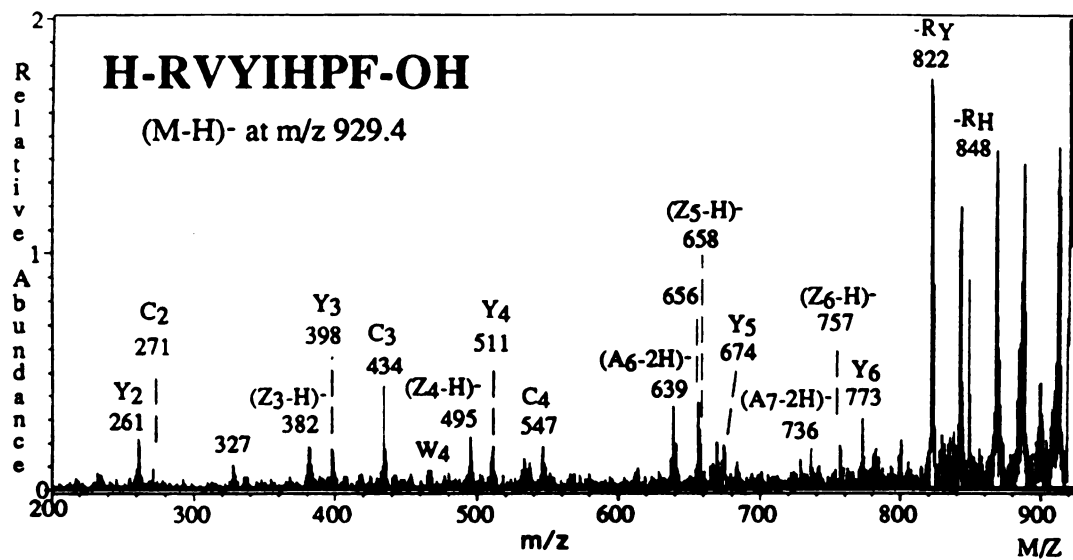
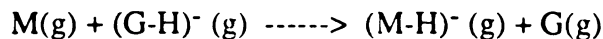


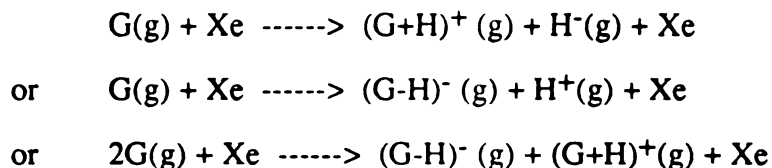
Figure 6.20 CID-B/E linked scan spectrum of (M-H)⁻ of H-RVYIHPF-OH.



where $G(g)$ and $M(g)$ designate gas-phase glycerol and peptide molecules respectively. Obviously, $(G-H)^-(g)$ has to be produced first for the above reaction to occur. The reaction rate R (deprotonation rate) is therefore directly proportional to the gas phase number density of deprotonated glycerol, assuming that the reaction is first order with respect to both M and $(G-H)^-(g)$.

$$R = k [M(g)] [(G-H)^-(g)]$$

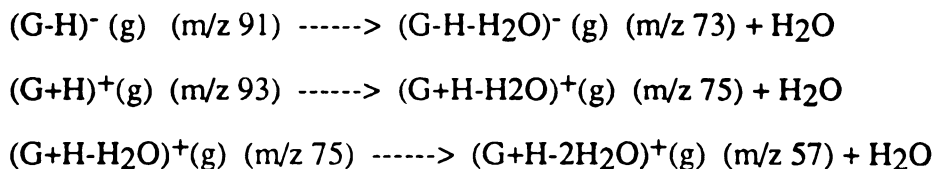
where k is the rate constant for the reaction. The formation of deprotonated glycerol in the gas phase can be assumed to be from the direct bombardment from high energy Xe atoms (3 keV):



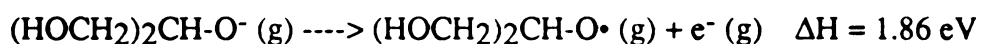
The above are simplified equations for protonation and deprotonation of glycerol matrix molecules. The dominant ions such as $(G+H)^+(g)$ and $(G-H)^-(g)$ in a mass spectrum are the major evidence for the above reactions.

During fast atom bombardment (protonation and deprotonation) processes, glycerol molecules are excited first by the high energy Xe atoms, and a small portion of their translational energy is converted into the internal energy of the neutral glycerol molecules, leading to the excitation of the glycerol molecules. The excited glycerol molecules then undergo ionization via reactions such as those shown above.

The ions formed during such processes may still be in excited states and they can undergo further degradation reactions. This statement can be partly supported by the ions formed via dehydration of protonated or deprotonated peptides.



With protonated glycerol, loss of an electron will produce multiply charged ions, which is not favored. Other pathways will produce positive ions which can act as protonation reagents. For deprotonated glycerol molecules, there is another important pathway which produces neutrals and electrons (can not be detected by a regular mass spectrometer) due to the very small electron affinity value:



Due to the small activation energy needed for such processes $\{\text{EA}[(\text{CH}_3)_2\text{CH-O}^-] = 1.86 \text{ eV} = 40 \text{ kcal/mol}\}$, this process is expected to be at least one of the major pathways for deprotonated glycerol. Note that the electron detachment reaction is expected to be much faster than other fragmentation reactions because there is no geometry requirement. Because of this additional pathway for deprotonated glycerol, the concentration (or number density) of deprotonated glycerol in the gas phase would be much lower than that of protonated glycerol.

If the rate constants for deprotonation and reprotonation of peptides are the same, and considering that the concentration of $(\text{G-H})^- (\text{g})$ is much less than that of $(\text{G+H})^+ (\text{g})$ in the gas phase, it is obvious that the rate of deprotonation of peptides is much less than that of protonation of peptides. Therefore, the number density of $(\text{M+H})^+ (\text{g})$ is much higher than that of $(\text{M-H})^- (\text{g})$, and the sensitivity of positive mode is better than that of negative mode.

The stability of deprotonated peptides: The poor stability of deprotonated peptides is another reason why the sensitivity of the negative mode in FAB is not as good as that of the positive mode. Protonated peptides are unlikely to be deprotonated (becoming neutral) due to the large proton-affinity values. Since an ion is positively charged, loss of an electron forming doubly charged ions, is also not favored. Other pathways such as loss of sidechains and hydrogen atoms, will produce fragments which can be detected.

With deprotonated peptides, the ions are not as stable as positive ions. One major pathway responsible for the instability is the easy loss of an electron and become electrically neutral species, which can not be detected by a mass spectrometer:



For this process, the energy required is only 3.4 eV (79 kcal/mol, from the data of acetic acid and alanine). With deprotonation at other sites, this number can be much lower. To cleave a peptide skeletal bond (homolytic cleavage), the lowest energy required is 79 kcal/mol (for CHR-CO bonds). Therefore, if the energy available can break a bond leading to fragmentation, then the same amount of energy can also remove an electron from a negatively charged species (the above equation). Removal of an electron could be favored because loss of an electron requires no arrangement of any atom and the steric hindrance is not a factor. Therefore, such processes directly lead to the loss of negative ion sensitivity in a regular FAB mass spectrometry.

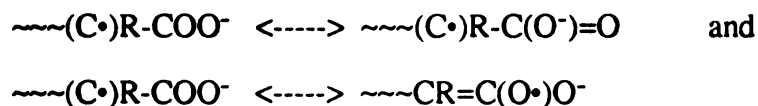
In CID experiments, the average internal energy deposition is determined to be about 3 eV with a high energy tail above 15 eV [28]. Therefore, immediately following collision activation, a large portion of the excited ions will undergo electron stripping and form neutrals, which is directly related to the poor fragment ion currents for negative ions.

2. Why are peak clusters formed?

The appearance of CID spectra of deprotonated peptides is generally not as good as that of protonated peptides. In positive mode, a peak representing an ion is accompanied by an isotopic peak. In negative mode, peak clusters for sequence ions are most frequently observed. For example, a $(Z-H)^-$ ion is frequently accompanied by a $(Z-2H)^-$ ion. Sidechain loss of leucine can lead to loss of 57 and 58, etc. In many cases, the formation and the nature of ions in peak clusters cannot be explained. It should be pointed out that the formation of clusters lowers the sensitivity of the technique because ion currents are distributed among more species.

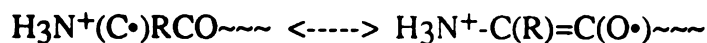
One explanation can be suggested based on the CID spectra of di- and tri- peptides in Bowie's work [1-9]. It has been shown that loss of a hydrogen atom from di- and tri-peptides is very common, especially when the precursor ion current is high. This loss of hydrogen radical lead to new series of new chemistry such as loss of H_2 molecule, or loss of another side chain radical to stabilize the radical formed. The easy loss of hydrogen radical is because the new species formed, also a radical, can be stabilized by radical delocalization.

When a hydrogen atom is removed from a negative charged peptide at the deprotonation site, the radical ion can be stabilized due to resonance structures (both the charge and the radical are stabilized).



Therefore, the product from loss of a hydrogen atom of CHR at a peptide chain is relatively stable.

{In positive mode, there is no similar situation. For example, if the N-terminus of a peptide is protonated.



Obviously, the charge cannot be delocalized by resonance structures. In such cases, $\text{H}_3\text{N}^+-\text{C}(\text{R})=\text{C}(\text{O}^\bullet)\sim\sim\sim$ may be the dominant species because the positive charge will make the double bond stay closer to the charge site. }

X. Conclusions

Preformation of $(\text{M}-\text{H})^-$ (l) in the liquid phase does not enhance the formation of $(\text{M}-\text{H})^-$ (g). Therefore, deprotonation of peptides occurs in the gas phase. Deprotonation of amides is favored over that of α -carbon positions because the former provide favorable intermediate leading to deprotonation.

Ions from CID of larger peptides are found to be different from what have been reported for smaller peptides such as di- and tri-peptides due to the smaller internal-energy deposition during a collision and the long life time of $(\text{M}-\text{H})^-$ ions. For di- and tri-peptides, the major sequence ions have been reported to be Y ions. With larger peptides, C ions are found to be another important ion series, which are as abundant as Y ions in a CID spectrum.

In CID spectra of deprotonated peptides, the situation becomes more complicated than that in the case for protonated peptides, especially for the high-mass ions. When a high-mass peak appears in a spectrum, it usually is not a single peak with its isotopic peak, instead a cluster of peaks is seen, which apparently cannot be explained simply by isotopic contributions. Because of the complexity, our efforts can only be put in explaining the formation of major ion series.

By using deuteration, derivatization and charge-localization, we have concluded that there is significant deprotonation at amide sites, which has not been considered as important sites of deprotonation previously by other groups. Also found is that deprotonation at the C-terminus is not as prevalent as people thought. These conclusions are important because they are the starting point for peptide fragmentation.

For most of the C ions observed, their formation does not involve the shift of α -hydrogen atoms. However, a small portion of C ions are formed via shifting of α -hydrogen atoms.

For the formation of Y ions in dipeptides, it has been reported that an α -hydrogen shift is involved. With larger peptides such as hexa-peptides, we find that α -hydrogen shifts do not occur, indicating totally different mechanisms.

With peptides of various deprotonation sites (derivatized and charge-localized peptides, we found that both Y ions and C ions are formed mainly from amide deprotonated peptides and the fragmentation processes are mainly charge-induced. Based on these conclusions, mechanisms for the formation of C ions and Y ions are proposed.

With charge-localized peptides, ions are formed via charge-remote fragmentation mechanisms. With the formation of Y ions, a hydrogen has to be shifted to the C-terminal side of the cleavage site. The formation of (Z-H)⁻ ions is simply from homolytic cleavage of NH-CHR bond.

CID-B/E linked scan spectra of deprotonated peptides can provide useful information for peptide sequencing. The major limitation of peptide sequencing with this technique is the relatively low sensitivity due to the facile loss of electron from deprotonated molecules. In addition, the easy loss of hydrogen atoms leads to the formation of clusters of peaks, which may complicate the interpretation of mass spectra.

References

1. Waugh, R. J. ; Bowie, J. H. *Rapid Commun. Mass Spectrom.* **1994**, 8, 169-173.
2. Echersley, M.; Bowie, J. H.; Hayes, R. N. *Org. Mass Spectrom.* **1989**, 24, 597-602.
3. Waugh, R.J.; Bowie, J. H.; Hayes, R. N. *Int. J. Mass Spectrom. Ion Processes* **1991**, 107, 333-347.
4. Waugh, R. J.; Bowie, J. H.; Hayes, R. N. *Org. Mass Spectrom.* **1990**, 26, 250-256.
5. Waugh, R. J.; Ekersley, M.; Bowie, J. H.; Hayes, R. N. *Int. J. Mass Spectrom. Ion Processes* **1990**, 98, 135-145.
6. Waugh, R. J.; Bowie, J. H.; Gross, M. L. *Rapid Commun. Mass Spectrom.* **1993**, 7, 623-625.
7. Waugh, R. J.; Bowie, J. H.; Gross, M. L. *Austral. J. Chem.* **1993**, 46, 693.
8. Waugh, R. J.; Bowie, J. H.; Gross, M. L. *Int. J. Mass Spectrom. Ion Processes* **1994**, 133, 165-174.
9. Barber, M.; Bordoli, R. S.; Sedgwick, R. D.; Tetler, L. W. *Org. Mass Spectrom.* **1981**, 16, 256.
10. Raftery, M. J.; Bowie, J. H. *Int. J. Mass Spectrom. Ions Processes* **1988**, 85, 167.
11. Knapp, D. R. "Chemical Derivatization for Mass Spectrometry" in *Methods in Enzymology*, vol. 93, McCloskey, J. A., ed., Academic Press: San Diego, 1990; pp314-328.
12. Sehgal, D.; Vijay, I. K. *Anal. Biochem.* **1994**, 218, 87-91.
13. Lias, S. G.; Bartmess, J. E.; Liebman, J. F.; Holmes, J. L.; Levin, R. D.; Marland, W. G. *J. Phys. Chem. Ref. Data*, **1988**, 17, Suppl. No. 1.
14. Roepstorff, P.; Fohlman, J. *Biomed. Mass Spectrom.* **1984**, 11, 601.
15. Huaqin Wu and John Allison, *J. Am. Soc. Mass Spectrom.* **1994**, 5, 564-475.

16. Renner, D.; Spiteller, G.; *Biomed. Environ. Mass Spectrom.* **1986**, 13, 405.
17. Johnson, Martin, Biemann, *Int J. Mass Spectrom. Ion Processes* **1987**, 86, 137.
18. Kidwell, D. A.; Ross M. M.; Colton, R. J. *J. Am. Chem. Soc.* **1984**, 106, 2219-
19. Vath, J. E.; Biemann, K. *Int. J. Mass Spectrom. Ion Proc.* **1990**, 100, 187.
20. Wagner, D.S.; Salari, A.; Gage, D. A.; Leykam, J.; Fetter, J.; Hollingsworth, R.;
Watson, J. T. *Biological Mass Spectrom.* **1991**, 20, 419-425.
21. Zaia, J.; Biemann, K. *41th Am. Soc. Mass Spectrom. Allied Topics* **1993**, San
Francisco, pp358.
22. Griffiths, W. J.; Zhang, J.; Sjoval, *Rapid Commun. Mass Spectrom.* **1993**, 7, 235-
240.
23. Wagner, D. S. *PhD Dissertation*, Michigan State University, **1992**.
24. Jessen, N. J.; Tomer, K. B.; Gross, M. L. *J. Am. Chem. Soc.* **1985**, 107, 1863-
1868.
25. Roepstorff, P.; Richter, W. J. *Int. J. Mass Spectrom. Ion Processes* **1992**, 118/119,
789-809.
26. Stults, J. T. *Peptide Sequencing by Mass Spectrometry* in "*Biomedical Application
of Mass Spectrometry*, vol. 34", Suelter, C. H. & Watson, J. T., ed.; Wiley: New
York; 1990.
27. Biemann, K.; Martin, S. A. *Mass Spectrom. Rev.* **1987**, 6, 1-76.

APPENDICES

APPENDIX I

Local Pressure at the Sample Holder in the Ion Source and Collision Frequency In K^+ IDS Experiments

I. Introduction

As has been seen from the previous chapters, K^+ IDS-MS can be viewed as a chemical ionization technique with K^+ ions as the reagent ions. The reagent ions are generated by a thermionic emitter. They react with thermally desorbed intact analyte molecules and their thermal degradation products forming K^+ -adducts. Because the adduct formation may be a second order reaction, the collision frequency between K^+ and desorbed species will be a direct indication of sensitivity. Since collision frequency, a function of source pressure and K^+ flux, is a function of pressure, let's first consider the ion-source pressure during the thermal desorption process.

The pressure in the ion source under K^+ IDS condition has been assumed to be high during early development of this technique. It was believed that the high pressure to a great extent stabilized the adduct ions after their formation.

However, there are some obvious observations which indicate low pressure in a K^+ IDS ion source, especially the local pressure at the sample holder. 1. There are no competitive reactions observed for K^+ attachment to mixtures. For example, in studying relative responses of various amino acids, ion chromatograms from all amino-acid are complete and symmetric, indicating that there is no equilibrium - no high collision

frequency - existing in K^+IDS ion source. 2. The sensitivity of K^+IDS technique is relatively low, even less sensitive than that of chemical ionization (CI). This suggests that there might be a low pressure in the ion source which leads to a low collision frequency, thus low sensitivity. 3. An assumed high pressure should lead to a high collision frequency, thus high adduct formation rates, high stabilization effects and thus high sensitivity of the technique. Unfortunately, this is not true, indicating that the high-pressure assumption may not be true.

The questions are: What is the local pressure at the sample holder in a typical K^+IDS experiment? What is the encounter frequency between K^+ ions and desorbed neutral molecules? After adduct formation, what is the average collision number between any adduct ion formed and desorbed neutral species? If the average collision number is less than one, what is the percentage of K^+ ions that undergo at least one collision?

Since the collision frequency is highly dependent on the pressure in the ion source (especially the small volume around the sample holder), a rough estimation of the ion source pressure or number densities for both K^+ ions and the neutral molecules will be necessary. Because the separation between the sample holder and K^+ emitter is 1 mm, a spherical volume with $r = 1\text{mm}$ is considered in this study.

II. Calculation of the local pressure at sample holder in the ion source

To find out the local pressure around the sample holder in the ion source, two methods for estimation are used. The consistency from these two methods suggests that the results are reliable.

A. Estimation Method #1

Considering a space 1 mm around the sample holder. If a gas is confined in this volume ($V = 1.333\pi r^3 = 4\text{ mm}^3$) and the volume has a imaginary surface A ($A = 4\pi r^2 =$

10 mm²), from which gas can diffuse to a lower pressure region (assuming 0 Pascal for the ion source).

Typical ion source conditions in K⁺IDS are as follows:

$$\text{Exit area: } A = 4\pi r^2 = 4 \times 3.14 \times 1 \text{ mm}^2 = 0.1 \text{ cm}^2 = 10^{-5} \text{ m}^2$$

$$\text{Volume considered (around bead): } V = 1.333\pi r^3 = 4 \text{ mm}^3 = 4 \times 10^{-9} \text{ m}^3$$

$$\text{Molar mass: } 200 \text{ g/mol}$$

$$\text{Sample load: } 20 \mu\text{g} = 10^{-7} \text{ mol}$$

$$\text{Desorption time: } 10 \text{ sec}$$

$$\text{K}^+ \text{ emission current : } 10 \mu\text{A}$$

$$\text{Average desorption rate:}$$

$$20\mu\text{g}/10\text{s} = 10^{-8} \text{ moles/s.}$$

$$m = M/N_{\text{av}} = 3.3 \times 10^{-25} \text{ Kg}$$

$$T = 300 \text{ K}$$

$$\text{Source Chamber Pressure: } 10^{-4} \text{ Pa}$$

If there is no diffusion from the imaginary surface from which gases diffuse, the pressure in the confined volume will build up to the following after one second of heating/desorption according to the ideal gas equation:

$$P = nRT/V = (10^{-8} \text{ mol} \times 8.314 \text{ J K}^{-1} \text{ mol}^{-1} \times 300 \text{ K}) / 4 \times 10^{-9} \text{ m}^3 = 6000 \text{ Pa}$$

however, the diffusion (the source pressure is only 10⁻⁴ Pa, which can be considered as 0; thus diffusion) of gas with a pressure of 6000 Pa from the imaginary surface cannot keep this high pressure at all, the gas flux J_n through the surface can be calculated as follows [1]:

$$J_n = P/(2\pi mkT)^{1/2}$$

$$= 6000 \text{ Pa} / (2 \times 3.14 \times 3.3 \times 10^{-25} \text{ Kg} \times 1.38 \times 10^{-23} \text{ JK}^{-1} \times 300 \text{ K})^{1/2}$$

$$= 6 \times 10^{25} \text{ s}^{-1} \text{ m}^{-2}$$

The diffusion rate of analyte in the gas phase through the imaginary surface at a pressure of 6000 Pa:

$$\begin{aligned} J_n \times A / N_{av} &= 6 \times 10^{25} \text{ s}^{-1} \text{ m}^{-2} \times 10^{-5} \text{ m}^2 / 6.022 \times 10^{23} \text{ mol}^{-1} \\ &= 1 \times 10^{-3} \text{ mol s}^{-1} \end{aligned}$$

It is easy to see that the diffusion rate (assuming that the pressure is maintained at 6000 Pa) is much faster than the desorption rate.

During desorption process, a steady-state desorption and diffusion can be assumed. Thus the diffusion rate must be equal to that of the desorption rate 10^{-8} mol/sec (steady-state approximation). Since the diffusion rate in mol/s is directly proportional to ion source pressure, the corresponding diffusion pressure with which steady-state condition is maintained is:

$$6000 \text{ Pa} \times (10^{-8}/10^{-3}) = 0.06 \text{ Pa}.$$

B. Estimation Method #2

The throughput of gases through the exit of the ion source can be calculated as follows [2]:

$$Q = AP_1 C' \left(\frac{kT}{m} \cdot \frac{2r}{r+1} \right)^{1/2} \left(\frac{2}{r+1} \right)^{1/(r-1)} \quad (\text{valid for } P_2/P_1 \leq (2/(r+1))^{r/(r-1)})$$

where Q is the gas flow through an orifice, A is the area of the orifice (a imaginary surface 1 mm around the sample holder), P_1 is the pressure inside the confined volume, P_2 is the pressure in the ion source (ion source chamber), C' is a correction factor for the orifice area (0.85 for thin orifice), r is the ratio of specific heat . The specific heat can be roughly estimated as $r = c_p/c_v = (2n+3)/(2n+1)$, where n is the number of atoms in a molecule. For small peptide molecules with molecular weights of 200, n is about 30 (for peptides, $n \approx \text{MW}/7$), and r is calculated to be about 1.024.

For $r = 1.024$, $[2/(r+1)][r/(r-1)] = 0.608$. It is apparent that the $P_2/P_1 \ll 0.608$ since the pressure outside the ion source is below 10^{-4} Pa. So the above equation is valid for the calculation of the flow rate at the imaginary surface 1 mm around the sample holder.

$$\text{Given } P_2 = 10^{-4} \text{ Pa, } T = 600 \text{ K, } r = 1.024, A = 0.1 \text{ cm}^2 = 10^{-5} \text{ m}^2$$

$$\begin{aligned} Q &= 10^{-5} \text{ m}^2 \times P_1 \text{ Pa} \times \{(8.314 \text{ JK}^{-1} \text{ mol}^{-1} \times 600 \text{ K} \times 2 \times 1.024) / [2 \text{ Kg/mol} \times 2.204]\}^{1/2} \\ &\quad \times [(2/(1+1.024))^{1/(1.024-1)} \times 0.85 \\ &= 10^{-5} \text{ m}^2 \times P_1 \text{ Pa} \times 158.9 \text{ m/s} \times 0.608 \times 0.85 \\ &= 8.2 \times 10^{-4} P_1 \text{ (Pa m}^3 \text{ s}^{-1}) \end{aligned}$$

$$\text{Given } r = 1.0328, Q = 8.1 \times 10^{-4} P_1 \text{ (Pa m}^3 \text{ s}^{-1})$$

$$\text{Given } r = 1.01 \text{ (n=100), } Q = 8.2 \times 10^{-4} \text{ (Pa m}^3 \text{ s}^{-1})$$

this clearly shows that r hardly affects the flow rate when it is very small.

The desorption rate is about 10^{-8} mol/sec, which is corresponding to

$$\begin{aligned} \Delta PV &= \Delta nRT = 10^{-8} \text{ mol s}^{-1} \times 8.314 \text{ J K}^{-1} \text{ mol}^{-1} \times 600 \text{ K} = 5 \times 10^{-5} \text{ J s}^{-1} \\ &= 5 \times 10^{-5} \text{ Pa m}^3 \text{ s}^{-1}. \end{aligned}$$

Obviously, to maintain the equilibrium, the diffusion rate (flow rate through the exit) should be equal to the desorption rate:

$$8.2 \times 10^{-4} P_1 \text{ m}^2 \text{ s}^{-1} = 5 \times 10^{-5} \text{ Pa m}^2 \text{ s}^{-1}.$$

$$P_1 = 0.06 \text{ Pa}$$

This means that the analyte pressure 1 mm around the emitter tip is kept at 0.06 Pa, which is consistent from the value estimated by method #1. Obviously, these numbers are not as high as many of us had imagined.

C. Collision diameter: The size of peptide molecules

To estimate the encounter frequency between K^+ ions and neutral molecules, the collision diameters of both peptide molecules and K^+ ions have to be estimated because the mean free path for analyte molecules can be calculated as follows:

$$\lambda_{aa} = kT / (2^{1/2} \pi d_a^2 P)$$

The problem is the effective collision diameter has to be figured out.

To calculate the collision diameter, the molecules can be treated as a ball in the gas phase. Suppose the density of peptide is 0.8 g/cm^3 , and the peptide is in the primitive cubic crystal form, with $\text{MW} = 200 \text{ g/mol}$.

Every one cm^3 contains moles of peptides: $0.8 \text{ g} / (200 \text{ g/mole}) = 4 \times 10^{-3} \text{ moles}$

of molecules in one cm^3 is $4 \times 10^{-3} \text{ moles} \times 6.022 \times 10^{23} / \text{mole}$

Each peptide molecule takes a volume of $(1.333\pi r^3) / 0.524$

$1 \text{ cm}^3 = 10^{-6} \text{ m}^3 = 4 \times 10^{-3} \text{ moles} \times 6.022 \times 10^{23} / \text{mole} \times (1.333\pi r^3) / 0.524$

$r = 6.6 \times 10^{-10} \text{ m}$

$d_{aa} = 2r = 1.32 \times 10^{-9} \text{ m}$

$\lambda_{aa} = kT / (2^{1/2} \pi d_{aa}^2 P)$

$= 1.38 \times 10^{-23} \text{ J K}^{-1} \times 300 \text{ K} / [1.414 \times 3.14 \times (1.32 \times 10^{-9} \text{ m})^2 \times P]$

$= 7.6 \times 10^{-4} / P \text{ m} \quad (\text{J m}^{-2} \text{ Pa}^{-1} = \text{m})$

$\lambda_{aa} = 0.76 / P \text{ mm} \quad \text{with } P \text{ in Pascal}$

If $T = 600 \text{ K}$ is used, $\lambda_{aa} = 1.5 / P \text{ mm}$

D. The mean free path of K^+ in the ion source

The K^+ emission rate in the ion source is $10 \text{ } \mu\text{A} = 10^{-5} \text{ A} = 10^{-10} \text{ moles/sec}$ (note 1 mole charge = $96487 \text{ C} \approx 10^5 \text{ C}$), which is only 1% of the desorption rate. The mean free path for K^+ ion in the analyte molecule gas can be calculated as follows:

$$\lambda_k = \frac{1}{\left[2^{1/2} \pi n_k d_k^2 + \left(1 + \frac{v_a^2}{v_k^2} \right)^{1/2} n_a \frac{\pi}{4} (d_k + d_a)^2 \right]}$$

where n_k is number density of K^+ ion in the gas phase, n_a is the number density of gas-phase analyte molecules; v_k is the velocity of K^+ ions, v_a is the velocity of analyte molecules in the gas phase, d_a is the diameter of analyte molecules, d_k is the diameter of

K^+ ions. λ_k is the mean free path of K^+ ions in the gas-phase analyte molecules. Since v^2 is inversely proportional to the mass of a molecule, the above equation can be rewritten as

$$\lambda_k = \frac{1}{\left[2^{1/2} \pi n_k d_k^2 + \left(1 + \frac{m_k}{m_a} \right)^{1/2} n_a \frac{\pi}{4} (d_k + d_a)^2 \right]}$$

since $n_a \gg n_k$, $d_a^2 \gg d_k^2$, the above equation can be simplified as following:

$$\lambda_k = \frac{1}{\left[\left(1 + \frac{m_k}{m_a} \right)^{1/2} n_a \frac{\pi}{4} (d_k + d_a)^2 \right]}$$

at this low pressure, the peptide in the gas phase may be treated as ideal gas, thus:

$$\lambda_k = \frac{kT}{\left[\left(1 + \frac{m_k}{m_a} \right)^{1/2} \frac{\pi}{4} (d_k + d_a)^2 P \right]}$$

Given $m_k = 39$, $m_a = 200$, $d_k \approx 10\% d_a$, plug all the numbers in the equation, then

$$l_k = 9.0 / P \quad \text{mm}$$

at the pressure of 0.06 Pa, $l_k = 9.0 / P \quad \text{mm} = 150 \text{ mm}$.

For the ion source used, the source center (EI source) to the exit is about 5 mm, which is much less than the mean free path of K^+ ions.

The low pressure of analyte and the low K^+ emission rate is the key factors for the low sensitivity of this K^+ IDS technique.

But why do we see adduct ions?

Do not misunderstand the mean free path, mean free path greater than the ion source dimension does not mean no collision! In fact, kinetic theory describes the distribution of free paths as follows:

$$N = N' e^{-x/l}$$

where N' is the number of molecules in the volume and N is the number of molecules that traverse the distance x before suffering a collision.

If the source dimension $x = 10\%l$, then $N/N' = 90\%$, 10% of the molecules or ions traversing the ion source will undergo a collision. If $x = 1/5 l$, $N/N' = 82\%$, 18% of molecules or ions will have a collision before getting out of the ion source.

x/l	3%	10%	1/5	2/5	1	5
% collision	3	10	18	33	63	99.7

so, even though the source dimension is only 3% (5 mm/150 mm) of the mean free path of K^+ ions, there are still 3% of K^+ ions collide with analyte molecules before leaving the ion source. Because of the low encounter frequency between K^+ and neutral species, the concentration of $(M+K)^+$ is low; thus the possibility of three-body collisions - the collisions between $(M+K)^+$ ions and neutral species - is small. Therefore, three-body collisions are unlikely to occur in K^+ IDS experiments.

Consider the above situation. 3% of the K^+ ions under collisions with neutral species is a reasonably high collision frequency. If each collision leads to the formation of one adduct ion, then the sensitivity can be very high. Assume ionization efficiency of 100% in FAB, the signal lasts 5 minutes, then it is only as sensitive as K^+ IDS. In fact, the FAB responses of peptides are much higher than K^+ IDS responses. This may suggest that the detachment of K^+ ions is very fast, which leads to poor sensitivity.

E. Comparison with Chemical Ionization (CI)

In CI, there are several factors changed. First, the most significant change is that the protonated molecules are much more stable than that of K^+ adducts of analyte molecules, Second, the collision diameter of CH_5^+ is increased by a factor of 2. Third, loss of reagent ion CH_5^+ and analyte molecules is also reduced because the collisions with the high-pressure reagent gas will keep them in the ion source for a much longer time.

$$\lambda_{CH_5^+(CH_4)} = \frac{kT}{\left[\left(1 + \frac{m_{CH_5^+}}{m_{CH_4}}\right)^{1/2} \frac{\pi}{4} (d_{CH_5^+} + d_{CH_4})^2 P \right]}$$

assume $d_{CH_5^+} = d_{CH_4} = 5\text{\AA}$, $T = 300\text{K}$, the result is $l_{CH_5^+(CH_4)} = 4/P$ mm.

The mean free path for collisions between CH_5^+ and analyte molecules are:

$$\lambda_{CH_5^+(a)} = \frac{kT}{\left[\left(1 + \frac{m_{CH_5^+}}{m_a}\right)^{1/2} \frac{\pi}{4} (d_{CH_5^+} + d_a)^2 P \right]}$$

assume $d_{CH_5^+} = 5\text{\AA}$, $d_a = 13\text{\AA}$, $T = 200\text{ K}$, $MW = 200$, $l_{CH_5^+(a)} = 1.6/P$ mm.

In a CI source, the pressure is usually set at 1 torr (133 Pa), the mean free path of the reagent ion with reagent gas is $l = 4/(133\text{ Pa}) = 0.03\text{ mm}$, which means that CH_5^+ will undergo hundreds of collisions with CH_4 or analyte molecules in the ion source. This high collision frequency ensures that the protonation process has a very high efficiency. The frequent collisions also stabilizes the protonated molecules due to thermalization, which results in little fragmentation of the protonated molecules.

The frequency of collisions between reagent ions and analyte molecules is determined by the number densities of both. If the sample quantity is the same as given in K^+IDS , the pressure can be kept much higher since the exit is now much smaller, plus the diffusion of the reagent gas is much faster than the analyte molecule. The diffusion rate ratio is $(16/200)^{1/2} \approx 1/3$, so the reagent gas diffuses 3 times as fast as the analyte molecules out of the ion source.

Note here the collisions between analyte molecules and reagent ion such as CH_5^+ is much less frequent than collisions between neutral molecules because of the much lower concentrations of both.

So what is the concentration of CH_5^+ like? Suppose filament current $300\text{ }\mu\text{A}$ and electron energy 300 eV , each electron ionized two neutral species. $300\text{ }\mu\text{A} = 3 \times 10^{-4}\text{ A} \approx 3 \times 10^{-9}\text{ moles/sec}$ since 1 mole of charge = 10^5 C . If this concentration can build up, the pressure can be as high as 10 Pa in the small ion source. If each collision between a CH_5^+

and an analyte molecule forms a protonated analyte, the chemical ionization rate will be the collision rate between CH_5^+ and analyte molecules.

There is a locally high concentration of CH_5^+ along the electron path, which will result in high ionization yield.

References

1. Alberty, R. A.; Sibley, R. J. *Physical Chemistry*, 1st ed.; Wiley & Sons: New York, 1992; pp609.
2. O'Hanlon, J. F. *A User's Guide to Vacuum Technology*, Wiley & Sons: New York, 1989; pp29.

Appendix II

Enthalpies of Thermal Degradation of Peptides from Model Compounds

1. Model Compounds:

Direct calculation or estimation of reaction enthalpies for thermal degradation of peptides are impossible at this time due to the lack of thermodynamic data of peptides. In order to estimate these data for the cleavages of peptide skeletal bonds (AX, BY and CZ bonds based on Roepstoff nomenclature) under various mechanisms, model compounds are selected to simulate these processes.

The three skeletal bonds in peptides are simulated with the following models:

I.	$\text{CH}_3\text{CO-NHCH}_3$	AX bond
II.	$\text{CH}_3\text{CH}_2\text{-COOH};$ $\text{NH}_2\text{CH}_2\text{-COOH};$ $\text{CH}_3\text{CH}_2\text{-COCH}_3$	BY bond
III.	$\text{CH}_3\text{NH-CH}_2\text{CH}_3$	CZ bond

The reaction enthalpies of these model compounds, based on the following data available, are used as the reaction enthalpies of peptides.

Table 1. Bond Dissociation Energies (BDE, kcal/mol)

BDE($\sim\text{CO-NH}\sim$)	93.6	amide bond
BDE(H-NHR)	101	Primary N-H bond.

BDE(H-NHR ₁ R ₂)	91.5	Secondary N-H bond.
BDE(H-i-C ₃ H ₇)	95.9	secondary C-H bond.
BDE(H-t-C ₄ H ₉)	93.3	tertiary C-H bond.

2. Estimation and Optimization of Bond Dissociation Energies

A. Modified Estimation of Amide N-H Bond Strength:

Consider the two N-H bonds in a peptide such as **H-NHCH₂CON(-H)CH₂~~~**,
which N-H bond is stronger ?

$$\text{BDE}(\text{CH}_3\text{NH-H}) = 100$$

$$\text{BDE}((\text{CH}_3)_2\text{N-H}) = 91.5$$

How does -CO- affect the bond strength?

$$\text{BDE}(\text{CH}_3\text{O-H}) = 104.4$$

$$\text{BDE}(\text{CH}_3\text{COO-H}) = 105.8, \text{ increased by } 1.4 \text{ kcal/mol.}$$

If this is true for amide/amide, then

$$\text{BDE}((\text{CH}_3)_2\text{N-H}) = 91.5$$

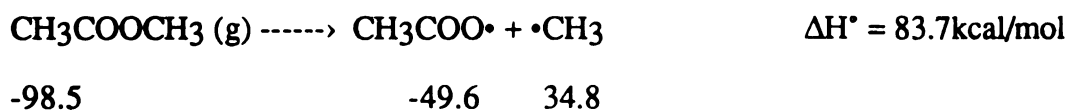
$$\text{BDE}((\text{CH}_3\text{CON}(\text{CH}_3)\text{-H}) = 91.5 + 1.4 = 93$$

Note here that the trend for C-H bond is different:

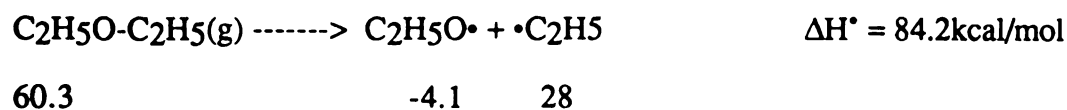
$$\text{BDE}(\text{CH}_3\text{CH}_2\text{-H}) = 100.3$$

$$\text{BDE}(\text{CH}_3\text{COCH}_2\text{-H}) = 98.3 \text{ decreased by } 2 \text{ kcal/mol.}$$

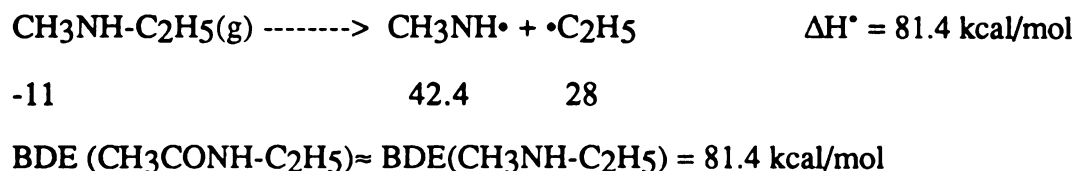
B. Estimation of C-O and C-N bond strengths



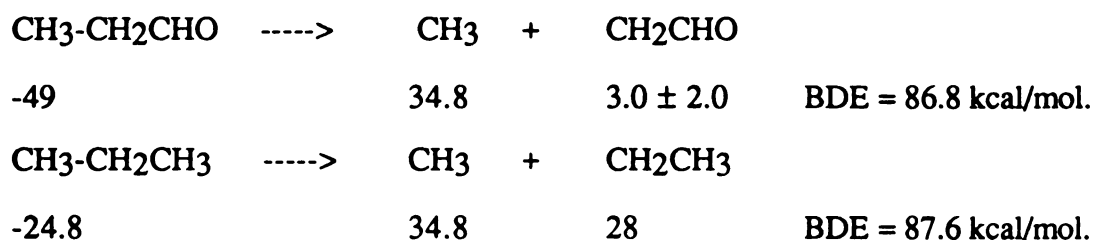
This bond is very similar to that formed in the (Z-H) fragment when cyclization occurs from the C-terminus.



The small difference indicates that the carbonyl group near the O does not affect the bond strength of O-C bond. In the same consideration, it is assumed that the carbonyl group near N will not affect the bond strength of N-C bond.



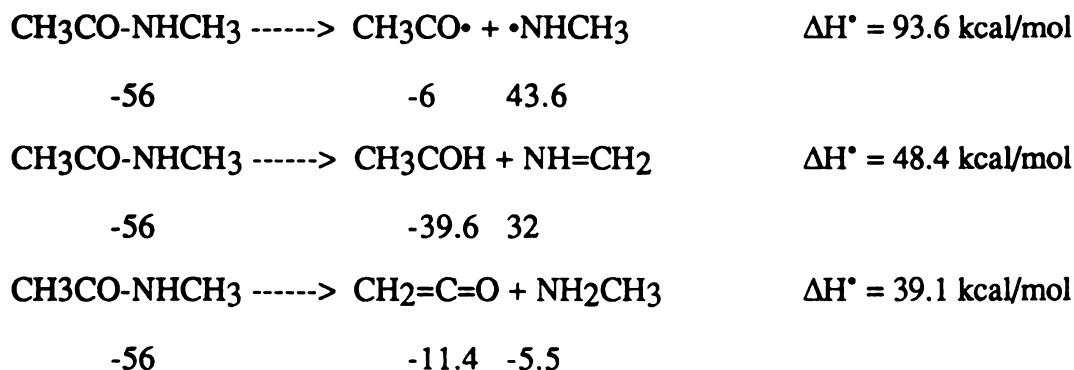
The small affect of carbonyl group can also be seen from the following example.



3. Enthalpies for Different Thermal-Degradation Pathways of Peptides

Model molecule: CH₃CO-NHCH₃

Model bond: -CHRCO-NHCHR'-, the BY bond.



Cyclization at BY bonds: for example, 1, 6 - Elimination:

$P \rightarrow \text{cyclo-(B-H)} + (Y+H) \quad \Delta H^\circ = 93 - 101 \approx -8$ if cyclization from an amide.

One secondary NH bond is broken and one primary N-H bond is formed.

$P \rightarrow \text{cyclo-(B-H)} + (Y+H) \quad \Delta H = 101 - 101 \approx 0$ if cyclization from the N-terminus. One primary N-H bond and an amide bond are broken while one primary N-H bond and one amide bond are formed.

Model Molecules: $\text{NH}_2\text{CH}_2\text{-COOH}$, $\text{CH}_3\text{-COCH}_3$, $\text{CH}_3\text{-COOH}$

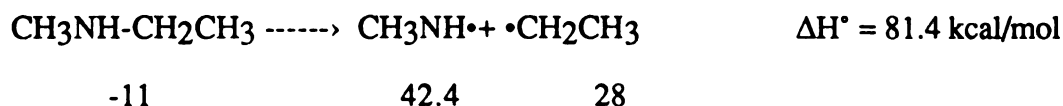
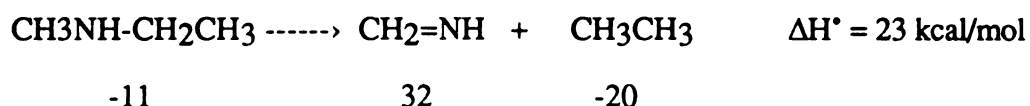
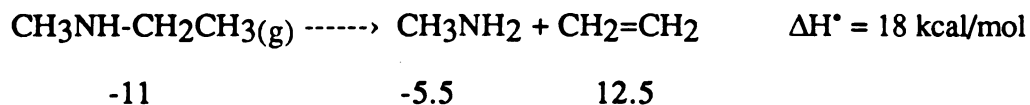
Model bond: -NHCHR-CONH- , the AX bond.

$\text{NH}_2\text{CH}_2\text{COOH} \rightarrow \text{NH=CH}_2 + \text{HCOOH}$	$\Delta H^\circ = 34.5 \text{ kcal/mol}$
-93 32 -90.5	
$\text{NH}_2\text{CH}_2\text{COOH} \rightarrow \text{NHCH}_2\bullet + \bullet\text{COOH}$	$\Delta H^\circ = 78 \text{ kcal/mol}$
-93 38 -53.3	
$\text{CH}_3\text{CH}_2\text{COCH}_3 \rightarrow \text{CH}_3\text{CH}_2\bullet + \bullet\text{COCH}_3$	$\Delta H^\circ = 79.5 \text{ kcal/mol}$
-57.5 28 -6	
$\text{CH}_3\text{CH}_2\text{COOH} \rightarrow \text{CH}_3\text{CH}_2\bullet + \bullet\text{COOH}$	$\Delta H^\circ = 82 \text{ kcal/mol}$
-107 28 -53.3	
$\text{CH}_3\text{COOH} \rightarrow \text{CH}_3\bullet + \bullet\text{COOH}$	$\Delta H^\circ = 85 \text{ kcal/mol}$
-103.3 34.8 53.3	
$\text{CH}_3\text{COCH}_3 \rightarrow \text{CH}_3\text{CO}\bullet + \bullet\text{CH}_3$	$\Delta H^\circ = 81 \text{ kcal/mol}$
-52 -6 -34.8	
$\text{CH}_3\text{CONH}_2 \rightarrow \text{CH}_4 + \text{O=C=N-CH}_3$	$\Delta H^\circ = 7 \text{ kcal/mol}$
-56 -17.8 -31	Unusually low

Cyclization at AX bonds: $P \rightarrow (A+H) + \text{Cyclo}-(X-H) \quad \Delta H = 93.3 - 96 \approx -3$
 because one secondary C-H is converted into a tertiary C-H bond.

Model Molecule: $\text{CH}_3\text{NH}-\text{CH}_2\text{CH}_3$

Model bond: $-\text{CHRNH}-\text{COCHR}'-$, the CZ bond.



Cyclization: There are two possibilities.

$P \rightarrow (C+H) + \text{Cyclo}-(Z-H) \quad \Delta H^\circ = 93 - 101 \approx -8 \text{ kcal/mol}$ if cyclization is not from the C-terminus. A primary N-H is formed while a secondary N-H bond is broken.

$P \rightarrow (C+H) + \text{Cyclo}-(Z-H) \quad \Delta H^\circ = 81.4 (\text{C-N}) - 84.3 (\text{C-O}) + 105.8 (\text{O-H}) - 101 (\text{N-H}) \approx 2 \text{ kcal/mol}$ if cyclization is from the C-terminus. A O-H bond and N-C bond are broken while a primary N-H bond and a C-O bond are formed.

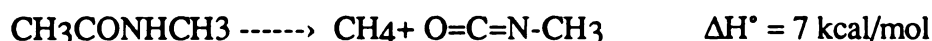
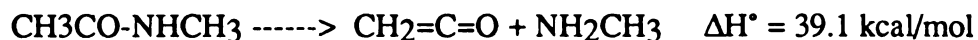
4. Data Rearranged in Types of Reactions

Homolytic cleavage:

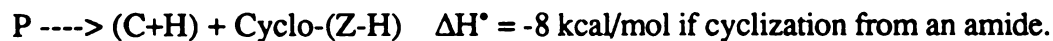
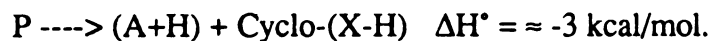




1,2 - Elimination:



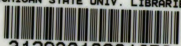
Cyclization: Cyclization involves bond changes from secondary amine to primary amine, from secondary carbon to tertiary carbon, etc.



Reference

1. CRC Handbook of Chemistry and Physics, 71th ed.

MICHIGAN STATE UNIV. LIBRARIES



31293010201659